

CONTENTS

71	H-type Hypertension and Recurrence of Ischemic Stroke Tan Song, Zhao Lu, Wang Haili, Song Bo, Li Zhuo, Gao Yuan, Lu Jiameng, Chandra Avinash, Xu Yuming	460-463
72	Stent displacement during the Y-stent assisted coil embolization of wide-neck basilar tip aneurysm Tan Song; Xu Hao-wen; Song Bo, Chandra Avinash , Xu Yu-ming	464-466
73	Withdrawn	467-476
74	The Health Status and Its Influence Factors of Stroke Patients in Community of Zhengzhou, 2010 Zhang Zhenxiang, Liu Lamei, Lin Beilei,Zhang Yaqi , Xie Junfang, Mei Yongxia, Zhang Weihong	477-481
75	Families of maps Singularities and its Gauss maps M. A. Soliman, Nassar. H. Abdel-All, Soad. A. Hassan and E. Dahi	482-487
76	Study of ladybirds (Col:Coccinellidae) in Khorramabad district and the first report of <i>Hyperaspis quadrimaculata</i> (Redtenbacher 1844) for Iranian fauna A. Ansari pour, J. Shakarami	488-495
77	Intracranial Stent Placement for Recanalization of Acute Cerebral Artery Occlusion Shilei Sun, Tan Song; Xu Haowen; Chandra Avinash , Xu Yuming	496-499
78	Helicobacter Pylori Infection and Immune Factors On Residents in High-incidence Areas of Cancer Along S River Ping LI, Jingyuan ZHU, Yue BA, Shiqun LI, Xuemin CHENG, Hua LI, Yutang XUE, Ruichang LIU, Qiting ZUO, Liuxin CUI	500-504
79	On Bipreordered Approximation Spaces A. Kandil QUOTE,M. Yakout QUOTE and A. Zakaria	505-509
80	Effect of Grape Seeds Extract in the Modulation of Matrix Metalloproteinase-9 Activity and Oxidative Stress Induced By Doxorubicin in Mice Monira A. Abd El Kader, Nermin M. El-Sammad, and Amal A.Fyiad	510-515
81	Effect of Powder and Essential Oil of Lemon grass on Aflatoxins Production in Dried Water Melon Seed Eman M. Hegazy	516-522
82	Histopathological and Ultrastructural Study of Experimental Spring Viraemia of Carp (SVC) Infection of Common Carp with Comparison between Different Immunohistodignostic Techniques Efficacy A.Y. Gaafar, Tomáš Veselý, T. Nakai, E.M. El-Manakhly, M.K. Soliman, H. Soufy, Mona S. Zaki, Safinaz G. Mohamed,Amany M. KenawyM. S. El-Neweshy and A. Younes.	523-533
83	PMF, Cesium & Rubidium Nanoparticles Induce Apoptosis in A549 Cells Faten. A. Khorshid; Gehan. A. Raouf ; Saleem. M. El-Hamidy; Gehan. S. Al-amri;	534-542

	Nourah. A. Alotaibi and Taha A. Kumosani	
84	Analysis of intraoperative complication of ruptured cerebral aneurysm with detachable coils embolization Xu Hao-wen; Tan Song; Song Bo, Sun Shi-lei, Xu Yu-ming	543-546
85	Construction of HSV-1 HF based replication defective vector Li Xiang, Xinjing Liu, Huitao Liu, Zhiqiang Han, Jiameng Lu and Yuming Xu	547-553
86	Structure, Electrical Conductivity and Dielectric properties of bulk, 2-amino-(4,5-diphenylfuran-3-carbonitrile) A.A. Hendi	554-559
87	Study of Electrical Properties of TlInses Layered Single Crystal S. E. Al Garni	560-563
88	Effect of Citrus Waste Substrate on the production of Bioactive Component, and Antioxidant and Antitumor Activity of <i>Grifola frondosa</i> Jung Hyun Kim, Min Young Kim	564-571
89	The Impact of Explicit Teacher Feedback on Micro and Macro Level Features of the Performance of the EFL Students in Descriptive Writing Afshin Soori , Arshad Abd. Samad , Kamariah Abu Bakar	572-576
90	Interleukin-4 Polymorphism in Egyptian Patients with Type-2 Diabetic Nephropathy Mohamed M. El-Shabrawi, Nervana M. K Bayoumy and Hamdi H. Hassan	577-582
91	Evaluation of changes the qualitative & quantitative yield of horse bean (<i>Vicia Faba L</i>) plants in the levels of humic acid fertilizer Simin Haghighi, Tayeb Saki Nejad, Shahram Lack	583-588
92	The Renoprotective Effect of Honey on Paracetamol - Induced Nephrotoxicity in Adult Male Albino Rats Basma K. Ramadan and Mona F. Schaalán	589-596
93	Non-Ulcer Dyspepsia: Abnormal Myoelectrical Activity and Gastric Emptying, Fact Or Fiction?. Amal S. Bakir, Adel A. Mahmoud, Tarek M. Yousef and Mohamed A. Mostafa	597-603

H-type Hypertension and Recurrence of Ischemic Stroke

Tan Song¹, Zhao Lu¹, Wang Haili¹, Song Bo¹, Li Zhuo¹, Gao Yuan¹, Lu Jiameng¹, Chandra Avinash¹, Xu Yuming¹

1. Department of Neurology, the First Affiliated Hospital of Zhengzhou University, Zhengzhou, Henan 450052, China.

Co-first author: Zhao Lu; Corresponding author: XU Yu-ming, xuyuming@zzu.edu.cn

Abstract: Both hypertension and hyperhomocysteinemia are important risk factors of ischemic stroke. The hypertension with hyperhomocysteinemia is defined as “H-type hypertension”, with a prevalence of 75% among Chinese hypertensive population. The correlation between H-type hypertension and recurrence of ischemic stroke needs to be confirmed. In this study, we prospectively recruited and followed up 602 ischemic stroke patients in Henan province, China. The average age of patients was 59.33±13.20 years and 67.3% being male. Average level of homocysteine was 19.09±11.19 mmol/L and 57% patients had hypertension. There were 310 (51.5%) H-type hypertension patients and 292 (48.5%) non H-type hypertension patients. 23.5% patients had past stroke history in H-type hypertension group and 15.1% in non H-type hypertension group. Stroke recurrence was recorded in 6.1% patients with H-type hypertension and in 1.7% patients non H-type hypertension group at 6-month follow-up. Multivariate Logistic analysis demonstrated a weak association between the H-type hypertension and stroke recurrence at 6-month follow-up. Thus, H-type hypertension could be a risk factor for stroke recurrence in Henan Chinese population.

[Tan Song, Zhao Lu, Wang Haili, Song Bo, Li Zhuo, Gao Yuan, Lu Jiameng, Chandra Avinash, Xu Yuming. **H-type Hypertension and Recurrence of Ischemic Stroke**. Life Science Journal. 2011;8(3):460-463] (ISSN:1097-8135). <http://www.lifesciencesite.com>.

Keywords: H-type hypertension; ischemic stroke; recurrence

1. Introduction

The strong interaction between hypertension and hyperhomocysteinemia has been reported [1], which increased 11 times risk of cardiovascular and cerebrovascular diseases more than the sole hypertension. In 2008, Dayi Hu et al proposed “H-type hypertension” in China, whose definition is hypertension with hyperhomocysteinemia [2]. H-type hypertension takes 75% among all Chinese hypertensive patients. A nested case-control study [3] in China, with a sample of 40 000 during an average of more than 6 years follow-up, revealed that the risk of the first cardiocerebrovascular events in patients with H-type hypertension was 12.1 times more than those of controls. However, we don't know whether H-type hypertension affect recurrence of stroke. This study was to investigate the association between H-type hypertension and recurrence of ischemic stroke by prospectively recruiting the ischemic stroke inpatients during a 30-month period and recording recurrence by 6-month follow-up. The inpatients were from the department of Neurology of the First Affiliated Hospital of Zhengzhou University.

2. Methods

The Stroke diagnosis is based on the stroke diagnostic criteria of World Health Organization 1976 [4]. Cerebral hemorrhage was excluded by CT/MRI. The time from onset to registry was less

than 15 days. Patients with hematological diseases or severe renal failure or hepatic failure and patients with dependence caused by any reason before onset as well as patients who could not cooperate to registry were excluded. Plasma homocysteine level was measured 2~5 days after stroke onset. The level of homocysteine >10μmol/L were set as the hyperhomocysteinemia [5]. Consecutive ischemic stroke patients were registered prospectively. Registry forms were filled by neurologists with unified training. The forms contain gender, age, National Institute of Health Stroke Scale (NIHSS) score after admission, hypertension, diabetes, hyperlipidemia, history of atrial fibrillation and coronary heart disease and TIA and smoking, previous stroke, fasting blood glucose, blood pressure on admission, the level of homocysteine and other laboratory tests and examinations, and the treatments. Patients were followed-up to document recurrent stroke and medication at 6 months. Multivariate logistic regression analysis was used to identify factors that increased the risk of recurrent stroke. Factors that contributed to the recurrence in the initial univariate analyses at P<0.1 were included in the multivariate model. In the final multivariate analyses, statistical significance was achieved if P<0.05. The Statistic Package for Social Science version (SPSS) 10.0 was used for statistical analysis.

3. Results

3.1 General profiles

634 patients who met the inclusion criteria were enrolled consecutively, and 32 (5%) patients missed the follow-up. Thus the final analysis involved 602 patients with acute ischemic stroke. Average level of homocysteine was 19.09 ± 11.19 mmol/L. Table 1 and table 2 demonstrate general data of the patients.

3.2 Baseline characteristics of patients with H-type hypertension or without H-type hypertension

There are 310 (51.5%) patients in H-type hypertension group and 292 (48.5%) in non H-type hypertension group. Diabetes and Coronary heart disease were more in H-type hypertension group than in non H-type hypertension group ($p < 0.05$). The patients in H-type hypertension group were obviously older and had more previous strokes than in non H-type hypertension group ($p < 0.01$). There was no significant difference in gender, history of hyperlipidemia and atrial fibrillation and TIA and moking, severity of

stroke on admission, treatment after onset ($p > 0.05$). (Table 3).

Table 1. Categorical variables

Variables	n	%
Male	405	67.3
Hypertension	343	57.0
Hyperhomocysteinemia	525	87.2
H-type hypertension	310	51.5
Diabetes	163	27.1
hyperlipidemia	142	23.4
Atrial fibrillation	24	4.0
Coronary heart disease	17	2.8
TIA	37	6.1
Previous stroke	117	19.4
smoking	208	34.6
Antiplatelet	523	86.9
Anticoagulation	35	5.8
Chinese traditional medicine	514	85.4
Rehabilitation	127	21.1

Table 2. Continuous variables

Variable	Minimal value	Maximal value	Mean \pm SD	Median
Age(years)	19	92	59.33 \pm 13.20	
NIHSS on admission	1	39		6
Fast blood glucose on admission (mmol/L)	3.0	25.57	6.11 \pm 2.69	
SBP on admission(mmHg)	90	210	143.85 \pm 20.79	
DBP on admission(mmHg)	57	160	87.37 \pm 13.56	

Table 3. Basline characteristics of patients with H-type hypertension or without H-type hypertension

Variable	H-type hypertension (310)	No H-type hypertension (292)	P value
Male,n(%)	212(68.4)	193(66.1)	0.549
Age (years)	60.87 \pm 12.46	57.68 \pm 13.782	0.003
NIHSS on admission	6.47 \pm 7.88	5.41 \pm 6.904	0.081
Diabetes,n(%)	97(31.3)	66(22.6)	0.017
Hyperlipidemia,n(%)	83(26.8)	59(20.2)	0.101
Atrial fibrillation,n(%)	13(4.2)	11(3.8)	0.789
Coronary heart diseas,n(%)e	13(4.2)	4(1.4)	0.037
TIA,n(%)	22(7.1)	15(5.1)	0.317
Previous stroke,n(%)	73(23.5)	44(15.1)	0.009
Smoke,n(%)	100(32.3)	108(36.9)	0.223
Antiplatele,n(%)	294(94.8)	273(93.4)	0.481
Anticoagulation,n(%)	16(5.2)	19(6.5)	0.481
Chinese traditional medicine,n(%)	262(84.5)	252(86.3)	0.811
Rehabilitation,n(%)	73(23.5)	54(18.6)	0.129

3.3 Relationship between H-type hypertension and stroke recurrence

6.1% (19/310) patients with H-type hypertension had recurrent stroke and 1.7% (5/292) patients without H-type hypertension had recurrent stroke at 6-month follow-up. We defined gender, age,

NIHSS on admission, H-type hypertension, diabetes, hyperlipidemia, history of atrial fibrillation and coronary heart disease and TIA, smoking history, antiplatelet, anticoagulation, Chinese traditional medicine and rehabilitation as concomitant variables, and recurrence at 6 month follow- up as dependent

variable. We used univariate logistic regression analyzing the data. Result showed that H-type hypertension was significantly associated with recurrence (P=0.006). Other variables associated with 6 month recurrence were age, NIHSS on admission, Diabetes, Hyperlipidemia and atrial fibrillation (Table

4). Then, we put all variables whose p value were less than 0.1 into multivariate logistic regression analysis. The results demonstrated that H-type hypertension had the weak association with stroke recurrence (P=0.037, OR=1.031, 95%CI 1.069-8.245)(Table 5)

Table 4. Results of univariate logistic regression analysis

Variable	Recurrence (n=24)	No recurrence (n=578)	Wald	P value
Male	16	389	0.004	0.948
Age (years)	65.58±9.103	59.07±13.28	-2.379	0.018*
NIHSS on admission	8.83±5.67	5.84±7.48	-2.371	0.026*
H-type hypertension	19	291	7.663	0.006*
Diabetes	11	152	4.454	0.035*
Hyperlipidemia	11	131	6.884	0.032*
Atrial fibrillation	3	21	4.733	0.030*
Coronary heart disease	1	16	0.145	0.704
TIA	3	34	1.749	0.186
smoke	12	196	2.638	0.104
Antiplatelet	19	504	1.303	0.254
Anticoagulation	2	33	0.259	0.611
Chinese traditional medicine	5	79	0.954	0.329
Rehabilitation	18	457	0.229	0.632

Table 5. Results of multivariate logistic regression analysis

Variable	OR	95%CI	P value
Age	1.031	0.993-1.069	0.104
H-type hypertesion	2.969	1.069-8.245	0.037**
Diabetes	1.855	0.777-4.429	0.164
Hyperlipidemia	2.750	1.174-6.442	0.020**
Atrial fibrillation	2.996	0.711-12.61	0.135
NIHSS on admission	1.018	0.970-1.067	0.470

4. Discussion

In China, within every 4 hypertensive patients, there will be 3 cases with hypercysteinemia^[6]. Previous study suggested that homocysteine might elevate blood pressure and increased the risk of hypertension^[7]. Also, homocysteinemia had interaction with hypertension for stroke risks^[1]. Thus, the terms of H-type hypertension was proposed in 2008^[8,9]. High frequency of H-type hypertension in China is one of important characteristics of Chinese hypertensive population different from other ethnic populations, which should be paid attention. Our hospital-based study showed that more than half of ischemic stroke inpatients in Henan province is with H-type hypertension.

American and European national stroke guidelines have identified hyperhomocysteinemia is an

independent risk factor for stroke in its primary prevention. Identifying stroke patients with H-type hypertension who may be more prone to have a second stroke than others is crucial and may affect the policy of secondary prevention. Our prospective study result indicated weak association of H-type hypertension with stroke recurrence. This result was independent of other risk factors such as age, atrial fibrillation, diabetes, hyperlipidemia and severity on admission. Above result indicated that H-type hypertensive stroke patients might be considered as high risk patients as compared to non H-type hypertensive stroke patients. The present analysis can't give a conclusion of an independent association because OR=1.031, which showed the association strength is weak. The reason for weak association is probably that the sample size is relatively

small and follow-up time is short (only 6 months). However, more H-type hypertension patients had previous stroke history, which is therefore complementary and supports above findings. Our analysis result supports an earlier published study that found a high plasma homocysteine level was associated with history of hypertension and recurrent stroke among patients presenting with acute ischemic stroke [10].

In conclusion, the present study demonstrates a tendency of association of H-type hypertension with recurrent stroke. This might have therapeutic implications for reducing the risk of recurrent stroke. Although the efficacy of stroke prevention by combination of lowering both high plasma homocysteine levels and blood pressure is still unproven, secondary prevention studies are needed. Once such interventions prove efficient, routine detection of plasma homocysteine levels in stroke patients may be advised and appropriate measures taken to prevent recurrent stroke especially for H-type hypertensive stroke patients.

References

- Graham IM, Daly LE, Refsum HM, et al. Plasma homocysteine as a risk factor for vascular disease. The European Concerted Action Project. *JAMA*. 1997; 277(22):1775-1781.
- Hu Dayi, Xu Xiping. Prevention of stroke relies on valid control H-type hypertension. *Chinese Journal of Internal Medicine*. 2008;47(12):976-977.
- Huo Y, Mao G, Venners S, et al. Homocysteine, hypertension and risks of vascular events and stroke: a prospective, nested case-control study. (paper under review).
- Hatano S: Experience from a multicentre stroke register: a preliminary report. *Bull World Health Organ*. 1976;54:541-553.
- Goldstein, LB, Adams, R & Alberts, MJ, et al.; American Heart Association/American Stroke Association Stroke Council; Atherosclerotic Peripheral Vascular Disease Interdisciplinary Working Group; Cardiovascular Nursing Council; Clinical Cardiology Council; Nutrition, Physical Activity, and Metabolism Council; Quality of Care and Outcomes Research Interdisciplinary Working Group; American Academy of Neurology. Primary prevention of ischemic stroke: a guideline from the American Heart Association/American Stroke Association Stroke Council: cosponsored by the Atherosclerotic Peripheral Vascular Disease Interdisciplinary Working Group; Cardiovascular Nursing Council; Clinical Cardiology Council; Nutrition, Physical Activity, and Metabolism Council; and the Quality of Care and Outcomes Research Interdisciplinary Working Group: the American Academy of Neurology affirms the value of this guideline. *Stroke*. 2006;37(6):1583–1633
- Li Jianping , Huo Yong , Liu Ping etc . Effectiveness and safety of lowering blood pressure and homocysteine with Enalapril Maleate and Folic Acid Tablets. *Beijing Da Xue Xue Bao* ,2007;39(6):614-618.
- Lim U; Cassano P A, Homocysteine and blood pressure in the Third National Health and Nutrition Examination Survey,1988-1994. *American Journal of Epidemiology*. 2002;156(12):1105–1113
- European Stroke Organisation (ESO) Executive Committee; ESO Writing Committee. Guidelines for management of ischaemic stroke and transient ischaemic attack 2008. *Cerebrovasc Dis*. 2008;25(5):457-507.
- Goldstein LB, Bushnell CD, Adams RJ, Appel LJ, Braun LT, Chaturvedi S, Creager MA, Culebras A, Eckel RH, Hart RG, Hinchey JA, Howard VJ, Jauch EC, Levine SR, Meschia JF, Moore WS, Nixon JV, Pearson TA; American Heart Association Stroke Council; Council on Cardiovascular Nursing; Council on Epidemiology and Prevention; Council for High Blood Pressure Research; Council on Peripheral Vascular Disease, and Interdisciplinary Council on Quality of Care and Outcomes Research. Guidelines for the primary prevention of stroke: a guideline for healthcare professionals from the American Heart Association/American Stroke Association. *Stroke*. 2011;42(2):517-84.
- Mizrahi EH, Noy S, Selab A, et al. Further evidence of interrelation between homocysteine and hypertension in stroke patients: a cross-sectional study. *Isr Med Assoc*,2003,5:791-794..

6/9/2011

Stent displacement during the Y-stent assisted coil embolization of wide-neck basilar tip aneurysmTan Song¹; Xu Hao-wen²; Song Bo¹, Chandra Avinash¹, Xu Yu-ming¹

1. Department of Neurology, the First Affiliated Hospital of Zhengzhou University, Zhengzhou, Henan 450052, China.

2. Department of Interventional Radiology, the First Affiliated Hospital of Zhengzhou University, Zhengzhou, Henan 450052, China

Co-first author: Xu Hao-wen; Corresponding author: Xu Yu-ming, xuyuming@zzu.edu.cn

Abstract: Y-stent technique has been widely used in the treatment of wide-neck basilar tip aneurysm. Compared to single stent assisted technique, one of the distinguished complications in Y-stent technique is the stent displacement. This is first report about analysis of stent displacement during the Y-stent assisted coil embolization of wide-neck basilar tip aneurysm. Two Cases with wide-neck basilar tip aneurysm were initially planned to introduce Y-stent assisted coil embolization; however, inadvertent migration of stent occurred during the procedure. In one case, the distal portion of the displaced stent migrated into the aneurysm lumen. In another case, the proximal portion of the stent displaced, resulting in a horizontal stent across the aneurysm neck. The two aneurysms were successfully embolized preserving important vessels. These cases highlight the potential tendency of stent displacement during procedure of Y-stent technique of wide-neck basilar tip aneurysm. The former stent seems to displace more easily than the latter stent, and longer length of stent may reduce the incidence of stent displacement.

[Tan Song, Xu Hao-wen, Song Bo, Chandra Avinash, Xu Yu-ming. **Stent displacement during the Y-stent assisted coil embolization of wide-neck basilar tip aneurysm.** Life Science Journal. 2011;8(3):464-466] (ISSN: 1097-8135). <http://www.lifesciencesite.com>.

Key words: Stent; Displacement; Coil; Aneurysm; Wide neck**1. Introduction**

Since bilateral PCA (posterior cerebral artery) and SCA (superior cerebellar artery) usually emanate from the lumen or neck of the basilar tip aneurysm. Single stent, dual microcatheter or balloon remodeling may not prevent coils from prolapsing into the parent artery¹⁻³. However, Y-stent technique may be a good alternative where there is to place two stents from bilateral P1 segments to BA (basilar artery), one stent passing through the interstices of another stent in a Y-configuration. Although there have been several reports of treating wide-neck basilar tip aneurysm with Y-stent technique successfully, nevertheless, the reports of complication of stent displacement are scarce⁴. Below are two cases with a wide-neck basilar tip aneurysm involving the stent displacement during the procedure of Y-stent technique.

2. Typical Patient 1

A 64-year-old man presented with SAH and Hunt-Hess grade II. Cerebral angiography demonstrated a 10×10×12 mm wide-neck basilar tip aneurysm (Fig 1-A). The condition of aneurysm and related vessels caused that Y-stent assisted coil embolization was suitable for the treatment of such aneurysm. Following induction of general anesthesia, a 6 F guide catheter (Envoy; Cordis) was navigated to the right vertebral artery. The patient was heparinized to an activated clotting time of 250 to 300 seconds. A

300 cm, 0.014 inch Transcend Floppy microwire (Boston Scientific) was placed into the left P3 segment and a 3.5 × 20 mm neuroform-3 stent delivery system (Boston Scientific) was positioned across the aneurysm neck through the microwire. The stent was subsequently deployed from left P1 segment back into BA (Fig 1-B). Abciximab was administered intravenously.

However, during the process of pulling back the microwire into the BA tip and then advancing the microwire into the right PCA through the interstices of the stent, the distal portion of stent migrated into the aneurysm lumen. No contrast was observed to leak from the aneurysm (Fig 1-C). The aneurysm was embolized with single stent assisted technique. An Excelsior 10 microcatheter was advanced into the dome of the aneurysm, and coil embolization proceeded in the usual fashion (Matrix 2, 360; Boston Scientific) (Fig1-D), however, the left side of the neck could not be packed tightly without coil loops herniation into the parent artery. Y-stent technique was reconsidered. Using the above method, a 4.0×20 mm neuroform 3 stent delivery system was placed through interstices of the first stent from left P1 segment to BA and then deployed, no stent displacement occurred. A so-called “Y” configuration was thus established (Fig1-E). Coil embolization proceeded in the usual fashion. Complete obliteration of the aneurysm cavity was

obtained without any compromise of distal flow (Fig1-F). The patient recovered completely.

Patient 1

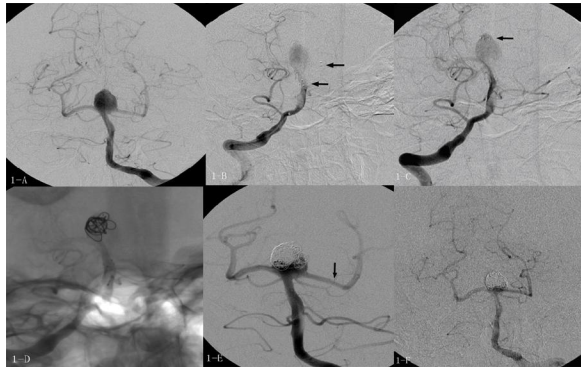


Fig 1-A. The wide-neck basilar tip large aneurysm with bilateral PCA involved; Fig 1-B. The neuroform stent was deployed from left P1 segment to BA; Fig 1-C. The distal portion of the stent migrated into the aneurysm; Fig 1-D. With single stent assisted technique; the coil was placed into the aneurysm lumen, the left portion of the aneurysm neck remained Fig 1-E, F. With Y- stent assisted technique, the aneurysm was embolized successfully and important vessels were preserved.

3. Typical Patient 2

A 29-year-old man presented with SAH and Hunt-Hess grade III. Cerebral CT showed subarachnoid hemorrhage in suprasellar cistern and cisterna ambiens. Cerebral angiography demonstrated a giant basilar tip aneurysm with wide neck ($17 \times 20 \times 20$ mm), bilateral PCA and SCA emanating directly from the dome and neck of the aneurysm (Fig 2-A, B). The Y- stent technique should be a good alternative.

Using the above method, a 300 cm, 0.014 inch microwire was placed into the right P3 segment, and then a 4×30 mm neuroform-3 stent delivery system was advanced over the wire into the proximal portion of right PCA, and then deployed the stent so as to bridge from right P1 segment to BA. However, the proximal portion of the stent jumped into the aneurysm when the microwire was pulling back into the BA. The displaced stent horizontally bestrode the aneurysm from right P1 segment to the ostium of left P1 segment and SCA. No contrast was observed to leak from the aneurysmal wall and abciximab was administered intravenously. A microcatheter was advanced into the dome of the aneurysm through the interstices of the stent. The aneurysm was embolized with 12 coils (microvention and cordis) without the coil being herniated into the parent artery (Fig 2-C). The angiogram showed excellent occlusion the lumen

of aneurysm and no branch occlusion was seen (Fig 2-D). The patient recovered in good condition.

Patient 2

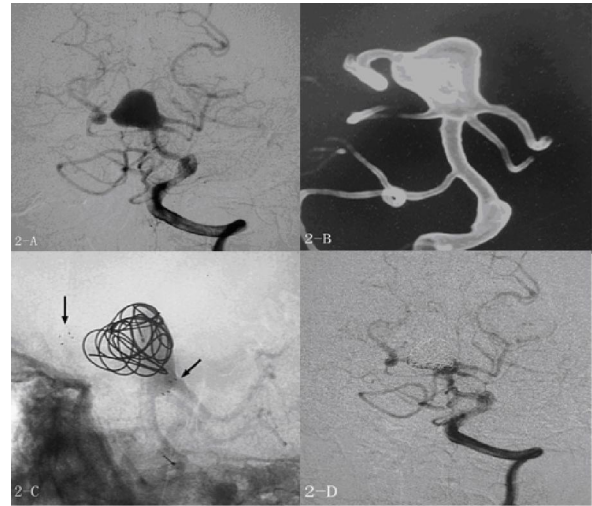


Fig 2-A. The basilar tip aneurysm with wide neck involving the bilateral PCA and SCA; Fig 2-B. 3D reconstruction showed the both P1 segments encroached into the aneurysm neck and SCA emanating directly from the base of the aneurysm; Fig 2-C. The proximal portion of the stent migrated into the aneurysm covered the ostium of the left PCA and SCA; Fig 2-D. After embolization with horizontal stent placement plus coiling, the aneurysm was occluded completely by coils with good flow in end branches;

4. Discussion

One potential complication of the “Y” configuration is stent displacement. Thorell et al described seven patients with wide neck basilar tip aneurysms treated with Y-stent assisted coil embolization. They found insignificant stent displacement occurred in all cases, displacement was always in the cephalad direction pertaining to the BA and laterally within the P1 segment, which did not interfere the effect of Y stent⁴.

The two cases demonstrated that either the distal or proximal portion of the stent could displace into the aneurysm. It's important to note that both stent displacements occurred during the process of pulling back the microwire from PCA, which is similar to the report of Broadbent et al who described two cases of stent malposition within internal carotid artery large aneurysms⁵. The manufacturers recommend that the length of neuroform stent should extend 4 mm proximal and distal to the aneurysm neck respectively to achieve reliable stent stability. We consider that the stent may need more “secure length” on condition that the stent bridge artery

bifurcation, which demand enough friction force to stabilize the stent.

When the stent bridging from PCA to BA, it could generate a certain longitudinal rebounding force which probably cause the stent displacement under outside factors, such as microwire, microcatheter or another stent. In the first cases, the length of first stent was 20 mm which exceeded more than 4 mm length on both ends of the aneurysm. When the microwire were pulling back into BA, the distal portion of the stent migrated into the aneurysm. In the second case, the neck of aneurysm was so wide that the proximal portion of the stent had not enough secure length (we used a 30 mm length stent that is the currently maximal length) which generated inadequate frictional force, therefore, the stability of the stent decreased. Under the circumstances, longer length of stent may be an alternative because it can increase the stability of the stent

5. Conclusion

These cases highlight the potential tendency of stent displacement during procedure of Y-stent technique of wide-neck basilar tip aneurysm, the former stent seems to displace more easily than the latter stent, and longer length of stent may reduce the incidence of stent displacement.

06/09/2011

References

1. Perez-Arjona E, Fessler RD. Basilar artery to bilateral posterior cerebral artery 'Y stenting' for endovascular reconstruction of wide-necked basilar apex aneurysms: report of three cases. *Neurological research*. 2004; 26(3):276–281
2. Andrew Lozen, Sunil Manjila, Richard Rhiew, Richard Fessler. Y-stent-assisted coil embolization for the management of unruptured cerebral aneurysms: report of six cases. *Acta Neurochir*. 2009; 151:1663–1672
3. Chow M, Woo HH, Massaryk TJ, Rasmussen PA. Endovascular treatment of a wide-necked basilar apex aneurysm using a Y-configuration double stent technique. *Am J Neuroradiology*. 2004; 25:509–512
4. Thorell WE, Chow M, Woo HH, Masaryk TJ, Rasmussen PA. Y-configured dual intracranial stent-assisted coil embolization for the treatment of wide-necked basilar tip aneurysms. *Neurosurgery*. 2005; 56:1035–1040
5. Broadbent LP, Moran CJ, Cross DT 3rd, Derdeyn CP. Management of neuroform stent dislodgement and misplacement. *Am J Neuroradiology*. 2003; 24:1819–1822
6. Castriota F, Martins EC, Dall Olmo CA, Molnar RG, Manetti R, Liso A, Oshoala K, Furgieri A, Ricci E, Cremonesi A. Stent migration as a late complication following carotid angioplasty and stenting. *Eurointervention*. 2008; 4:397-404

The Health Status and Its Influence Factors of Stroke Patients in Community of Zhengzhou, 2010

Zhang Zhenxiang, Liu Lamei, Lin Beilei, Zhang Yaqi, Xie Junfang, Mei Yongxia, Zhang Weihong

The Nursing College of Zhengzhou University, Zhengzhou, 450052, China.

Zhangzx6666@126.com

[Abstract] Objective Learning about the health status and analyzing its influence factors of stroke patients in communities, to improve the health level of the patients. **Methods** Choosing 177 cases of stroke patients as the study objects from communities of Zhongyuan, Erqi, Jinshui, in Zhengzhou. Using the brief questionnaire of SF-36 to investigate the health status of the patients. **Results** Health status scores of the 177 cases of patients are lower than normal people. Each dimension score of the forty to sixty years old patients is lower than normal people, except the social function dimension. Every dimension score of the male stroke patients that sixty or above sixty years old is lower significantly than the normal people. This is the same to female patients except body pain, energy, social function and mental health. The factors that influencing the health status of stroke patients are working situation, medical insurance, types of diagnose, frequency of incidence and duration of illness. **Conclusions** There is varying degrees of decline of the health status of stroke patients in communities comparing with normal people. And its influence factors are various. So the suggest is that the health of stroke patients should be taken seriously and carrying out corresponding rehabilitation nursing service to improve the patients' health level.

[Zhang Zhenxiang, Liu Lamei, Lin Beilei, Zhang Yaqi, Xie Junfang, Mei Yongxia, Zhang Weihong. **The Health Status and Its Influence Factors of Stroke Patients in Community of Zhengzhou, 2010**. Life Science Journal. 2011;8(3):477-481] (ISSN: 1097-8135). <http://www.lifesciencesite.com>.

Key words: Stroke; Health status; Factors

Stroke, namely apoplexy in other words, is a common intractable disease that seriously harms human health and life safety, with high incidence, mortality, morbidity, and recurrence rate, etc. According to statistics, the number of stroke happening every year in China is up to 2 million and now the existing stroke patients are 7 million, in which 4.5 million patients have different degrees of labor losing and self-care obstacle, the rate of disability is up to 75%^[1]. Its high rate of disability seriously affect of patients' physical and mental health and the quality of life. In view of this, in order to learning about the health status of stroke patients in communities of Zhengzhou, we did a follow-up survey to 177 cases of stroke patients in Zhengzhou from July to September, 2010, which help to understand the patient's health status and its influencing factors, and to provide the corresponding help and guidance and to improve their health level and quality of life.

1 Objects and methods

1.1 Objects

According to the level of economic development of Zhengzhou and the actual situation in this study, we adopt the convenient sampling method to select stroke patients in convalescence from communities of Zhongyuan, Erqi, Jinshui in Zhengzhou as the objects of the survey. There are inclusion criteria as follows: ① up to the diagnostic criteria of stroke that established in Fourth National Cerebrovascular

Disease Conference in 1995, and confirmed by CT or MRI; ② patients with clear consciousness, no intelligence obstacle and aphasia, can understand and voluntarily complete all evaluations.

1.2 Methods

1.2.1 Contents

General information of patients, health status and daily living conditions were included in the contents.

1.2.2 Instruments

The brief health status questionnaire SF-36 was used to investigate the stroke patients in community. Liu Chaojie and other researchers' researches^[2] shows that, SF-36 has a good reliability, validity and applicability in the population of our country, and it can be used to evaluate the health status of different populations. SF-36 roundly learning about the health status of respondents from eight dimensions that are physical function (PF), response of physical (RP), body pain (BP), general health (GH), vitality (VT), social function (SF), response of emotion (RE) and mental health (MH). There are 36 questions in all; each question is endowed scores from 0 to 6 according to alternative answers, the higher the scores, the better the health status. In order to be convenient, the eight dimensions of SF-36 were father classified into physical comment summary (PCS) and physical comment summary (PCS)^[3] at the time of analyzing the influence factors of affecting health status. And the

physical comment summary summed from PF, BP and GH, the health comment summary summed from VT, SF, RE, and MH.

The Activity of Daily Living Scale (ADL) was used to evaluate the activity situation of daily living. This scale is consist of ten items, including eating, transferring between bed and chair, embellishing, toileting, bathing, walking on flat, up and down stairs, dressing, bowel and bladder controlling. According to patients whether need help or not and the degree of help, it divides each entry into 0, 5, 10, 15 four ranks, the total score is 100 points. Patients that Score 100 points are divided into completely independent, 75 to 95 points are divided into mild dependence, 50 to 70 points are moderate dependence, 25 to 45 points are divided into severe dependence, and 0 to 20 points are divided into completely dependent.

1.2.3 Methods of data collection

The investigation team is made up of researchers, undergraduate students of nursing department and community nursing staff. All members sent questionnaires in home after a uniform training, explained the precautions of filling in, and recovered the questionnaires that completed on the spot. The survey distributes questionnaires 200 copies in total, and taking back effective questionnaires 177 copies, the effective reclaimed rate is 88.5%.

1.2.4 Statistical Methods

Adopting SPSS13.0 statistical software to process the data. Using mean \pm standard deviation to describe the measurement data. Describing constituent ratio by percentage. Comparing the differences between stroke patients and the normal by t test. Analyzing the influence factors of patients' health status by using multielement regression analysis.

2 Conclusion

2.1 The general information of the patients

In the 177 cases of stroke patients, there are 109 male cases (61.1%), 68 female cases (38.4%); aging from 36 to 87 (67.3 ± 10.8), one case of below 40 years (0.6%), 45 cases of 40 to 60 years old (25.5%), 131 cases of above 60 (73.9%); 21 cases of following primary education (19.9%), 23 cases of primary education (13.0%), 51 cases of high school or technical school education (28.8%), 23 cases of junior school education (13.3%); 158 cases of married (89.3%), one case of divorced (0.6%), 18 cases of widowed; 148 cases of retirement or rest for sick

(83.6%), 18 cases of no fixed profession (10.2%), 6 cases of workers (3.4%), 5 cases of resign (2.8%). There are 47 cases whose income is less than 1000 Yuan (26.6%), 92 cases of 1000 to 1999 Yuan (52.0%), 16 cases of 2000 to 2999 Yuan (9.0%), 22 cases of above 3000 Yuan (12.4%); 12 cases of self-pay (6.8%), 140 cases of having medical insurance (79.1%), and 25 cases else (14.2%), 19 cases of cerebral hemorrhage (10.7%), 92 cases of cerebral infarction (52.0%), 42 cases of cerebral embolism (23.7%), and 24 cases else (13.6%); 108 cases of stroke once (61.0%), 41 cases of twice (23.2%), 12 cases of third (6.8%), 16 cases of more times (9.0%); 51 cases of suffering for illness less than one year (28.8%), 16 cases of suffering for one to two years (9.0%), 14 cases of suffering for two to three years (7.9%), 96 cases of suffering for more than three years (54.4%).

2.2 The health status of patients

Thinking the proximity of geographical and the comparability of data, we adopt the reference value of people's health status that educed by Shi Ping and others people^[4] that surveyed 930 cases of general population by using SF- 36 in the city of Wuxi. And we use T-test to compare the different ages of stroke patients with the corresponding standard norm in Wuxi to learn about the health status of stroke patients. The resultss are shown in Table 1.

It can be seen from table 1: stroke patients scored lower than normal people in each dimension. Each dimension score of the forty to sixty years old patients is lower than normal people except social function dimension; every score is lower for male patients above sixty years old, as same as female except body pain, energy, social function and mental health.

2.3 Patients' activity of daily living

63 cases (35.6%) scored 100 in ADL of all 177 patients, displayed complete independence in daily life, the rest 144 cases (64.4%) scored below 95 in ADL, displayed incomplete independence, part or all need help in daily life.

2.4 Influence factors of patients' health status

Take the patients' general information such as gender, age, marital status as the independent variables, and the total score of patient's health as the dependent variables. Analyze the influence factors of patients' health status by using multielement regression analysis. The results are shown in Table 2.

Table 1 the health status of stroke patients in different ages

Age	SF-36	Male ($\bar{x} \pm s$)		t value	P value	Female ($\bar{x} \pm s$)		t value	P value
		Patients	Norm			Patients	Norm		
40~60	PF	51.5±35.8	86.1±10.2	-7.3	0.00 ²⁾	51.4±34.8	81.9±13.9	-6.9	0.00 ²⁾
	RP	35.8±42.1	84.7±30.1	-11.4	0.00 ²⁾	34.5±42.9	81.0±33.5	-8.6	0.00 ²⁾
	BP	71.4±20.7	85.5±12.9	-6.9	0.00 ²⁾	67.9±20.4	77.0±16.7	-3.6	0.002)
	GH	51.8±14.4	61.9±20.5	-7.0	0.00 ²⁾	50.7±12.5	64.6±20.5	-8.9	0.002)
	VT	59.3±23.2	64.9±17.9	-2.4	0.02 ¹⁾	59.1±23.9	68.9±15.6	-3.3	0.002)
	SF	74.8±33.1	81.4±20.9	-2.0	0.05	76.7±32.2	79.2±20.2	-0.7	0.54
	RE	51.3±45.5	83.3±30.9	-7.0	0.00 ²⁾	50.0±44.8	83.3±33.1	-5.9	0.002)
	MH	65.1±20.9	70.0±16.7	-2.3	0.02 ¹⁾	65.0±18.9	72.5±16.0	-3.2	0.002)
	PF	49.3±35.5	83.7±10.5	-8.1	0.00 ²⁾	47.3±34.0	79.1±15.4	-6.6	0.002)
≥60	RP	37.9±41.7	82.4±29.9	-8.7	0.00 ²⁾	39.5±44.6	59.0±46.1	-3.1	0.002)
	BP	69.9±22.4	82.5±17.9	-4.7	0.00 ²⁾	66.3±20.9	69.4±21.8	-1.1	0.29
	GH	41.1±11.8	67.8±16.4	-18.8	0.00 ²⁾	40.3±10.1	62.8±18.2	-16.0	0.002)
	VT	58.4±23.1	75.2±16.4	-6.0	0.00 ²⁾	60.1±24.6	66.8±15.7	-2.0	0.06
	SF	74.5±33.1	83.3±21.1	-2.2	0.03 ¹⁾	76.4±34.0	78.5±21.6	-0.4	0.66
	RE	54.6±45.4	83.3±33.1	-5.3	0.00 ²⁾	55.1±44.7	77.3±35.6	-3.6	0.002)
	MH	65.4±22.2	78.8±16.9	-5.0	0.002)	66.2±18.4	70.8±17.6	-1.8	0.08

Note: PF: physical function, RP: response of physical, BP: body pain, GH: general health, VT: vitality, SF: social function, RE: response of emotion, MH: mental health; 1) P<0.05, 2) P<0.01

Table 2 Multielement regression analysis of the total scores of patients' health status

Items	Influence factors	Standard regression coefficient	t value	P value
Scores of health status	Constant term		1.424	0.169
	Current work situation (retired or in sick)	-0.783	-2.314	0.031 ¹⁾
	Medical insurance (yes)	0.572	2.334	0.030 ¹⁾
	Diagnosis of type (cerebral infarction)	0.965	2.414	0.025 ¹⁾
	Diagnosis of type (cerebral embolism)	0.972	2.591	0.017 ¹⁾
	Times of sick	-0.494	-2.475	0.022 ¹⁾
	Constant term		1.371	0.184
	Concomitant diseases(no) regularly rehabilitation therapy(no)	0.487	2.723	0.012 ¹⁾
Health status	Current work situation (retired or in sick)	-0.485	-2.793	0.011 ¹⁾
	Current work situation (retired or in sick)	-0.854	-2.901	0.008 ²⁾
	Medical insurance (yes)	0.488	2.226	0.037 ¹⁾
	Years of suffering	-0.465	-2.769	0.011 ¹⁾
Status of mental health	Scores of ADL	0.699	3.694	0.001 ²⁾
	Constant term		0.729	0.475
	Diagnosis of type (cerebral infarction)	1.109	2.877	0.008 ²⁾
	Diagnosis of type (cerebral embolism)	1.037	2.786	0.010 ¹⁾

Note:1) P<0.05, 2) P<0.01

3 Discussions

As our population ages, the morbidity of stroke has also increased, and the mortality of stroke decreased. With the advances in medical technology,

but the disabled survivors has increased year by year. Physical disability and dysfunction caused by stroke severely limit patient's participation in work and daily activities, and bring larger impact to their physical and

mental health. Studies^[5] have shown that health status of stroke patients was significantly lower than the normal population at the same age, particularly in physiological function and mental health, which is similar to the results of this study. Through investigating the 177 cases of stroke patients in communities, the results of the study show that there are slightly differences of stroke patients in different age, sex health status, but the dimensions of their health status scores are lower than the normal population in general. Each dimension score of the forty to sixty years old patients is lower than normal people except social function dimension; and compared with the normal at the same age, every score is lower for male patients above sixty years old; this is the same to female patients except body pain, energy, social function and mental health. The results suggest that the health status of stroke patients that 40 to 60 years old is worse, which may relate to the characteristics of this age groups. People of 40 to 60 years old are in middle age, and have reached the stage of full maturity. On the one hand, they have the sound and perfect physical function; on the other hand, their body has well-adapted to environment. So they can complete variety of role tasks and they are the mainstays of the family and society. If there is a stroke, it not only can decrease the patient's physical and mental health, but also can bring a great influence to the family and society. Men's health conditions were significantly lower than the normal population of crowd aged 60 and over, and women scores is lower in physical pain, energy, social functioning and mental health, but there is no statistical significant, which suggests that the influence of stroke is greater on the health status of male patients. This may relate to the different social roles that both undertook. In China's traditional cultural values, man takes charge of external matters and woman takes charge of the internal. Compared with women, men bear greater pressures of family and social, and thus the impact of stroke is relatively large.

The results of multielement regression analysis reveal that many factors impacted the health status of stroke patients, including current work situation, medical assurance, types of disease, times of sick, whether merging other diseases or not, ect. Among them, the current work situation (retired or rest for sick) was negatively correlated with the physical health status and the overall health of patients, namely the physical health status and the overall health of patients of retired or rest for sick are worse than the patients that still working. This may relate to the age and severity of the disease of patients. Patients that retired or rest for sick is elder or couldn't continue to engage in heavy work because of disease, while patients that still working haven't reached retirement

age, and could continue to work currently, which indicates that their physical condition is better. Whether having medical insurance or no has a significant effect on overall health and physical health, the status is better of patients with insurance. Researches^[6] shows that the medical costs of stroke is growing fastest in all chronic diseases, in China, the medical expenses of cerebrovascular disease are as much as \$ 25 billion each year, the huge financial burden restrains some patients to receive continuous treatment and rehabilitative care. Compared with self-paid patients, having medical insurance makes the economic burden lighter, the patients could accept more health care services, and their health status will be relatively good. Types of disease significantly affect the overall health and mental health of patients, which might because the severity of the symptoms that different types of diseases exists certain differences. In addition, the times of sick, whether merging other disease, years of suffering, and scores of ADL also have a significant effect on overall health and physical health of patients, patients with more times in sick, suffering longer, having concomitant diseases and scored high in ADL are in worse status.

After all, we find that the health status of stroke patients have different degrees of decline compared with the normal at the same age through investigating the 177 cases of patients in communities. And current work situation, medical insurance, types of disease, the times of sick, etc, have different degrees of impact on the health status of patients. So, suggest communities should pay attention to the health of stroke patients, take rehabilitation care and appropriate measures to improve the patients' health and quality of life, according to their health status and its influence factors.

Acknowledgements:

The authors would like to acknowledge the work of teacher in the Nursing College of Zhengzhou University who were involved in the collection of the original data.

Corresponding Author:

Dr. Zhang Weihong The Nursing College of Zhengzhou University Zhengzhou, 450052, China.
E-mail: zwhong306@zzu.edu.cn

References

- [1] Baidupedi . Stroke [EB/OL]. <http://baike.baidu.com/view/122124.htm.2010.12.25>.
- [2] Liu Chaojie, Li Ningxiu, Ren Xiaohui. Applicability study of 36 Short Form scale in Chinese population [J]. Huaxi Yida Science, 2001,32(1):43-47.
- [3] Li Chunbo, HeYanling. Introduction of the health

status questionnaire SF-36. *International Journal of Psychiatry*, 2002, 29(2):116-119.

[4] Shi Ping, Qian Yun, Xu Ming. Quality evaluation of life and its influencing factors analysis among the general population in Wuxi [J]. *Chinese Primary Health Care*, 2007,21(6):14-17.

[5] Zhang Meixia, Zhang Ruying, Zhang Meirong, etc.

Multi-center study of the quality of life of stroke patients [J]. *Nursing Research*, 2004, 18(1):37-38.

[6] Liu Yahong, Xu Gelin. Research progress of the influence factors of affecting stroke patients' economic burden and the countermeasures [J]. *Journal of Modern Nursing*, 2009,15(15):1498-1500.

8/16/2011

Families of maps Singularities and its Gauss maps

M. A. Soliman¹, Nassar. H. Abdel-All¹, Soad. A. Hassan¹ and E. Dahi²

¹ Department of Mathematics, Faculty of Science, Assiut University, Assiut 71516, Egypt

² Department of Mathematics, Faculty of Science, Al-Azhar University, Assiut 71524, Egypt
saodali@ymail.com

Abstract: This paper mainly studies the Singularities of smooth mapping. The singularities of the families of Gauss maps corresponding to the family of mappings are studied and the shape of these families and their singularities using mathematica program are illustrated and plotted.

[M. A. Soliman, Nassar. H. Abdel-All, Soad. A. Hassan and E. Dahi. **Families of maps Singularities and its Gauss maps**. Life Science Journal. 2011;8(3):482-487] (ISSN: 1097-8135). <http://www.lifesciencesite.com>.

Keywords: extrinsic differential geometry, Families of Maps, Gauss map, theory of singularities.

1. Families of Maps (Scaler Function)

Let

$$z = f(u^1, \dots, u^n, a^1, \dots, a^r)$$

be the family of r parameter of hypersurface in \mathbb{R}^n .

Where $u^\alpha \in U \subset \mathbb{R}^{n+1}$, $a = a^r \subset \mathbb{R}^r$, the vector a is a vector of control parameter.

The discriminate set of these families can be calculate by the solution of these (n) equations

$$p^\alpha = 0 \text{ such that } p^\alpha = \frac{\partial z}{\partial u^\alpha} \text{ and finding } u^\alpha \text{ 's as}$$

function in a^r say $u^\alpha = u^\alpha(a^\alpha)$ and substitution in the relation $f = 0$ we obtain the discriminate set for the considered formal as in the following form

$$\Delta = f(a^1, \dots, a^r) = 0$$

By changing the control parameters we find some singular points for the family which can be classified according to the famous theorems in singularity theory. Using the Hessian matrix we can obtain the singular points and singular set. Geometrically these singularities can be plotted but the classification of them can't be a valuable for all points. Using the terminology of level set which tell us the type of singular points like folds (level sets is start line), cusp (level set is semicubical parabola). In general there is no existence of some famous types.

Remark 1 For the simple ideas for finding and calculated singular points and singular sets see [1, 2, 3].

Definition 1 [1] The level set attached to the hypersurface M is defined as the following: let $u_n = Z(u_1, u_2, \dots, u_{n-1}) = c$, c is constant, if $c = 0$ that given the level set $V_0 = \{(u_1, u_2, \dots, u_{n-1}): u_n = 0\}$ and the other level sets are

$$V_c = \{(u_1, u_2, \dots, u_{n-1}): u_n = 0\}, \quad c \neq 0$$

Another version of the definition of level sets is contours as given in the following

Definition 3 We say the point p on a surface M with a parametric representation is a contour point if and only if $N \cdot pc = 0$

where N is the normal vector field on the surface M and c is the view point. The contour line or contour, for short, of a surface is the set of all its contour points.

The determination of the contour line of a surface in the general case involves a numerical method to find the zeros of a real-valued function of n real variables in a domain $(u^1, u^2, \dots, u^n) \in U$. An algorithm and its implementation can be found in [6].

2. Application

Let us consider a 3-parameter family of surfaces defined by mong's form as the following:

$$Z = f(u, v; a, b, c) = au^4 + bu^2v + u^2 + cv^2, \quad a, b, c \in \mathbb{R} \quad (1)$$

This family is denoted by σ , where a, b, c are the parameters of the family σ . The bifurcation diagram of the zeroes of this family (of functions of $u; v$ depending on the parameters (a, b, c) is given from:

$$\Delta = c = 0 \quad (2)$$

where Δ is the discriminant set and it is a plan.

Remark 4 The family of contours is given from $z = k$ (constant), and the family of zero level set corresponding to $k = 0$ are given through the figurers [1, 2, 3].

The families (1) are classified into serval subclasses as the following:

- 1) $a = b = c = 0$, in this case the family f has A_1 singularity (fold).
- 2) $b = c = 0$, $a < 0$ then f has a singularity (cusp).
- 3) $b = c = 0$, $a > 0$ in this case the family f has A_1 singularity (fold).
- 4) $a = c = 0$, $b < 0$ or $b > 0$ in this case the family f has a fold.
- 5) $a = b = 0$, $c < 0$ or $c > 0$ in this case the family f has $\pm B_2$ singularity (the normal form of this set is $B_k = x^k + y^2; k \geq 2$).
- 6) $a; b; c > 0$, $a; b; c < 0$.
- 7) $a = 0, b < 0; c < 0$.

- 8) $a = 0, b > 0; c > 0.$
- 9) $a = 0, b < 0; c > 0.$
- 10) $a = 0, b > 0; c < 0.$
- 11) $b = 0, a < 0; c < 0.$
- 12) $b = 0, a > 0; c > 0.$
- 13) $b = 0, a < 0; c > 0.$
- 14) $b = 0, a > 0; c < 0.$
- 15) $c = 0, a < 0; b < 0.$
- 16) $c = 0, a > 0; b > 0.$
- 17) $c = 0, a < 0; b > 0.$
- 18) $c = 0, a > 0; b < 0.$

The previous families are plotted by $\sigma_i, i = 1, 2, \dots, 18$ which corresponding to the conditions (1), 2),..., 18)) and their geometric interpretations are given through the figures [4]- [16].

we denote the previous families by $\sigma_i, i = 1, 2, \dots, 18$ which corresponding to the codomain (1), 2),..., 18)).

The normal vector field to the family of surfaces (1), is given by:

$$N(u, v; a, b, c) = \{-2(u+2au^3+bu^2v), -(bu^2+2cv), 1\} \quad (3)$$

For the subfamily σ_i , it is easy to see that the normal vector fields has a planer swallowtail when $a, b, c > 0$ or $a, b, c < 0$ as shown in figure (17).

Since the family (3) of function lies in the plane $z = 1$, so we can make a modification to the families $(N(u, v; a, b, c))$ as in the following:

$$N_{mod}(u, v; a, b, c) = \{-2(u+2au^3+bu^2v), -(bu^2+2cv)\} \quad (4)$$

The singularities of this family can be deferral using the rank of its Jacobian matrix which is given by:

$$\begin{pmatrix} -2(1+6au^2+bu^2) & -2bu \\ -2bu & -2c \end{pmatrix} \quad (5)$$

so the discriminant set(singular set) is given as:

$$S := 4c-4b^2u^2+24acu^2+4bcv = 0 \quad (6)$$

From which we have :

$$S := u^2 = \frac{bc}{b^2 - 6ac} \left(v + \frac{1}{b} \right), \quad b^2 \neq 6ac, b \neq 0 \quad (7)$$

This relation represents a parabola in the plan u, v with $\left(0, -\frac{1}{b} \right)$, i. e, is non defined for all

points lies on the hyperbolic paraboloid. Thus the image of singular set under the modified normal vector field N is

$$N_{mod}(S) = \left\{ -\frac{2(b^2 - 4ac)}{c}u^3, \frac{2c}{b} - \frac{3(b^2 - 4ac)}{b}u^2 \right\} \quad (8)$$

It is easy to see that the normal vector field of the family has a cusp point for all points except for the points lies on the hyperbolic paraboloid $b^2 - 4ac = 0$ with conditions $b; c \neq 0$ see figures (18). The shapes of discriminate set, zero level sets, for the family subclasses σ_i of the given family and the normal vector field for the subclasses σ_i and singular point are shown in fig [1] to [18].

3. Gauss and Mean Curvature

The notion of curvature of a surface is a great deal complicated than the notion of curvature of a curve. Let α be a curve in R^3 . and let p be a point in on the trace of α . The curvature of α at p measures the rate at which α leaves the tangent line to α at p . By analogy. the curvature of a surface $M \subset R^3$ at $p \in M$ should measure the rate at which M leaves the tangent plane to M at p . But for surface a difficulty arises that was not present for curves: although a curve can separate from one of its tangent lines in only two direction. a surface separates from one of its tangent planes in infinitely many directions. In general the rate of departure of a surface from one of its tangent planes depends on the direction.

It is usually possible to glance at almost any surface and recognize which points are elliptic, hyperbolic, parabolic or planer. at the planer points we find the Gauss curvature achieves to maximum value at thats points and mean curvature is planer. I. e Gauss curvature and mean curvature have a relation with elliptic, hyperbolic, parabolic and planer points.

Now we calculate the Gauss curvature and mean curvature of that family of functions. The shapes of Gauss curvature and mean curvature and their contour are plotted to show the singularities of these families.

The first fundamental coefficients of the family under consideration are given as:

$$G_{11} = 1 + 4(u+2au^3+bu^2v)^2, \quad G_{22} = 1 + (bu^2+2cv)^2 \quad \text{and} \quad G_{12} = 2(bu^2+2cv)(u+2au^3+bu^2v)$$

and its discriminant (metric) is given by:

$$G = 1 + 16a^2u^6 + 4c^2v^2 + u^4(b^2 + 16a(1 + bv)) + 4u^2(1 + bv(2 + c + bv))$$

The second fundamental coefficients L_{ij} of this family are:

$$L_{11} = 2(1+6au^2+bu^2)Q, \quad L_{22} = 2cQ, \quad L_{12} = 2buQ \quad (9)$$

Where $Q = \sqrt{1 + (bu^2 + 2cv)^2 + 4(u + 2au^3 + bu^2v)^2}$

and the discriminant $L = \det(L_{ij})$ is given by

$$L = 4(c-b^2u^2+6acu^2+bcv)Q \quad (10)$$

From above equations and by simple calculation we obtain the Gauss and mean curvatures as the following:

$$K = \frac{4(c-b^2u^2+6acu^2+bcv)}{(1+16a^2u^6+4c^2v^2+u^4(b^2+16a(1+bv))+4u^2(1+bv(2+c+bv)))^2} \quad (11)$$

$$H = ((1+6au^2+4c^2v^2(1+6au^2+bu^2)+b(v-bu^4(3+2au^2+3bv)))$$

$$\frac{+c(1 + 4u^2((1 + 2au^2)^2 + b(1 + 6au^2)v))}{(1 + (bu^2 + 2cv)^2 + 4(u + 2au^3 + buv)^2)^{3/2}}$$

respectively.

From (11) its easy to see that $K = 0$ when $u; v$ lie on the parabola equation:

$$u^2 = \frac{bc}{b^2 - 6ac} \left(v + \frac{1}{b} \right)$$

i. e., $K = 0$ when $u; v$ lie on the singular set (6). Finally the shapes of Gauss Curvature and Mean Curvature and its contours corresponding some σ_i are plotted in figure [19] - [29].

Figures

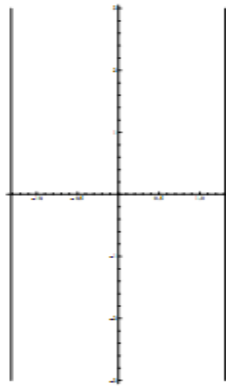


Figure 1: zero level set $b = c = 0, a < 0$

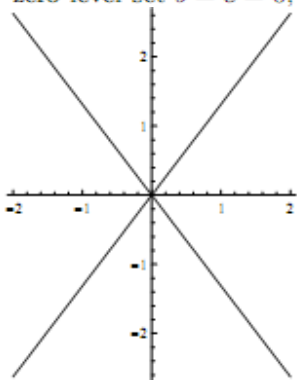


Figure 2: zero level set $a = b = 0, c < 0$

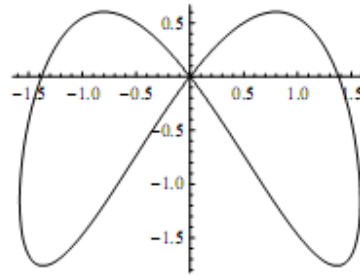


Figure 3: zero level set $a, b, c < 0$

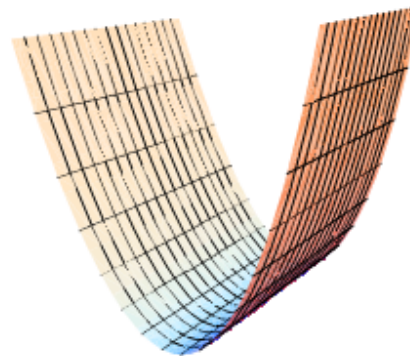


Figure 4: $\sigma_1 : a = b = c = 0$ (fold)

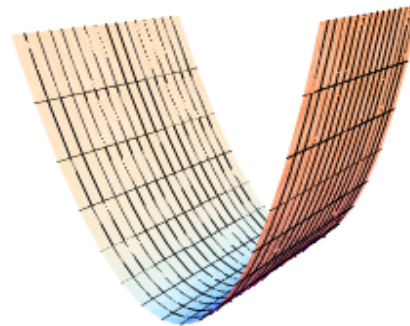


Figure 4: $\sigma_1 : a = b = c = 0$ (fold)

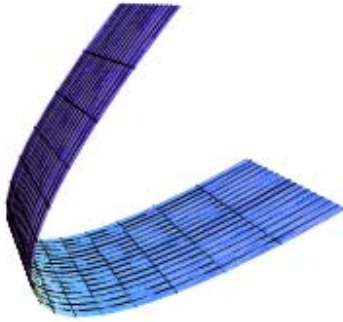


Figure 6: $\sigma_3 : b = c = 0, a > 0$

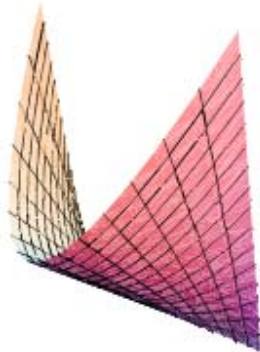


Figure 7: $\sigma_4 : a = c = 0, b < 0$

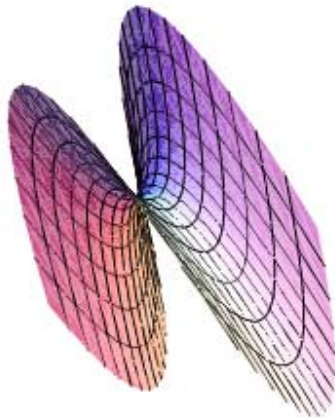


Figure 8: $\sigma_5 : a = b = 0, c < 0$



Figure 9: $\sigma_5 : a = b = 0, c > 0$



Figure 10: $\sigma_6 : a, b, c, > 0$ or $a, b, c, < 0$

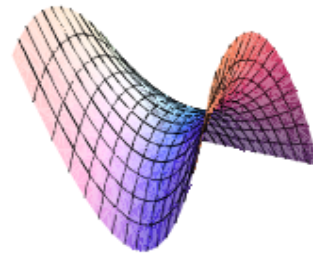


Figure 11: $\sigma_7 : a = 0, b < 0, c < 0$

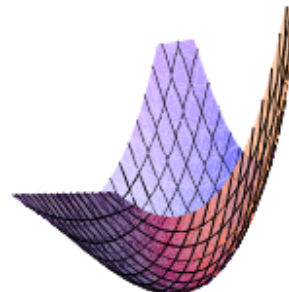


Figure 12: $\sigma_8 : a = 0, b > 0, c > 0, \sigma_9 : a = 0, b < 0, c > 0$

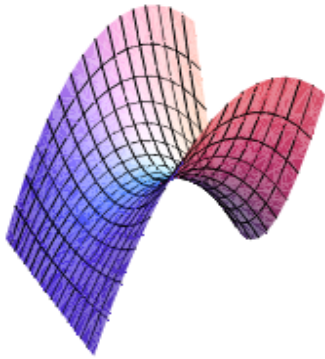


Figure 13: $\sigma_{10} : a = 0, b > 0, c < 0, \sigma_{14} : b = 0, a > 0, c < 0, \sigma_{18} : c = 0, a > 0, b < 0$

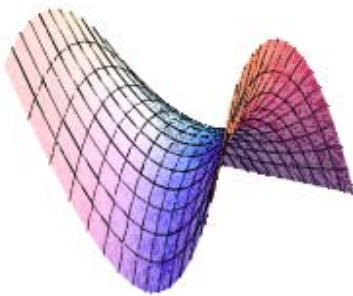


Figure 14: $\sigma_{11} : b = 0, a < 0, c < 0, \sigma_{15} : c = 0, a < 0, b < 0$

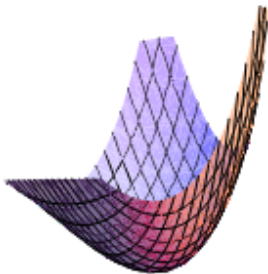


Figure 15: $\sigma_{12} : b = 0, a > 0, c > 0, \sigma_{16} : c = 0, a > 0, b > 0$



Figure 16: $\sigma_{13} : b = 0, a < 0, c > 0, \sigma_{17} : c = 0, a < 0, b > 0$

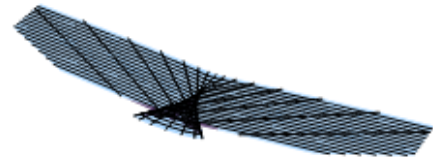


Figure 17: normal vector field when $a, b, c > 0$

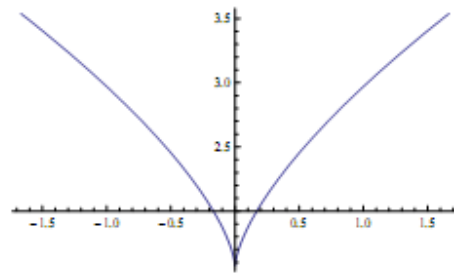


Figure 18: singular set under the N_{mod}

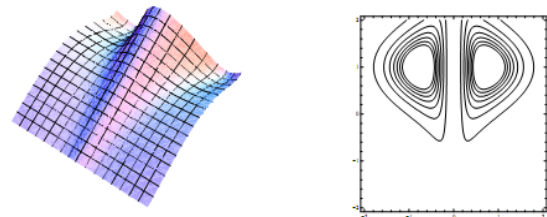


Figure 19: Gauss curvature $a = c = 0, b < 0, a = c = 0, b > 0$

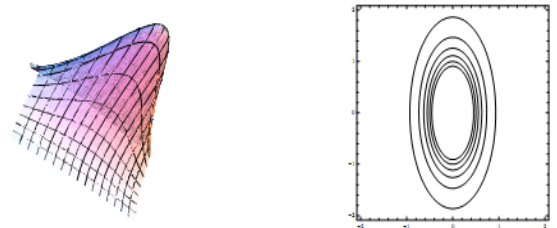


Figure 20: Gauss curvature $a = b = 0, c < 0$ or $c > 0$

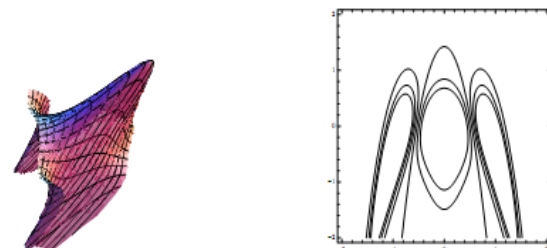


Figure 21: Gauss curvature $a, b, c < 0$

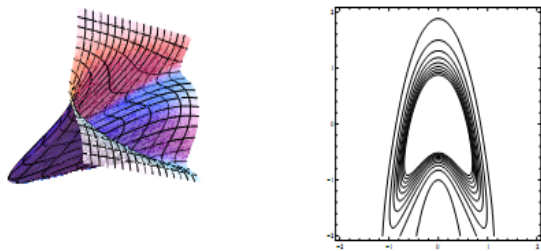


Figure 22: Gauss curvature $a, b, c > 0$

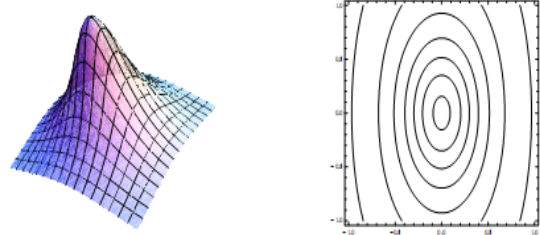


Figure 27: Mean curvature $a = b = 0, c > 0$

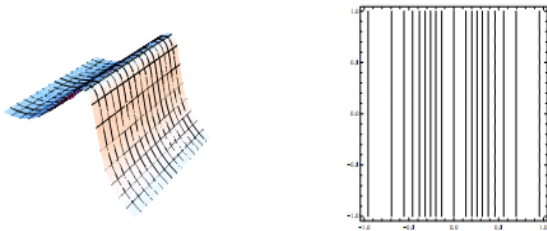


Figure 23: Mean curvature $a = b = c = 0$

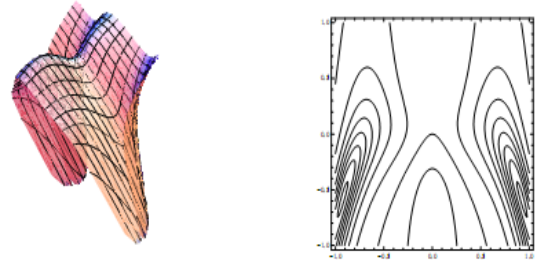


Figure 28: Mean curvature $a, b, c < 0$

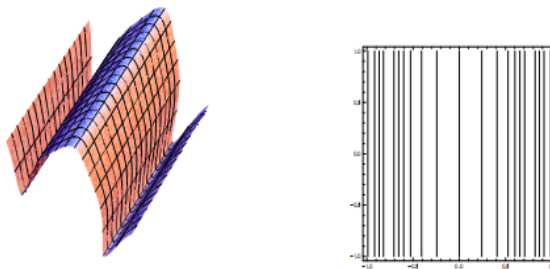


Figure 24: Mean curvature $b = c = 0, a < 0$

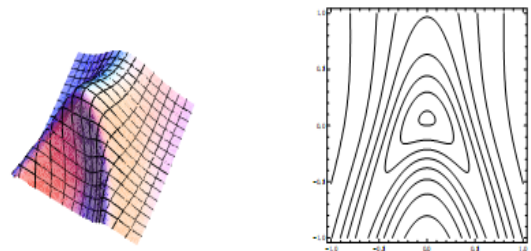


Figure 29: Mean curvature $a, b, c > 0$

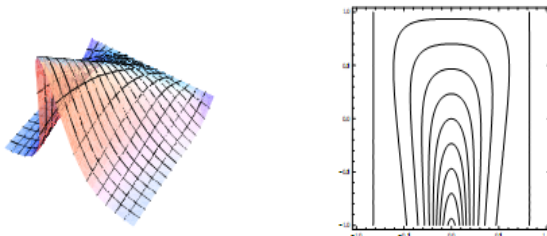


Figure 25: Mean curvature $a = c = 0, b < 0$ or $b > 0$

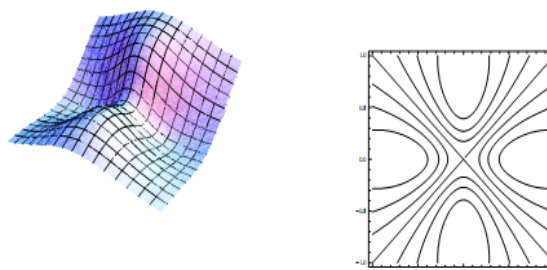


Figure 26: Mean curvature $a = b = 0, c < 0$

References

1. V. I. Arnol'd, S .M. Gusein-Zade and A. N. Varchenko, Singularities of Differentiable Maps vol. I. Birkhauser (1986).
2. V. I. Arnol'd: The Theory of Singularities and Its Applications ; Cambridge Univ. Press, Cambridge, (1991).
3. T. Banchoff, " Cusps of Gauss mappings" Publisher: Longman Science Technology, May, (1986).
4. M. P. Do Carmo, Differential Geometry of Curves and Surfaces, Prentice-Hall, (1976).
5. M. P. Do Carmo, Rimannian Geometry, Birkhuser Basel, (1992).
6. M. Failing, E. Malkowsky, Ein effizienter Nullstellenalgorithmus zur computergrafis chen Darstellung spezieller Kurven und Flächen, Mitt. Math. Sem. Giessen, 229, (1996), 11-25.
7. M. Golubitsky, V. Guillemin, Stable mappings and thier singularities; Springer Verlag, New York, Inc, (1973).
8. A. Gry, Modern differential Geometry of Curves and Surfaces, studies in advanced mathematics. CRC press, Inc, (1993).
9. L. u. Yung-Chen: Singularity Theory and an Introduction to Catastrophe Theory Springer-Verlag, New York, Inc (1976).

8/21/2011

Study of ladybirds (Col:Coccinellidae) in Khorramabad district and the first report of *Hyperaspis quadrimaculata* (Redtenbacher 1844) for Iranian fauna

A. Ansari pour¹, J. Shakarami²

1- Graduated University of Arak, Arak, Iran.

2- Faculty at the University of Lorestan, Khorramabad, Iran.

Abstract: Ladybird fauna of the farms, orchards and pastures of Khorramabad city were studied during 2009 and 2010. In this study, a total of 22 species belonging to 13 genus of ladybird were detected, among them four new species for the province of Lorestan (marked *) and one for Iranian fauna (marked **) were identified. Samples were collected using a valid key and identified by characteristics of their appearance and their genitalia. The species identified are as follows:

1. *Adalia bipunctata* (Linnaeus 1758)
2. *Adalia decempunctata* (Linnaeus 1758)
3. *Chilocorus bipustulatus* (Linnaeus 1758)
4. *Coccinella septempunctata* (Linnaeus 1758)
5. *Coccinella undecimpunctata* (Linnaeus 1758)*
6. *Coccinula elegantula* (Weise, 1980)*
7. *Cryptolaemus montrouzieri* (Mulsant 1853)*
8. *Exochomus flavipes* (Goeze 1777)
9. *Exochomus pubescens* (Kuster 1848)
10. *Exochomus quadripustulatus* (Linnaeus 1758)
11. *Exochomus undulatus* (Linnaeus 1758)
12. *Hippodamia variegata* (Goeze 1777)
13. *Hyperaspis quadrimaculata* (Redtenbacher 1844) **
14. *Oenopia conglobata* (Linnaeus 1758)
15. *Oenopia oncina* (Olivier 1808)*
16. *Propylea quatuordecimpunctata* (Linnaeus 1758)
17. *Psyllobora vigintiduopunctata* (Linnaeus 1758)
18. *Scymnus apetzi* (Mulsant 1846)
19. *Scymnus flavicollis* (Redtenbacher 1844)
20. *Scymnus syriacus* (Marseul 1868)
21. *Stethorus gilvifrons* (Mulsant 1850)
22. *Stethorus siphonulus* (Kapur 1948)

[Study of ladybirds (Col:Coccinellidae) in Khorramabad district and the first report of *Hyperaspis quadrimaculata* (Redtenbacher 1844) for Iranian fauna. Life Science Journal. 2011;8(3):488-495] (ISSN:1097-8135).

<http://www.lifesciencesite.com>.

Keywords: ladybird, Khorramabad, Lorestan, Iran

1. Introduction

Lorestan province is located in western Iran and its center is Khorramabad. This study has been done to identify species of ladybird in the Khorramabad district. Ladybirds (Coccinellidae) are a popular, widely recognized and highly regarded insect group due to their bright color and role in controlling insect pests (Gordon, 1985). Useful application of this insect has in many cases has proven successful and case studies of this type of pest control around the world have been recorded (Sadeghi, 1991; Farahi & Sadeghi Namghi, 2009). The first successful, classical biological control was related to the use of the ladybird *vedalia*, *Rodolia cardinalis* (Mulsant) against the Australian crab

louse, *Icerya purchasi* Maskell (Heteroptera: Margarodidae) in the orange farms of California, in 1880 AD (Caltagirone and Doust, 1989). Ladybird classification, together with that of other animals was first conducted in the mid-seventeenth century by Linnaeus, and then over 100 years later the classification of ladybirds, together with that of other insects, was progressed by Fabricius, Degger, Thunberg and Herbst (Gordon, 1985). Ladybird classification was revised by Mulsant in 1850; he presented a new basis for ladybird classification. Today further detection of new ladybird species takes place by observation of the characteristics of insect genitalia (Sadeghi, 1991; Bagheri & Mossadegh, 1995; Haji zade, 1995) adult male genitalia have two

distinct parts, Observations of tegmen as well as the siphon that may be symmetrical or asymmetrical are also used to determine ladybird species (Sadeghi, 1991). Research on the diversity of ladybird species in the world has studied the taxonomy and morphology of adult and larval ladybird (Hodek, 1973) and has been used to name ordinary species of ladybird in alfalfa fields throughout the United States; as a result the species *Hippodamia convergens* Goeze was introduced. The Ladybird *Stethorus* has been reported for China in a list of new species, determined by the sex of the insects in China by Yu, (1996). Ladybird fauna of the Himalayan country Nepal and the surrounding region has been compiled by Canepari (1997) and the study recorded new species. A list of the ladybird species of East Russia was published by (Kuznetsov, 1997). A family of predatory ladybirds was identified in India (Afroze, 1999). The published list of identified ladybird fauna of India included ladybird *Epilachna* (Poorani, 2002) List of ladybird by Durverger, (1983) was published. Naeem, in the year 1972 published a list of the ladybirds of Iran (Sadeghi, 1991). Various lists of ladybird fauna in different regions have subsequently been registered (Fatemi, 1982; Sadeghi, 1991; Montazeri and Mosadegh, 1995; Haji zade *et al*, 2001; Yaghmaei and Kharazi Pakdel, 2005; Farahi and Sadeghi Namghi, 2010; Ansari pour, 2010).

2. Material and Methods

Samples collected

Ladybird samples were collected from March 2009 to September of 2010, from farms, agricultural land, gardens and parks within and around the city of Khorramabad. Samples were collected weekly and sometimes daily. The sampling procedure was to record the name of the place, its geographical location (using a GPS device) and the names of the tree and shrub varieties from which the samples were taken. Samples were collected from within cultivated fields, especially alfalfa fields with insect nets or by hand directly from the plant or from the surface of the farm land. samples were also collected from within gardens, from trees and shrubs on a glazed tray by hitting several branches and an aspirator was used for the removal of leaves from trees to collect ladybirds.

Maintenance and identification of samples

Collected insects were killed with ethyl acetate and some of these samples for identification were placed in a 70% alcohol solution After separation of the genitalia, cleared (by 10% potassium hydroxide), and dewatering with alcohol of varying purity, permanent slides were kept for identification. Samples were catalogued using valid

keys (Hodek, 1973) and (Gordon, 1985) and a team of internal and external experts assisted in the sex determination of the insects and then species were identified and described. Some species were identified and confirmed by Dr. Fursch from Germany.

3. Results and discussion

In this study, a total of 22 ladybird species were identified, among which four species of fauna for Lorestan province and a new species for the country's fauna were identified as follows:

Adalia bipunctata (L.)

A total of 40 ladybirds of this species were collected and identified, of which 18 were male and the others female. This species of ladybird was identified from samples taken from fruit orchards, wheat fields and alfalfa fields of Khorramabad. It should also be noted that this ladybird has reportedly been found in other regions of Iran, the province of Kerman (Koochpayezadeh & Mossadegh, 1991), Mazandaran (Montazeri & Mossadegh, 1995), south-eastern province of Khorasan (Moadi & Mossadegh, 1995), in Mashhad (Yaghmaei & Kharazi Pakdel, 1995), Chahar Mahal and Bakhtiari province (Bagheri & Mossadegh, 1995), Mazandaran and Lorestan province (Jafari & Kamali 2007). The geographical location of the collection site was 33°48.40'N, 48°57.74' E at an altitude of 1638 m.

Adalia decempunctata (L.)

A total of 19 species of this ladybird species were collected and identified, of which 12 were male and the others female. This species was collected from fruit gardens in the city of Khorramabad. The ladybird has reportedly been found in other areas (Montazeri & Mossadegh, 1995), in the south-eastern province of Khorasan (Moadi & Mossadegh, 1995), Mazandaran and Lorestan province (Jafari & Kamali, 2007). The geographical location of the collection site was 33° 48.40'N, 48°57.74'E at an altitude of 1638 m.

Chilocorus bipustulatus (L.)

A total of 10 species of this ladybird species were collected and identified, of which 3 were male and the others female. This species of ladybird was identified from samples taken from cedar trees of Khorramabad. The ladybird has reportedly been found in other areas: Khorasan Province (Farahi & Sadeghi Namghi, 2009). The geographical location of the collection site was 33°48.24'N, 48°25.17' E at an altitude of 1333 m.

Coccinella septempunctata (L.)

A total of 150 ladybirds of this species were collected and identified, of which 49 were male and the others female. The ladybirds were collected from all regions of Khorramabad city in wheat, barley, cucumber, tomato, alfalfa fields, from fruit gardens and on weeds. This species has spread to all parts of the country and has been reported in all ecosystems. The geographical location of the collection site was 33°48.40'N, 48°57.74'E at an altitude of 1638 m.

***Coccinella undecimpunctata* (L)**

A total of 17 ladybirds of this species were collected and identified, of which 9 were male and the others female. The ladybirds were collected from alfalfa fields. The ladybird has reportedly been found in other areas: Kerman Province (Koohpayezadeh & Mossadegh, 1991), Mazandaran province (Montazeri & Mossadegh, 1995), south-eastern province of Khorasan (Moadi & Mossadegh, 1995), Mashhad province (Yaghmae & Kharazi Pakdel, 1995). The geographical location of the collection site was 33°48.40'N, 48°57.74'E at an altitude of 1638 m.

***Coccinula elegantula* (Weise)**

A total of 37 ladybirds of this species was collected and identified, of which 16 were male and the others female. The ladybird has an adult body length of 3 to 3.5 mm, white elytra with orange spots on them: several were seen with five white and orange spots visible on the pronotum. The insect body is very soft. The ladybirds were collected whilst feeding on two-spotted spider mite from cypress trees in the region of Khorramabad. The geographical location of the collection site was 33°48.40'N, 48°57.74'E at an altitude of 1638 m.

***Cryptolaemus montrouzieri* (Mulsant)**

A total of 25 of this ladybird species were collected and identified, 10 of these were male and the others female. They were collected from ladybird crypts found in apple orchards and fruit gardens city of Khorramabad, (especially from apple and peach trees). But most of the ladybird was Kakareza of Khorramabad region. The geographical location of the collection site was 33°47.15'N, 48°57.74'E at an altitude of 1556 m.

***Exochomus flavipes* (Goeze)**

A total of 75 of this ladybird species was collected and identified, of which 33 were male and the others female. They were collected from the city of Khorramabad, from alfalfa hay fields and fruit orchards, especially peach and apricot trees. The ladybird has been reported in other areas and provinces, cited as follows; in Chahar Mahal and Bakhtiari (Bagheri & Mossadegh, 1995), in Mashhad

(Yaghmae & Kharazi Pakdel, 1995), in Mazandaran (Ghahari *et al.* 2004), Lorestan province (Jafari & Kamali, 2007), Khorasan Province (Farahi & Sadeghi Namghi, 2009). The geographical location of the collection site was 33°48.40'N, 48°57.74'E at an altitude of 1638 m.

***Exochomus pubescens* (Kuster)**

A total of 33 of this ladybird species were collected and identified, of which 13 were male and the others female. They were collected from alfalfa hay fields and fruit orchards, especially peach and apricot trees in the city of Khorramabad. Other areas where this ladybird has been reported are cited by Ghahari *et al.* (2004), also in Mazandaran by Montazeri & Mossadegh (1995), south-eastern province of Khorasan (Moadi & Mossadegh, 1995) and Lorestan province (Jafari & Kamali, 2007). The geographical location of the collection site was 33°48.40'N, 48°57.74'E at an altitude of 1638 m.

***Exochomus quadripustulatus* (L.)**

A total of 29 ladybirds of this species were collected and identified, of which 12 were male and the others female. The Ladybirds were collected from fruit gardens in the city of Khorramabad and from peach trees and alfalfa fields around the fruit orchards. The ladybird has been reported in other areas, cited as follows; in the province of Kerman by (Koohpayezadeh & Mossadegh, 1991), in Mashhad by (Yaghmae & Kharazi Pakdel, 1995) and Chahar Mahal and Bakhtiari by (Bagheri & Mossadegh, 1995). The geographical location of the collection site was 33°48.40'N, 48°57.74'E at an altitude of 1638 m.

***Exochomus undulatus* (Weise)**

A total of 23 of this ladybird species were collected and identified, of which 10 were male and the others female. The ladybirds were collected from trees in city parks, and especially in Khorramabad from oleander shrub and fruit trees such as peach, nectarine and apricot. The ladybird has been reported in other areas; the province of Chahar Mahal and Bakhtiari (Bagheri & Mossadegh, 1995), Mazandaran (Montazeri & Mossadegh, 1995), south-eastern province of Khorasan (Moadi & Mossadegh, 1995), Lorestan province (Jafari & Kamali, 2007) and Khorasan (Farahi & Sadeghi Namghi, 2009). The geographical location of the collection site was 33°49.51'N 48°35.39'E at an altitude of 1211 m.

***Hippodamia variegata* (Goeze)**

A total of 312 of this species of ladybird was collected and identified, of which 154 were male and the others female. This kind of ladybird was found in

most of all alfalfa fields of Khorramabad district. Its presence been reported in most areas of the country (Sadeghi, 1991; Koohpayezadeh & Mossadegh, 1991; Yaghmae & Kharazi Pakdel, 1995; Bagheri & Mossadegh, 1995; Ghahari *et al.* 2004). The geographical location of the collection site was 33°48.40'N 48°57.74'E at an altitude of 1638 m.

***Hyperaspis quadrimaculata* (Redtenbacher)**

Description:

A total of 3 of this species of ladybird was collected and identified, 2 of which were male and the other was female. The Ladybird has a length of 3 – 3.5 mm and a width of 2 – 2.4 mm, Elytra shiny black hair is not elytra level, two red spots on each elytron can be seen, in the middle of the patches of spots on the elytra and other spots are located at the end of the elytra. The genitalia Tegmenin males of this genus is asymmetric and can therefore be easily distinguished from other types of ladybird. This was the first time this ladybird has been collected and reported in Khorramabad city. This species has been identified by Dr. Fursch form Germany. The geographical location of the collection site 33°48.41'N 48°57.72'E at an altitude of 1641 m.

***Oenopia conglobata* (L.)**

A total of 45 of this species of ladybird was collected and identified, of which 19 were male and the others female. The ladybird has been reported in other areas, cited as follow; in the province of Kerman (Koohpayezadeh & Mossadegh, 1991), Mazandaran (Montazeri & Mossadegh, 1995), the south-eastern province of Khorasan (Moadi & Mossadegh, 1995), Chahar Mahal and Bakhtiari (Bagheri & Mossadegh, 1995), in Mashhad (Yaghmae & Kharazi Pakdel, 1995), Gilan (Haji zade *et al.*, 2001), Mazandaran (Ghahari *et al.* 2004), Lorestan province (Jafari & Kamali, 2007) and in Khorasan (Farahi & Sadeghi Namghi, 2009). The geographical location of the collection site was 33°48.40'N 48°57.74'E at an altitude of 1638 m.

***Oenopia oncina* (Olivier)**

A total of 15 ladybird species were collected and identified, of which 7 were male and the others female. The adult length is 3 - 4/5 mm, with black elytra and 10 yellow spots were observed in the spot test, which observed that elytra on each side were L shaped. Two yellow spots were visible on the black side area of the pronotom. The geographical location of the collection site was 33°48.40'N, 48°57.74'E at an altitude of 1638 m.

***Propylea quatuordecimpunctata* (L.)**

A total of 16 ladybird species were collected and identified, a number of which were male and the others female. Other areas where this ladybird has been reported are cited by (Montazeri & Mossadegh, 1995), in Chahar Mahal and Bakhtiari (Bagheri and Mossadegh, 1995), in Mashhad (Yaghmae & Kharazi Pakdel, 1995), Gilan (Haji Zade *et al.*, 2001), Lorestan province (Jafari & Kamali, 2007), Khorasan (Farahi & Sadeghi Namghi, 2009) and in Golestan (Afshari, 2010). The geographical location of the collection site was 33°48.40'N, 48°57.74'E at an altitude of 1638 m.

***Psyllobora vigintiduopunctata* (L.)**

A total of 19 ladybird species were collected and identified, a number of which were male and the others female. The ladybird has been reported in other areas of the province of Kerman (Koohpayezadeh & Mossadegh, 1991), Mazandaran (Montazeri & Mossadegh, 1995), south-eastern province of Khorasan (Moadi & Mossadegh, 1995), Chahar Mahal and Bakhtiari (Bagheri & Mossadegh, 1995), in Mashhad (Yaghmae & Kharazi Pakdel, 1995), Gilan (Haji Zade *et al.*, 2001), Lorestan province (Jafari & Kamali, 2007) and Khorasan (Farahi & Sadeghi Namghi, 2009). The geographical location of the collection site was 33°48.40'N, 48°57.74'E at an altitude of 1638 m.

***Scymnus apetzi* (Mulsant)**

A total of 35 ladybird species were collected and identified, of which 16 were male and the others female. The ladybird was collected from Khorramabad district in the fruit gardens and alfalfa fields. The ladybird has been reported in other areas of Fars province (Yazdani & Ahmadi, 1991), Mazandaran (Montazeri & Mossadegh, 1995), Chahar Mahal and Bakhtiari (Bagheri & Mossadegh, 1995), Mazandaran (Mafi, 1997), Guilan (Haji Zade *et al.*, 2001), Lorestan province (Jafari & Kamali, 2007), and Khorasan (Farahi & Sadeghi Namghi, 2009). The geographical location of the collection site was 33°40.73'N 48°61.25'E at an altitude of 1639 m.

***Scymnus flavicollis* (Redtenbacher)**

A total of 26 ladybird species were collected and identified, of which 15 were male and the others female. The adult length is 2 – 2.5 mm, elytra color is black and covered with hair on them is a shiny gray. Elytra a spot on each orange to dark brown inclined, there have been a way that are seen as two eyes. This is the first report of ladybird from this province that has been collected from the fruit gardens in city of Khorramabad. The geographical location of the

collection site was 33°49.16'N, 48°35.12'E at an altitude of 1185.5 m.

***Symnus syriacus* (Marseul)**

A total of 25 ladybird species were collected and identified, 9 of which were male and the others female. The ladybird was collected from fruit orchards in Khorramabad city. The ladybird has been reported in other areas of the province of Fars (Yazdani & Ahmadi, 1991), south-eastern province of Khorasan (Moadi & Mossadegh, 1995), in Mashhad (Yaghmae & Kharazi Pakdel, 1995), Gilan (Haji Zade *et al.*, 2001) and Khorasan (Farahi & Sadeghi Namghi, 2009). The geographical location of the collection site was 33°48.41'N, 48°57.72'E at an altitude of 1641 m.

***Stethorus gilvifrons* (Mulsant)**

A total of 8 Ladybirds of this species were collected and identified, of which 1 was male and the rest were female. This species was collected from cedar tree in the city of Khorramabad and was identified after separation of the genitalia.

The ladybird has been reported in other areas of the province of Kerman (Koochpayezadeh & Mossadegh, 1991), Mazandaran (Montazeri & Mossadegh, 1995), south-eastern province of Khorasan (Moadi & Mossadegh, 1995), Tehran province (Haji zade, 1995), in Mashhad (Yaghmae & Kharazi Pakdel, 1995), Chahar Mahal and Bakhtiari (Bagheri & Mossadegh, 1995), Gilan (Haji zade *et al.*, 2001), Lorestan province (Jafari & Kamali, 2007) and Razavi province (Farahi & Sadeghi Namghi, 2009). The geographical location of the collection site was 33°48.41'N 48°57.72'E at an altitude of 1641 m.

Table 1: List of ladybird Khorramabad and host from which they were collected.

Ladybirds	Feeding preferences
<i>Adalia bipunctata</i> Linnaeus 1758	<i>Sitobium avenae</i> (F.), <i>Schizaphis graminum</i> (Roud.) & <i>Therioaphis maculata</i> (Bukt.)
<i>Adalia decempunctata</i> Linnaeus 1758	<i>Brachycaudus schwartzi</i> (Borner), <i>Eriosoma lanigerum</i> (Hausm.) & <i>Aphis pomi</i> (Deg.)
<i>Coccinella septempunctata</i> Linnaeus 1758	Aphididae
<i>Coccinella undecimpunctata</i> Linnaeus 1758	<i>Sitobium avenae</i> (F.), <i>Schizaphis graminum</i> (Roud.) & <i>Aphis fabae</i> (Scop.)
<i>Coccinula elegantula</i> Weise, 1980*	<i>Leucaspis pusillai</i> (Loew.), <i>Planococcus vovae</i> (Nasanov)
<i>Cryptolaemus montrouzieri</i> Mulsant 1853	<i>Pseudococcidae</i>
<i>Exochomus flavipes</i> Goeze 1777	<i>Brachycaudus schwartzi</i> (Borner), <i>Eriosoma lanigerum</i> (Hausm.), <i>Myzus persicae</i> (Sulz.) & <i>Aphis pomi</i> (Deg.)
<i>Exochomus pubescens</i> Kuster 1848	<i>Brachycaudus schwartzi</i> (Borner), <i>Eriosoma lanigerum</i> (Hausm.), <i>Myzus persicae</i> (Sulz.) & <i>Aphis pomi</i> (Deg.)
<i>Exochomus quadripustulatus</i> Linnaeus 1758	<i>Myzus persicae</i> (Sulz.) & <i>Aphis pomi</i> (Deg.)
<i>Exochomus undulatus</i> Linnaeus 1758	<i>Aphis nerii</i> (Boyer de Fon.) & <i>Myzus persicae</i> (Sulz.)
<i>Hippodamia variegata</i> Goeze 1777	<i>Aphis nerii</i> (Boyer de Fon.), <i>Aphis pomi</i> (Deg.), <i>Therioaphis maculata</i> (Bukt.), <i>Aphis gossypii</i> (Glov.) & <i>Myzus persicae</i> (Sulz.)
<i>Hyperaspis quadrimaculata</i> Redtenbacher 1844	<i>Aphis gossypii</i> (Glov.)
<i>Oenopia conglobata</i> Linnaeus 1758	<i>Myzus persicae</i> (Sulz.) & <i>Aphis gossypii</i> (Glov.)
<i>Oenopia oncina</i> Olivier 1808	
<i>Propylea quatuordecimpunctata</i> Linnaeus 1758	<i>Myzus persicae</i> (Sulz.) & <i>Aphis gossypii</i> (Glov.)
<i>Psyllobora vigintiduopunctata</i> Linnaeus 1758	
<i>Scymnus apetzi</i> Mulsant 1846	Aphididae
<i>Scymnus flavicollis</i> redtenbacher 1844	Aphididae
<i>Scymnus syriacus</i> Marseul 1868	Aphididae
<i>Stethorus gilvifrons</i> Mulsant 1850	<i>Tetranichus urticae</i> (Koch)
<i>Stethorus siphonulus</i> Kapur 1948	<i>Tetranichus urticae</i> (Koch)

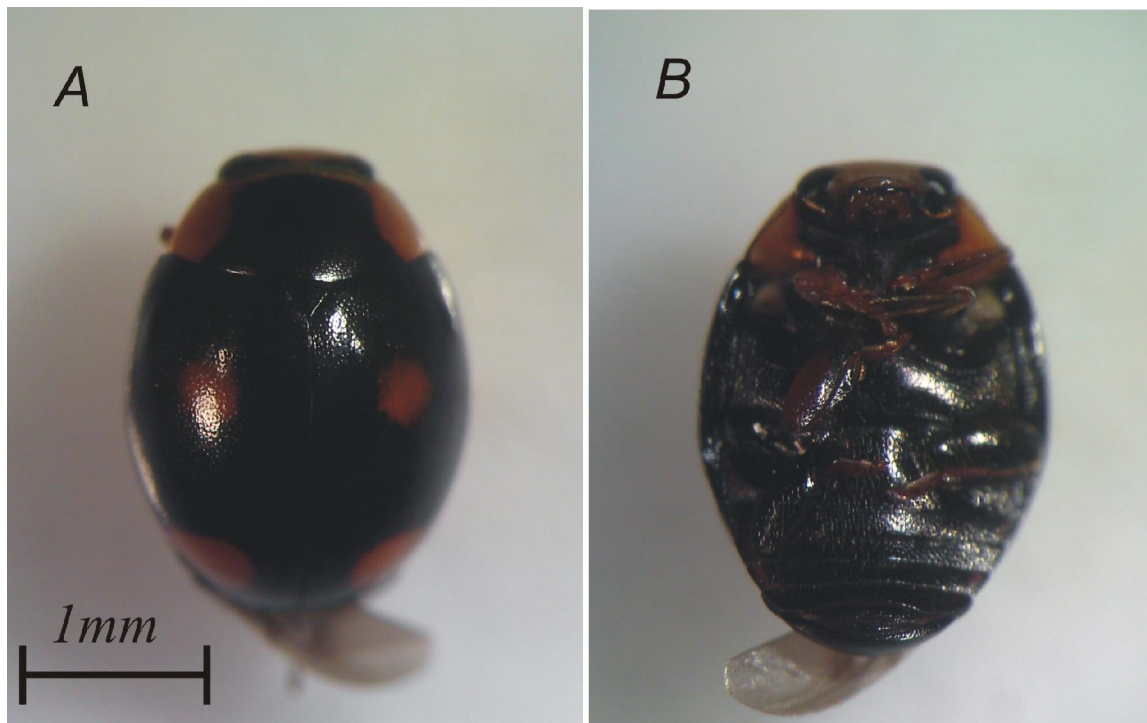


Fig 1: *Hyperaspis quadrimaculata* (Redtenbacher 1844), A: Front surface of body, B: Dorsal surface of body.

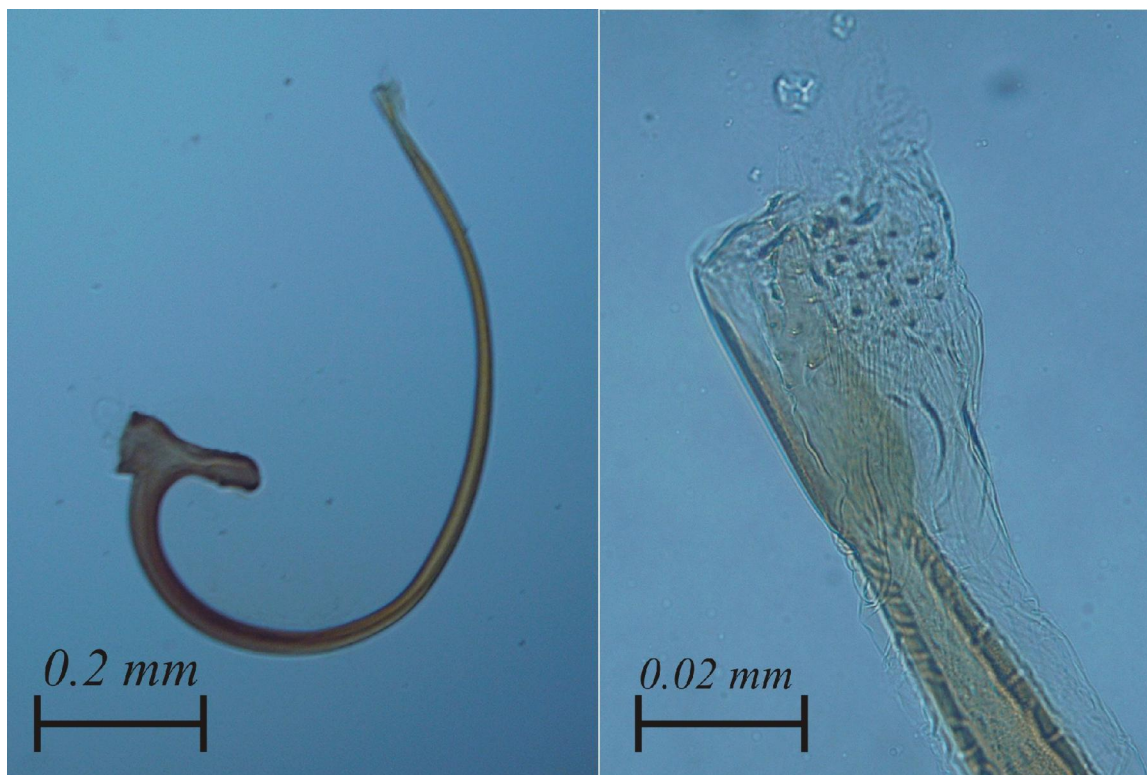


Fig 2: Male genitalia (Siphon) of *H. quadrimaculata*

***Stethorus siphonulus* (Kapur)**

A total of 7 of this ladybird species was collected and identified, of which 2 were male and the others female. The ladybird has a length of 1.1 – 1.5 and width of 1 – 1.2 mm. The body is an elliptical shape and is convex. The body has a black color, antennae, mouth parts, leg and the toe tip is yellow / brown. The ladybird has been reported for the first time in the province. The geographical location of the collection site was 33°48.41'N 48°57.72'E at an altitude of 1641 m.

4. Discussion

The study of fauna conducted in this survey show that 22 species of ladybird in the city of Khorramabad have been identified, among them the five species as follows:

1. *Coccinella undecimpunctata**
2. *Coccinula elegantula**
3. *Cryptolaemus montrouzieri**
4. *Hyperaspis quadrimaculata***
5. *Oenopia oncina**

The species marked * are new fauna of Lorestan province and the species marked ** are the new fauna of Iran. The results are agreed with former study (Jafari and Kamali, 2007).

Contact: Amir.ansar2010@gmail.com ,

Reference

1. **Afroze, S. 1999.** Some Indian predaceous Coccinellidae (Coleoptera). Indian Journal of Systematic Entomology, 11: 27-34.
2. **Afshari, A. 2010.** Relative abundance, spatial distribution and sequential sampling for four main predators of cereal aphids in winter wheat fields of Gorgan, northern Iran. M.S.c thesis. dissertation, Shahid chamran university, Ahwaz. 156 pp.
3. **Ansari pour, A. 2010.** Study of Ladybird fauna (Col.: Coccinellidae) in khorramabad district and population dynamic of dominant species. M.Sc. thesis, Islamic Azad University, Arak. Iran.
4. **Bagheri, M.R. and Mossadegh, M. S. 1995.** The faunistic studies of Coccinellidae in Charmahal Bakhtiari province. p: 308. In: Proceeding of the 12th plant protection congress of Iran 2-7 September 1995, Karaj, Iran.
5. **Caltagirone L. E. and Douth, R. L. 1989.** The history of the Vedalia beetle importation to California and its impact on the development of biological control. Annu. Rev. Entomol. 34:1-16.
6. **Canepari, C. 1997.** Coccinellidae (Coleoptera) from the Nepal Himalayas. Stuttgarter Beitrage zur Naturkunde, Serie A (Biologie), 565 (65): 1-65.
7. **Duverger, P. C. 1983.** Contribution ALA connaissances coccinellidae D' Iran. Nour. Rew. Entomol. 13(1) : 73-79. with English abstract
8. **Farahi, S. and Sadeghi namghi, H. 2009.** Species diversity of aphids and ladybird Mashhad district (Khorasan razavi province). Journal of Plant Protection, 23(2): 89-95.
9. **Gordon, R. 1985.** The coccinellidae (coleoptera) of America North of Mexico. J. Entomol. Soc. 93(1) : 1-912.
10. **Haji zade, J. 1995.** A survey for identification of Coccinellid species of *Stethorus* Weise particular reference on biology, efficiency and mass rearing possibilities of *S. golvifrons* (Mulsant) in Tehran province. M.S.c thesis. dissertation, Tarbiat modares university, Tehran. 196 pp.
11. **Haji zade, J., Jalali sanadi, J. and Peyrovi chashnasar H. 2001.** Introduction part of ladybirds (Col.: coccinellidae) in Guilan province. Agricultural science and natural resources, 4: 99-112.
12. **Hedek, I. 1973.** Biology of coccinellidae. Academia, Czechoslovak Acad. Sci., Prague, 260pp.
13. **Jafari, R. and Kamali, k. 2007.** Faunistic study of ladybird (Col.: Coccinellidae) in Lorestan province and report of new records in Iran. New findings in agriculture, 4: 349-359.
14. **Koohpayezadeh N. and Mossadegh M. S. 1991.** Some of the ladybirds (Coccinellidae) fauna of Kerman province, p: 64. In: Proceeding of the 10th plant protection congress of Iran 1-5 September 1991, Kerman, Iran.
15. **Kuznetsov, V. N. 1997.** Lady Beetles of the Russian Far East. Memoir No. 1, Center for Systematic Entomology, 248 pp.
16. **Mafi, Sh. 1997.** Identification of mealybug species (Pseudococcidae) in Mazandaran province and study on dominant species and its natural enemies. M.S. thesis. dissertation, Tarbiat modares university, Tehran. 112 pp.
17. **Moadi, S. Mossadegh, M. S. 1995.** The coccinellids (Coleoptera) of southeast Khorasan province, Iran, p: 326. In: Proceeding of the 12Th plant protection congress of Iran 2-7 September 1995, Karaj, Iran.

18. **Montazeri, M. M. Mossadegh, M. S. 1995.** The coccinellids (Coleoptera) fauna of Gorgan plain and Gonbad Kavus, p: 325. In: Proceeding of the 12Th plant protection congress of Iran 2-7 September 1995, Karaj, Iran.
19. **Poorani, J. 2002.** An annotated checklist of the Coccinellidae (Coleoptera) (excluding Epilachninae) of the Indian subregion. *Oriental Insects* 36: 307-383.
20. **Sadeghi, I. 1991.** An investigation on the Coccinellidae fauna of alfalfa fields and determination of dominant species at Karaj. M.S. thesis. dissertation, Tarbiat modares university, Tehran. 284 pp.
21. **Yaghmaee, F. and Kharazi Pakdel, A. 1995.** A faunestic survey of Coccinellids in mashhad region, p: 307. In: Proceeding of the 12Th plant protection congress of Iran 2-7 September 1995, Karaj, Iran.
22. **Yu, G. 1996.** A list on *Stethorus* Weise (Coleoptera: Coccinellidae) from China with description of a new species. *Entomotaxonomia*, 18: 32-36.

8/18/2011

Intracranial Stent Placement for Recanalization of Acute Cerebral Artery Occlusion

Shilei Sun¹, Tan Song¹; Xu Haowen²; Chandra Avinash¹, Xu Yuming¹

1. Department of Neurology, the First Affiliated Hospital of Zhengzhou University, Zhengzhou, Henan 450052, China.

² Department of Interventional Radiology, the First Affiliated Hospital of Zhengzhou University, Zhengzhou, Henan 450052, China

Co-first author: Tan Song; Corresponding author: Xu Yuming, xuyuming@zzu.edu.cn

Abstract: To retrospectively evaluate the feasibility, efficacy, and safety of intracranial artery recanalization for acute ischemic stroke (AIS) using a self-expandable stent. All patients treated with an intracranial stent for acute cerebral artery occlusion were included. Treatment comprised intraarterial thrombolysis, balloon angioplasty and stent placement. Recanalization result was assessed by follow-up angiography immediately after stent placement. Complications related to the procedure and outcome at 3 months were assessed. Twelve patients (median NIHSS 14, mean age 63 years) were treated with intracranial stents for AIS. Occlusions were located in the posterior vertebrobasilar circulation (n=6) and in the anterior circulation (n=6). Stent placement was feasible in all procedures and resulted in partial or complete recanalization (TIMI 2/3) in 92%. No vessel perforations, subarachnoid, or symptomatic intracerebral hemorrhages occurred. Three patients (25%) had a good outcome (mRS 0 to 2), 3 (25%) a moderate outcome (mRS 3), and 6 (50%) a poor outcome (mRS 4 to 6). Mortality was 33.3%. Intracranial stent placement for AIS management has an excellent recanalization rate. However, it is associated with high complication risks as our series showed. We believe that the decision to treat acute ischemic stroke with intracranial stent placement should be made after careful consideration of potential benefits and risks.

[Shilei Sun, Tan Song; Xu Haowen; Chandra Avinash, Xu Yuming. **Intracranial Stent Placement for Recanalization of Acute Cerebral Artery Occlusion.** Life Science Journal. 2011;8(3):496-499] (ISSN:1097-8135). <http://www.lifesciencesite.com>.

Keywords: Intracranial stent; Recanalization

1. Introduction

Various treatment modalities for AIS have gradually evolved during the past decade.[1-2] Among them, stents have been reported as an option for improvement of the recanalization rate and have shown excellent results with an acceptably low complication rate.[3-4] The authors have also used intracranial stents in failed cases of intraarterial thrombolysis (IAT) with pharmacologic and mechanical methods since 2004. We also experienced good results in terms of recanalization. But at the same time, we felt that stent should be selected as an option with care. Its use has often been accompanied by complications that could be directly and indirectly related to the stent. In this article, we summarize the radiologic and clinical outcomes of 12 patients with AIS treated with intracranial stents.

2. Methods

All patients treated at our department with intracranial stent placement for acute cerebral artery occlusion were retrospectively analyzed. Data had been collected prospectively and entered into our stroke database. Inclusion criteria for intracranial stent treatment were confirmed vessel occlusion by digital subtraction angiography (DSA), failed IAT, or contraindication to perform intravenous thrombolysis

(IVT) or IAT. Inclusion criteria for IAT were (1) clinical diagnosis of acute stroke established by a stroke neurologist; (2) baseline NIHSS score 4 to 24; (3) exclusion of hemorrhage by cranial Computed Tomography (CT) or Magnetic Resonance Imaging (MRI); (4) vessel occlusion correlating to neurological deficit confirmed by 4-vessel angiography; (5) initiation of treatment within 6 hours of symptom onset for hemispheric stroke and within 24 hours for vertebrobasilar stroke; (6) no clinical or laboratory contraindications for IAT; (7) for patients >80 years that their general condition before stroke did not advise against it.

Intracranial Stent Placement Procedures

All procedures were performed with local anesthetics. A standard transfemoral approach was used, and a 6F guide sheath was placed in the lesion side of the common carotid artery and a 6F conventional guide catheter was placed coaxially into the ICA.

Dual oral antiplatelet agents (clopidogrel 300mg and aspirin 300mg) were given orally or through a nasogastric tube after confirming no intracranial hemorrhage on postprocedural brain CT. Clopidogrel (75 mg) and Aspirin (100 mg) were administered daily thereafter. IV heparin was not

administered during and after IAT. However, in case of cardiac embolic occlusion, low molecular heparin was added 24 hours after IAT, which was changed to oral warfarin several days later. Activated clotting time was not checked during IAT. Mechanical IAT was performed with microwires, microcatheters, and balloons (Gateway balloon, Boston Scientific company US). In all patients a self-expandable stent (Wingspan stent system, Boston Scientific) designed for intracranial use was applied. Stents were slightly oversized to allow proper adjustment to the vessel wall (2.5 to 4.5 mm diameter, 15 to 20 mm length). The stent catheter was navigated to the occlusion site using a road map, and the stent was placed during fluoroscopic control. Aspirin (300 mg) was administered intravenously immediately after stent placement. PTA was carried out before or after stent placement at the discretion of the operator. Recanalization result was assessed by DSA immediately after stent placement according to the Thrombolysis in Myocardial Infarction (TIMI) trial criteria: Grade 0, no recanalization; grade 1, minimal recanalization; grade 2, partial recanalization; grade 3, complete recanalization. Thrombus formation or residual thrombus inside the stent lumen as well as side wall irregularities corresponding to residual atherosclerotic stenosis or fixated thrombotic material between stent and vessel wall were recorded. Dissection and vessel perforation were assessed. Flow in the lenticulostriate arteries (LA) after stent placement in the middle cerebral artery (MCA) was evaluated and perfusion of major branches (eg, M2 segments, cerebellar arteries, posterior cerebral artery) after recanalization of the main vessel was assessed.

Management of post-procedure and follow-Up

After the intervention patients were transferred to the intensive care unit. Brain CT or MRI was performed in the first 24 hours after intervention as well as in case of neurological deterioration to exclude intracranial hemorrhage and to estimate brain edema. sICH was defined as clinical deterioration (4-point or greater increase in the NIHSS score or a 1-point deterioration in the level of consciousness) combined with space-occupying brain hematoma.^{15,18} After exclusion of hemorrhage was made, long-term Aspirin (100 mg/d) was given and Clopidogrel (75 mg/d) was added for the next 30 days. Clinical outcome was assessed at 3 months observation according to the modified Rankin scale (mRS).¹⁹ Outcome was stratified to “good outcome” (mRS 0 to 2), “moderate outcome” (mRS 3), and “poor outcome” (mRS 4 to 6).

3. Result

From May 2009 until July 2011, 12 patients (7 men and 5 women, mean age 63 ± 13 years) were treated with intracranial stent placement for acute occlusion of cerebral artery in our hospital. Median NIHSS score at admission was 14 (range 5 to 38). In 11 patients 1 stent was placed, and in 1 patient two stents were delivered. Stent placement was feasible in all 13 stent procedures. Occlusion sites are given in the Table. All patients had collateral flow grade 2. We made the decision to place a stent in 4 patients in whom PTA had been unsuccessful. PTA was performed in a further 4 patients before and in 3 patients after stent placement. Partial or complete recanalization (TIMI 2 and 3) was achieved in 11/12 patients (91.6%). Median time from symptom onset to recanalization was 393 minutes (range 20 to 510 minutes.). Preservation of LA was possible in all stent placements in the middle cerebral artery (MCA). Occlusion of a major vessel branch at the site of stent placement persisted in 6 patients. Assessment of the dependent vessel branch territory by follow-up MRI or CT showed infarction in 3 of 6 patients (50%), whereas no infarction of this particular territory was noted in the remaining 3 patients. In 8 patients major branches at the site of the stent showed sufficient perfusion.

At 3 months follow-up 3 patients (25%) had a good outcome (mRS 0 or 1), 3 (25%) had a moderate outcome (mRS 3), and 6 (50%) had a poor outcome (mRS 4 to 6). Mortality was 33.3%.

4. Discussion

A recent meta-analysis of several stroke studies revealed a strong association of recanalization and good outcome after acute ischemic stroke.^[1] IVT has been shown to improve patient outcome and is approved by the FDA and EMEA.^[5] However, only a minority of patients admitted for acute stroke receive IVT.^[6] IAT is also effective for vessel recanalization and is supposed to achieve higher recanalization rates than IVT.^[7] On the other hand, application of thrombolytic drugs increases the risk of sICH.^[8] These factors as well as failure of thrombolysis to achieve sufficient recanalization in a subgroup of patients led to the introduction of MT. The Merci Retriever System got FDA approval in 2004. However, recanalization rate remained at 46% to 57% with the Merci retriever and risk of SAH attributable to intracranial vessel perforation has increased.^[9] Intracranial stent placement for recanalization of cerebral arteries has been performed in a limited number of acute stroke patients.^[10] The present study confirms the high technical success rate using a self-expandable stent system introduced for treatment of atherosclerotic stenosis in the setting of

complete acute intracranial vessel occlusion.[11] No technical failure was encountered in our study. The stent catheter was navigated easily up to the intracranial vasculature and placed beyond the occlusion site. High recanalization rates of 79% to 90% after intracranial stent placement have been reported and are confirmed in the present study (92%).[11] Whereas Levy et al reported results obtained at 4 different clinical centers and used the Neuroform stent in a majority of patients, we report a single center experience with the more recently introduced Wingspan stent system. Compared to the Neuroform stent, the Wingspan stent has an improved delivery system, a higher radial force, and a higher number of struts. The improved delivery system increases stent safety and feasibility. The higher radial force and tighter struts are supposed to compress and fixate the thrombus more reliably.[12]

Mortality (33%) was similar to former studies (32% to in a quarter of the patients.[11] However, stenting was performed as a rescue therapy in patients with major artery occlusions after failure of other techniques. 40%), and a good outcome after 3 months was observed only in a quarter of the patients.

From our point of view important side branches like the LA can be preserved if the thrombus is passed on the ipsilateral side by the microwire and the stent. Stent expansion will fixate the thrombus at the contralateral wall. This technique was successfully performed in all 5 of our patients suffering MCA occlusion and can be translated to the BA and P1 segments with their perforating arteries as well. However, occlusion of major vessel branches (eg, M2 segment, superior cerebellar artery) at the site of stent placement persisted in 6 patients. Remarkably, no infarction occurred in the dependent vessel territory in half of those patients, pointing to a sufficient collateral circulation. In 3 patients follow-up MRI or CT revealed infarcts in the dependent vessel territory. These infarcts were apparent to some extent at MRI before the interventional treatment, and it remains uncertain whether they are related to the primary occlusive disease or to the stent placement.

In our experience care has to be taken if the deployed stent has to be passed repeatedly with other devices. As long as the stent is not covered by neointima, devices might get caught in the stent struts with subsequent complications. Hence stent placement was performed to reestablish sufficient cerebral blood flow with as little mechanical manipulation as possible, additional postdilatation was performed in only 25% of our patients. Before the introduction of stents for the treatment of atherosclerotic stenosis of intracranial vessels, PTA

performed alone for acute ischemic stroke yielded some success. However, when treating thrombus rather than atherosclerotic stenosis, reocclusion attributable to thromboaggregation and thrombus expansion might occur. In our study, all PTAs performed for vessel recanalization failed to establish sufficient flow.

Reference

1. Tissue plasminogen activator for acute ischemic stroke: The National Institute of Neurological Disorders and Stroke rt-PA Stroke Study Group. *N Engl J Med* 1995; 333: 1581–87.
2. Furlan A, Higashida R, Wechsler L, et al. Intra-arterial prourokinase for acute ischemic stroke: The PROACT II study—a randomized controlled trial. *Prolyse in Acute Cerebral Thromboembolism. JAMA* 1999; 282:2003–2011.
3. Gupta R, Vora NA, Horowitz MB, et al. Multimodal reperfusion therapy for acute ischemic stroke: factors predicting vessel recanalization. *Stroke* 2006; 37: 986–990.
4. Brekenfeld C, Schroth G, Mattle HP, et al. Stent placement in acute cerebral artery occlusion: use of a self-expandable intracranial stent for acute stroke treatment. *Stroke* 2009; 40:847–852.
5. Tissue plasminogen activator for acute ischemic stroke. The National Institute of Neurological Disorders and Stroke rt-PA Stroke Study Group. *N Engl J Med.* 1995; 333: 1581–1587.
6. Barber PA, Zhang J, Demchuk AM, Hill MD, Buchan AM. Why are stroke patients excluded from TPA therapy? An analysis of patient eligibility. *Neurology.* 2001; 56:1015–1020.
7. Brekenfeld C, Remonda L, Nedeltchev K, Arnold M, Mattle HP, Fischer U, Kappeler L, Schroth G. Symptomatic intracranial haemorrhage after intra-arterial thrombolysis in acute ischaemic stroke: assessment of 294 patients treated with self-expandable stents. *J Neurol Neurosurg Psychiatry.* 2007; 78:280–285.
8. Nedeltchev K, Brekenfeld C, Remonda L, Ozdoba C, Do DD, Arnold M, Mattle HP, Schroth G. Internal carotid artery stent implantation in 25 patients with acute stroke: preliminary results. *Radiology.* 2005; 237: 1029–1037.
9. Smith WS, Sung G, Saver J, Budzik R, Duckwiler G, Liebeskind DS, Lutsep HL, Rymer MM, Higashida RT, Starkman S, Gobin YP; Multi MERCI Investigators, Frei D,

- Grobelny T, Hellinger F, Huddle D, Kidwell C, Koroshetz W, Marks M, Nesbit G, Silverman IE. Mechanical thrombectomy for acute ischemic stroke: final results of the Multi MERCI trial. *Stroke*. 2008; 39:1205–1212.
10. Grobelny T, Hellinger F, Huddle D, Kidwell C, Koroshetz W, Marks M, Nesbit G, Silverman IE. Mechanical thrombectomy for acute ischemic stroke: final results of the Multi MERCI trial. *Stroke*. 2008; 39:1205–1212.
11. Sauvageau E, Levy EI. Self-expanding stent-assisted middle cerebral artery recanalization: technical note. *Neuroradiology*. 2006; 48: 405– 408.
12. Levy EI, Mehta R, Gupta R, et al. Self-expanding stents for recanalization of acute cerebrovascular occlusions. *AJNR Am J Neuroradiol* 2007; 28: 816–822.

8/22/2011

Helicobacter Pylori Infection and Immune Factors On Residents in High-incidence Areas of Cancer Along S River

Ping LI*, Jingyuan ZHU*, Yue BA*, Shiqun LI*, Xuemin CHENG*, Hua LI#, Yutang XUE#, Ruichang LIU#, Qiting ZUO, Liuxin CUI*1

*Department of Public Health, Zhengzhou University, 450001, Zhengzhou, China

^ Department of Water and Environment, Zhengzhou University, 450001, Zhengzhou, China

Centers of Disease Control and Prevention, ShenQiu town, Zhoukou, China

Clx@zzu.edu.cn

Abstract: This study was conducted via questionnaire among the residents from 30 to 60 years old in two areas to explore the influence of water pollution on people's health condition. The Contaminated area situated less than 2 km away from S river whereas the control area was chosen at least 20 km away from the river. The subjects were divided into four groups according to family history of cancer, gastrointestinal diseases history, gastrointestinal symptoms and smoking or drinking habit, including high-risk group (group 1) and normal group (group 2) who lived in Contaminated area, high-risk group (group 3) and normal group (group 4) who lived in control area respectively. Immunoblotting method was applied to test HP antibodies in serum, levels of IL-2 and INF- γ in serum were measured by ELISA method. We found that type I HP infections (CagA or VacA-positive) in group 1, group 2 and group 3 were all significantly higher than that in group 4 ($p < 0.001$), while type II HP infection (UreA or UreB positive) had no significant difference among groups ($p > 0.05$), which points out that the residents living in the contaminated area along S River had significantly higher *Helicobacter pylori*. Values of IL-2 and INF- γ in group 1 was significantly higher than that in the other groups ($p < 0.05$), while levels of IL-2 in group 2 and group 3 were higher than group 4 ($p < 0.05$). Group 1 had a higher level of INF- γ than group 2 ($p < 0.05$), these results indicated that the contaminated area residents along S River also had significantly higher immune factors. Both of which are risk factors of gastrointestinal cancer.

[Ping LI, Jingyuan ZHU, Yue BA, Shiqun LI, Xuemin CHENG, Hua LI, Yutang XUE, Ruichang LIU, Qiting ZUO, Liuxin CUI. **Helicobacter Pylori Infection and Immune Factors On Residents in High-incidence Areas of Cancer Along S River.** Life Science Journal. 2011;8(3):500-504]. (ISSN:1097-8135). <http://www.lifesciencesite.com>.

Key words: Cancer; High-incidence areas; Residents; *Helicobacter pylori*; Immune factors.

1. Introduction

The Huai River Basin is the third largest river in China, which has a total length of 1000 km and covers an area of 270,000 km². About 150 million people are brought up by the Huai River. Since the 1980s, the water quality has been getting worse and worse because of the dramatic population growth, economic development, the rapid acceleration of urbanization and the large quantities discharging of domestic sewage, industrial effluent and agricultural pollutants. The most polluted section is S river, because various types of wastewaters from 31 cities were poured into the river without any sewage disposal. The monitoring (Wang et al, 2007; Gao et al, 2010; Tian et al, 2011) data showed that S River had accepted so many municipal and agro-industrial pollutants that it had already lost its self-purification capacity of environment, in which numbers of indicators had been classified as Class V of surface water quality standards or even worse. Some researches (Xu, 2007) have already reported that water pollution of Huai River has caused great harm to the health of surrounding residents resulting in multiple

high-incidence area of cancer around the basin. We had analyzed the cause of death in contaminated area and control area, and found that the proportion of people dying of cancer, accounted to 29.83%, was significantly higher in contaminated area, especially gastrointestinal cancer. The high-incidence areas of cancer assumed a focal distribution along S river and are consistent with the river pollution.

The effect of HP infection on health of people is a major issue of social concern. Many literature (Amieva et al, 2008; Takahashi et al, 2004) indicated that high incidence of gastrointestinal cancer related with HP infection. However, most of investigations were about clinical patients. It was reported rarely in normal population using strain typing method. There were also many scholars (Dimitrios et al, 2010; Mantovani et al, 2008; Hussain et al, 2007; Henson et al, 2011) who did believe cancer had a certain correlation with inflammation, yet mainly paid more attention to patients. In an early phase, the influence of Huai River pollution on the health of residents mainly focused on the incidence of cancer while less for the levels of

immune factors. Therefore, the objects of this study were designed to research HP infection and levels of immune factors (IL-2 and INF- γ) in serum of the residents between contaminated area and control area in order to explore the impact of water pollution on people's health condition and provide the scientific basis for selecting monitoring indicators.

2. Materials and Methods

Location

According to the data about disease spectrum and water monitoring from relevant health and environmental departments, and opinions of experts, S county which is the last place that S River flows through in Henan Province was chosen as the survey scene for this cross sectional study. The polluted area and control area were selected randomly from the villages that less than 2 km and more than 20 km away from the river respectively. And the two villages both have 3,000,000 people and are similar in the economic level, natural condition, demographic composition and living habits and so on.

Subjects

Villagers aged from 30 to 60 years old who has been living in these two survey areas were recruited. Based on some elements such as family history of cancer, history of digestive system diseases, obvious gastrointestinal symptoms and smoking or drinking habit, they were divided into four groups: high-risk group (group 1) and normal group (group 2) who lived in Contaminated area, high-risk group (group 3) and normal group (group 4) who lived in control area respectively. Then 65 subjects were randomly selected in each group using random number table. Every subject was drawled 10ml fasting blood, then the samples were centrifuged to separate serum and stored at -80°C for use.

Analysis of Cause of Death

All data about a three-year period from 2007-01-01 to 2009-12-31 were obtained via direct reporting death registration network system of S County that included the entire population data, the list of all death, cause of death, death symptoms, treatment hospitals and diagnostic basis, etc. Household survey was used on the death list in order to further verify cause of death and diagnosis according to ICD-10 Classification of Diseases, while the demographic in 2009 of S County was used to calculate gender mortality, age-specific mortality and the cause of death.

Questionnaire

The questionnaire included villagers' general condition, vocational and life behavior, the types of

drinking water and fuel, dietary structure, clinical symptoms, two weeks and six months of illness and so on. Investigators were trained in advance and the villagers were asked by face to face interview survey.

HP Infection Analyses

HP was tested by Immunoblotting, kits were purchased from Shenzhen Bo Lao te Biological Products Co., Ltd. The experiment was done according to steps on the introduction and then compared with the "standard zone" to judge results. There are totally three different results ① CagA or VacA antibodies simultaneously or either positive is type I HP infection. ② only Ureas antibodies positive is type II HP infection. ③ CagA, VacA and Ureas all negative is Hp-negative.

Immune Factors in Serum Testing

IL-2 and INF- γ levels in serum were measured by ELISA. At the end of the measure in all samples, 10 samples which selected randomly were retested. kits were supported by Shanghai Yuan Valley Technology Development Co., Ltd.

Statistical Analysis

The data utilized double people enter into the database which was established using Epidata 3.0 software (Epidata 3.0 for windows, Epidata Association Odense, Denmark). HP infection, the top eight causes of death and the mortality of the top eight cancer were assessed using Fisher exact value method and χ^2 test. The levels of immune factors (IL-2 and INF- γ) were summarized with descriptive statistics. One-way analysis of variance (ANOVA) test and SNK test were used to compare mean differences in four groups. SPSS17.0 statistical package was used for statistical analysis. (significance level $\alpha = 0.05$).

3. Results

3.1 The Top Eight Causes of Death in Contaminated Area and Control Area (Table 1)

Compared with control area, we can observe that the percentage of tumor and cerebrovascular disease was significantly higher ($P < 0.05$), while others have no significant differences in two areas ($P > 0.05$) (Table 1).

3.3 HP Infection in Four Groups

As was shown in table 3, Type I HP infection (CagA or VacA-positive) in group 1, group 2 and group 3 all were significantly higher than that in group 4 ($p < 0.001$); while type II HP infection (Ur eA or Ur eB positive) had no significant difference among groups ($p > 0.05$).

TABLE 1. The top eight causes of death and their percentage (%) in two areas

death cause	contaminated area		control area	
	name	percentage (%)	name	percentage (%)
1	tumor	29.83*	tumor	13.22
2	cerebrovascular disease	23.05*	cerebrovascular disease	8.82
3	cardiovascular diseases	15.43	respiratory diseases	8.58
4	respiratory diseases	15.08	cerebrovascular diseases	7.43
5	accidental death	11.86	accidental death	5.57
6	infectious and parasitic diseases	1.36	infectious and parasitic diseases	0.81
7	endocrine, nutritional and metabolic diseases	1.19	endocrine, nutritional and metabolic diseases	0.58
8	digestive diseases	0.85	genitourinary diseases	0.46
	others	1.35*	others	54.48

Note. * $p < 0.05$ compared with control area

3.2 The Mortality of the Top Eight Cancer in Contaminated Area and Control Area

Compared with control area, the mortality of liver cancer, Rectal cancer, Pancreatic cancer and Lung cancer in contaminated area was significantly higher ($P < 0.05$). while others have no significant differences in two areas ($P > 0.05$) (Table 2).

3.4 IL-2 of Human Serum in Four Groups

As were shown in table 4, Values of IL-2 in group 1, group 2 and group 3 were all significantly higher than that in group 4 ($p < 0.05$). Values of IL-2 in group 1 and group 3 were significantly higher as compared with group 2 ($p < 0.05$). Group 1 had a higher level than group 3 ($p < 0.05$).

TABLE 2. Comparison of the mortality of the top eight cancer in two areas (1/100,000)

name	Contaminated area	Control area	χ^2	<i>P</i>
Esophageal cancer	25.9	16.2	1.999	0.157
liver cancer	45.4	18.2	10.582	0.001*
Rectal cancer	13.0	4.1	4.321	0.038*
Pancreatic cancer	7.8	0.0	5.569	0.018*
Gastric cancer	22.0	18.2	0.315	0.574
leukemia	6.5	3.0	0.499	0.480
Breast cancer	11.7	4.1	3.398	0.065
Lung cancer	66.1	26.3	15.645	0.000*

Note. * $p < 0.05$ indicating statistical significance of difference

TABLE 3. Comparison of HP infection in serum of four groups in two areas

groups	type I HP infection	type II HP infection	negative infection	No
1	61*	4	0	65
2	56*	2	7	65
3	60*	2	3	65
4	36	6	23	65
total	213	14	33	260

Note. * $p < 0.05$ compared with group 4.

TABLE 4. Values of IL-2 in serum of four groups in two areas

groups	NO	IL-2 ($\bar{x} \pm s$) (pg/ml)
1	65	1006.455 ± 146.603*a
2	65	608.060 ± 144.056#
3	65	754.570 ± 83.021#a
4	65	312.881 ± 16.881#a

Note. a $p < 0.05$ compared with group 2, * $p < 0.001$, # $p < 0.05$ compared with group 4.

3.5 INF- γ of Human Serum in Four Groups

As shown in table 5, Values of INF- γ in group 1 and group 3 were all significantly higher than that in group 4 ($p < 0.05$); and group 1 had a higher level than group 2 ($p < 0.05$).

TABLE 5. Values of INF- γ in serum of four groups in two areas

groups	NO	INF- $\gamma(\bar{x} \pm s)$ (ng/ml)
1	65	154.991 \pm 27.210*#
2	65	81.192 \pm 21.999
3	65	125.076 \pm 19.989*
4	65	60.231 \pm 8.896

Note. # $p < 0.05$ compared with group 2, * $p < 0.05$ compared with group 4.

4. Discussions

The cause of death has been influenced by S River Pollution

In recent years, according to the monitoring data, it showed that about 50% of the Huai River Basin were exceeding class V standards of surface water quality in 2004 and it can directly affects the local people who live around the Basin (Wang et al, 2007). More and more attention had been paid to the incidence of cancer.

The results of this study showed that: 1) the percentage of tumor and cerebrovascular disease was significantly higher ($P < 0.05$). 2) the mortality of liver cancer, Rectal cancer, Pancreatic cancer and Lung cancer in contaminated area was significantly higher ($P < 0.05$), while others have no significant differences in two areas.

The research indicated that the proportion of people in contaminated area dying of cancer accounted to 29.83% and was significantly higher, especially gastrointestinal cancer. It suggested that the cause of death has been influenced by the polluted river spread horizontally.

HP Infection in Contaminated Area and Control Area

HP was divided into two types in clinic: type I HP, producing cytotoxic strain, can be easy to cause stomach diseases. Conversely, people have no clinical symptoms when suffered type II HP which is less toxic. HP infection is common in crowd. And HP is not only the main cause for chronic gastritis and ulcer, but also closely related with gastric cancer and gastric mucosa-associated lymphomas (Amieva et al, 2008; Takahashi et al. 2004). Wang et al, etc, (Wang and Wang 2003) conducted a Meta-analysis on the epidemiology of HP infection in China and indicated that HP widely distributed in China and its average infection rate was 58.07%. According to the research of Huang et al, etc, (Huang et al, 2011) the results had showed that HP infection and gastric disease history had a closely relationship.

The results of this study showed that 1) HP infection was lowest in group 4 in which type I HP infection was 55.2% and consistent with the level of our national. 2) type I HP infection in group 1, group 2 and group 3 all were significantly higher than that in group 4 ($p < 0.001$) and the average level, which is consistent with the disease spectrum data from health departments of S county showing that the incidence of cancer especially gastrointestinal cancer in contaminated area is much higher than that of the national average.

The Levels of Immune Factors in Contaminated Area and Control Area

IL-2 and INF- γ , important immune factors, can lead to immune tolerance (Michele et al, 2008; Robert et al, 2011) by affecting regulatory T cells via signal transformation. Some researches indicated that tumors prone to happen if the immune function was inhibited as levels of IL-2 and INF- γ increased. Previous researches (Du et al, 2004) also had showed IL-2 in patients with gastrointestinal cancer was significantly higher than that in non-cancer group.

The result of this study showed that ① the levels of IL-2 and INF- γ in high-risk groups were significantly higher than that in normal groups ($p < 0.05$), ② group 1 has a higher IL-2 level than group 3 ($p < 0.05$). ③ the levels of IL-2 and INF- γ in group 1 were significantly higher compared with that in group 4. ④ there is no statistically difference of levels of IL-2 and INF- γ between group 2 and group 3 ($P > 0.05$).

According to the above results, it demonstrated that both polluted factors and other risk factors can together lead to levels of IL-2 and INF- γ significantly changing, so did the polluted factors only, which has some necessary link with the pollutants which affect human immune function in S River.

Recently some data (Wang et al, 2006) have shown high prevalence of type I HP can reduce the function of immune system, meanwhile the reduce of immune factors conversly add the incidence of HP infection. They are high risk factors of all gastrointestinal tumors and may have some combined effect.

This study has indicated that the residents living in the contaminated area along S River had significantly higher *Helicobacter pylori* infection and immune factors, both of which are risk factors of gastrointestinal cancer. Therefore, residents living along S River can adopt some measures including early prevention and treatment of HP infection, and improving their immune function to reduce the incidence of cancer to improve the quality of life. At the same time, HP infection and immune factors can be used as monitoring indicators in the evaluation on effect of pollution control to obtain residents' attention.

Acknowledgements

We are extremely grateful to all the investigators and most importantly the residents for their participation in our study. We appreciate all the leaders for their supporting. The Center for Disease Control and Prevention of Shengqiu provided invaluable information and Experimental Equipment for this study. Besides, we should also thank Prof. Zuo Qiting and the School of Public Health for Technical guidance and financial support.

Corresponding Author:

Prof. Liuxin Cui
Department of Public Health, Zhengzhou University,
Henan, China
Tel: 0371-67781796; Fax: 0371-67781796
E-mail: clx@zzu.edu.cn

References

1. Wang X K, Zuo Z J, Luo W J, *et al.* (2007). Water quality and pollution characteristics of shallow groundwater in Huai River basin [J]. *Engineering investigation*, 9: 40-43.
2. Gao H L, Li H T, Zhao F L (2010). Spatial and temporal distribution of water pollution in Shaying River [J]. *Water resources protection*, 26(3):23-26.
3. Tian D, Zheng W, Wei X, *et al.* (2011). Eutrophication of water bodies and pollutions of microcystins in water and sediments in X county in the Huai River Basin [J]. *Health Research*, 40(2):158-162.
4. Xu X L (2007). Investigation evaluation of groundwater pollution in the Huai River basin (in the part of An hui) and the counter-measure [J]. *Geol An hui*, 17:128-133.
5. Amieva M R, El-Omar E M (2008). Host-bacterial interactions in *Helicobacter pylori* infection

[J]. *Gastroenterology*, 134(1):306-323.

6. Takahashi T, Yujiri T, Shinohara K, *et al.* (2004). Molecular mimicry by *H. Pylori* CagA Protein may be involved in the Pathogenesis of *H. Pylori* associated chronic idiopathic thrombocytopenic Purpura. *Br J Haematol*, 124:91-96.
7. Dimitrios Iliopoulos, Savina A, Heather A, *et al.* (2010). STAT3 Activation of miR-21 and miR-181b-1 via PTEN and CYLD Are Part of the Epigenetic Switch Linking Inflammation to Cancer. *Molecular Cell*, 39(10):493-506.
8. Mantovani A, *et al.* (2008). Tumor immunity: effector response to tumor and role of the microenvironment. *Lancet*, 371, 771 – 783.
9. Hussain S P, Harris C C (2007). Inflammation and cancer: an ancient link with novel potentials. *Int J Cancer*, 121: 2373 – 2380.
10. Henson M S, Curtsinger J M, Larson V S, *et al.* (2011). Immunotherapy with autologous tumour antigen-coated microbeads (large multivalent immunogen), IL-2 and GM-CSF in dogs with spontaneous B-cell lymphoma. *veterinary and comparative oncology*, 9(2) : 95-105.
11. Wang K J, Wang R T (2003). Meta analysis on the epidemiology of *Helicobacter pylori* infection in china [J]. *Chinese Journal Epidemiology*, 24(6):443-446.
12. Huang R G, Wang C M, Lv M H, *et al.* (2011). The correlation analysis of *Helicobacter pylori* infection in medical groups [J]. *Chinese Journal of Modern Medicine*, 21(5):671-446.
13. Du X T, Wang S K, Wang Z Z, *et al.* (2004). The detection of IL-2, TNF- α and IFN- γ , and its clinical significance in peripheral blood cells of lung cancer patients [J]. *Clinical Laboratory Science*, 1: 32-33.
14. Zhang W B, Liu J T, Dang X J (2001). The observation of the expression of IL-2 and IL-2R, and activity changes about CD_3, CD_4, CD_8 and NK cells in peripheral blood of cancer patients [J]. *Chinese Journal of Modern Medicine*, 5: 30-31.
15. Li R N, Liu Y P (2004). The effect of IL-2 and its receptor in malignant prognosis [J]. *Chinese Clinical Oncology*, 4: 428-430.
16. Wang S K, Wu G L, Wang Z Z, *et al.* (2006). Cellular immune responds in gastric lesion associated with *Helicobacter pylori* infection and its relationship with occurrence of gastric cancer. *Doctoral thesis of Nanjing Medical University*, 1-130.

8/20/2011

On Bipreordered Approximation Spaces

¹A. Kandil, ²M. Yakout, and ^{*2}A. Zakaria

¹Mathematics Department, Faculty of Science, Helwan University, Cairo-Egypt.

²Mathematics Department, Faculty of Education, Ain Shams University, Egypt.

*amr_zakaria2008@yahoo.com

Abstract: We used preordered relations to define a bipreordered space and hence bitopological space and introduced a condition (*) on these relations such that $\overline{R}(A \cup B) = \overline{R}(A) \cup \overline{R}(B)$, where $\overline{R}(A) = \overline{R}^1(A) \cap \overline{R}^2(A)$, and hence we get a topology $\tau_{R_{12}}$ on X satisfies

$$\overline{A} = \overline{R}(A) = \overline{R}^1(A) \cap \overline{R}^2(A) = \{x \in X: xR_1 \cap xR_2 \cap A \neq \emptyset\} = \overline{A}^1 \cap \overline{A}^2$$

and $\tau_{R_{12}} = \tau_{R_1 \cap R_2} = \tau_{R_1} \vee \tau_{R_2}$. We deal with bitopological spaces (X, τ_1, τ_2) which satisfying a certain condition (***) and proved that the family of all such bitopological spaces $BT\mathcal{S}^{***}$ is equivalent to the family of all bipreordered spaces $BP\mathcal{S}^*$.

[A. Kandil, M. Yakout, and A. Zakaria. **On Bipreordered Approximation Spaces**. Life Science Journal. 2011; 8(3):505-509] (ISSN: 1097-8135). <http://www.lifesciencesite.com>.

Keywords: Bipreorder; Approximation; Space

1. Introduction

A classic paper of Z. pawlak [17] is the Rough Sets (RS), published in 1982, which declared the birth of the RS theory. A lot of mathematicians, logicians, and researchers of computers have become interested in the RS theory and have done a lot of research work of RS in theory [6, 14, 15] and application. Its applications are showed in wide fields such as machine learning [5], data mining [4], decision- making support and analysis [16, 18, 23], process control [22] and expert system [26].

Different kinds of generalizations of pawlak RS model can be obtained by replacing the equivalence relation with an arbitrary binary relation [3, 19, 20, 25]. It was proved that, the pair of lower and upper approximation operators induced by reflexive and transitive relations is exactly a pair of interior and closure operators of a topology [27, 29]. Some surveys of RS theory and applications are presented in [21, 28]. Many properties of RS were obtained when the approximation space is finite. When the universe is infinite, the relationship between generalized RS induced by binary relation and topologies were investigated in [11] and [24]. In [11], a kind of compactness condition (comp) was proposed and it was proved that a topology which satisfies (comp) can determine the lower and upper approximation operators induced by reflexive and transitive relation. In [24], the topology induced by reflexive and transitive relation does not satisfy (comp) in general. Another kind of compactness condition (COMP) is proposed and it is proved that there exists a one-to-one correspondence between the set of all reflexive and transitive relations and the set of all topologies which satisfy condition (COMP).

The formation and progress of the theory of bitopological spaces introduced in [10]. The theory acquires special importance in the light of applications of its results. The theory of bitopological space has been developed in [1, 7, 8, 12].

the order relations used to define a topology or bitopologies on a set X were often equivalence relations (e.g.[2]). In this paper we used only preordered relations(i.e. reflexive and transitive) to define topologies, however, $A \cup B = A \cup B$ still does not hold, where $\overline{A} = \overline{A}^1 \cap \overline{A}^2$, so, we introduced the condition (*) for preordered relations R_1 and R_2 making the preceding equality holds and hence we could generate a topology by two preordered relations, $\tau_{R_{12}}$ and proved that for all $A \subseteq X$,

$$\overline{A} = \overline{R}(A) = \overline{R}^1(A) \cap \overline{R}^2(A) = \{x \in X: xR_1 \cap xR_2 \cap A \neq \emptyset\} = \overline{A}^1 \cap \overline{A}^2$$

and many other properties are proved, especially, $\tau_{R_{12}} = \tau_{R_1 \cap R_2} = \tau_{R_1} \vee \tau_{R_2}$ and many examples on finite and infinite universes are given. If a bitopological space (X, τ_1, τ_2) is given, we introduced a condition (***) such that $C(A \cup B) = C(A) \cup C(B)$ becomes hold, and hence we obtained a topology $\tau_{A^{c1}} = \{A \subseteq X: A^{c1} \cup A^{c2} = A\}$ and proved that there exists a one-to-one correspondence between the family of all bitopological space satisfying the condition (***) which denoted by $BT\mathcal{S}^{***}$ and the family of all bipreordered spaces satisfying (*) which denoted by $BP\mathcal{S}^*$.

2. Material and Methods

2 Preliminaries

2.1 Definition[3]

Let R be any relation on X , $x \in X$ and $A \subseteq X$. The afterset(foreset) of x is defined respectively, by $xR_1 = \{y \in X: xRy\}$, $R_1x = \{y \in X: yRx\}$, and the upper(lower) approximation of A is defined by

$$\bar{R}(A) := \{x \in X: xR \cap A \neq \emptyset\} \quad (1)$$

$$\underline{R}(A) = (\bar{R}(A'))' \quad (2)$$

2.2 Theorem[24]

If R is reflexive, then the operator \bar{R} on $P(X)$, defined by (1), is Čech closure operator and hence it generates a topology on X given by

$$\tau_R = \{A \subseteq X: \bar{R}(A) = A\} \quad (3)$$

Moreover, if R is a preorder relation on X , then \bar{R} satisfies kuratowski's axioms i.e. for all $A \subseteq X$, $\bar{R}(A)$ represents the closure of A w.r.t. the induced topology τ_R and τ_R satisfies the following condition

COND: for all $x \in X$ and $A \subseteq X$, $x \in \bar{A} \iff \exists y \in A$ s.t. $x \in \bar{y}$ (4)

Let (X, τ) be a topological space (TS) and $\bar{}$ be its closure operator. We define a preorder relation on X by:

$$xRy \iff x \in \overline{\{y\}} \quad \forall x, y \in X \quad (5)$$

2.3 Theorem[24]

Let (X, τ) be a TS, $\bar{}$ be its closure operator and R be as defined in (5). If (X, τ) satisfies the condition (4), then:

1. $\bar{R}(A) = \bar{A} \quad \forall A \subseteq X$
2. $\tau_R = \tau$, where τ_R defined in (3)
3. $R_{\tau_R} = R$

2.4 Lemma

If R_1 and R_2 are two preorder relations on a non empty set X , then

$$x(R_1 \cap R_2) = xR_1 \cap xR_2$$

Proof. Straightforward.

2.5 Theorem[9]

Let (X, τ) be a TS. Then the following are equivalent:

1. (X, τ) satisfies the condition (4)
2. $\bigcup_{j \in J} \bar{A}_j = \overline{\bigcup_{j \in J} A_j}$
3. (X, τ) is an Alexandrov space.

2.6 Theorem[24]

There exists a one-to-one correspondence between the family of all preorder relations on X and the family of all topologies which satisfies (4).

3 Bipreordered Spaces

3.1 Definition

Let R_1 and R_2 be two preorder relations on a non empty set X . Then (X, R_1, R_2) is called bipreordered space (BPS).

3.2 Lemma

Let (X, R_1, R_2) be a BPS. Then pre-upper approximation operator $\bar{R}: P(X) \rightarrow P(X)$ given by:

$$\bar{R}(A) = \bar{R}^1(A) \cap \bar{R}^2(A) \quad (6)$$

where $\bar{R}^j(A)$, $j = 1, 2$ be defined in (1), satisfies the following properties:

1. $A \subseteq \bar{R}(A)$
2. $\bar{R}(A) \cup \bar{R}(B) \subseteq \bar{R}(A \cup B)$
3. $\bar{R}(A \cap B) \subseteq \bar{R}(A) \cap \bar{R}(B)$
4. $\bar{R}(\bar{R}(A)) = \bar{R}(A)$
5. $\bar{R}(X) = X$
6. $\underline{R}(A) = (\bar{R}(A'))'$

Proof. Straightforward

The following example shows that $\bar{R}(A) \cup \bar{R}(B) \neq \bar{R}(A \cup B)$.

3.3 Example

Let $X = \{a, b, c\}$, $R_1 = \Delta \cup \{(c, a), (b, c)\}$, $R_2 = \Delta \cup \{(c, a), (a, c)\}$, $A = \{c\}$ and $B = \{b\}$. Then $\bar{R}(A) \cup \bar{R}(B) \neq \bar{R}(A \cup B)$.

3.4 Definition

The BPS (X, R_1, R_2) is called BPS^* if it satisfies the following condition

(*): If $(R_1y \cap R_2z) \setminus \{y, z\} \neq \emptyset$, then yR_1z or zR_2y .

3.5 Examples

Let X be a non empty set, $a \in X$ and $A \subseteq X$. Then the following spaces (X, R_1, R_2) are examples for BPS^*

1. $R_1 = \Delta \cup \{(x, a): x \in X\}$, $R_2 = \Delta \cup \{(a, y): y \in X\}$
2. $R_1 = \Delta \cup \{(x, y): y \in A\}$, $R_2 = \Delta \cup \{(x, y): x \in A\}$

3.6 Theorem

If (X, R_1, R_2) is BPS^* , then

1. $\bar{R}(A \cup B) = \bar{R}(A) \cup \bar{R}(B)$, where $\bar{R}(A)$ as defined in(1)
2. $\bar{R}(A) = \{x \in X: xR_1 \cap xR_2 \cap A \neq \emptyset\}$
3. If we define $\tau_{R_{12}} = \{A \subseteq X: \bar{R}(A) = A\}$ then $\tau_{R_{12}}$ is a topology on X . Moreover, $\bar{A} = \bar{R}(A) = C(A) = \bar{A}^1 \cap \bar{A}^2$, where \bar{A}^j is the closure of A w.r.t. τ_{R_j} , $j = 1, 2$

Proof.

1. By Lemma (3.2).2

$$\overline{R}(A) \cup \overline{R}(B) \subseteq \overline{R}(A \cup B) \quad (7)$$

Let $x \in \overline{R}(A \cup B)$. Then $x \in \overline{R}^1(A \cup B)$ and $x \in \overline{R}^2(A \cup B)$ i.e. $xR_1 \cap (A \cup B) \neq \emptyset$ and $xR_2 \cap (A \cup B) \neq \emptyset$, i.e. there exists $y \in xR_1 \cap (A \cup B)$ and $z \in xR_2 \cap (A \cup B)$.

We have the following cases:

- If $y, z \in A$ then $xR_1 \cap A \neq \emptyset$ and $xR_2 \cap A \neq \emptyset$ which implies that $x \in \overline{R}(A)$ and then $\overline{R}(A) \cup \overline{R}(B) = \overline{R}(A \cup B)$.

- Similarly if $y, z \in B$.

- If $y \in A, z \in B$ and $y \in xR_1, z \in xR_2$, hence by (*) yR_1z or zR_2y . Since R_1, R_2 are transitive we have xR_1z or xR_2y , and hence $(xR_1 \cap B \neq \emptyset, xR_2 \cap B \neq \emptyset)$ or $(xR_1 \cap A \neq \emptyset, xR_2 \cap A \neq \emptyset)$. Hence $x \in \overline{R}(B)$ or $x \in \overline{R}(A)$, accordingly,

$$\overline{R}(A \cup B) \subseteq \overline{R}(A) \cup \overline{R}(B) \quad (8)$$

From (6) and (7) we get $\overline{R}(A \cup B) = \overline{R}(A) \cup \overline{R}(B)$.

- Similarly if $y \in B, z \in A$.

2. Let $x \in \overline{R}(A)$. Then $x \in \overline{R}^1(A)$ and $x \in \overline{R}^2(A)$, i.e. $xR_1 \cap A \neq \emptyset$ and $xR_2 \cap A \neq \emptyset$, i.e. there exists $y \in xR_1 \cap A$ and $z \in xR_2 \cap A$, hence by (*) yR_1z or zR_2y . Since R_1, R_2 are transitive we have xR_1z or xR_2y and hence $xR_1 \cap xR_2 \cap A \neq \emptyset$, i.e. $\overline{R}(A) \subseteq \{x \in X: xR_1 \cap xR_2 \cap A \neq \emptyset\}$. $\{x \in X: xR_1 \cap xR_2 \cap A \neq \emptyset\} \subseteq \overline{R}(A)$ is trivial. 3. Straightforward.

3.7 Theorem

Let (X, R_1, R_2) be a BPS*. Then τ_{R_1, R_2} satisfies condition (4).

Proof. Let $x \in C(A)$. It follows that $x \in \overline{R}(A)$ and hence $xR_1 \cap xR_2 \cap A \neq \emptyset$, i.e. $x \in \overline{R}(y) = C(\{y\})$.

3.8 Theorem

Let (X, R_1, R_2) be a BPS*. Then the family $\{xR_1 \cap xR_2: x \in X\}$ is a basis for τ_{R_1, R_2} .

Proof. Let $x \in G$ be an open subset of X . It follows that $x \in G = \underline{R}(G)$ and hence $x \in xR_1 \cap xR_2 \subseteq G$.

3.9 Lemma

Let (X, R_1, R_2) be a BPS*. Then

1. Since $xR_1 \cap xR_2$ is the smallest possible neighborhood of x
2. A subset A of X is open if and only if $A = \cup_{x \in A} (xR_1 \cap xR_2)$.

Proof.

1. Since R_1 and R_2 are reflexive relations. Then $x \in xR_1 \cap xR_2 \forall x \in X$, hence $xR_1 \cap xR_2$ is a neighborhood of x .

Let A be any neighborhood of x . It follows that $x \in i(A) = \underline{R}(A)$, hence $xR_1 \cap xR_2 \subseteq A$, i.e. $xR_1 \cap xR_2$ is the smallest possible neighborhood of x .

2. By Theorem 3.8. the result follows immediately.

3.10 Theorem

If (X, R_1, R_2) is BPS*, then

$$\tau_{R_1, R_2} = \tau_{R_1 \cap R_2}$$

Proof. For simplicity put $R_1 \cap R_2 = Q$. $A \in \tau_Q \Leftrightarrow \underline{Q}(A) = A \Leftrightarrow \{x: xQ \subseteq A\} = A \Leftrightarrow \{x: xR_1 \cap xR_2 \subseteq A\} = A \Leftrightarrow \underline{R}(A) = A \Leftrightarrow A \in \tau_{R_1, R_2}$, for all $A \subseteq X$. Then the result.

3.11 Theorem

If (X, R_1, R_2) is BPS*, then

$$\tau_{R_1, R_2} = \tau_{R_1} \vee \tau_{R_2}$$

i.e. τ_{R_1, R_2} is the least upper bound topology containing τ_{R_1}, τ_{R_2} .

Proof. We want to show that $\tau_{R_1} \vee \tau_{R_2} \subseteq \tau_{R_1, R_2}$ and the other inclusion is clear.

Let $A \in \tau_{R_1} \vee \tau_{R_2}$. Then

$$\begin{aligned} A &= \overline{R}(\cap_{i,j} (B_i' \cup B_j')) \\ &\subseteq \cap_{i,j} \overline{R}(B_i' \cup B_j') = \cap_{i,j} (\overline{R}(B_i') \cup \overline{R}(B_j')), \quad \text{by} \\ &\text{theorem 3.6(1)} \\ &= \cap_{i,j} (B_i' \cup B_j'), \text{ by (1)} \\ &= A'. \text{ Hence } \overline{R}(A'), \text{ and then } A \in \tau_{R_1, R_2}. \end{aligned}$$

4 Special Kinds of Bitopological Spaces

4.1 Definition

The bitopological space (BTS) (X, τ_1, τ_2) is called BTS** if it satisfies the following condition

$$(**): (\overline{\{y\}}^{\tau_1} \cap \overline{\{z\}}^{\tau_2}) \setminus \{y, z\} \neq \emptyset \Rightarrow y \in \overline{\{z\}}^{\tau_1} \text{ or } z \in \overline{\{y\}}^{\tau_2}, \text{ where } \tau_1 \text{ and } \tau_2 \text{ satisfy the condition (4).}$$

4.2 Example

Let X be a non empty set, $a \in X$ and $A \subseteq X$ Then the following spaces (X, τ_1, τ_2) are examples for BTS**

1. $\tau(a) = \{A \subseteq X: a \in A\} \cup \{\emptyset\}, \tau_2 = \{A \subseteq X: a \notin A\} \cup \{X\}$
2. $\tau_A = \{B \subseteq X: A \subseteq B\} \cup \{\emptyset\}, \tau^A = \{B \subseteq X: B \subseteq A\} \cup \{X\}$

The following example shows that the two topologies satisfy (**) but one of them does not satisfy (4)

4.3 Example

Let X be an infinite set and $a \in X$. The BTS (X, τ_{aa}, τ_a) where
 $\tau_{aa} = \{A \subseteq X: A' \text{ finite}\} \cup \{\emptyset\}$,
 $\tau_a = \{A \subseteq X: a \notin A\} \cup \{X\}$. Then each of τ_{aa}, τ_a satisfies (**) and (X, τ_{aa}) does not satisfy (4).
 The following example shows that the two topologies satisfy (**) but neither of them is COMP.

4.4 Example

The BTS $(\mathbb{R}, \tau_{aa}, \tau_N)$ where
 $\tau_{aa} = \{A \subseteq \mathbb{R}: A' \text{ finite}\} \cup \{\emptyset\}$,
 $\tau_N = \{G \subseteq \mathbb{R}: \forall x \in G \exists \varepsilon > 0 \text{ s.t. } (x - \varepsilon, x + \varepsilon) \subseteq G\}$
 satisfy (**), but neither (\mathbb{R}, τ_{aa}) nor (\mathbb{R}, τ_N) satisfies (4).

4.5 Theorem

Let (X, τ_1, τ_2) be a BTS^{**}. Then
 1. $C(A \cup B) = C(A) \cup C(B)$, where
 $C(A) = \overline{A^1} \cap \overline{A^2}, \forall A \in P(X)$, (9)
 $\overline{A^j}$ denotes the closure of A w.r.t $\tau_j, j = 1, 2$;
 2. $C(A)$ defined in (8) satisfies kuratowski's axioms and hence it generates a topology $\tau_{12} = \{A \subseteq X: i(A) = A\}$, where the interior of A
 $i(A) = (C(A'))'$ (10)
 3. τ_{12} satisfies condition COMP

Proof.

1. it's clear that
 $C(A) \cup C(B) \subseteq C(A \cup B)$ (11)
 Now, we want to prove the another inclusion
 Let $x \in C(A \cup B)$. Then $x \in \overline{A \cup B^1}$ and $x \in \overline{A \cup B^2}$. Hence by condition COMP, there exists $y \in A \cup B$ such that $x \in \overline{\{y\}^1}$ and $z \in A \cup B$ such that $x \in \overline{\{z\}^2}$.

we have the following cases:
 - if $y, z \in A$ then $x \in \overline{\{y\}^1} \subseteq \overline{A^1}$ and $x \in \overline{\{z\}^2} \subseteq \overline{A^2}$ and hence $x \in \overline{A^1} \cap \overline{A^2} = C(A)$. It follows that $C(A \cup B) = C(A) \cup C(B)$.
 - Similarly if $y, z \in B$.
 - If $y \in A, z \in B$ and $x \in \overline{\{y\}^1} \cap \overline{\{z\}^2}$. Hence by (**)
 $y \in \overline{\{z\}^1}$ or $z \in \overline{\{y\}^2}$. It follows that $x \in \overline{\{z\}^1}$ or $x \in \overline{\{y\}^2}$, and hence $x \in C(z)$ or $x \in C(y)$. it implies that $x \in C(B)$ or $x \in C(A)$, accordingly,
 $C(A \cup B) \subseteq C(A) \cup C(B)$ (12)
 From (10) and (11) we get
 $C(A \cup B) = C(A) \cup C(B)$.
 - Similarly if $y \in B, z \in A$.

2. Straightforward

3. Let $x \in C(A)$. Hence $x \in \overline{A^1} \cap \overline{A^2}$. It implies that there exists $y, z \in A$ such that $x \in \overline{\{y\}^1} \cap \overline{\{z\}^2}$. Hence by (**) $y \in \overline{\{z\}^1}$ or $z \in \overline{\{y\}^2}$, and hence $x \in \overline{\{z\}^1}$ or $x \in \overline{\{y\}^2}$. It follows that $x \in C(z)$ or $x \in C(y)$.

4.6 Theorem

There exists one-to-one correspondence between the family of all BPS^{**} and family of all BTS^{**}.

Proof. It suffices to prove that

$$(*) \Leftrightarrow (**) \quad (13)$$

Let $(\overline{\{y\}^1} \cap \overline{\{z\}^2}) \setminus \{y, z\} \neq \emptyset$. Then there exists $x \in X$ such that $x \in (\overline{\{y\}^1} \cap \overline{\{z\}^2}) \setminus \{y, z\} \neq \emptyset$. Hence xR_1y and xR_2z , and hence by (*) yR_2z or zR_1y . It implies that $y \in \overline{\{z\}^1}$ or $z \in \overline{\{y\}^2}$. Necessity of (12) is similar

Corresponding author

A.Zakaria
 Mathematics Department, Faculty of Education,
 Ain Shams University, Egypt.
amr_zakaria2008@yahoo.com

References

- [1] Abdalla Tallafha, Adnan Al-Bsoul, Ali Fora, Countable dense homogeneous bitopological space. Tr. J. of mathematics, 23 (1999) 233-242.
- [2] M. E. ABD EL-MONSEF, A.A Abo Khadra, A.A. Zedan, On Biapproximation space,
- [3] A. A. Allam, M. Y. Bakeir, E. A. Abo-tabl, Some methods for generating topologies by relations, Bull. Malays. Math. Sci. Soc., 31 (2008) 35-45.
- [4] C. C. Chan, A rough set approach to attribute generalization in data mining, J. Inf. Sci., 107 (1998) 169-176.
- [5] M. R. Chmielewshi and J. W. Grzymala-Busse, Global discretization of continuous attributes as preprocessing for machine learning. Int. J. Approx. Reason., 15 (1966) 319-331.
- [6] B. Davvaz, Roughness in rings, Inf. Sci., 164 (2004) 147-163.
- [7] B. P. Dvalishvili, The lower and Upper Topologies as Bitopological. Proc. Tbilisi state Univ., 55 (2003) 37-52.
- [8] B. P. Dvalishvili, Bitopological Spaces: Theory, Relations with Generalized Algebraic Structures, and Applications, North Holland, 2005.
- [9] Hua-Peng Zhang, Yao Ouyang, Zhudeng Wang, Note on "Generalized rough sets based on reflexive and transitive relations", Information Sciences, 179 (2009) 471-473.
- [10] G. C. Kelly, Bitopological space. Proc. London Math. Soc., 13 (1963) 71-89.

- [11] M. Kondo, On the structure of generalized rough sets, information sciences, 176 (2006) 589-600.
- [12] R. Koppermqn, J. D. Lawson, Bitopological and Topological orderd K-spaces. Topology and its Applications 146-147,385-396, 2005.
- [13] E. P. Lane, Quasi-proximities and bitopological space, Portugal Math. 28 (1969) 181-159.
- [14] H. J. Lee, J. B. Park, and Y. H. Joo, Robust load-frequency control for uncertain nonlinear power systems: A fuzzy logic approach, Inf. Sci., 176 (2006) 3520-3537.
- [15] W. N. Liu, Y. JingTao and Y. Yiyu, Rough approximations under level fuzzy sets, in Proc. 4th Int. Conf., RSCTC, S. S. Tsumoto, K. J. Roman et al. Eds., (2004) 78-83.
- [16] D. Mcsherry, Knowledge discovery by inspection, Decis. Support Syst., 21 (1997) 43-47.
- [17] Z. Pawlak, Rough sets, Int. J. Comput. Inf. Sci., 11 (1982) 341-356.
- [18] Z. Pawlak, Rough set approach to knowledge-based decision support, Eur. J. Oper. Res., 99 (1997) 48-57.
- [19] Z. Pawlak, A. Skowron, Rudiments of rough sets, Information Sciences, 177 (2007) 3-27.
- [20] Z. Pawlak, A. Skowron, Rough sets: some extensions, Information Sciences, 177 (2007) 28-40.
- [21] Z. Pawlak, A. Skowron, Rough sets and Boolean reasoning, Information Sciences, 177 (2007) 41-73.
- [22] J. F. Peters, K. Ziaei, and S. Ramanna, Approximate time rough control: Concepts and application to satellite attitude control, in Proc. RSCTC, (1998) 491-498.
- [23] J. C. Pomerol, Artificial intelligence and human decision making, Eur. J. Oper. Res., 99 (1997) 3-25.
- [24] K. Qin, J. Yang, Z. Pei, Generalized rough sets based on reflexive and transitive relations, information sciences, 178 (2008) 4138-4141.
- [25] A. Skowron, J. Stepaniuk, Tolerance approximation spaces, Fundamenta Informaticae 27 245-253, 1996.
- [26] M. E. Yahia, R. Mahaod, N. Sulaiman, and F. Ahamad, Rough neural expert systems, Expert Syst. Appl., vol. 18, no. 2, pp. 87-99, Feb. 2000.
- [27] Y.Y. Yao, Two views of the theory of rough sets in finite universes, International Journal of Approximate Reasoning 15 291-317, 1996.
- [28] Y.Y. Yao, Constructive and algebraic methods of the theory of rough sets, Information Sciences 109 21-47, 1998.
- [29] Y.Y. Yao, T Y Lin, Generalization of rough sets using modal logics, Intelligent Automation and Soft Computing 2 103-120, 1996.

8/18/2011

Effect of Grape Seeds Extract in the Modulation of Matrix Metalloproteinase-9 Activity and Oxidative Stress Induced By Doxorubicin in Mice

*Monira A. Abd El Kader, Nermin M. El-Sammad, and Amal A.Fyiad

Biochemistry Department, National Research Center, Dokki, Cairo, Egypt

*mkader1233@yahoo.com

Abstract: The therapeutic value of doxorubicin as antitumor agent is limited by its cardiotoxicity. Matrix metalloproteinases activation is an early event in doxorubicin-induced cardiotoxicity. Because Matrix metalloproteinases are up-regulated by increased formation of reactive oxygen species, the present study was designed to test whether the grape seeds extract could attenuate the increases in matrix metalloproteinase-9 activity and prevent the doxorubicin-induced cardiotoxicity in mice. Mice were dosed with a single injection of doxorubicin (20 mg/kg b.wt, i.p) with or without pretreatment of grape seeds extract. The protective role of grape seeds extract against doxorubicin-induced cardiac damage was evaluated on the aspects of the release of cardiac enzymes into serum, the formation of malondialdehyde, the activation of matrix metalloproteinase-9 and the histopathological changes in heart tissues. The results showed that doxorubicin led to increase in serum metalloproteinase-9 activity, heart injury as shown by increased serum creatine kinase, lactate dehydrogenase, alanin aminotransferase and aspartat aminotransferase. Oxidative stress was also increased in cardiac tissue as shown by increased malondialdehyde and decrease of antioxidants (superoxide dismutase, catalase and reduced glutathione). This damage was accompanied with histopathological changes in the heart tissue. Pretreatment with GS extract (100mg/kg b.wt daily for 12 days) effectively hindered the adverse effect of doxorubicin and protect against cardiac damage via suppression of oxidative stress.

[Monira A. Abd El Kader, Nermin M. El-Sammad, and Amal A.Fyiad. Effect of Grape Seeds Extract in the Modulation of Matrix Metalloproteinase-9 Activity and Oxidative Stress Induced By Doxorubicin in Mice. [Life Science Journal. 2011; 8(3):510-515] (ISSN: 1097-8135). <http://www.lifesciencesite.com>.

Keywords: matrix metalloproteinase-9, reduced glutathione, lipid peroxidation, cardiotoxicity.

Abbreviations: Dox, doxorubicin; ROS, reactive oxygen species; MMPs, matrix metalloproteinases; MMP-9, matrix metalloproteinase-9; TIMPs tissue inhibitors of metalloproteinase; GS, grape seed; LDH, lactate dehydrogenase; CK, creatine kinase; MDA, malondialdehyde; SOD, superoxide dismutase; CAT, catalase; GSH, reduced glutathione.

1. Introduction

The anthracycline antibiotic doxorubicin [Adriamycin[®], (Dox)] is one of the most effective chemotherapeutic agents against a wide variety of cancers, but its clinical use is limited by development of cardiotoxicity, which may ultimately lead to severe and irreversible cardiomyopathy^[1]. The cause of Dox cardiotoxicity is multifactorial, even though most Dox-induced cardiac effects can be attributed to the formation of reactive oxygen species (ROS), which ultimately results in myocyte apoptosis (or programmed cell death)^[2]. Several studies suggest that ROS play a major role in the activation of matrix metalloproteinases (MMPs). These are an endogenous family of zinc-dependent enzymes that have an important role in vascular dysfunction and tissue remodeling in many cardiovascular conditions as a result of increased oxidative stress^[3,4]. MMPs are regulated at multiple levels including transcription, secretion, and activation of inactive zymogens while their activity is under the strict control of specific tissue inhibitors of

metalloproteinase (TIMPs)^[5]. Dox was found to be induced matrix metalloproteinase-9 (MMP-9) expression and activation in the heart^[6]. A great deal of effort has been made to identify which agents might mitigate the cardiotoxic effects of Dox. Because of free radical plays important role in Dox-induced cardiotoxicity, it is logical to consider antioxidants as primary potential therapeutic agent to prevent such toxic effect. In fact, several compounds with antioxidant properties (carvedilol, sesame oil and statin) have been investigated with some degree of success^[7-9]. In spite of up regulation of MMPs was reported in animal models of Dox-induced cardiotoxicity^[6,10,11], few studies examined whether antioxidants could prevent the increases in MMP-9 level associated with Dox-induced cardiotoxicity^[12].

Grape seed extract (GS extract) is a natural extract from the seed of grape^[13]. It is a rich source of one of the most beneficial groups of plant flavonoids and pro-anthocyanidins oligomers^[14]. It improves hepatic ischemia-reperfusion injury and reduces the size of the infarct in cardiac ischemia in

the rat^[15]. GS extract involves in ameliorating the oxidative stress *in vitro* and *in vivo*^[16]. The aim of the present study was to investigate the possible potential role of GS extract in the modulation of the increased activity of MMP-9 and oxidative stress induced by Dox in mouse model.

2. Material and Methods

Chemicals

Doxorubicin (Adriablastina) was purchased in a vial contains 10 mg powder from Pharmacia & Upjohn Co. S.P.A, Milan, Italy. GS extract (proanthocyanidins 95%) was obtained from Arab Company for Pharmaceuticals and Medicinal Plants (MEPACO-Egypt), which is patented as Gervital (patent ARE 312034-vrs1). All other chemicals and solvents that required for the biochemical assays were of highest purity and analytical grade and purchased from Sigma-Aldrich Chemic (Deisenhofen, Germany). Reagent Kits for MMP-9 was purchased from Quantikine, RnD Systems Co. (UK). Commercially available reagent kits for assays aspartate aminotransferase (AST), alanine aminotransferase (ALT), lactate dehydrogenase (LDH), and creatine kinase (CK) were obtained from Stanbio Laboratory (USA). Reagent Kits for determination of malondialdehyde (MDA), reduced glutathione (GSH), catalase (CAT) and superoxide dismutase (SOD) were purchased from Biodiagnostics (Egypt).

Animals and experimental design:

Forty eight male adult Swiss albino mice weighing (20-25g) were obtained from the Animal House in National Research Centre, Egypt. Animals were housed in plastic cages at an environmentally controlled room (constant temperature 25-27°C, with 12h light / dark cycle) for one week prior to starting the experiments and they were fed on standard feed, water *ad libitum*. All animals received humane care in compliance with the international guiding principles for animal research. The experimental procedure used in this study met the guidelines of the ethics committee of the National Research Centre. The animals were fasted for 16-18 hrs before sacrificing. Doxorubicin was reconstituted in 5ml of dist. water and injected intraperitoneally to animals at a single dose of 20 mg/ kg body weight which was evaluated to cause cardiotoxicity^[8,9]. GS extract was dissolved in de-ionized water (5mg/ml) and administered to animals by oral gavages at a dose of 100 mg / kg b.w. The dose of GS extract used was selected on the basis of the previous studies^[17].

The animals were randomly assigned into four groups containing twelve mice each one.

Control group: Mice were received 0.5 ml vehicle (distilled water) through oral intubation for 12 days,

GS extract group: Mice were received 0.5 ml (2.5 mg) of GS extract through oral intubation for 12 consecutive days.

Dox group: Mice were received vehicle for 7 days and afterwards treated with a single i.p injection of Dox, then vehicle treatment continued for 5 days.

(GS extract+Dox) group: The mice were administered with 0.5ml (2.5 mg) GS extract orally for 7 days prior to i.p injection of Dox followed by administration 0.5 ml (2.5 mg) of GS extract for other 5 days.

At the end of the experiment, the mice were sacrificed under anesthesia. Blood was collected and serum was separated by centrifugation at 3000 rpm. The serum was used for the determination of AST and ALT activities by colorimetric method^[18]. LDH^[19] and CK^[20] activities were estimated by kinetic procedures. MMP-9 activity was assayed by Immunoassay method^[5]. The hearts were dissected out and portions of them were preserved in 10% formalin (pH7.2) and subjected to histopathological examination^[21]. The remaining parts of the hearts were immediately washed in ice cold physiological saline and homogenized in 100 mM tris- HCl buffer (pH 7.4) to render 10% homogenate. Aliquots of homogenate were used for MDA^[22], GSH^[23], SOD^[24] and CAT^[25] estimation.

Statistical Analysis

The results were expressed as mean \pm SD of different groups. The differences between the mean values were evaluated by ANOVA followed by student's "t" test. All analyses were performed using Statistical Package for the Social Sciences software (SPSS Inc., Chicago, IL). Values of $P < 0.05$ were regarded as significant.

3. Results

Serum markers of heart damage: There was a significant ($P < 0.001$) increase in the activities of LDH, CK and AST as well as a significant ($P < 0.01$) increase for ALT activity in the Dox group as compared with control group. The administration of GS extract along with Dox significantly attenuated elevation of these enzymes (Table 1). There was insignificant difference in the activities of above enzymes between control and GS extract group.

Serum MMP-9 activity: As shown in Table 1, Dox injection produced a significant increase in the serum activity of MMP-9 (3.6000 \pm 0.8075 ng/ml; $P < 0.001$) as compared with control group (0.8383 \pm 0.1585 ng/ml). This effect was significantly ($P < 0.001$) modulated by the administration of GS

extract which decreased the activity of MMP-9 (0.7750 ± 0.2034 ng/ml) as compared with Dox

group. Treatment with GS extract alone has no effect on MMP-9 activity.

Table (1): Effect of administration of Dox alone and along with GS extract on serum markers of cardiotoxicity and MMP-9 activity

Group	LDH U/L	CK U/L	AST U/ml	ALT U/ml	MMP-9 ng/ml
Control group	155.85 ± 35.55	112.71 ± 15.08	28.83 ± 6.59	27.67 ± 7.17	0.8383 ± 0.1585
GS extract group	175.56 ± 16.66	119.16 ± 16.77	32.75 ± 8.48	31.33 ± 5.32	0.7367 ± 0.1946
Dox group	538.09 ± 140.54 ^{ac}	409.65 ± 124.76 ^{ac}	90.67 ± 15.36 ^{ac}	43.83 ± 9.84 ^{ab}	3.6000 ± 0.8075 ^{ac}
(GS extract+Dox) group	222.29 ± 41.77 ^c	172.56 ± 38.44 ^b	44.50 ± 8.78 ^c	37.67 ± 7.39	0.7750 ± 0.2034 ^{ac}

Values are expressed as mean ± SD (n=12). P values: a < 0.05, b < 0.01, c < 0.001 vs Dox and aa < 0.05, ab < 0.01, ac < 0.001 vs control (one way ANOVA).

Heart oxidative stress and antioxidant activity:

The concentrations of MDA (a marker of lipid peroxidation) & GSH (a non-enzymatic antioxidant) and the activities of SOD & CAT (enzymatic antioxidants) were shown in Table 2. GS extract administration alone did not alter the previous measurements. There was a significant ($P < 0.001$) increase of MDA concentration (139.57 ± 18.85 nmol/g) in the Dox-treated group as compared with control (73.67 ± 9.22 nmol/g). Treatment with GS extract along with Dox significantly ($P < 0.001$) reduced the MDA level (83.51 ± 11.29 nmol/g) as compared to Dox group. The activity of SOD which was observed to be lower in the Dox group

(354.24 ± 106.14 U/g tissue ; $P < 0.05$) as compared with control (615.71 ± 281.04 U/g) , was also attenuated by GS extract (636.99 ± 136.85 U/g; $P < 0.001$). Administration of Dox also produced a significant decrease in the activity of CAT (0.52 ± 0.14 U/g; $P < 0.01$) as compared to that of control group (1.98 ± 0.73 U/g). Treatment with GS extract significantly attenuated the CAT activity (0.99 ± 0.38 ; $P < 0.01$) as compared to Dox group. The GSH level showed marked reduction in the Dox group (5.29 ± 1.31 mg/g; $P < 0.001$) as compared to control group (10.64 ± 1.54 mg/g). Similarly, treatment with GS extract reversed this effect (9.06 ± 0.87 mg/g; $P < 0.001$).

Table (2): Effect of administration of Dox alone and along with GS extract on biomarkers of oxidative stress

Group	MAD nmol/g tissue	SOD U/g tissue	CAT U/g tissue	GSH mg/g tissue
Control group	73.67 ± 9.22	615.71 ± 281.04	1.98 ± 0.73	10.64 ± 1.54
GS extract group	72.23 ± 7.23	726.23 ± 134.62	1.67 ± 0.90	10.76 ± 1.33
DOX group	139.57 ± 18.85 ^{ac}	354.24 ± 106.14 ^{aa}	0.52 ± 0.14 ^{ab}	5.29 ± 1.31 ^{ac}
(GS extract + DOX) group	83.51 ± 11.29 ^c	636.99 ± 136.85 ^c	0.99 ± 0.38 ^b	9.06 ± 0.87 ^c

Values are expressed as mean ± SD (n=12). P values: a < 0.05, b < 0.01, c < 0.001 vs Dox and aa < 0.05, ab < 0.01, ac < 0.001 vs control (one way ANOVA).

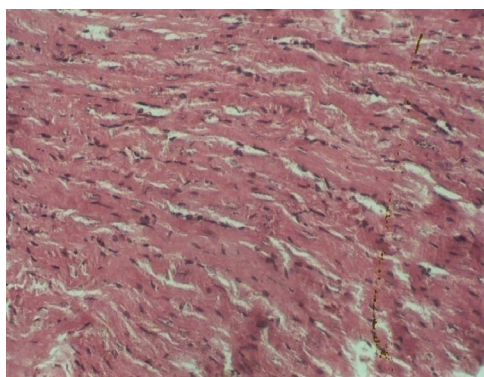


Fig (1): The cardiac muscle of control mouse revealing longitudinally sectioned cardiac muscle branching. The centrally located nucleus is surrounded by clear area. (H&E, X20).

Histopathological effects of Dox:

Fig.1 shows the light micrograph of cardiac muscle of control mice revealing longitudinally sectioned cardiac muscle branching. The centrally located nucleus is surrounded by clear area. Light micrograph of heart of mice treated with GS extract alone showed normal structure (Fig.2). Degenerations of the myofibrils, vacuolated cytoplasm, separation and focal hemorrhage in-between cardiac muscle fibers were clearly seen in the Dox treated group (Fig.3). Animals treated with GS extract along with Dox showed better-preserved appearance of cardiac muscle fibers with slight pyknosis of nucleus of cardiac muscle fibers (Fig.4).

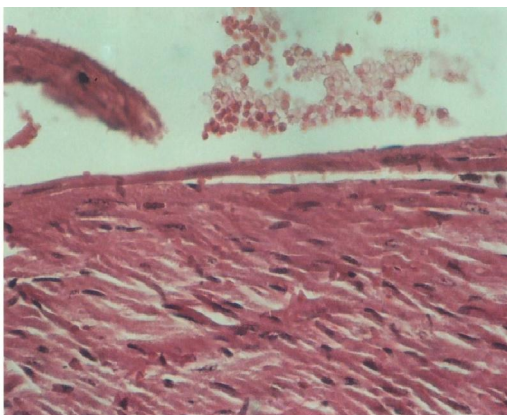


Fig (2): The cardiac muscle of a mouse after treatment with GS extract alone revealing normal structure (H&E, X40).

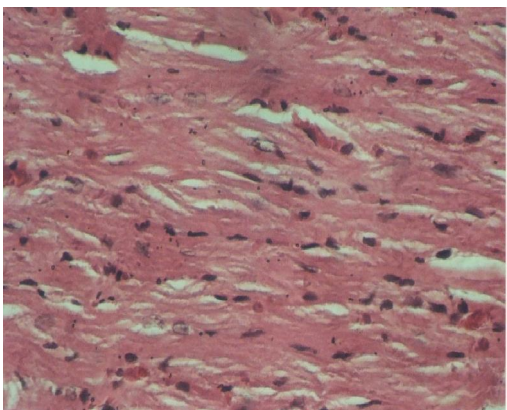


Fig (3): The cardiac muscle of a mouse after treatment with Dox showing degenerations of the myofibrils, vacuolated cytoplasm, separation and focal hemorrhage in-between cardiac muscle fibers (H&E, X40)

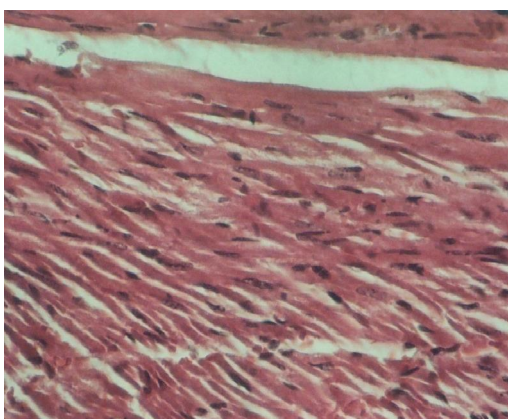


Fig (4): The cardiac muscle of a mouse after treatment with GS extract along with Dox revealing better-preserved appearance of cardiac muscle fibers with slight pyknosis of nucleus of cardiac muscle fibers (H&E, X40).

4. Discussion

The clinical use of Dox is marred by its unwanted side effects that include cardiomyopathy and congestive heart failure¹. Many studies indicated that oxidative stress from Dox disposition is significantly correlated with the Dox -induced cardiotoxicity^[8,9,26].

The present study demonstrates that GS extract administered along with Dox is an effective scavenger of toxic free radicals and inhibitor of lipid peroxidation. Oxidative stress is increased after Dox treatment due to overproduction of ROS and decreased efficiency of endogenous antioxidant defenses in heart, liver, kidney and brain^[27]. In this study, intraperitoneal administration of Dox at a single dose of (20 mg/kg b.w.) induced cardiovascular changes by increase in free radical production as indicated by significant increase in LDH, CK, AST, ALT and MDA. These results are consistent with earlier studies^[26,28]. In our study, the increase in serum CK and LDH might indicate the leakage of these enzymes through the membranes. The activities of serum CK and LDH have been widely used as parameters for the diagnosis of cardiac dysfunction and the increase of CK level in serum and in myocytes culture media as a result of possible cell damage is occurring in concert with the decrease of CK activity in the cardiac tissue^[29].

The present study also confirmed that treatment with Dox significantly increased the MDA level (a marker of lipid peroxidation and an indicator of oxidative injury) and decreased the SOD and CAT activities and GSH level in cardiac tissues. These results are in accordance with the findings from other animal models treated with Dox^[26,28]. The observed decrease in GSH level in our study group treated with Dox could be possibly due to its conversion to oxidized glutathione or due to decreased synthesis under oxidative stress. Comporti^[30] reported that, the depletion of GSH resulted in enhanced lipid peroxidation, and excessive lipid peroxidation caused increased GSH consumption.

In the present work, the observed depletion in GSH levels and decreased activities of SOD and CAT can be correlated with significant increment in cardiac lipid peroxidation in Dox-treated mice and indicate higher susceptibility of myocardium to oxidative damage. SOD protects cells from oxidative damage by converting superoxide radicals into hydrogen peroxide, which gets further metabolized by CAT to molecular oxygen and water^[31]. Lipid peroxidation which has been linked with altered membrane structure and inactivation of SOD and CAT resulting in accumulation of superoxide anion, which further damages the myocardium. Therefore, according to the present data, it seems that increased

CK and LDH in serum paralleled the inhibition of SOD and CAT activities and decreased GSH level and production of MDA in heart of Dox treated mice. Thus, the present findings might confirm that the heart damage resulting in leakage and increase in CK and LDH levels in serum as a consequence of cellular oxidative injury induced by Dox mediated ROS production.

The present study demonstrated that the levels of AST, ALT, CK and LDH were greatly attenuated in serum of mice receiving GS extract for twelve days during Dox treatment. This is accompanied by a marked protection against lipid peroxidation as well as amelioration of the inhibition of SOD and CAT activities and GSH level in heart. Furthermore, light microscopy of all the mice tissue sections treated with GS extract showed a well-preserved normal morphology of cardiac muscle. Such amelioration effect might be due to that the grape seeds are rich sources of monomeric phenolic compounds such as catechin, epicatechin, dimeric, trimeric and tetrameric proanthocyanidins^[32] which confers on them an antioxidant property and their protection against cardiac cell apoptosis via the induction of endogenous antioxidant enzymes which may be an important mechanism underlying the protective effects of GS extract observed with various forms of cardiovascular disorders^[33]. Moreover, GS extract inhibits enzyme systems that are responsible for the production of free radicals^[34].

The increase in serum MMP-9 activity in mice treated with Dox in this work are in accordance with the findings of Bai *et al.*,^[6] and Li *et al.*,^[12] who reported that MMPs activation is an early event in Dox-induced cardiotoxicity. Spallarossa *et al.*,^[10] showed that low doses of Dox, which had previously been found to induce apoptotic, and not necrotic cell death in cardiomyocytes, also induce early transcription and activation of MMP-9 in these cells without changing the transcript levels of their inhibitors, TIMP-1 and TIMP-2. However, when MMPs activity is increased with insufficient quenching activity by TIMPs, progressive disruption of the collagen network occurs, thus leading to progressive dilation and remodeling of the left ventricle^[35]. Interestingly, the present study, revealed that GS extract reduced the activity of serum MMP-9 that induced by Dox treatment, thus offering a mechanistic insight into protective effect associated with antioxidant therapy against the alterations induced by Dox.

Conclusion

Our study suggests that GS extract produce cardioprotective effects against Dox- induced cardiotoxicity, which may be through re-modulation

of MMP-9 and reducing oxidative stress, but further studies are needed to evaluate the possible effect of GS extract on TIMPs to confirm whether GS extract is possible as an early inhibitory therapy before myocardial injury induced by Dox treatment.

Acknowledgments

The authors are grateful to Prof. Dr. Menha Swellam at Biochemistry Dept. at National Research Center for her great help to perform the statistical analysis and also to the members of histology unit at Research Institute of Ophthalmology, Giza for their help to perform the histological part of the paper.

Corresponding author

Monira A. Abd El Kader
Biochemistry Department, National Research Center,
Dokki, Cairo, Egypt
mkader1233@yahoo.com

References

1. Minotti, G., Menna, P., Salvatorelli, E., Cairo, G. and Gianni, L. (2004). Anthracyclines: molecular advances and pharmacologic developments in antitumor activity and cardiotoxicity. *Pharmacol. Rev.*, 56: 185–229.
2. Spallarossa, P., Garibaldi, S., Altieri, P., Fabbi, P., Manca, V. *et al.* (2004). Carvedilol prevents doxorubicin-induced free radical release and apoptosis in cardiomyocytes in vitro. *J. Mol. Cell Cardiol.*, 37: 837– 846.
3. Siwik, D.A., Pagano, P.J. and Colucci, W.S. (2001). Oxidative stress regulates collagen synthesis and matrix metalloproteinase activity in cardiac fibroblasts. *Am. J. Physiol. Cell. Physiol.*, 280: C53-60.
4. Castier, Y., Brandes, R. P., Leseche, G., Tedgui, A. and Lehoux, S. (2005). p47phox-dependent NADPH oxidase regulates flow-induced vascular remodeling. *Circ. Res.*, 97:533–540.
5. Nagase, H. and Woessner, J.r. (1999). Matrix metalloproteinases. *J. Biol. Chem.*, 274:21491–21494.
6. Bai, P., Mabley, J.G., Liaudet, L., Virág, L., Szabó, C. *et al.*(2004). Matrix metalloproteinase activation is an early event in doxorubicin induced cardiotoxicity. *Oncol. Rep.*, 11: 505-508.
7. Oliveira, P. J., Bjork, J. A., Santos, M. S., Leino, R. L., Froberg, M. K. *et al.*(2004). Carvedilol-mediated antioxidant protection against doxorubicin-induced cardiac mitochondrial toxicity. *Toxicol. App. Pharmacol.*, 200: 159-168.
8. Shad, K. F., Al-Salam, S. and Hamza, A.A. (2007). Sesame oil as a protective agent against doxorubicin induced cardio toxicity in rat. *American J. Pharmacol. Toxicol.*, 2: 159-163.
9. Riad, A., Bien, S., Westermann, D., Becher, P., Loya, K. *et al.* (2009). Pretreatment with Statin

- Attenuates the Cardiotoxicity of Doxorubicin in Mice. *Cancer Res.*, 69: 695-699.
10. Spallarossa, P., Altieri, P., Garibaldi, S., Ghigliotti, G., Barisione, C. *et al.* (2006). Matrix metalloproteinase-2 and -9 are induced differently by doxorubicin in H9c2 cells: The role of MAP kinases and NAD(P)H oxidase. *Cardiovasc. Res.*, 69 : 736 – 745.
 11. Goetzenich, A., Hatam, N., Zerneck, A., Weber, C., Czarnotta, T. *et al.* (2009). Alteration of Matrix Metalloproteinases in Selective Left Ventricular Adriamycin-Induced Cardiomyopathy in the Pig. *The Journal of Heart and Lung Transplantation*, 28: 1087-1093.
 12. Li, L., Pan, Q., Han, W., Liu, Z., Li, L. *et al.* (2007). Schisandrin B Prevents Doxorubicin-Induced Cardiotoxicity via Enhancing Glutathione Redox Cycling. *Clin. Cancer Res.*, 13: 6753-6760.
 13. Asl, M.N. and Hosseinzadeh, H. (2009). Review of the pharmacological effects of *Vitis vinifera* (grape) and its bioactive compounds. *Phytotherapy Res.*, 10 : 1002.
 14. El-Ashmawy, I.M., Saleh, A. and Salama, O.M. (2007). Effects of marjoram volatile oil and grape seed extract on ethanol toxicity in male rats. *Basic & Clin. Pharmacol. Toxicol.*, 101:320-327.
 15. Sehirlı, O., Ozel, Y., Dulundu, E., Topaloglu, U., Ercan, F. *et al.* (2008). Grape seed extract treatment reduces hepatic ischemia reperfusion injury in rats. *Phytother Res.*, 22: 43-48.
 16. Martinez-Florez, S., Gonzalez-Gallego, J. and Culebras, J. M. (2002). Flavonoids: properties and antioxidizing action. *Nutr. Hosp.*, 17:271-278.
 17. Çetin, A., Kaynar, L., Kocyigit, I., Hacıoglu, S. K., Saraymen, R. *et al.* (2008). The effect of grape seed extract on radiation-induced oxidative stress in the rat liver. *Turk. J. Gastroenterol.*, 19: 92-98.
 18. Reitman, A. and Frankel, S.A. (1957). Colorimetric method for determination of serum glutamic oxaloacetic and glutamic pyruvic transaminases. *Am. J. Clin. Path.*, 28:56-63.
 19. Buhl, S.N. and Jackson, K.Y. (1978). Optimal conditions and comparison of lactate dehydrogenase catalysis of the lactate to pyruvate and pyruvate to lactate reactions in serum at 25, 30, and 37degrees C. *Clin Chem.*, 24: 828-831.
 20. Tietz, N. W. (1986). *Textbook of Clinical Chemistry*, W.B. Saunders Co., Philadelphia, p. 678-686.
 21. Ross, M.H., Reith, E.J. and Romrell, L.J. (1989). *Histology: A Text and Atlas* (2nd ed). Baltimore. Williams & Wilkins, p. 51–84.
 22. Ohkawa, H., Ohishi, W. and Yagi, K. (1979). Assay for lipid peroxides in animal tissues by thiobarbituric acid reaction. *Anal. Biochem.*, 95 : 351.
 23. Beutler, E., Duron, O. and Kelly, B. (1963). Improved method for the determination of blood glutathione. *J. Lab. Clin. Med.*, 61: 882-88.
 24. Nishikimi, M., Roa, N.A. and Yogi, K. (1972). Measurement of superoxide dismutase. *Biochem. Biophys. Res. Commun.*, 46: 849-854.
 25. Aebi, H. (1984). Catalase *in vitro*. *Methods Enzymol.*, 5: 121-126.
 26. Li, W., Xu, B., Xu, J. and Wu, X.L. (2009). Procyanidins Produce Significant Attenuation of Doxorubicin-Induced Cardiotoxicity via Suppression of Oxidative Stress. *Basic & Clin. Pharmacol. Toxicol.*, 104 : 192–197.
 27. Pristos, C.A. and Ma, J. (2000). Basal and drug-induced antioxidant enzyme activities coelate with age dependant doxorubicin oxidative toxicity. *Chem. Biol. Interact.*, 127: 1–11.
 28. Andreadou, I., Sigala, F., Iliodromitis, E.K., Papaefthimiou, M. and Sigalas, C. (2007). Acute doxorubicin cardiotoxicity is successfully treated with the phytochemical oleuropein through suppression of oxidative and nitrosative stress. *J. Mol. Cell. Cardiol.*, 42 : 549–558.
 29. Miura, T., Muraoka, S. and Fujimoto, Y. (2000). Inactivation of creatin kinase by adriamycin during interaction with horseradish peroxidase. *Biochem. Pharmacol.*, 60 : 95–99.
 30. Comporti, M. (1985). Biology of disease: lipid peroxidation and cellular damage in toxic liver injury. *Lab Invest.*, 53 : 599–623.
 31. Rajadurai, M. and Mainzen Prince, P.S. (2006). Preventive effect of naringen on lipid peroxides and antioxidants in isoproterenol-induced cardiotoxicity in Wistar rats: Biochemical and histopathol. evidences. *Toxicol.*, 228 :259-268.
 32. Monagas, M., Hernandez-Ledesma, B., Gomez-Cordoves, C. and Bartolommeo, B. (2006). Commercial ingredients from *Vitis vinifera* L. leaves and grape skins: Antioxidants and chemical characterization. *J. Agric. Food Chem.*, 54: 319-327.
 33. Du, Y., Guo, H. and Lou, H. (2007). Grape Seed Polyphenols Protect Cardiac Cells from Apoptosis via Induction of Endogenous Antioxidant Enzymes. *J. Agric. Food Chem.*, 55: 1695–1701.
 34. Maier, T., Schieber, A., Kammerer, D. and Carle, R. (2009). Residues of grape (*Vitis vinifera* L.) seed oil production as a valuable source of phenolic antioxidants. *Food Chem.*, 112: 551-559.
 35. Spinale, F.G. (2002). Matrix metalloproteinases: regulation and dysregulation in the failing heart. *Circ. Res.*, 90: 520– 530.

Effect of Powder and Essential Oil of Lemon grass on Aflatoxins Production in Dried Water Melon Seed**Eman M. Hegazy**Food Toxicology and Contaminants Department, National Research Center, Dokki, Giza, Egypt
eman_hegazy@hotmail.com

Abstract: Antifungal activity of powder and essential oil from dried ground leaves of Lemon grass (*Cymbopogon citratus*) to control aflatoxin production by *Aspergillus flavus* NRRL 5096 on dried water melon seed by sun, oven, smoke and solar drying were studied. The powdered dry leaves and essential oil from lemon grass were mixed with seeds at levels ranging from 5-75 g and 0.1 to 2.0 % respectively. Obtained results revealed that the Minimal Inhibitory Concentration (MIC) on fungi was mixture of 75g powder and 0.1% oil. Also the moisture content ranged between 8.94-6.26% for dried water melon seed in addition, *A. niger* was the most frequent genus isolated from water melon seed before and after drying. Toxigenic of *A. flavus* were isolated from water melon seed dried by sun drying produced aflatoxin B₁ and B₂ at concentration 3.50 and 2.67 µg/L in liquid broth media respectively. Oven drying was the best method for drying water melon seed.

[Eman M. Hegazy. **Effect of Powder and Essential Oil of Lemon grass on Aflatoxins Production in Dried Water Melon Seed**] Life Science Journal. 2011; 8(3):516-522] (ISSN: 1097-8135).
<http://www.lifesciencesite.com>.

Key words: powder and essential oil of *Cymbopogon citrates*, aflatoxins, dried water melon seed, Lemon grass.

1. Introduction

Aflatoxins are, the toxic metabolites produced by *Aspergillus flavus* and *Aspergillus parasiticus*. It is the most potent hepatocarcinogen and mutagen among mycotoxins. Several mycotoxins in agricultural products cause health hazards to people and animals and economical problem (IARC, 1993).

Dangerous mycotoxins are naturally present in foods, feeds and our environment (Dragan *et al.*, 2010).

Water melon seed (*Citrullus vulgaris*) are smooth and black color. In Egypt, water melon seeds can be dried, roasted with salt and served as snacks. It is cultivated in the tropics for its seed which are a source of protein in important soup condiment in African diet (Ekundayo, 1987). Water melon seed are priced for highly nutritive contain protein, starch, vitamins, especially vitamin B and C and oils at level 27% (oleic, linoleic, palmitic and stearic) which used as vegetable oil. Also seeds are consumed in various forms such as (equisi) soup, melon ball snacks and ogori (fermented melon seed condiment used in seasoning) (Odunfa, 1981). Melon seed proteins contain low level of lysin, large amounts of glutamic acid, aspartic acid and arginine (King and Onuora, 1984). Also, cooked Nigeria sausages with full fat egusi (melon seed) meal was produced with up 30% meat replacement, which had acceptable sausage with fat content and juiciness increased (Akobundu, 1989). A beverage from melon seeds in Turkey was produced to make a waste product available for human consumption which was a good source of iron, magnesium and a fair of source of protein, with a concentration of 0.31 mg/100g vitamin C (Karakaya *et al.*, 1995).

Essential oils from different species of genus *Cymbopogon* are known for their antimicrobial activity (Mishra and Dubey, 1994), antibacterial and antifungal activity as they contain some essential oils which inhibit mycotoxin formation (Bullerman *et al.*, 1984). *Cymbopogon* had some important aromatic with remarkable commercial value. Also, essential oil of the *cymbopogon* are used in perfumery, cosmetic and soap industries and have antifungal and insecticide activity Hajieghrari *et al.* (2006).

Dry grains keep longer, safe from insects and moulds. Most African farmers spread their harvests to dry under the sun, which often require longer durations for the product to attain "safe" moisture level (Begum 1991). Since sun drying may be a difficult task due to the high rainfall at the time of harvest, a lot of work has been done on the design of solar and mechanical dryers for use by farmers in the tropics, These dryers are not in use by farmers because large capital investment in involved. So, other methods of drying that are much effective and rapid including microwave, oven but these could not be implemented in the sub-region because farmers do not have the requisite facilities, for that mechanical dryers could be set up in strategic locations, which farmers can utilize if sun drying is proven difficult. Smoking is also an efficient method of protecting maize against infestation by fungi and this practice was found to decrease aflatoxin levels in farmer's stores. The problem with smoking is that if not carefully applied, it may discolor the product and change the test (Carruthers and Rodriguez, 1992).

This study aimed to compare the traditional sun drying with other drying methods of water melon seed and to evaluate the activity of dry powdered leaves and essential oil from lemon grass

against toxigenic fungi and aflatoxins production in dried water melon seed.

2. Materials and Methods

Aspergillus flavus NRRL 5906 was obtained from standard Association of Australia North Sydney.

Aflatoxins standards (B₁, B₂, G₁ and G₂) at concentrations 5µg/ml were purchased from Sigma and Chemical Company PO Box 4508 St. Louis, US.

Samples of water melon seed apparently healthy were collected from different house keeper in summer 2008. Seeds were manually extracted from the fruits, washed and mixed.

Natural leaves of lemon grass (*Cymbopogon citratus*) with no chemicals and aflatoxins were purchased from Siwa Oasis, Egypt. The Crispy dry leaves were powdered in a coffee grinder, and sieved with a 0.5mm size mesh.

Drying methods of water melon seeds

Seed were dried by four methods sun, oven, and smoke and solar dried. Sun drying was done by sun, at night the seeds were covered with polyethylene bags. The vacuum oven with hot air was done continuously for at 80°C. For smoke drying a wire mesh on which water melon seeds were spread above a burning wood fire, where the temperature was between 50°C to 60°C. Solar drying by the dryer absorber was made from black in plate with 0.4mm thickness, coated by black coating (70°C). Drying was terminated when the seeds had attained constant moisture, the time taking for the seeds to attain constant weight as 30, 9, 10, and 18 h for sun oven, smoke and solar drying respectively (Bankole *et al.* 2005).

Extraction of essential oil from lemon grass:

Two hundred grains of the powdered leaves of lemon grass was put in a round bottom flash, 1000ml of distilled water was added and then subjected to hydro distillation in modified cleverger apparatus for 8 hours. The oil recovered was dried over anhydrous sodium sulphate and kept in the refrigerator at 4°C before use (Bankole, 1997).

Determination of moisture content (MC)

Moisture content (MC) was determined for water melon seed before and after drying according the method of AOAC (2007).

Aflatoxins analysis

The extraction and assay of aflatoxin (B₁, B₂, G₁ and G₂) were performed using the EEC method (Bankole *et al.*, 1996). Five hundred grams of each seed samples was crushed with a Moulinex blender then homogenized in 250 ml of 7:3 methanol: water for 30 min and defatted twice with 25ml n-hexane

in a separator funnel. Aflatoxins were qualitative and quantitative by thin layer chromatography (TLC) and high performance liquid chromatography (HPLC). The average recovery of 86.5% for ten spiked melon seed samples.

Isolation of *Aspergillus spp*

100 seeds from each sample after drying by oven, sun, smoke and solar were surface sterilized for 1 min in 1% Na Cl , (5 per plate) were placed on Potato Dextraose Agar (PDA) plus chloromphoniced and incubated for 7 days at 28°C. The percentage of seeds with *Aspergillus spp.* was determined then identification was done according to Barnett and Hunter (1987).

Variability of aflatoxins production by *Aspergillus spp.*

Colonies of the isolated aflatoxins (B₁, B₂, G₁ and G₂) producing strains of *Aspergillus flavus* or *A. parasiticus* were characterized microscopically; colonies were suspended and grown in Yeast Extract Sucrose medium (YES) broth containing 15% sucrose and 2% yeast extract. After incubation for 2 weeks at 28°C under stationary culture conditions the culture filtrate and extracted twice with 3 volumes of chloroform and were analyzed for aflatoxins by HPLC (Reddy and Farhana, 2011).

Effect of drying methods on the growth of toxic *A. flavus* and aflatoxins production in vitro

Aspergillus flavus NRRL 5906 a high aflatoxins producing strain. The preparation of conidia suspension was done by flooding the surfaces of 7-10 day old cultures of fungi with 10 ml of 0.05% tween 80 in sterile distilled water (Bankole, 1997). 100g of each the dried water melon seeds (Sun, oven, smoke and solar) as well as the control (fresh seed) were distributed in each of stopper flask. The seed moisture content was equilibrated to approximately 14% by addition of sterile distilled water. The flasks were incubated in incubation at 28°C with manual shaking twice daily. After 14 days the aflatoxins level in each flask was determined according to AOAC (2007).

Effect of lemon grass powder and essential oil

The effect of lemon grass powder and essential oil on the growth and aflatoxins production of toxic *A. flavus* NRRL 5906 on water melon seeds by preparation on conidia suspension pure cultures was maintained on potato dextrose agar and the preparation of conidia suspension, the concentration of fungi was adjusted to approximately 10⁶ Conidia/ml (Bankole and Joda, 2004).

Determination of Minimal Inhibitory Concentration (MIC)

Was conducted according to (Bankole and Joda, 2004). The MIC was determined as the lowest concentration at which no growth occurs. 500g of water melon seeds after drying (Sun oven, smoke and solar) were distributed in conical flasks the seed moisture content was equilibrated to approximately 14% by the addition of sterile distilled water. After autoclave and inoculated with 5 ml conidia suspension of the toxigenic *A. flavus* NRRL 5906.

Experiments were carried out to determine the potential of using the powder, essential oil and mixed of powder plus essential oil. The powder leaves was used at level 5, 10, 25, 50 and 75 g (W.W). Different dosages of the oil to give concentrations of oil, 0.1, 0.25, 0.5, 1 and 2% (V/W). Powder leaves and oil were put together. The control was also similarly set up but without powdered leaves or essential oil. The aflatoxins were determined after 14 days incubation in incubator at 28°C according to Bankole *et al.* (1996).

Statistical analysis

Data analysis of variance using the SUPER ANOVA (Abacus Concepts Inc CA, USA) computer and significant differences between means were determined by the least significant difference technique at 95% confidence level according to Peterson (1985).

3. Results and Discussion

Concerning aflatoxins detection; obtained results revealed that aflatoxins (B₁, B₂, G₁ and G₂) were not detected in any of the investigated samples. These results were agreement with Ogunsamwo *et al.* (1989) and Ubani *et al.* (1993), they screened for aflatoxins in melon seed and they not detected aflatoxins in any of melon seed. Also, 27% of melon seed samples from farmer's stored contained aflatoxin B₁ with mean levels of 14 µg/kg in forest and 11 µg/kg in savanna of Nigeria were detected (Bankole and Adebajo, 2004).

Concerning moisture content; as shown in table (1). It was significantly lowest for oven dried seeds, followed by that with smoke dried and solar-dried, while moisture content was highest in sun dried. Nearly similar results were reported by Bankole *et al.* (2005), who Found seed moisture content of one hundred and thirty seven samples of melon seed from Nigeria Varied ranged between 5.3 to 10.4%.

The obtained results also revealed that percentage of seeds infected with *Aspergillus spp.* Samples after drying showed that *A. niger* was the most frequent genus flowed by *A. flavus* (table 2). The results presented in Table (2) shows that, *A. niger* was isolated from water melon seed before drying had largest count (70.0%). Also, water melon seed after drying by solar energy had the

four species belonged to *Aspergillus*. The most frequently associated with melon in Nigeria (Bankole, 1993 and Bnkole *et al.*, 2004). In these respect, Fungi associated with three cultivars of melon seed (*Colocynthis citrullus*, *Citrullus vulgaris* and *Citrullus lanatus*) in Nigeria were investigated by Chiejina (2006) who found the genus, *Aspergillus* was the most predominant, *A. niger* was the topping the list of fungi.

Concerning identification of *Aspergillus* isolates and their ability to produce aflatoxins, it was found that, aflatoxin B₁ and B₂ at concentration 4.50 and 3.67 µg/L respectively, were isolated from dried melon seed by sun drying. On the other hand all *A. parasiticus* isolated from water melon seed dried by solar energy produced aflatoxins B₁, B₂, G₁ and G₂ at concentration 8.11, 4.00, 6.29 and 3.37 µg/L, respectively. In these respect, Dorner (2004) found toxigenic of *A. flavus* could produce only two aflatoxins, B₁ and B₂ but most of *A. parasiticus* could produce all of the four types of aflatoxins.

These results may be due to the time taking for drying which was 30 and 18 h for sun and solar drying, respectively make spores of fungi activation. Hell *et al.* (2009) studied the mycoflora and occurrence of aflatoxin in dried vegetables include melon seed in Benin, Mali and Togo, West Africa and found mycotoxigenic fungi belong to *Aspergillus* species had ability to produce aflatoxin was found on dried vegetable products sample from African markets.

As shown in Table (3), the lowest concentration of total aflatoxins Produced by *A. flavus* NRRL 5906 which grow on dried seed by oven which recorded 3.204 µg/kg aflatoxins (B₁ and B₂). While it was highest in water melon seed before dried which recorded 17.540 µg/kg, in this respect, Ekundayo and Idzi (1990) found the mean quality 0.40 µg/g of aflatoxin in healthy shelled seed infected with spores of *A. flavus* after 14 days of inoculation, also he reported the shelled melon seeds served as a utilizable nutrient source for growth of the fungi hence the rapid colonization by the diverse range of fungi.

On the other hand *A. flavus* NRRL 5906 produced aflatoxins at level 9.270µg/kg when grow on water melon seed dried by smoking. These findings not agree with those reported by Bankole and Adebajo (2003), who reported that 12% of farmers in various ecological zones in Nigeria used smoke to preserve their grains and decrease aflatoxin levels in farmer's stores. Also the efficacy of smoking was also confirmed by Hell *et al.* (2000) in survey conducted in Benin.

Concerning the effect of different concentrations of powder and essential oil of *cymbopogon citrates*, results in figures 1-3, the powdered dry leaves and essential oil from lemon grass were mixed with the inoculated seed at level 75 g and 0.1% respectively and had the highest

effect to inhibition the effect of toxigenic *A. flavus* in dried water melon seed. **Adegoke and Odelusola, (1996)**, found that, the essential oil and powder extracts of *cymbopogon citratus* inhibited the growth of fungi including toxigenic species such as *A. flavus*. Moreover, dried seed with powder lemon grass at concentration 50g decreased the growth of *A. flavus* in dried seed by oven, smoke and solar drying, followed by dried seed by

oven and solar drying with extracted oil (0.25%) treatment. Similar results were obtained by **Singh et al. (2010)**, **Helal et al. (2007)**, **Bonkole & Joda (2004)** and **Bankole & Adebajo (2003)**.

Citral, geraniol and citronellol showed the highest antifungal activities among terpenoids, the main component found in lemon grass oil was citral 68.4%. (**Viollon and Chaumont, 1994**).

Table (1) moisture content % of water melon seed dried by different methods

Moisture content (%)			
Drying methods			
Oven	Sun	Smoke	Solar
6.26±0.41 ^d	8.50±0.26 ^b	7.00±0.08 ^c	7.35±0.17 ^b
Moisture content (%) of water melon seed before drying was 8.94±0.52 ^a			

Mean of three determination ± Standard deviations.

The same letter is not significantly different according to Duncan's Multiple Range test at, the 95% confidence level.

Table (2) Effect of drying methods on the percentage of *Aspergillus spp.* isolated from water melon seed.

<i>Aspergillus spp.</i>	Water melon seed before drying	Water melon seed after drying by			
		Oven	Sun	Smoke	Solar
<i>A. flavus</i>	10.20	25.00	33.33	14.29	33.33
<i>A. niger</i>	70.00	68.75	66.67	71.43	57.15
<i>A. parasiticus</i>	7.50	6.25	ND	ND	4.76
<i>A. Ochraceus</i>	12.30	ND*	ND	14.28	4.76

*ND: Non Detected

Table (3): Quantitative estimation of aflatoxins content of water melon seed

Dried water melon seed by	Aflatoxins content µg/kg				Total aflatoxins
	B ₁	B ₂	G ₁	G ₂	
Oven	2.001	1.203	ND*	ND	3.204
Sun	5.388	3.507	3.146	3.075	15.116
Smoke	3.450	2.019	3.280	0.971	9.720
Solar	4.001	2.112	3.753	1.304	11.170
Water melon seed before drying	6.951	3.282	5.053	2.54	17.540

ND*: Non Detected.

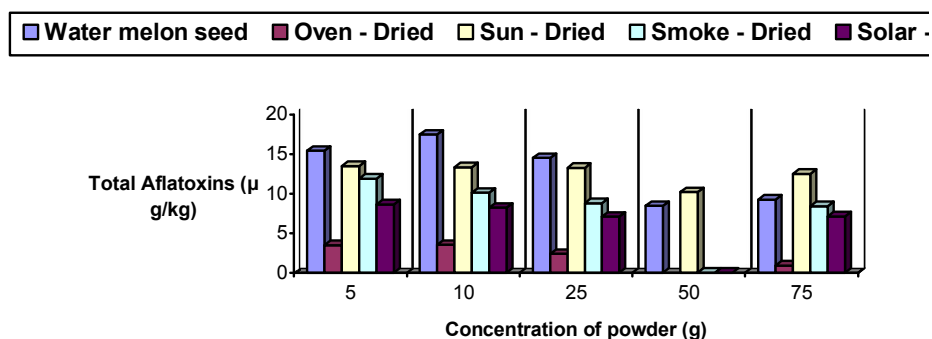


Figure 1 Effect of different concentration of powder of *cymbopogon citrates* and aflatoxins production on water melon seed

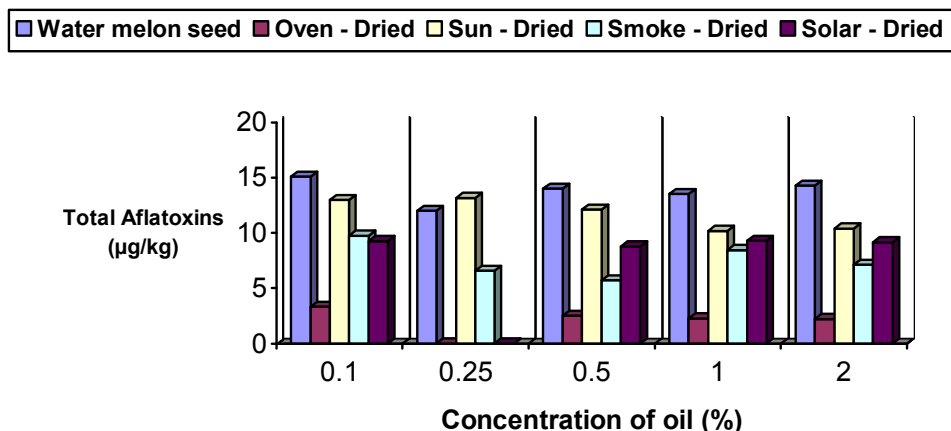


Figure 2 Effect of different concentration of essential oil of *cymbopogon citrates* and aflatoxins production on water melon seed.

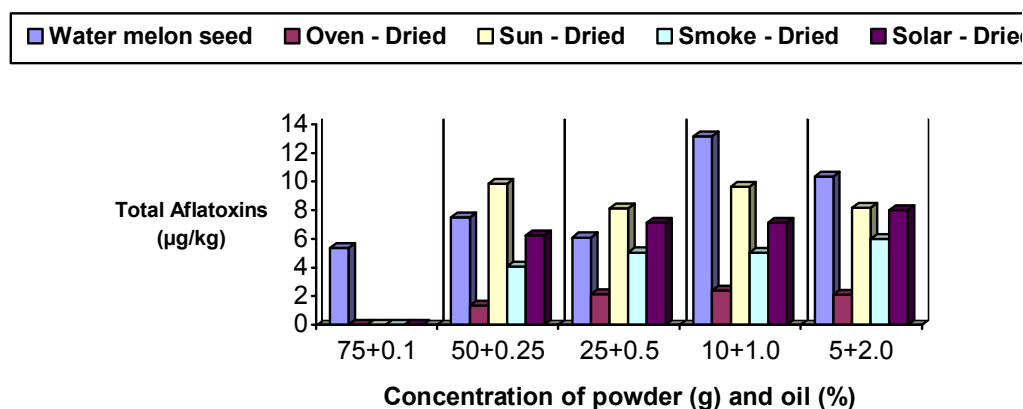


Figure 3 Effect of different concentration of powder plus essential oil of *cymbopogon citrates* and aflatoxins production on water melon seed.

The plasma membrane of *A. flavus* in the presence of 1µl/ml *C. citratus* essential oil was seemed to be irregular. The marked action of terpenic alcohols E-citraltus myrecene and Z-citral (the main constituents of *C. citratus* oil), may be attributed to the polarity of the OH-group, making these compounds relatively soluble in water, which confers these molecules their lipophilic properties and the ability to penetrate the plasma membrane (Knobloch *et al.* 1989).

On conclusion, Oven drying is the best method for drying the crops and *Cymbopogon citratus* (powder, essential oil and powder plus oil), owing to its antifungal, anti-aflatoxigenic properties, may be recommended for its practical application as a botanical fungi toxicant for enhancing the shelf-life of food commodities.

Corresponding author

Eman M. Hegazy
Food Toxicology and Contaminants Department,
National Research Center, Giza, Dokki, Egypt
eman_hegazy@hotmail.com

References

- Adegoke, G.O. and Odelusola, B.A. (1996):** Storage of maize and Cowpea and inhibition of microbial. Agents of biodeterioration using the powder and essential oil of *Cymbopogon citratus*. Internat. Biodeter, Biodegrad. 37: 81-84.
- Akobundu, E. (1989):** Effect of Jull-fat egusi (melon seed) meal on quality of cooked Nigerian sausage. Food Quality and Preference, 1: 109-111.

- AOAC (2007):** Official Methods of Analysis of AOAC International 20th Edition. Gaithersburg, MD, USA.
- Bankole, S.A. (1993):** Moisture content, mould invasion and seed germinability of stored melon. *Mycopathologia* 122:123-126.
- Bankole, S.A. (1997):** Effect, of essential oil from two Nigerian medicinal plants (*Azadirachta indica* and *Morinda lucida*) on growth and aflatoxin B₁ production in maize grain by a toxigenic *Aspergillus flavus*. *Lett. Appl. Microbiol.* 24: 190-192.
- Bankole, S.A. and Adebajo, A. (2003):** Mycotoxins in food in West Africa: current situation and possibilities of controlling it. *African Journal of Biotechnology* 2: 545-263.
- Bankole, S.A. and Adebajo, A. (2004):** Fungal infection and aflatoxin contamination of melon seeds from the humid forest and Northern Guinea savanna of Nigeria. *Trop. Sci.* 15-25.
- Bankole, S.A.; Esegbe, D.A. and Enikuomehim, O.A. (1996):** Mycoflora and aflatoxin production in pigeon pea stored in jute sacks and iron lins. *Mycopathologia* 132: 155-160.
- Bankole, S.A. and Joda, A.O. (2004):** Effect of lemon grass (*Cymbopogon citratus* Stapf) Powder and essential oil on mould determination and aflatoxin contamination of melon seeds (*Colocynthis citrullus* L.). *African Journal of Biotechnology* 3: 52-59.
- Bankole, S.A.; Lawal O.A. and Adebajo A. (2004):** Storage practices and aflatoxin B₁ contamination of 'egusi' melon seed in Nig. *Trop. Sci.* 44: 150-153.
- Bankole, S.A.; Osho, A.; Joda, A.O. and Enikuomehim, O.A. (2005):** Effect of drying method on the quality and storability of 'egusi' melon seeds (*Colocynthis citrullus* L.). *African Journal of Biotechnology* 4: 799-803.
- Barnett, H.L., Hunter, B.B., (1987):** Illustrated Genera of Imperfect Fungi. MacMillan Publ. Co., New York.
- Begum, S. (1991):** The economics of small-scale drying. In Axtell B, Bush a (Eds), Case studies in the dissemination of tray drying technology. Intermediate Technology Publications, London, 7: 41-47.
- Bullerman, L.B., Schroeder, L.L. and Park, K., (1984):** Formation and control of mycotoxins in food. *J. Food Prot.* 47: 637-646.
- Carruthers, I. and Rodriguez, M. (1992):** Tools for agriculture: a guide to appropriate equipment for smallholder farmers. Intermediate Technology Publication, Center for Agricultural Technology. Wageningen.
- Chiejina, V. (2006):** Studies on seed-borne pathogens of some Nigeria melons. *J. of Agriculture, Food Environment and Extension* 5: 13-16.
- Dorner, J.W. (2004):** Biological control of aflatoxin contamination of crops. *J. Toxicol. Toxin Rev.*, 23:425-450.
- Dragan, R.; Milicevic, I. ; Skrinjar, M. and Baltic, T. (2010):** Real and Perceived Risks for Mycotoxin Contamination in Foods and Feeds: Challenges for Food Safety Control. *Toxins* 2: 572-592.
- Ekundayo, C.A. (1987):** Mycoflora and vitamin content of sun-dried food condiments in Nigeria. *Plant Foods Hum. Nutr.* 37:247-252.
- Ekundayo, C.A. and Idzi, E. (1990):** Mycoflora and nutritional value of shelled melon seeds (*Citrulus vulgaris* Schrad.) in Nigeria. *Plant Foods for Human Nutrition* 40: 215-222.
- Hajjehgari, B.; Mohammadi, M.R.; Hadian, D. (2006):** Antifungal activity of *Cymbopogon parkeri* stapf. essential oil on some important phytopathogenic fungi. *Commun Agric Appl Biol Sci.* 71:937-41.
- Helal, G.A.; Sarhan, M.M.; Abu Shahla, A.N.K. and Abou El-Khair, E.K. (2007):** Effect on *Cymbopogon citratus* L. essential oil on the growth, morphogenesis and aflatoxin production of *Aspergillus flavus* ML2-strain. *Journal of Basic Microbiology*, 47: 5-15.
- Hell, K.; Cardwell, K.F., Setamou, M., Poehling, H.M. (2000):** The influence of storage practices on aflatoxin contamination in maize for agro ecological zones of Benin, West Africa, *J. Stored Prod. Res.* 36: 365-382.
- Hell, K.; Gnonlonfin, B.G., Kodjoghbe, G.; Lamoni, Y. and Abdourhamane, I.K. (2009):** Mycoflora and occurrence of aflatoxin in dried vegetable in Benin, Mali and Togo, West Africa. *Int J Food Microbiol* 31: 99-104.
- IARC (1993):** IARC Monographs on the Evaluation of Carcinogenic Risks to Humans, volume 56. Some naturally occurring substances. Food items and constituents, Heterocyclic Amines and Mycotoxins, Lyon, IARC Press, pp. 445-466.
- Karakaya, S.; Kavas, A.; El Nehir, S.; Gunduc, N. and Akdogan, L. (1995):** Nutritive value of a melon seed beverage. *Food Chemistry*, 52: 139-141.
- King, R.D. and Onuora O. (1984):** Aspects of melon seed protein characteristics. *Food Chemistry*, 14: 65-77.
- Knobloch, K.; Pauli, P.; Iberl, B.; Weigand, H. and Weiss, N. (1989):** Antibacterial and antifungal properties of essential oil components. *J. Essen. Oil Res.*, 1: 119-128.
- Mishra, A. K. and Dubey, N. K. (1994):** Evaluation of some essential oil for their toxicity against fungi causing deterioration of stored food commodities. *App. Environ. Microbiol.* 60:1101-1105.

- Odunfa, S.A. (1981):** Microbiology and amino acid. Composition of 'ogiri' – a food condiment from melon. Seeds. *Nahrung* 25: 811-816.
- Ogunsanwo, B.M.; Faboya, O.O.; Idowu, O.R.; Ikotun, T and Akano, D.A. (1989):** The fat of aflatoxins during the production of "oyiri" a West African fermented melon seed condiment from artificially contaminated seeds. *Nahrung* 33: 983-988.
- Peterson, R.G. (1985):** Design and analysis of experiments. Marcel Dekker. Inc. New York and Basel, 429 pp.
- Reddy, K.R.N. and Farhana, N.I. (2011):** Occurrence of *Aspergillus spp.* and Aflatoxin B₁ in Malaysian Foods Used for Human Consumption. *Journal of Food Science*. 76:99-104.
- Singh, P.; Shukla, R.; Kumar, A.; Prakash, B.; Singh, S. and Dubey, N.K. (2010):** Effect of *Citrus reticulata* and *Cymbopogon citratus* essential oils on *Aspergillus flavus* growth and aflatoxin production on *Asparagus racemosus*. *Mycopathologia*, 170: 195-202.
- Ubani, O.N.; Opadokun, J.S. Williams, J.O.; Akimnusi, D.A.; Akano, A. and Ikeorah, J.N. (1993):** Storage properties of melon seeds (*Cucumeriopsis edulis*). *Food Chemistry*, 47: 7-10.
- Viollon, C and Chaumont, J. P. (1994):** Antifungal properties of essential oils and their main components upon *Cryptococcus neoformans*. *Mycopathologia*, 128: 151-153.

8/8/2011

Histopathological and Ultrastructural Study of Experimental Spring Viraemia of Carp (SVC) Infection of Common Carp with Comparison between Different Immunohistodignostic Techniques Efficacy

A.Y. Gaafar^{1*}, Tomáš Veselý², T. Nakai³, E.M. El-Manakhly⁴, M.K. Soliman⁵, H. Soufy¹, Mona S. Zaki¹, Safinaz G. Mohamed⁶, Amany M. Kenawy¹, M. S. El-Neweshy⁴ and A. Younes¹.

¹Veterinary Research Division, National Research Centre, Cairo, Egypt.

²Veterinary Research Institute, Hudcova 70, 621 32 Brno, Czech Republic.

³Graduate School of Biosphere Science, Hiroshima University, Higashi-Hiroshima 739-8528, Japan.

⁴Faculty of Veterinary Medicine - Alexandria University, Edfina, Egypt.

⁵Faculty of Veterinary Medicine - Damanhour University, Bostan City, Egypt.

⁶National Institute of Oceanography and Fisheries, Alexandria, Egypt.

*Correspondence to A.Y. Gaafar, (e-mail: alkhateibyg@yahoo.com).

Abstract: Spring viremia of carp (SVC) is an important disease affecting cyprinids, mainly common carp *Cyprinus carpio*. The disease is widespread in European carp culture, where it causes significant morbidity and mortality. This study describes some Histopathological, Immunohistological, and Ultra-microscopical characteristics of infection by this virus in experimentally infected target species; common carp. In this study the pathological changes in naturally and experimentally infected fish existed mainly in the hepatopancreas, kidney, spleen and gills. On the other hand, the changes were evoked to a lesser extent in the intestine and brain. The alterations were ranging between minor degenerative changes to severe necrotic picture. Immunostaining and immunofluorescence studies revealed the presence of antigen in SVCV infected tissue specimens. Transmission Electron Microscopy studies of liver, kidney and spleen samples revealed the presence of pullet-shaped electron-dense intra-cytoplasmic particles, with approximate length of 180-200 nm and approximate width of 90-100 nm. These particles resemble the characteristics of *Rhabdovirus* viral particles.

[A. Y. Gaafar, Tomáš Veselý, T. Nakai, E.M. El-Manakhly, M.K. Soliman, H. Soufy, Mona S. Zaki, Safinaz G. Mohamed, Amany M. Kenawy, M. S. El-Neweshy and A. Younes. **Histopathological and Ultrastructural Study of Experimental Spring Viraemia of Carp (SVC) Infection of Common Carp with Comparison between Different Immunohistodignostic Techniques Efficacy.** [Life Science Journal. 2011; 8(3):523-533] (ISSN: 1097-8135). <http://www.lifesciencesite.com>, #82

Keywords: Spring Viraemia of Carp, SVC, *Rhabdovirus carpio*, common carp, *Cyprinus carpio*, Histopathology, Immunohistochemistry, Immunofluorescence, TEM.

1. Introduction

Spring Viraemia of Carp (SVC) is an acute, systemic, contagious disease caused by Rhabdovirus (Bootsma and Ebregt, 1983; Wolf, 1988; Ahne *et al.*, 2002 and Saad 2005). The term SVC and *Rhabdovirus carpio* (RVC) were firstly introduced by Fijan *et al.* (1971). Tropism and replication of virus are confined to capillary endothelium, as well as in haemopoietic and excretory kidney tissues, causing an impaired salt-water balance, which is often lethal (Fijan *et al.*, 1971). The systemic character of Spring Viraemia of Carp virus (SVCV) infection has been demonstrated by experimental infection of specific pathogen free (SPF) carp (Ahne 1977, 1978). It affects primarily common carp (*Cyprinus carpio*), while other cyprinids and non-cyprinid species are also susceptible including Koi carp (*Cyprinus carpio koi*), Crucian carp and Goldfish (*Carassius auratus*), Bighead carp (*Aristichthys nobilis*), Grass carp (*Ctenopharyngodon idella*), Silver carp (*Hypophthalmichthys molitrix*), Sheatfish, (*Silurus glanis*), Orfe (*Leuciscus idus*), Tench (*Tinca tinca*)

and Roach (*Rutilus rutilus*) as stated by Haenen & Davidse (1993), And *Oreochromis niloticus* (Abo Eisa 2008).

SVC disease is very important fish disease because of its world-wide distribution. The disease was firstly discovered in Yugoslavia 1969 (Fijan *et al.*, 1971), then Czechoslovakia (Tesarcik *et al.*, 1977), Scotland (Richards and Buchanon, 1978), Malaysia (Armstrong and Ferguson, 1989), Spain (Lupiani *et al.*, 1989), Indonesia (Glazebrook *et al.*, 1990), Russia (Oreshkova *et al.*, 1995), Brazil (Alexandrino *et al.*, 1998), Hawaii (Johnson *et al.*, 1999), Northern Ireland (Rowley *et al.*, 2001), United States in North Carolina and Virginia (APHIS, 2003), China (Liu *et al.*, 2004), Egypt (Saad *et al.*, 2005), Canada (Garver *et al.*, 2007) and Iran (Haghighi *et al.*, 2008)

In European countries including Russia where the Carp is an important fish, SVCV causes high mortalities among carp farms with reduction of total returns from fish selling leading to severe economic

losses (Richenbach-Klinke, 1973; Oreshkova *et al.*, 1995; Björklund *et al.*, 1996; Siwicki *et al.*, 2003). Details about the specific histopathologic lesion induced by virus infection can be used as a tool for viral infection diagnosis.

2. Material and Methods

Fish

In the present study, European common carp (*C. carpio carpio*) of the R3×R8 strain which are the offspring of a cross between fish of Hungarian origin (R8 strain) and of Polish origin (R3 strain) were used (Irnazarow, 1995). In this study, we refer to the European common carp subspecies as carp, unless stated otherwise. Carp were bred in the central fish facility of Wageningen University, The Netherlands, and raised at the Veterinary Research Institute (VRI), Brno, Czech Republic, in recirculating UV-treated water and fed pelleted dry food (Trouvit, Nutreco) daily.

Viral infection of carp

Spring viraemia of carp virus (SVCV) strain CAPM V 539 (Koutna *et al.*, 2003) was propagated in EPC (Epithelioma Papulosum Cyprini, (Fijan *et al.*, 1983)) cells at 15 °C. Cells were grown in Eagle's Minimal Essential Medium (MEM) containing 2% fetal bovine serum (FBS) and standard concentration of antibiotics. The virus titers, given as tissue culture infective dose (TCID₅₀/ml), were calculated by the method of Reed and Muench (1938).

Ten-month-old carp were raised at 15 °C to an average weight of 30–40 g. This temperature is optimal for SVCV infectivity (Ahne *et al.*, 2002). Fish ($n = 110$) were exposed, by immersion, to SVCV-infected tissue culture (10^3 TCID₅₀/ml) for 2 hours. Control fish ($n = 62$) were treated similarly and exposed to control cultures only. Infected fish were divided over two replicate tanks for subsequent representative tissue sampling at 2 weeks and 3 weeks postinfection, six fish were killed to collect tissue samples. Infection of carp with SVCV was performed at the central fish facility of the Veterinary Research Institute (VRI), Brno, Czech Republic.

Detection of SVCV

To confirm that all fish used in our experiment were infected by the SVC virus, virus-specific primers were used in a single tube reverse transcription (RT)-PCR and nested PCR reaction (Koutna *et al.*, 2003).

Histopathological examination

After complete necropsy of experimentally infected fish, fresh tissue specimens were collected

from gills, liver, spleen, kidney, brain, gas bladder, musculature and intestine for histological examination. These specimens were rapidly fixed in Davidson's fixative for 24 hours then transferred to 70% ethanol till processing proceeds. The fixed specimens were processed through the conventional paraffin embedding technique (dehydration through ascending grades of ethanol, clearing in xylen and embedding in paraffin wax at 60° C). Paraffin blocks were prepared and cutting 3 µm-thick tissue sections by using microtome (Leica 2155). Then 5 replicates from the same section were mounted on silane (Sigma Aldrich)-pretreated slides, and then the slides were divided between H&E staining, Immunohistochemistry and Immuno-fluorescent techniques.

Immuno-histological examination

In all Immunohistodetection methods in this study heat-induced antigen retrieval was required for optimal staining with SVCV antibodies. So paraffin sections mounted on slides were heated to 60° C for 30 minutes to retrieve the viral antigen inside the tissue. Anti-SVCV Rabbit antiserum was kindly provided by Prof. Dr. Peter Dixon (SVC OIE Reference Laboratory, Centre for Environment, Fisheries and Aquaculture Science CEFAS, Weymouth Laboratory, The Nothe, Weymouth, Dorset DT4 8UB, UK).

Immunohistochemistry

Immunohistochemical staining for SVC antigen was performed by two methods for comparing the efficacy.

The first method was by using peroxidase activity as antigen indicator. After deparaffinization, 3 µm-thick tissue sections were incubated in methanol with 3% hydrogen peroxide to block endogenous peroxidase activity. The sections were incubated overnight with primary SVC rabbit antiserum (1:100 dilution) at 4°C. For negative controls, normal rabbit serum was used at equivalent concentrations. Thereafter, endogenous nonspecific antigens were blocked by placing sections in 2.5% skimmed milk for 20 minutes. Then sections were incubated with secondary antibody-conjugated universal immuno-enzyme polymer; Histofine Simple Stain MAX-PO kit (Nichirei, Japan); for 30 minutes at room temperature. The bound antibody was visualized using 0.016% diaminobenzidine tetrahydrochloride (DAB) substrate, 0.24% H₂O₂ in PBS (Wako, Japan) revealing brown precipitate. Sections were counterstained with Gill's hematoxylin and "Blued" with 0.1% ammonia water.

The second method was using avidin/biotin conjugate alkaline phosphatase (ABC) procedure. After deparaffinization, 3 µm-thick tissue sections

were incubated overnight with primary SVC rabbit antiserum (1:100 dilution) at 4°C. For negative controls, normal rabbit serum was used at equivalent concentrations. Thereafter, endogenous nonspecific antigens were blocked by placing sections in 2.5% skimmed milk for 20 minutes. Then sections were incubated with secondary antibody-Alkaline Phosphatase Conjugated Swine Anti-Rabbit polyclonal Immunoglobulin (Dako, Denmark) for 30 minutes at room temperature. Sections were developed in New Fuchsin chromogen/substrate solution (Dako, Denmark) within 15 minutes at room temperature revealing red precipitate. Sections were counterstained with Gill's hematoxylin and "Blued" with 0.1% ammonia water.

Immuno-flourescent Technique

The technique was done according to (Hayat, 2002). As after deparaffinization, 3 µm-thick tissue sections were incubated overnight with primary SVC rabbit antiserum (1:100 dilution) at 4°C. For negative controls, normal rabbit serum was used at equivalent concentrations. Thereafter, endogenous nonspecific antigens were blocked by placing sections in 2.5% skimmed milk for 20 minutes. Then sections were incubated with secondary antibody- FITC Conjugated Swine Anti-Rabbit polyclonal Immunoglobulin (Dako, Denmark) for 1 hour at 4°C in dark place. Sections were mounted by anti-fading water based mountant (glycerol-PVD 1:1) then cover-slipped. Positive antigenic signals appears as green fluoresce under FITC-specific UV wave length when viewed by UV microscope (Nikon Eclipse E200 + Hamamatsu CCD Camera).

Transmission Electron Microscopic (TEM) examination

At the beginning of sample processing we had lack of samples fixed specially for TEM examination by glutaraldehyde, only Davidson's fixed paraffin embedded specimens were present. So retrieval of tissue from histological wax blocks for TEM is used despite the previous fixation method (Kuo, 2007). In some cases an area of interest, which may not be discovered by simply processing more tissue, can be retrieved from the wax block. The area of interest on the microscope slide was Identified by ringing it with a marker pen, and then matched against the specimen in the wax block and cut around with a razor blade. Carefully the piece of tissue was levered out. Ascending re-hydration of the specimen is done. Then the usual processing schedule for TEM specimens was continued with post fixation in osmium tetroxide, and epoxy resin embedding, then specimens were cut on ultra-microtome (Ultracut Reichert, Austria) into firstly nearly 1µm semi-thin

sections by glass knives, which is observed after toluidine blue staining to perform more trimming, to facilitate further ultrathin sectioning. After making nearly 0.1 µm ultrathin sectioning by diamond knife the grey floating sections were selected for better TEM results, which were caught over carbon-copper grids. After drying, the grids were subjected to negative staining by 2% uranyl acetate and lead citrate method (Kuo, 2007). TEM observation is made by transmission electron microscope (JEOL 1200. Japan).

3. Results and Discussion

Table (1) summarizes the histopathological picture of examined fish tissue sections. Example pictures are shown in figure (1).

In the positive samples in immunohistological detection (immunohistochemistry and immunofluorescence) antigenic expression is noticed as seen in figure (1). While control negative samples, showed absence of antigenic expression.

The present study showed that the pathological changes in naturally and experimentally infected fish existed mainly in the hepatopancreas, kidney, spleen and gills. On the other hand, the changes were evoked to a lesser extent in the intestine and brain.

Microscopically, the hepatopancreas showed congestion, acute cellular swelling of the hepatocytes. Moreover, necrotic areas with corresponding alterations in nuclear and cytoplasmic staining characteristics indicating abnormal hepatocytes were also evident. These changes may be due to virus replication inside the cytoplasm of hepatocytes which lead to exhaustion of cellular resources leading to vacuolations progressed as necrosis and subsequent viral shedding, thus because of the hepatic multiple metabolic functions, such damage could have serious effects on all metabolic processes (Roberts, 2001). The aforementioned alterations were partially similar to those described by Negele (1977) and Osadcaja and Rudenko (1981) who denoted that liver parenchyma showed multifocal necroses, adipose degeneration and hyperemia.

Bucke and Finlay (1979) described degenerative and necrotic changes in the hepatopancreas, with marked areas of karyorrhexis and hepatocyte cell-membrane breakdown, moreover Saad (2005), Abo Eisa (2007) and Soliman *et al.* (2008) denoted hepatic lesions as pyknosis and necrosis, while Haghghi *et al.* (2008) found that the microarchitecture of the hepatic tissue was almost destroyed, with small parts of healthy tissue were visible in certain places, while the remaining tissue was atrophied due to pressure of the cellular infiltrate.

Table (1) The histopathological picture of examined fish tissue.

	2 nd week		3 rd week	
Hepatopancreas				
• Circulatory Disturbances	Blood vessels and sinusoidal congestion	++*	Blood vessels and sinusoidal congestion	++
• Degenerative Changes	Vacuolar degeneration	+	Multifocal vacuolar degeneration	++
• Proliferative Changes	-		-	
• Necrosis	-		Hepatocellular necrosis Nuclear pyknosis and karyolysis	++ +
• Infiltrations	-		-	
Spleen				
• Circulatory Disturbances	-		Hemorrhages	++
• Degenerative Changes	-		-	
• Proliferative Changes	-		-	
• Necrosis	Multifocal depletion of white pulp	+	Multifocal depletion of white pulp	++
• Infiltrations	-		-	+
Posterior kidney				
• Circulatory Disturbances	Edema infiltrating renal interstitium	++	Hemorrhages	+
• Degenerative Changes	Vacuolation of tubular epithelial cells Intracellular hyaline droplet formation	++ ++	Vacuolation of tubular epithelial cells	+++
• Proliferative Changes	Stimulation of interstitial hemopoietic tissue	+	-	
• Necrosis	Nuclear changes such as pyknosis	+	Tubular necrosis Interstitial necrosis	 +
• Infiltrations	-		Diffuse mononuclear cell infiltration	+
Intestine				
• Circulatory Disturbances	-		-	
• Degenerative Changes	Villar vacuolation	+	Villar vacuolation	++
• Proliferative Changes	-		-	
• Necrosis	-		-	
• Infiltrations	-		-	
Gills				
• Circulatory Disturbances	Congestion	++	Congestion Edema	++ +
• Degenerative Changes	Intracytoplasmic vacuoles in-between the proliferated malpighian cells	++	Lamellar subepithelial spongiosis of secondary gill lamellae	+++
• Proliferative Changes	Diffuse lamellar fusion Hyperplasia of the epithelial lining at the base of secondary gill lamellae	++ ++	Diffuse lamellar fusion Hyperplasia of the epithelial lining at the base of secondary gill lamellae	++ +++
• Necrosis	-		-	
• Infiltrations	Eosinophilic Granular cells	+	Eosinophilic Granular cells	++

*Score value: - = none, + = mild, ++ = moderate, +++ = severe

Semiquantitative scoring: Histopathological alterations were assessed using a score ranging from - to + + + depending on the degree and extent of the alteration: (-) none, (+) mild occurrence, (++) moderate occurrence, (+++) severe occurrence.

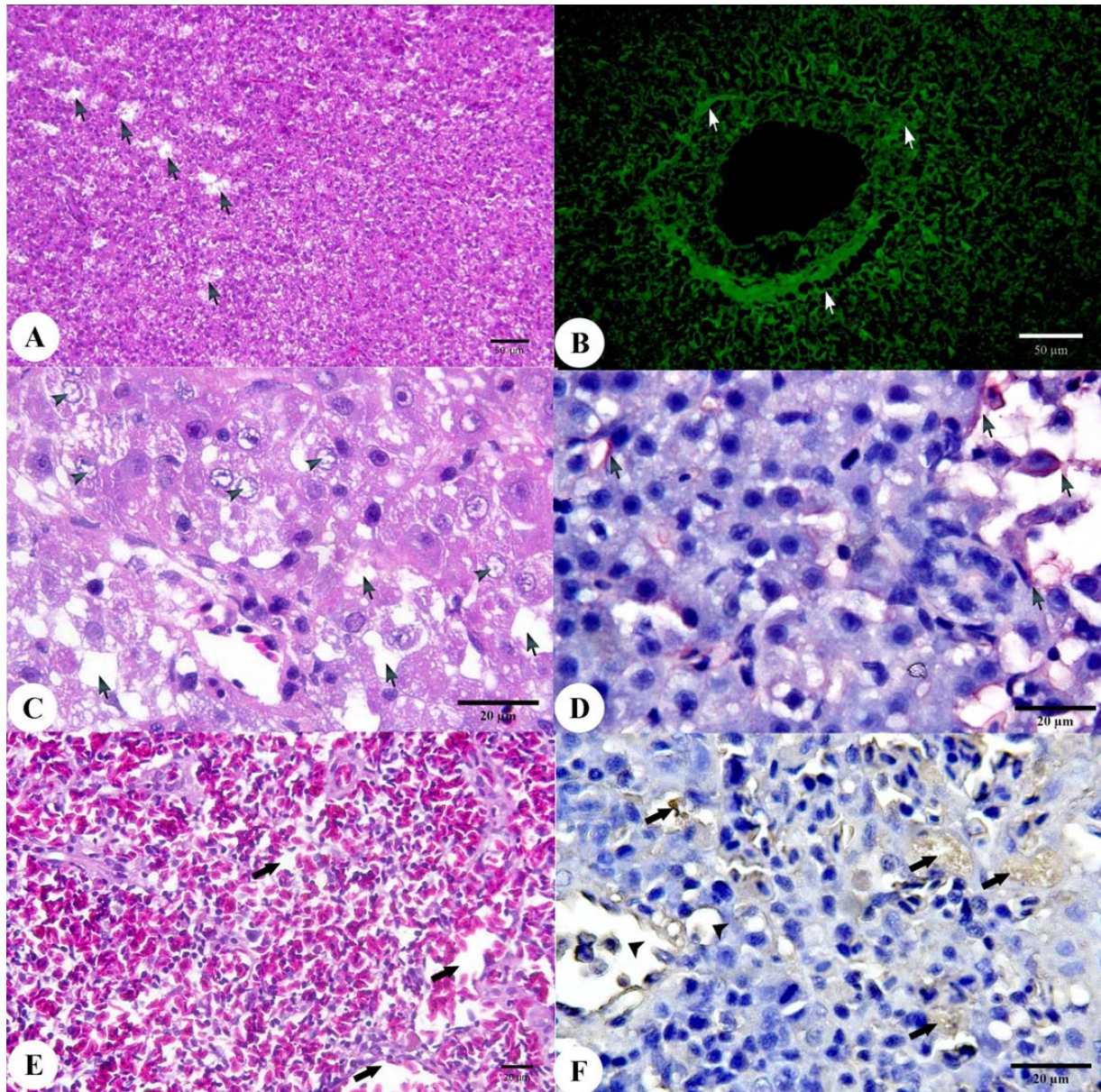


Figure (1): (A) - Common carp after 2 weeks of experimental SVCV infection showing ascitis (arrowhead) with haemorrhagic prolapsed anal opening (arrow). (B) - Hepatopancreas of common carp after 2 weeks of experimental SVCV infection showing green fluorescence (arrows) concentrated at peripancreatic acinar area and surrounding vacuolated hepatic tissue. Immuno-Fluorescence Technique. (C) - Hepatopancreas of common carp after 3 weeks of experimental SVCV infection showing hepatic necrosis represented by nuclear karyolysis (arrowheads) and vacuolations (arrows). H&E. (D) - Hepatopancreas of common carp after 2 weeks of experimental SVC infection showing positive antigenic red staining concentrated at necrotic areas. Immuno-Alkaline Phosphatase, New Fuchsin substrate – Gill's Hematoxylin counterstain. (E) - Spleen of common carp after 3 weeks of experimental SVCV infection showing multifocal depletion of white pulp and hemorrhages (arrows). H&E. (F) - Spleen of common carp after 3 weeks of experimental SVCV infection showing brown staining (arrows) within splenocytes. Immuno-Peroxidase, DAB substrate – Gill's Hematoxylin counterstain.

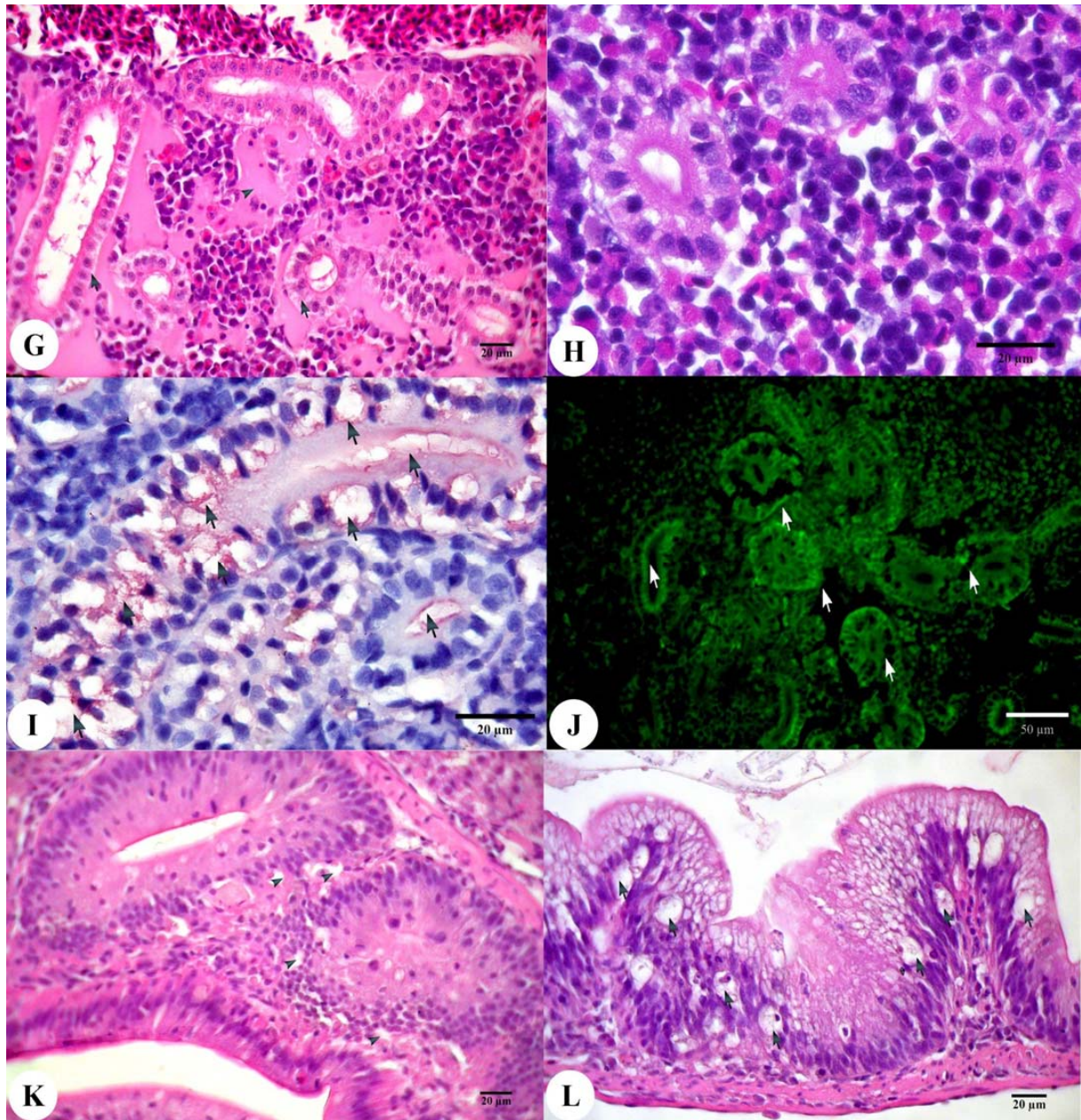


Figure (1) continued: (G) - Posterior kidney of common carp after 2 weeks of experimental SVCV infection showing diffuse amorphous eosinophilic material (arrowhead) infiltrating renal interstitium with tubular necrosis (arrows). H&E. (H) - Posterior kidney of common carp after 3 weeks of experimental SVC infection showing diffuse interstitial infiltration of mononuclear cells with some vacuolation inside the cytoplasm of tubular epithelium. H&E. (I) - Higher magnification of Fig (36) showing posterior kidney of common carp after 2 weeks of experimental SVCV infection showing red staining concentrated in vacuolated tubular epithelial cells and inside tubular lumina. Immuno-Alkaline Phosphatase, New Fuchsin substrate – Gill's Hematoxylin counterstain. (J) - Posterior kidney of common carp after 2 weeks of experimental SVCV infection showing green fluorescence (arrows) in the tubular epithelial cells and from the interstitial tissue and also inside the tubular lumina. Immuno-Fluorescence Technique. (K) - Intestine of common carp after 2 weeks of experimental SVCV infection showing mild villar vacuolation (arrowheads). H&E. (L) - Intestine of common carp after 3 weeks of experimental SVCV infection showing villar vacuolation (arrows). H&E.

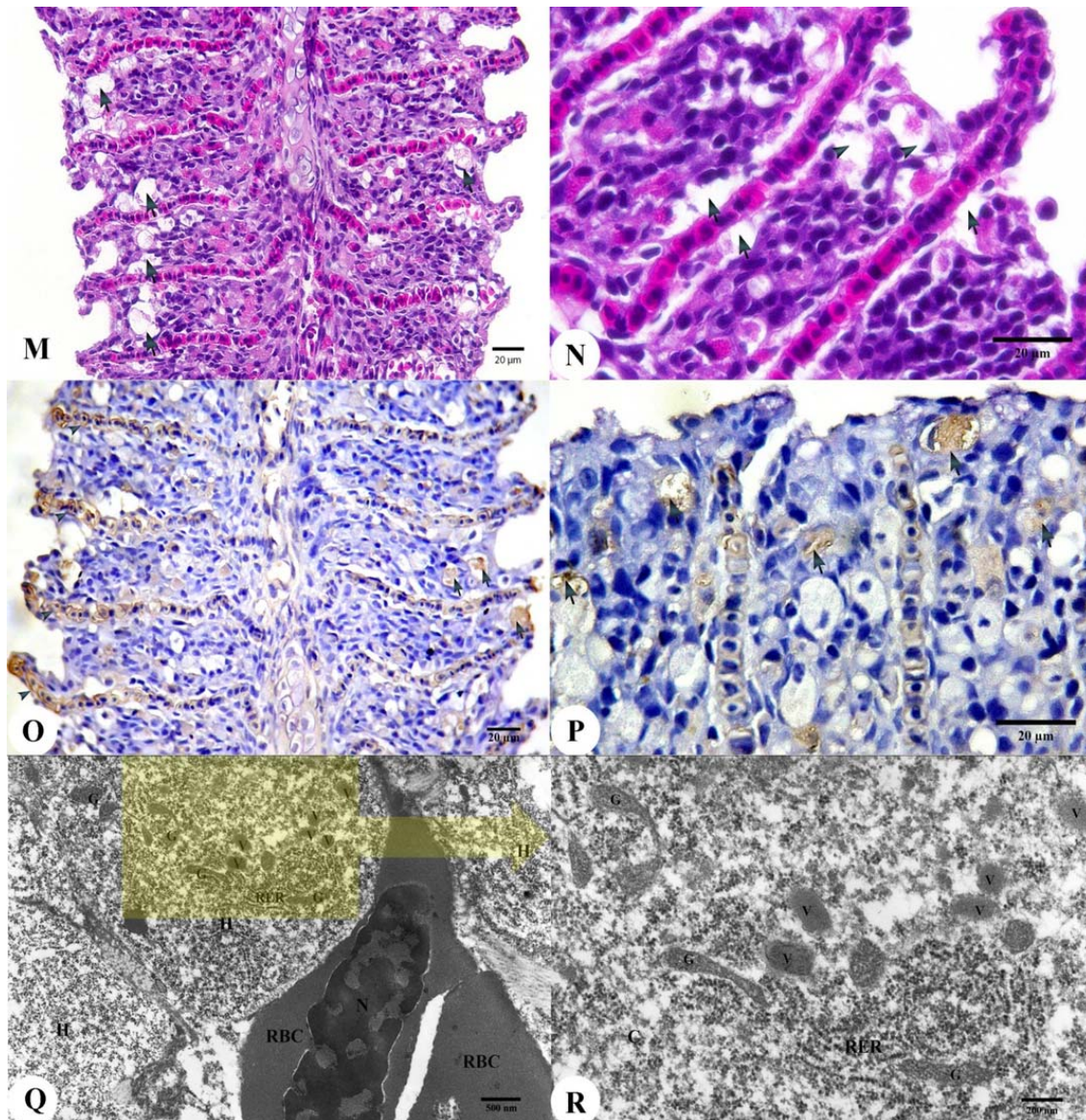


Figure (1) continued: (M) - Gills of common carp after 2 weeks of experimental SVCV infection showing diffuse lamellar fusion due to hyperplasia of the epithelial lining at the base of secondary gill lamellae with development of vacuoles (arrows) in the proliferated malpighian cells. H&E. (N) - Gills of common carp after 3 weeks of experimental SVCV infection showing degenerative changes of epithelial lining of secondary gill lamellae; subepithelial spongiosis; (arrowheads) with development of focal necrotic areas of the proliferated malpighian cells (arrows). H&E. (O) - Gills of common carp after 2 weeks of experimental SVCV infection showing brown staining demarcating the lamellar blood capillaries and inside vacuolated malpighian cells (arrows). Immuno-Peroxidase, DAB substrate – Gill's Hematoxylin counterstain. (P) - Higher magnification of Fig (43) showing gills of common carp after 2 weeks of experimental SVCV infection showing brown staining demarcating the lamellar blood capillaries and inside vacuolated malpighian cells (arrows). Immuno-Peroxidase, DAB substrate – Gill's Hematoxylin counterstain. (Q) - Electron micrograph of SVCV infected hepatocytes of common carp 2 weeks post-infection showing intra-cytoplasmic presence of SVCV as clear pullet shaped electron-dense particles (V) in the vicinity of Golgi apparatus. C= cytoplasm, G= Golgi apparatus & RER= rough endoplasmic reticulum. (R) - Electron micrograph of SVCV infected hepatocytes of common carp 3 weeks post-infection. Note the numerous virions (V) scattered in the cytoplasm at the vicinity of the nucleus. N= nucleus, C= cytoplasm, NM= nuclear membrane & RER= rough endoplasmic reticulum.

In pancreatic acini necrotic changes which were concurrent with hepatic changes were greatly similar to those observed by **Bucke and Finlay (1979)** as the exocrine tissue showed degenerative changes in the hepatopancreas and in free pancreatic tissue, there was moderate to marked necrosis of the acini. The Microscopical picture of posterior kidney showed proteinaceous dystrophy in the form of vacuolar degeneration of the tubular epithelium. Furthermore, tubular necrosis with lymphocytic infiltration was noticed. These results may be a sequelle of virus replication. Hyaline droplet in the tubular epithelium and eosinophilic detritus in their lumina were noticed, with evident mononuclear cell infiltration. These results may be due to virus replication in glomerular capillary tuft, which became more permeable to plasma protein including albumin. The marked depletion in haemopoietic elements; which was evident in spleen and kidney; was probably caused by virus cytopathic effect. The aforementioned alterations were seemingly similar to those described by **Negele (1977)** and **Osadcaja and Rudenko (1981)** who stated that the tubules of the kidney were clogged by the tube casts, vacuolation and hyaline degeneration. **Bucke and Finlay (1979)** denoted moderate to marked glomerulonephritis were evident in kidney. Meanwhile **Sulimanovic et al. (1986)** described trunk kidney to have diffuse necrosis of haematopoietic tissue as almost all cells of haematopoietic tissue were necrotic, with a varying degree of cell degeneration and some necrosis in tubules, also focal infiltration in haematopoietic tissue and peritubular oedema with apparent partial degeneration and necrosis in tubules were present.

The Microscopical picture of spleen revealed various degrees of degenerative and necrotic changes as lymphocytic (white pulp) depletion which appeared as focal areas of empty spaces in splenic parenchyma, this may be attributed to cytopathic effect of SVCV on splenic tissue and/or relocation of lymphocytes into other viral-infected organs. The detectable lesions in spleen were in agreement with those reported by **Negele (1977)** who stated also that spleen was hyperemic and showed a considerable hyperplasia of the reticuloendothelium, with siderocytes and cells with increased lipofuscin storage were present. Also **Osadcaja and Rudenko (1981)** and **Way et al. (2003)** described haemorrhage and inflammation in the spleen. The activation of melanomacrophage centers in spleen, was commonly noticed. It is quite known as an unusual sequel to infection or irritation in fish and is related to fish immune response as reported by **Robert (2001)**.

Various degrees of pathological harm in gills due to SVCV infection were evident. The remarkable

lesions were severe hyperplasia of basal malpighian cells of primary gill lamellae, progression of this migration lead to lamellar fusion, with presence of malpighian cell vacuolations (spongiosis) which might be attributed to the drastic cytopathic effects of the SVCV. After that separation of the proliferated cells from the capillary bed supervened leaving subepithelial vacuolation, which might be attributed to viral replication in capillary wall. As a result of epithelial hyperplasia, inter-lamellar spaces decreased interfering with gaseous exchange. Moreover, as gills are important also for osmoregulation and excretion of toxic waste products as mentioned by **Robert (2001)**, thus any harm in the gills leads to impairment of such vital functions revealing respiratory distress, impaired osmoregulation and retention of toxic wastes. The detectable lesions in gills were reported by **Bucke and Finlay (1979)** as a moderate hyperplasia of the lamellar epithelium with associated macrophage cells at the tips of the lamellae in the gill tissue were observed. **Sanders et al. (2003)** described multifocal branchial necrosis and melanomacrophage proliferation in gills. Furthermore **Haghighi et al. (2008)** described fusion in secondary gill lamellae with necrotic foci due to SVCV infection in fish.

The Microscopical picture of gasbladder revealed degenerated gas gland cells with the loss of connective tissue symmetry due to heavy infection with virus and its destructive effects during multiplication. **Negele (1977)** denoted that lamina epithelia of the gasbladder changed into a discontinuous multilayer and in the submucosa dilated vessels and hemorrhages were evident. While **Wunner and Peters (1991)** described petechial haemorrhages occurred in the internal wall of gasbladder. Also **Haghighi et al. (2008)** described oedema of all internal organs as well as of the wall of gasbladder

The Microscopical picture of intestine revealed villar vacuolation which agreed with **Negele (1977)** who observed perivascular inflammation and desquamation of epithelium with a subsequent atrophy of the intestinal villi. Also with some extent with **Bucke and Finlay (1979)** who recorded marked degenerative and necrotic changes, with desquamation of the epithelial linings with complete destruction of the mucosal rugae in the posterior intestine, also **Osadcaja and Rudenko (1981)** denoted acute catarrhal enteritis, with necrosis and desquamation of the epithelium, as well as **Sulimanovic et al. (1986)** described necrosis and sloughing off of the epithelial layer of the intestine, oedema and necrosis in submucosa and oedema between internal and external muscular layer and in visceral peritoneum.

By using immunohistochemistry and Immunofluorescence the localization of viral antigen was concentrated intra-cellular in hepatocytes, pancreatic acinar cells, renal tubular epithelium, gas gland cells and gill basal epithelium of primary filaments (malpighian cells), neuronal bodies. While intercellular distribution

In conclusion, we report that there are similarity in accuracy between various methods of both immuno-staining techniques (Immuno-peroxidase and Immuno-alkaline phosphatase) and Immunofluorescence technique in demonstration of SVCV in histological tissue sections with the preference of authors for immuno-staining techniques despite it takes more time in processing than Immunofluorescence, as it doesn't need sophisticated equipments such as fluorescent microscope and it produces permanent slides can be used for scientific demonstration, this statement is agreed by **Faisal and Ahne (1984)**.

In Transmission Electron Microscopy, rehydration of paraffin blocks and then re-processing for TEM observation produced satisfactory results and revealed the viral particles in SVCV infected fish specimens.

In the present study, electron microscopy of SVCV infected fish tissue revealed the presence of virus particles inside the cytoplasm especially nearby Golgi apparatus, this finding agreed with **Granzow et al. (1997)** who stated that SVCV particles adsorb to the plasma membrane and enter the host cell by receptor mediated endocytosis, and the first sign of viral replication is the formation of inclusion bodies in the cytoplasm, then virus budding at the plasma membrane and at membranes of dilated Golgi vesicles followed by maturation and release of virus from the cells. And the finding disagreed with **Saad (2005)** and **Abo Eisa (2007)** who referred to the presence of intra-nuclear viral inclusion bodies.

Acknowledgments

We thank **Dr. Peter Dixon**, Fisheries and Aquaculture Science CEFAS, Weymouth Laboratory, The Nothe, Weymouth, Dorset DT4 8UB, UK, for providing us SVCV antiserum. Also **Dr. Motohiko SANO** Director of National Research Institute of Aquaculture, Hiruta 224-1, Tamaki, Watarai, Mie 519-0423, JAPAN, for experimental technical help. And **Dr. Olga L.M. Haenen**, Head of the fish and shellfish diseases laboratory, central veterinary institute, Wageningen University, Netherland, **Dr. Geert F. Wiegertjes**, Department of Animal Sciences, Cell Biology and Immunology Group, Wageningen University, Netherland, **Dr. Jim R.Winton**, chief of the fish health section at the U.S.

Geological. Survey's Western Fisheries Research Center, Seattle, WA, USA, and **Dr. Niels Jørgen Olesen**, senior research scientist, Community Reference Laboratory for Fish Diseases, Section for Fish Diseases, National Veterinary Institute, Technical University of Denmark for providing us with some valuable publications and technical advice.

References

1. **Abo eisa, (2007)**: Some studies on the Spring Viraemia of Carp in cultured freshwater fish. M.V.Sc. Thesis, Faculty of Veterinary Medicine, Alexandria University.
2. **Ahne, W. (1977)**: Evidence for the systemic character of Rhabdovirus carpio infection. Bulletin de l'Office International des Épidémiologies. 87:435-436.
3. **Ahne, W. (1978)**: Uptake and multiplication of Spring Viraemia of Carp virus in carp, *Cyprinus carpio* L. Journal of Fish Diseases.1:265-268.
4. **Ahne, W., Björklund, H.V., Essbauer, S., Fijan, N., Kurath, G., Winton, J.R., (2002)**: Spring viraemia of carp (SVC). Diseases of Aquatic Organisms. 52:261-272.
5. **Alexandrino, A.C., Ranzani-Paiva, M.J.T. and Romano, L.A. (1998)**: Identificación de Viraemia primaveral de la carpa (VPC) *Carrassius auratus* en San Pablo, Revista Ceres (Brasil).45:125-137.
6. **APHIS, (2003)**: USA Animal and Plant Health Inspection Service Report. Washington, March 25, 2003.
7. **Armstrong, R.D. and Ferguson, H.W. (1989)**: Systemic viral disease of the orange chromide cichlid *Etropus maculatus*. Diseases of Aquatic Organisms. 7:155-157.
8. **Björklund, H.V., Higman, K.H. and Kurath, G. (1996)**: The glycoprotein genes and gene junctions of the fish rhabdoviruses Spring Viraemia of Carp virus and Hirame rhabdovirus: analysis of relationships with other rhabdoviruses. Virus Research. 42:65-80.
9. **Bootsma, R. and Ebregt, D. (1983)**: Spring Viraemia of Carp. In: Anderson, D.P., Dorson, M. and Dubourget, P. (eds) Antigens of Fish Pathogens. Collection Fondation Marcel Merieux, Lyons, France, pp. 81-86.
10. **Bucke, D. and Finlay, J. (1979)**: Identification of Spring Viraemia in Carp (*Cyprinus carpio* L.) in Great Britain. Veterinary Record 104:69-71.
11. **Faisal, M. and Ahne, W. (1984)**: Spring Viraemia of Carp virus (SVCV): comparison of immunoperoxidase, fluorescent antibody and cell culture isolation techniques for detection of antigen. Journal of Fish Diseases. 7:57-64.

12. **Fijan, N., Petrinec, Z., Sulimanović, D. and Zwillenberg, L.O. (1971):** Isolation of the viral causative agent from the acute form of infectious dropsy of carp. *Veterinarski Arhiv* 41, 125-138.
13. **Fijan, N., Sulimanovic, D., Bearzotti, M., Muzinic, D., Zwillenberg, L.O., Chilmoneczyk, S., Vautherot, J.F. and de kinkelin, P. (1983):** Some properties of the *Epithelioma papulosum cyprini* (EPC) cell line from carp *Cyprinus carpio*. *Annals of Virology (Institut Pasteur)* 134: 207-220.
14. **Garver, K.A., Dwilow, A.G., Richard, J., Booth, T.F., Beniac, D.R., and Souter, B.W., (2007):** First detection and confirmation of Spring Viraemia of Carp virus in common carp, *Cyprinus carpio* L., from Hamilton Harbour, Lake Ontario, Canada. *Journal of Fish Diseases*. 30:665-671.
15. **Glazebrook, J.S., Heasman, M.P. and DeBeer, S.M. (1990):** Picorna like viral particles associated with mass mortalities in larval barramundi, *Lates calcarifer* block. *Journal of Fish Diseases*. 12:245-249.
16. **Granzow, H., Wieland, F., Fichtner, D. and Enzmann, P.J. (1997):** Studies on the ultrastructure and morphogenesis of fish pathogenic viruses grown in cell culture. *Journal of Fish Diseases*. 20:1-10.
17. **Haenen, O.L.M. and Davidse, A. (1993):** Comparative pathogenicity of two strains of pike fry rhabdovirus and Spring Viraemia of Carp virus for young roach, common carp, grass carp and rainbow trout. *Diseases of Aquatic Organisms*. 15:87-92.
18. **Haghighi, A., Asl, K., Bandehpour, M., Sharifnia, Z. and Kazemi, B. (2008):** The First Report of Spring Viraemia of Carp in Some Rainbow Trout Propagation and Breeding by Pathology and Molecular Techniques in Iran. *Asian Journal of Animal and Veterinary Advances*. 3(4):263-268.
19. **Hayat, M. A. (2002):** Microscopy, Immunohistochemistry, and Antigen Retrieval Methods for Light and Electron Microscopy. Kluwer Academic Publishers, Kean University Union, New Jersey.
20. **Irnazarow, I. (1995):** Genetic variability of Polish and Hungarian carp lines. *Aquaculture Research*. 129: 215-219.
21. **Johnson, M.C., Maxwell, J.M., Loh, P.C. and Leong, J.A. (1999):** Molecular characterization of the lycoproteins from two warm water rhabdoviruses: snakehead rhabdovirus (SHRV) and rhabdovirus of penaeid shrimp (RPS)/ Spring Viraemia of Carp virus (SVCV). *Virus Research*. 64(2):95-106.
22. **Koutna, M., Vesely, T., Psikal, I. and Hulova, J. (2003):** Identification of spring viraemia of carp virus (SVCV) by combined RT-PCR and nested PCR. *Diseases of Aquatic Organisms*. 55: 229-235.
23. **Kuo, J. (2007):** Electron microscopy: methods and protocols. 2nd ed., Methods in molecular biology; v. 369, Humana Press Inc.
24. **Liu, H., Gao, X., Shi, T., Gu, Y., Jiang, H., Chen (2004):** Isolation of Spring Viraemia of Carp virus (SVCV) from cultured koi (*Cyprinus carpio koi*) and common carp (*C. carpio carpio*) in P.R.China. *Bulletin of European Association of Fish Pathologists*, 24(4): 194.
25. **Lupiani, B., Dopazo, C.B., Ledo, A., Fouz, B., Barja, J.L., Hetrick, F.M. and Toranzo, A.E. (1989):** New syndrome of mixed bacterial and viral etiology in cultured turbot *Scophthalmus maximus*. *Journal of Aquatic Animal Health*. 1:197-204.
26. **Negele, R.D. (1977):** Histopathological changes in some organs of experimentally infected carp fingerlings with *Rhabdovirus carpio*. *Bulletin de l'Office International des Épidémiologistes* 87: 449-450.
27. **Oreshkova, S.F., Tikunova, N.V., Shchelkunov, I.S. and Ilyichev, A.A. (1995):** Detection of Spring Viraemia of Carp virus by hybridization with biotinylated DNA probes. *Veterinary Research*. 26:533-537.
28. **Osadcaja, E.F. and Rudenko, A.P. (1981):** Patogennost virusov, vydelennyh pri krasnuhe (vesennej viremii) karpov i kliniko-morfologičeskaja harakteristika estestvennogo tečhenija bolezni i v eksperimente. *Rybnoe hozjajstvo (Kiev)* 32, 66-71. (In Ukrainian.)
29. **Reed, R.J., Muench, H., (1938):** A simple method of estimating 50% endpoints. *American Journal of Hygiene*. 27:493-497.
30. **Richards and Buchanon. (1978):** Studies on *Herpesvirus scophthalmi* infection of turbot *scophthalmus maximus* (L): Histopathological observation. *Journal of Fish Diseases*. 1:251-258.
31. **Richenbach-Klinke, H.H. (1973):** Fish pathology. T.F.H. Publ., Neptune, N.J. P.512.
32. **Roberts, R.J. (2001):** Fish pathology. Third edition. Harcourt publishers limited 2001.
33. **Rowley, H., Graham, D.A., Campbell, S., Way, K., Stone, D.M., Curran, W.L. and Bryson, D.G. (2001):** Isolation and characterization of rhabdovirus from wild common bream *Abramis brama*, roach *Rutilus*, farmed brown trout *salmo trutta* and rainbow trout *Onchorhynchus mykiss* in Northern Ireland. *Diseases of Aquatic Organisms*. 48 (1):7-15.
34. **Saad, T.T., (2005):** Some Studies on the effects of Spring Viraemia of Carp Virus on cultured

- Carp species. Ph.D. Thesis, Faculty of Veterinary Medicine, Alexandria University.
35. **Sanders, G. E., Batts, W. N. and Winton, J. R. (2003):** Susceptibility of Zebrafish (*Danio rerio*) to a Model Pathogen, Spring Viraemia of Carp Virus. *Comparative Medicine*. 53(5):501-508.
 36. **Siwicki, A. K., Pozet, E., Morand, M., Kazun, B., Trapkowska, S. and Malaczwska, J. (2003):** Influence of methisoprinol on the replication of rhabdoviruses isolated from Carp (*Cyprinus carpio*) and Catfish (*Ictalurus melas*): in vitro study. *Polish Journal of Veterinary Sciences*. 6(1):47-50.
 37. **Soliman, M. K., Aboeisa, M. M., Safinaz G. M., Saleh, W.D. (2008):** First record of isolation and identification of Spring Viraemia of Carp virus from *Oreochromis niloticus* in Egypt. 8th International Symposium on Tilapia in Aquaculture. 533-533.
 38. **Sulimanovic, M., Bambir, S., Sabocanec, R., Culjak, K. and Miyazaki, T. (1986):** Spring Viraemia of Carp: microscopic pathology. In: Abstracts, International Symposium Ichthyopathology in Aquaculture. October 21-24, 1986. Yugoslav Academy of Sciences and Arts, Veterinary Faculty. Dubrovnik, p.21.
 39. **Tesarcik, J., Macura, B., Dedek, L., Valicek, D. and Smid, B. (1977):** Isolation and electron microscopy of rhabdovirus from the acute form of infectious dropsy of carp (Spring Viraemia of Carp). *Zentralblatt für Veterinärmedizin (B)* 24, 340-343.
 40. **Way, K., Bark, S.J., Longshaw, C.B., Denham, K.L., Dixon, P.F., Feist, S.W., Gardiner, R., Gubbins, M.J., Le Deuff, R.M., Martin, P.D., Stone, D.M. and Taylor, G.R. (2003):** Isolation of a rhabdovirus during outbreaks of disease in Cyprinid fish species at fishery sites in England. *Diseases of Aquatic Organisms*. 57 (1-2): 43-50.
 41. **Wolf, K. (1988):** Fish Viruses and Fish Viral Diseases. Cornell University Press, Ithaca.
 42. **Wunner, W.H. and Peters, D. (1991):** Family Rhabdoviridae. In: Francki, R.I.B., Fauquet, C.M., Knudson, D.L. and Brown, F. (eds): Classification and Nomenclature of Viruses. Fifth Report of the International Committee on Taxonomy of Viruses. *Archives of Virology, Supplement*. 2, 250-262.

3/3/2011

PMF, Cesium & Rubidium Nanoparticles Induce Apoptosis in A549 Cells

Faten. A. Khorshid¹; Gehan. A. Raouf² *; Salem. M. El-Hamidy³; Gehan. S. Al-amri¹; Nourah. A. Alotaibi² and Taha A. Kumosani²

King Fahd Medical Research Centre, ¹Tissue Culture Unit, ²Medical Biophysics Laboratory, Biochemistry Department, ³ Electron Microscopy Unit, Biological Science Department and ²Biochemistry Department, Faculty of Science, King Abdulaziz University
*jahmed@kau.edu.sa

Abstract: Cancer becomes one of the leading cause of death in many countries over the world. Fourier-transform infrared (FTIR) spectra of human lung cancer cells (A549) treated with PMF (natural product extracted from PM 701) for different time intervals were examined. Second derivative and difference method were taken in comparison studies. Cesium (Cs) and Rubidium (Rb) nanoparticles in PMF were detected by Energy Dispersive X-ray attached to Scanning Electron Microscope SEM-EDX. Characteristic changes in protein secondary structure, lipid profile and changes in the intensities of DNA bands were identified in treated A549 cells spectra. A characteristic internucleosomal ladder of DNA fragmentation was also observed after 30 min of treatment. Moreover, the pH values were significantly increases upon treatment due to the presence of Cs and Rb nanoparticles in the PMF fraction. These results support the previous findings that PMF is selective anticancer agent and can produce apoptosis to A549 cells.

[Faten. A. Khorshid; Gehan. A. Raouf; Salem. M. El-Hamidy; Gehan. S. Al-amri¹; Nourah. A. Alotaibi and Taha A. Kumosani, PMF, Cesium & Rubidium Nanoparticles Induce Apoptosis in A549 Cells] Life Science Journal, 2011; 8(3):534-542] (ISSN: 1097-8135). <http://www.lifesciencesite.com>.

Keywords: Apoptosis, FTIR spectroscopy, pH therapy, Scanning Electron Microscope- Energy Dispersive X-ray (SEM-EDX).

1. Introduction

Nanotechnology has considerable promise for the detection, staging and treatment of cancer [1]. The past two decades have witnessed rapid advances in the ability to structure matter at the nanoscale with sufficient degree of control over the material size, shape, composition, and morphology [2]. The combination of the unique properties with the appropriate size has motivated the introduction of nanostructure into biology [3, 6] Cells and their constituent organelles lie on the sub-micron to micron size scale. Further, proteins and macromolecules found throughout the cell are on the nanometer size scale [7]. Thus nanoparticles ranging from a few to a hundred nanometers in size become ideal as labels and probes for incorporation into biological systems [5,6]

Despite significant investment and research, cancer is still responsible for 25% of all deaths in developed countries [8]. There is a pressing need for more sensitive, selective and cost-effective methods for detecting and treating cancer.

The presence of natural occurring nanoparticles that can produce apoptosis in cancer cells would be of great help. PMF, the active fraction separated from PM 701 [(natural product previously proved to be selective anticancer agent) [9-15] would give a promising therapeutic criterion in treating cancer. The effect of PMF on lung cancer cells A549

will be monitored by Fourier-transform infrared (FTIR) spectroscopy.

FTIR spectroscopy has become a useful analytical tool in biomedical science in the past decade, e.g., for the characterization of microorganisms[16], isolated cells or cell lines[17-20], body fluids and tissues [21,26] The ability to detect drug action, disease or dysfunction rapidly has obvious benefits, including early intervention of therapeutic strategies, hopefully in a prognostic fashion, significant reduction in mortality and morbidity, and the freeing up of much needed economic resources within health care systems [27]. With these highly sensitive techniques, the frequency and the intensity of light in the resulting spectrum provide biochemical information regarding the molecular composition, structure and interaction in cells and tissues.

Apoptosis, as a pre-programmed physiological mode of cell death, plays an important role in the pathogenesis and progression of cancer. Understanding of the basic mechanisms that underlie apoptosis will point to potentially new targets of therapeutic treatment of diseases that show an imbalance between cell proliferation and cell loss. As an active process, apoptosis involves biochemical changes on three essential cellular components, DNA, protein and lipid. There are three steps in apoptosis, the initiation phase triggered by a stimulus

received by the cell, the decision phase during which the cell commits itself to live or to die, and the degradation phase when the cells acquire the morphological and biochemical hallmarks of apoptosis [28]. Clearly, it would be desirable to detect apoptosis at an early stage, i.e. before phase that entails the visible changes of apoptosis.

In this study we will explore the potential of PMF as a selective anticancer agent which produces apoptosis in lung cancer cells (A549) by using FTIR spectroscopy technique and to bring to light the role of Cesium (Cs) and Rubidium (Rb) nanoparticles - found in PMF.

2- Material and Methods

Media

The following commercially available media were prepared according to published literature, these include: Ordinary media, Minimal essential medium (MEM, supplemented with 10%FCS): MEM is a rich, multipurpose medium that was used for cultivation of human lung cancer cells (A549). Phosphate Buffer Saline (PBS) is a Phosphate-Buffered physiological Saline solution. Calcium and Magnesium free Solution Trypsin [29] Examined media: PMF (extracted from PM 701) is a natural product, easily available, cheap, sterile, and non-toxic according to our chemical and microbiological testing. PMF added to the ordinary media with ratio 2.5 μg : 1 ml (w/v) media.

Human Lung Cancer Cells line:

Human Lung Cancer Cells, non- small cell carcinoma (A549) was obtained from cell strain from (ATCC) American Type Cultural Collection, available in the cell bank of Tissue Culture Unit, King Fahd Medical Research Center (KAU, Jeddah).

In vitro proliferation of cells

Human Lung Cancer Cells (A549) were suspended in culture medium MEM.

The cells were dispensed in 3X (6wells plate), $1 \times 10^5/\text{ml}$ in each well.

Each group of cells was incubated 24 hrs in suitable media and apoptosis was induced by incubating cells in PMF at different time points.

Infrared spectroscopy

At various time points, the cells treated with PMF were harvested and washed twice (by centrifugation for 3 min at 300 g). The cell pellet was kept at -80°C and freeze dried prior to IR measurements. The lyophilized samples - from three different separated experiments - were dispersed in potassium bromide (KBr) discs by mixing them gently in an agate mortar and with pestle to obtain

homogenous mixture as described previously [14, 30]. The mixture then pressed in a die at 5 metric tons force for 3 s, creating a 1.1 cm diameter transparent disc with imbedded sample. The FTIR spectra were recorded in absorbance form using Shimadzu FTIR-8400 s spectrophotometer with continuous nitrogen purge. The spectra were obtained in the wavenumber range of $4000-400\text{ cm}^{-1}$ with an average of 20 scans to increase the signal to noise ratio and at spectral resolution of 4 cm^{-1} . All the samples were baseline corrected and normalized to amide II band by using IR Solution software. The parameters studied were nucleic acid, proteins and lipids. Second derivative and difference method measurements were taken in comparison studies.

Scanning Electron Microscopy (SEM)

Detecting of Cs and Rb nanoparticles in PMF:

For SEM studies the PMF were suspended in distilled water, then treated in an ultrasonic bath (BRANSON, 1510) about 20 min. A small drop of this suspension placed on the double side carbon tape on Al- Stub and dried in air. The specimens were analyzed - without gold coating- by using energy dispersive analyzer unit (EX-23000BU) which attached to the scanning electron microscope (JSM-6360LA, JEOL, Tokyo, Japan). The microscope was operated at an accelerating voltage of 20 kV. Quantitative method ZAF and characterization method as pure.

Cs and Rb level measurements

Cs and Rb levels were measured in The Ministry of Petroleum-The Egyptian Mineral Resources Authority- Central Laboratories Sector by using Inductively Coupled Plasma (ICP) the results were multiplied by the dilution factor 20.1.

DNA fragmentation and pH measurements

DNA was extracted according to the method described by Kneipp et al., [23] by electrophoresis in agarose gel. The genomic DNA was run in a 1.5% agarose gel for 20min.

The pH values of the A549 cell's media were measured immediately by Jenway 3200 pH meter at the end of each treating time. These measurements were repeated for three different experiments.

3. Results and Discussion

IR spectral features and assignments

The addition of PMF to A549 cells after 5, 15, 30 min and 2, 24hr of treatment caused a series of changes in the spectra of these cell lines (Fig.1). The absorption profiles are typical of tissue infrared spectra, which are dominated by protein, lipids and DNA represents the most absorption IR spectral

peaks and the proposed biomolecular assignments (Table I). Fig.1a. shows a noticeable decrease in the intensities of proteins (amide I & amide II), nucleic acids band, and an increase in the intensity of the weak shoulder located at 1737 cm⁻¹ after PMF treatment.

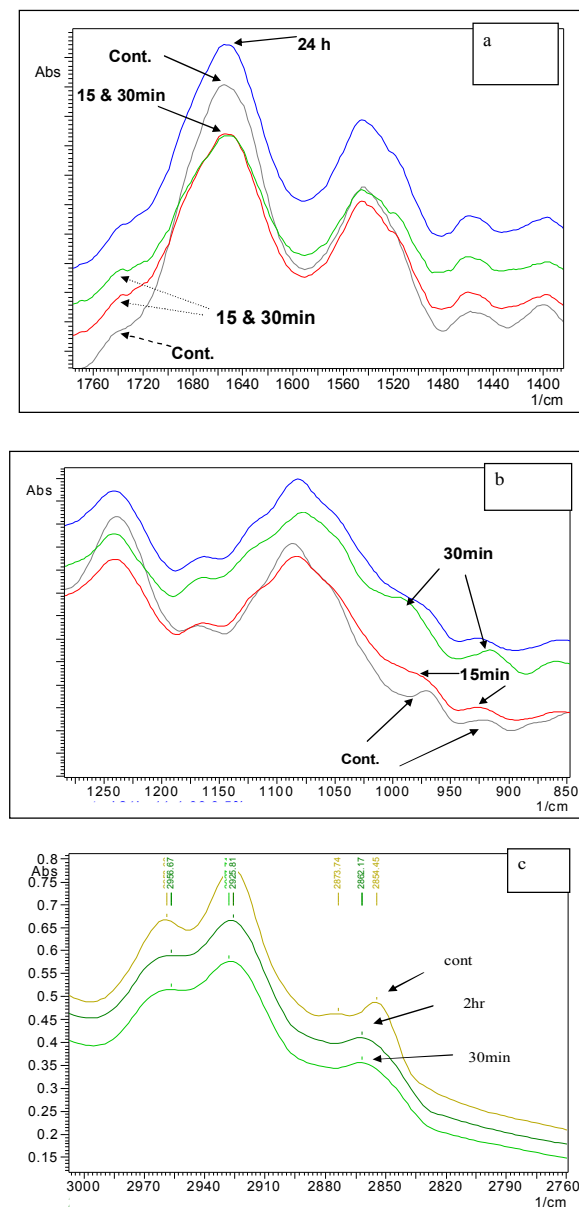


Fig. 1 Raw FTIR spectra of A549 cells treated with PMF at different times (a) shows the amide I band shift and the increase in the intensity of the band located at 1735 cm⁻¹ (C=O ester group) in range 1760-1400 cm⁻¹. (b) shows the decrease in DNA peaks at the onset of apoptosis (5-15min) and the increase in 970 cm⁻¹ peak after 30 min of PMF treatment. (c) shows the band shift in CH₂ bands.

TABLE 1. Major IR Spectral Peaks Of A549 Cells and Proposed Biomolecular Assignments

Wave number (cm ⁻¹)	Proposed biomolecular assignment
2963	C-H stretch (asymmetric) of CH ₃ in fatty acids, lipids, proteins.
2926	C-H stretch (asymmetric) of CH ₂ in fatty acids, lipids, proteins.
2873	C-H stretch (symmetric) of CH ₃ in fatty acids, lipids, proteins.
2853	C-H stretch (symmetric) of CH ₂ in fatty acids, lipids, proteins.
1737	Ester C=O stretching of phospholipids.
1652	Amide I of α -helix protein structures (C=O) stretch.
1542	Amide II (N-H) bend
1460	CH ₃ antisymmetric bend
1430-1360	COO ⁻ stretch
1240	PO ₂ ⁻ asymmetric stretch of phosphodiester group in nucleic acids and phospholipids
1168	C-O, C-C stretch, C-O-H, C-O-C deformation of carbohydrates or C-OH stretch of serine, threonine, tyrosine in cell proteins
1085	PO ₂ ⁻ symmetric stretch of phosphodiester group in nucleic acids and phospholipids
975	PO ₃ ²⁻ stretch

We also observed that the amide I band shifted towards lower frequency from 1652 cm⁻¹ in the control cells to 1649 cm⁻¹ in the cells treated with PMF for 15, 30 min, 2hr and 24hrs. These amide I frequencies are compatible with the fact that overall protein structure in the control cells consists primarily of α -helix, whereas after 5min up to 24hr of PMF treatment the cells have a relatively high proportion of β -sheet and a relatively high proportion of unordered proteins. A similar shift in the amide I and amide II bands during apoptosis was reported earlier [14,35,39].

Alterations in lipid content/structure can also be obtained by examining the dominant lipid bands in the range 2800-3050 cm⁻¹ that originate from CH stretching vibrations of the fatty acyl chains of all cellular lipids (Fig.1b). The CH₂ band provide information about the membrane fluidity [40], the higher the frequency, the higher the fluidity. Therefore, we analyzed the CH₂ band position in the cells before and after PMF treatment and found that for control A549 cells this band was centered at 2931 cm⁻¹ while it is shifted to 2929 cm⁻¹ in the treated cells. This observed shift in CH₂ band could be explained. It can be considered now as a strong evidence in decreasing membrane fluidity, which would be in agreement with oxidative damage having occurred [36, 39].

Absorbance of infrared in the region 900-1300cm⁻¹ of the samples is shown in Fig.1c. The figure shows the decrease in DNA peaks at the onset

of apoptosis (5-15min) and the increase in 970 cm^{-1} peak after 30 min of PMF treatment. Early apoptotic cells appear in the cell cycle distribution as cells with a hypodiploid DNA. This alteration in DNA content results from degradation of cellular DNA by activation of endogenous endonucleases during apoptosis [36]. Cells in the pre-Go/G1 phase (M4) were therefore defined as apoptotic cells. These results are also consistent with the finding that at the early stage of apoptosis, initiation phase is triggered by a stimulus received by the cell, this can be explained by the first disappearance of nucleic acid bands at 975 and 923 cm^{-1} at 5 and 15 min upon PMF treatment. A549 cells treated up to 30 min with PMF showed clear absorbance bands of DNA at 975 and 923 cm^{-1} which may referred to the degradation of DNA. Jamin et al. [41] reported a large increase in the DNA signals of apoptotic cells. In apoptosis DNA is degraded into oligonucleotides with a few hundreds of base pairs that subsequently diffuse out of the nucleus. This observation suggests that the DNA, although highly condensed in the nucleus, has a low absorption, yet its degradation products in late apoptosis are detected by IR spectroscopy.

Fig. 2 represents the raw IR spectra of A549 cells treated with PMF from 5 min up to 24hr without normalization. The figure shows a dramatic decrease in bands intensities over the rang 1800-900 cm^{-1} . The same results were obtained from normal human fetal lung fibroblast IMR-90 in G1, S-, and G2M-phase of the cycle [39]. Hoi-Ying et al., [39] showed that the IR spectra of these three phases are clearly different. During the S-phase the DNA was undergoing replication and they observed that the absorption in the DNA/RNA spectral region increased relative to the G1-phase spectra. When a G2/M-phase cell was measured they observed a large increase in the overall absorbance ([like the uppermost spectrum in Fig. 2. This may have been a result of more material in the cell or because of the thickness may have been different in the M-phase.

Second Derivative Analysis

Since apoptosis involves the modification of existing proteins, as well as the synthesis of new proteins [35, 39] we analyzed the changes of protein structure after PMF treatment in more detail. Fig. 3 shows only the mean spectra of control and PMF treated cells for 30 sec - for clarity reason - in the region of the amide I (1600-1700 cm^{-1}) and amide II (1500-1600 cm^{-1}) bands. Spectra are shown as second derivative, a method commonly used for narrowing broad IR bands for better visualization. The spectrum of a dying cell due to treatment shows significant shifts in the amide I peak compared to the spectrum of a living A549 cell. The changes in the secondary

structure of the proteins appeared after 15 min of treatment. The dying cell shows two characteristic spectral signatures indicative of death [36, 41]. First, the centroids of the protein amide I and II peaks shift to lower energy, indicating a change in the overall protein conformational states within the cell. Second; the appearance of a peak at around 1743 cm^{-1} [39]. These structural changes in the cellular proteins could be due to a different distribution of proteins during apoptosis or to denaturation of the existing proteins.

The lipids in the plasma membrane are composed mainly of phospholipids that determine membrane stability, fluidity and membrane enzymatic activity [40]. Thus, monitoring lipid absorbance in the treated samples is an important for detecting apoptosis. The peak at 1737 cm^{-1} - which is associated with the non-hydrogen bonded ester carbonyl C=O - splits into two bands in the second derivative analysis (Fig 3.) centered at 1743 and 1725 cm^{-1} . the reason that the 1743 cm^{-1} peak in Fig.3 is significantly more intense than the 1725 cm^{-1} peak implies that the C=O ester carbonyl groups of lipids in the cell are becoming predominantly non-hydrogen bonded, which would be in agreement with oxidative damage having occurred [39]. Apoptosis is associated with, among other factors, increased oxidative damage [42, 43]. The positive intensity at 1740 cm^{-1} suggest an increase in the C=O ester components in the plasma membranes following PMF treatment.

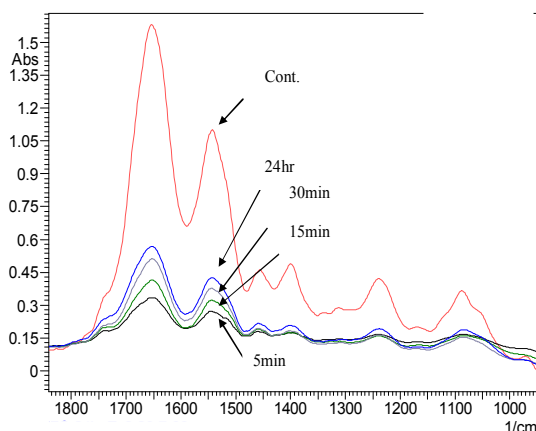


Fig. 2 The raw FTIR spectra of A549 cells treated with different times with PMF. The spectra were not normalized.

Difference Method

In order to further assess and identify these membrane changes, typical IR marker bands for lipids were evaluated by creating a difference spectrum' in the range of 2800-3050 cm^{-1} Fig. 4(a).

The two methyl bands at 2870 and 2954 cm^{-1} , which originate from the symmetric and asymmetric stretching vibrations of the acyl chain CH_3 groups,

are negative in the IR 'difference spectrum' in contrast, the two methylene bands at 2851 and 2931cm^{-1} , attributed to the symmetric and asymmetric stretching vibrations of acyl chain CH_2 groups are positive, indicating that PMF treatment increases the lipid content in the plasma membranes of A549 cells.

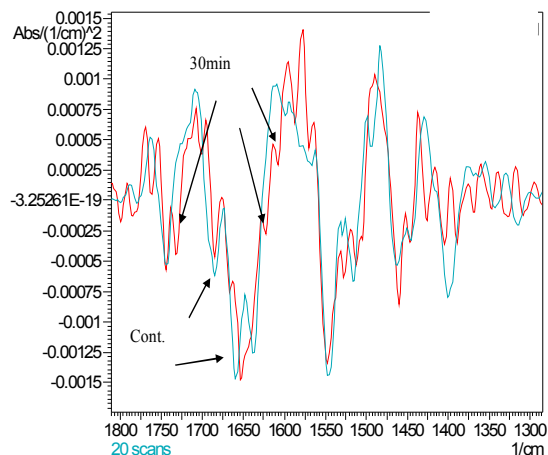


Fig. 3 Infrared second derivative spectra of control and PMF-treated A549 cells for 30 min.

The characteristic CH_3 group stretching vibration bands at 2870 & 2954cm^{-1} show a negative band in the difference spectrum. These results may reflect structural changes of phospholipids rather than relative changes of lipid in the treated cells [34, 35]. PMF contains mainly peptides and amino acids [44]. Thus, PMF may contact with A549 cell membrane and may form some sort of an ion channel or pore in the cell membrane thereby, enhancing the ion permeability of the membrane and destroying the cell i.e. induce apoptosis. References [45-47] suggested that the peptide could perturb membrane functions responsible for osmotic balance.

The mode of action of PMF with the membrane phospholipids bilayers could possibly be due to the aggregation of peptides on the surface of the membrane and then inserts into the bilayer forming a so-called barrel-stave pore. Another possibility is that the accumulation of peptide on the membrane surface forms a destabilizing carpet, leading to a local disintegration of the bilayer. A third possibility is that peptide chains aggregate on the membrane surface, possibly forming a carpet, partially submerge, and then blend with lipids so that peptide chains and lipid head groups together line the wall of a toroidal pore [35, 44-48].

The present and our previous study [14] extend these findings and suggest that PMF may alter the conformation of membrane proteins such as

nucleoside transporters, ion channels and proof the formation of pores.

The Transmission Electron microscope (TEM) Photograph (Fig. 5) was taken after 5 sec only from adding PMF to the media "unpublished paper" [49]. The arrow in the Fig. pointed to the entrance of nanoparticles to inside the nucleus via temporary created artificial pore (T) in the nuclear envelope. The nanoparticle interpenetrated the nuclear envelope and the underneath euchromatin. The normal nuclear pore was also seen in other place, whereas no underneath chromatin prevent the normally entrance and exit of molecules.

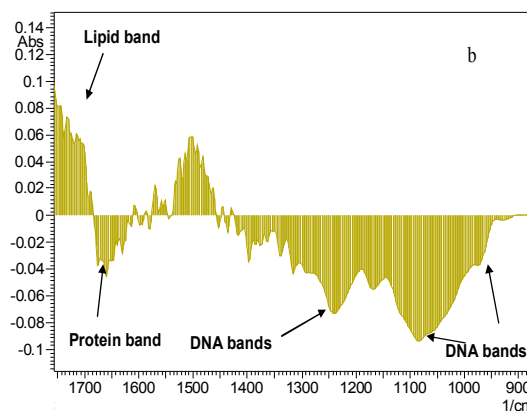
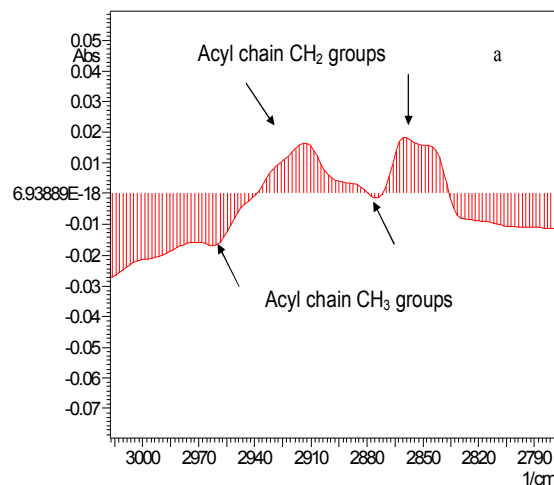


Fig. 4 The IR difference spectrum between control and PMF treated A549 cells for two hours in range $3000\text{-}2800\text{cm}^{-1}$ (a). Difference spectra between control A549 cells and that treated with PMF for 5 min. The figure shows negative DNA bands (at 930cm^{-1} , 1085cm^{-1} and 1240cm^{-1}), negative band of proteins (1652cm^{-1}) and positive band of lipids (1735cm^{-1}) (b).

Difference spectra between control A549 cells and that treated with PMF for 5 min in range $1700\text{-}900\text{cm}^{-1}$ were presented in Fig. 4b. The figure

shows negative DNA bands (at 930cm^{-1} , 1085cm^{-1} and 1240cm^{-1}), negative band of proteins (1652cm^{-1}) and positive band of lipids (1735cm^{-1}). From the difference spectrum one can clearly observe that DNA content in the cells treated with PMF has significantly decreased. These results are consistent with the finding that condensation of chromatin during the early stage of apoptosis takes place which in turn decreases the path length [41,50]. This is may referred to dark DNA, one would expect that less photons are transmitted within the strong absorption bands of DNA (which make up the chromatin) by particles of such relatively high optical density. Furthermore, given the entire highly condensed chromatin would be virtually opaque [41, 50]. These results are in good agreement with the results obtained earlier [10,14] who studied the effect of PM701 as anticancer agent in vitro on the same type of cancer A549 cells. Live images of the cells showed that the severe lethal effects of PM701 on cancer cells started immediately after 5-6min since adding the examined substrate. They continued that the cancer cells incubated in PM701 showed that the substrate attacks the cell's nuclei, which is indicated by the appearance of pale ring around the nucleus of the lung cancer cell after 30 min of incubation. This leads to the degradation of the cells, which could not be reversed to recover the cells by re-growing the cells in ordinary media again.

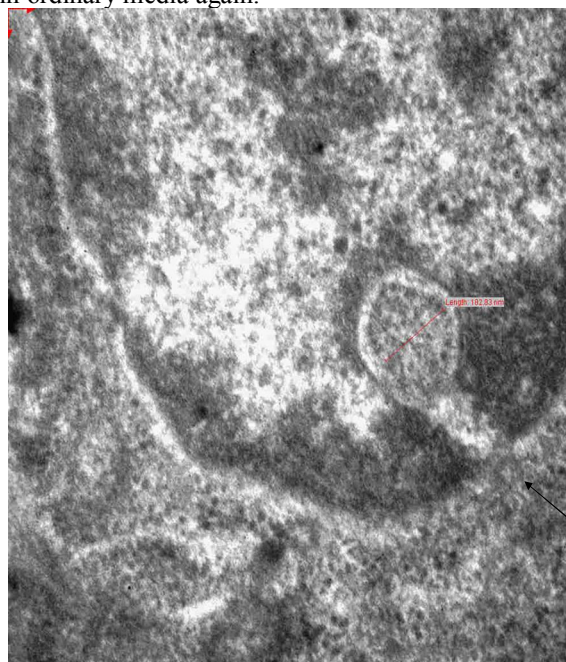


Fig. 5 TEM image of A549 cells after 5 sec of PMF treatment. The figure shows the induced pore formation in the nucleus membrane upon PMF treatment.

Electrophoresis and pH measurements

We extracted DNA from A549 control and the treated cells to confirm the finding that PMF induces apoptosis and analyzed DNA fragmentations using gel electrophoresis. A characteristic internucleosomal ladder of DNA fragmentation was observed in A549 cells treated with PMF for 30 min (Fig. 6). These results are in good consistent with the above results obtained from infrared spectroscopy observations.

The pH values of the A549 cells were measured as described earlier. The relationship between the time of treatment and the pH values were shown in Fig. 7. For all times of treatment, the pH values increased significantly after adding PMF to the media of A549 cells the maximum value was obtained at 2hrs of treatment. Our results consistent with the previous reported results describing the pH value of cancer cells and the using of high pH therapy in cancer patients [48, 51, 52]. The cancer cells contain high amounts of hydrogen ions rendering them acidic and they also contain higher Na^+ levels than found in normal cells. If Cs^- or Rb^- enters the cancer cells, their pH increases. At a pH of 7.6 the cancer cell division will stop, and at a pH of 8.0 to 8.5 the life span of cancer cells is considerably shortened to only hours [51]. Cs, Rb, and the other elements were detected in PMF by using SEM-EDX (Fig. 8) (Table II). The presence of Cs or Rb in the fluids adjacent to the tumor cells is believed to raise the pH of the cancer cells where cell mitoses will then cease resulting in reduction of life span of the cancer cell [52].

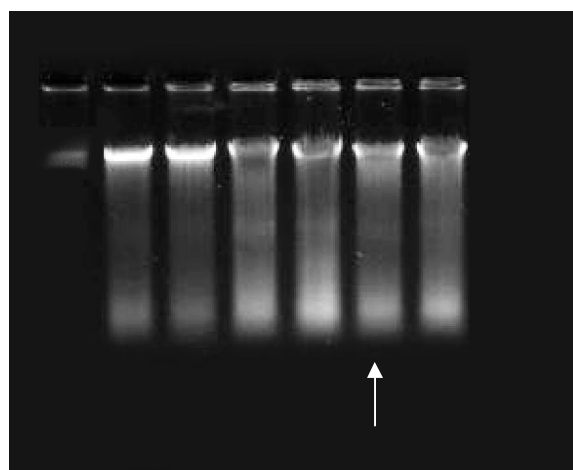


Fig. 6 Detection of DNA fragmentation by agarose electrophoresis. A549 cells were treated with PMF for 5, 15, 30 min, 2hr and 24hr with PMF (Lane from left to right). The arrow points to DNA maximum fragmentation after 30 min of treatment.

(Ag) and gold (Au) nanoparticles [49]. Noble metal, especially Au, nanoparticles have immense potential for cancer diagnosis and therapy [7].

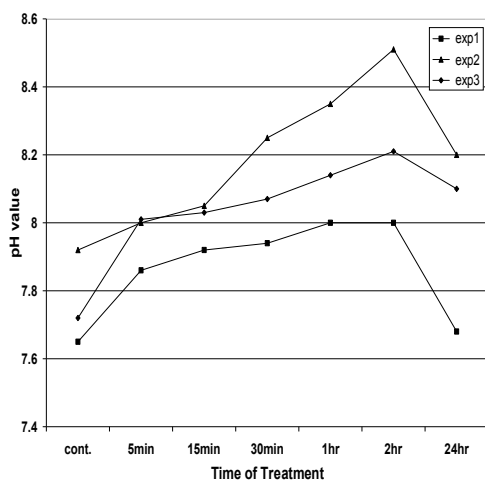


Fig. 7 The pH values of three different measurements to the A549 cells' media for different PMF treating time. The results obtained from three different separated experiments.

The mechanism of action of Cs in cancer has been little studied. That both Cs⁻ and Rb⁻ can specifically enter cancer cells and embryonic cells, but not normal adult cells[51]. PMF contain 70.9128, 8.04 ppm Rb and Cs respectively and thus may explain the selectivity action of this new anticancer agent (PMF). It is clear from (Table II) that PMF contain also silver

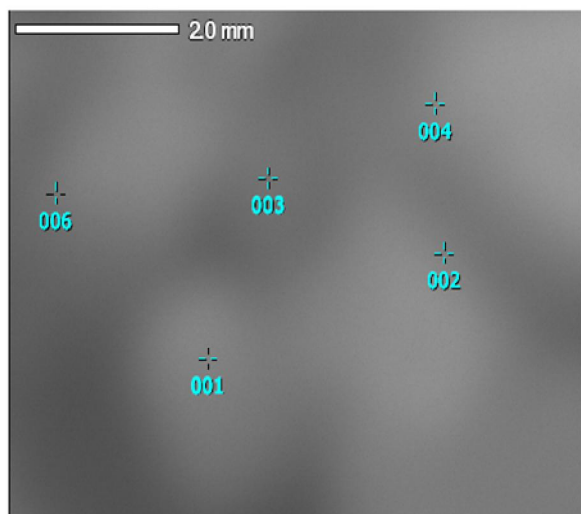


Fig. 8 SEM-EDX image of PMF

TABLE II The most important nanoparticles detected in PMF by SEM-EDX

mass%	N	Na	Mg	P	S	Cl	K	Ca	Cu	Zn	Rb	Ag	Cs	Au	Total
001	55.45	14.04	2.32		1.02	15.96	8.74	1.07	0.10	0.07	0.23	0.88			1.33
002	47.36	21.07	1.74	0.20	0.96	21.18	7.28	0.30		0.22	0.28				100.00
003	52.78	17.77	1.65		0.93	17.87	8.38	0.26	0.05			0.15		0.78	100.00
004	52.58	16.34	0.82		0.22	17.94	9.76	0.21		0.14	0.95	0.52	0.23		100.00
006	53.23	17.78	1.42		0.75	17.64	8.84	0.54	0.03	0.28	0.43	0.63	0.42		100.00

Conclusion

To conclude, we can state that PMF can induce apoptosis to A549 cells. The dominant protein secondary structure shifts from α -helix structure to unordered, indicating an altered protein profile in the apoptotic cells. In addition the total cellular lipid content increases starting from the first 5 to 15 min up to 24hr of treatment while the amount of DNA decreases dramatically during treatment with PMF as observed in difference spectrum

It should mention here that condensation of chromatin at the early stage of apoptosis was observed after 5 to 15 min of PMF treatment in the FTIR spectra indicated by the disappearance of the DNA absorbance bands. On the other hand, fragmentation of chromatin after 30 min of PMF treatment was evident by both FTIR spectroscopy and formation of DNA Ladder in the electrophoresis analysis. This study indicates that PMF contains Cs and Rb nanoparticles which proved to have a role in attacking cancer cells by elevating the pH. Thus, PMF as a natural product gives promising hope in cancer therapy with its prosperity of different potentially variable nanoparticles. These nanoparticles nowadays are all represent the new trend in treating cancer.

Corresponding author

Nahla AG Ahmed Refat

Department of Pathology, Faculty of Veterinary Medicine, Zagazig University, Egypt

Nahla_kashmery@hotmail.com

References

- [1] Paolo F., J. K. Larry, J. G. David, P. Jason, H. Terry, T. Felicia, H. Naomi, S. Saul, A. W. Scott, 2007. "Applications of nanoparticles to diagnostics and therapeutics in colorectal cancer," *TREND Biotechnology*, 25, : 145-152
- [2] Burda C., X. Chen, R. Narayanan, and M. A. El-Sayed, 2005. "Chemistry and properties of nanocrystals of different shapes," *Chem. Rev.*, 105: 1025-1102.
- [3] Katz E., I. Willner, 2004. "Integrated Nanoparticle-Biomolecule Hybrid Systems: Synthesis, Properties, and Applications," *Angew. Chem. Int. Ed. Vol.*, 43: 6042.

- [4] Rosi N. L., C. A. Mirkin, 2005. "Nanostructures in Biodiagnostics," *Chem Rev.*, 105: 1547.
- [5] Salata O. V., 2003. Applications of nanoparticles in biology and medicine, *J. Nanobiotech.* 2:3.
- [6] Whitesides G. M., 2003 "The 'right' size in nanobiotechnology," *Nat. Biotech.*, 21:1161.
- [7] Prashant K. J., H. Ivan, M. A. El-Sayed, 2007. "Au nanoparticles target cancer.," *Nanotoday*, 2: 18-29.
- [8] **Jemal A.**, T. Murray, E. Ward, A. Samuels, R. C. Tiwari, A. Ghafoor, E. J. Feuer, and M. J. Thun, 2005. Cancer Statistics, *CA. Cancer J. Clin.*, 55:, pp. (4):259.
- [9] Khorshid F. A., S. S. Moshref, N. Heffny, , 2005. An ideal selective anticancer agent in vitro, I-Tissue culture study of human lung cancer cells A549," *JKAU- Medical Sciences*, 12: 3-18.
- [10] Moshref S. S., F. A. Khorshid, Y. Jamal, 2006. The effect of PM 701 on mice leukemic Cells: I - Tissue culture study of L1210 (in vitro) II - In vivo study on mice," *JKAU- Medical Sciences*. 13:3-19. vol 13 (1), pp. 3-19.
- [11] Khorshid F. A., S. S. Moshref ,2006 "In vitro anticancer agent, I - Tissue culture study of human lung cancer cells A549 II - Tissue culture study of mice leukemia cells L1210," *International Journal of Cancer Research*, vol., 2, no. 4, pp. 330-344.
- [12] Moshref S. S., 2007 "PM701 a highly selective anti cancerous agent against L1210 leukemic cells: II – In vivo clinical and histopathological study," *JKAU- Medical Sciences*, vol., 14, no. 1, pp. 85-99, 2007.
- [13] Khorshid F.A., 2009 "Potential anticancer natural product against human lung cancer cells," *Trends Med. Res.*, vol., 4, no. 1, pp. 9-15.
- [14] Raouf G. A. , F. A. Khorshid , T. Kumosani, 2009 "FT-IR Spectroscopy as a Tool for Identification of Apoptosis-Induced Structural Changes in A549 Cells Dry Samples Treated with PM 701," *Int.J. Nano and Biomaterials*, vol., 2, no. 1/2/3/4/5, pp. 396-408.
- [15] Khorshid F. A., A. M. Osman, E. Abdel-Sattar, 2009 "Cytotoxic activity of bioactive fractions from PM 701," *EJEAFChe*, vol., 8, no. 11, pp. 1091-1098.
- [16] Naumann D, D. Helm, Labischinski, 1991 "Microbiological characterization by FT-IR spectroscopy," *Nature*, vol., 351, pp. 81-2.
- [17] Diem M., S. Boydston-White, & L. Chiriboga, 1999 "Infrared spectroscopy of cells and tissues: shining light on a novel subject," *Appl. Spectrosc.*, vol., 53, 148A-161A ,.
- [18] Fabian H., D. Chapman, H. Mantsch, 1996 "Infrared Spectroscopy of Biomolecules," Mantsch, H. H., Chapman, D., Eds., *Wiley-Liss*: New York, pp 341-352.
- [19] Schulz, C. P., L. Kan-Zhi, B. J. James, H. M. Henry, 1997 "Prognosis of chronic lymphocytic leukemia from infrared spectra of lymphocytes," *J. Mol. Struc.*, vol., 408, no. 40, pp. 253-256.
- [20] Baker M. J., E Gazi, M.D. Brown, J.H. Shanks, P. Gardner, N.W. Clarke, 2008 "FTIR-based spectroscopic analysis in the identification of clinically aggressive prostate cancer," *British J. Cancer*, vol., 99, pp. 1859-1866.
- [21] Lasch P., D. Naumann, 1998 "FT-IR microspectroscopic imaging of human carcinoma thin sections based on pattern recognition techniques," *Cell. Mol. Biol.* vol., 44, no. 1, pp. 189-202.
- [22] McIntosh L., M. Jackson, H. Mantsch, M. Stranc, D. Pilavdzic, A. Crowson, 1999 "Infrared spectra of basal cell carcinomas are distinct from non-tumor-bearing skin components," *J. Invest. Dermat.*, vol., 112, pp. 951-956.
- [23] Kneipp J., P. Lasch, E. Baldauf, M. Beekes, D. Naumann, 2000 "Detection of pathological molecular alterations in scrapie-infected hamster brain by fourier transform infrared (FT-IR) spectroscopy" *Biophys. Acta.*, vol., 1501, no. 2-3, pp. 189-99.
- [24] Roeges N. P., 1994 "A Guide to complete interpretation of Infrared Spectra of Organic Structures," *Wiley*, Chichester, UK.
- [25] Mantsch H. H., D. Chapman, 1996 "Infrared Spectroscopy of Biomolecules" *Wiley-Liss*, New York.
- [26] Brandenburg K., U. Seydel, 1998 "Infrared Spectroscopy of Glycolipids," *Chem. Phys. Lipids*, vol., 96, pp. 23.
- [27] David I., G. Royston, 2006 "Metabolic fingerprinting in disease diagnosis: biomedical applications of infrared and Raman spectroscopy," *Analyst*, vol., 131, pp. 875-885.
- [28] Huilu Y., T. Zhanhua, A. Min, P. Lixin, W. Guiwen, H. Bijuan, L. Yong-qing, 2009 "Raman spectroscopic analysis of apoptosis of single human gastric cancer cells" *Vibrational Spectroscopy*," *Vib. Spectrosc.* vol.50, pp.193-197.
- [29] Giaever I., C. R. Keese, 1986 *IEEE Transactions on Biomedical Engineering BME-33* (2), pp. 242-247.
- [30] Paul G. L., D. S. Robert, 1998 "Cancer grading by Fourier transform infrared spectroscopy," vol., 4, pp. 37-46.
- [31] Montpetit S. A., I. T. Fitch, P. T. O'Donnell, 2005 "A simple automated instrument for DNA extraction in forensic casework," *J. Forensic Sci.*, vol., 3, no. 555-63.

- [32] Jackson M., M.G. Sowa, H. H. Mantsch, 1997 "Infrared spectroscopy: a new frontier in medicine," *Biophys. Chem.*, vol. 68, 109-125.
- [33] Wong P. T., R. K. Wong, T.A. Caputo, T. A. Godwin, B. Rigas, 1991 "Infrared spectroscopy of exfoliated human cervical cells: evidence of extensive structural changes during carcinogenesis," *Proc. Natl Acad. Sci., USA* vol., 88, pp. 10988-10992,.
- [34] Mantsh H. H., 2001 "Apoptosis-induced structural changes in leukemia cells identified by IR spectroscopy," *J. Mol. Str.*, vol., 565-566, pp. 299-304,.
- [35] Liu K-Z, Li Jia., S. M. Kelsey, A. C. Newland, H. H. 2001 "Mantsch, Quantitative determination of apoptosis on leukemia cells by infrared spectroscopy," *Apoptosis*, vol., 6, pp. 269-278.
- [36] Rigas B., & P. T. Wong, 1992 "Human colon adenocarcinoma cell lines display infrared spectroscopic features of malignant colon tissues," *Cancer Res.*, vol., 52, pp. 84-88.
- [37] Benedetti E., E. Bramanti, F. Papineschi, & I. Rossi, 1999 "Determination of the relative amount of nucleic acid of the relative amount of nucleic acids in leukemic and normal lymphocytes by means of FT-IR microscopy" *Appl. Spectrosc.*, vol., 51, pp. 792-797,.
- [38] Boydston-White S., T. Gopen, S. Houser, J. Bargonetti, & M. Diem, 1999 "Infrared spectroscopy of human tissue. V. Infrared spectroscopic studies of myeloid leukemia (ML-1) cells at different phases of the cell cycle" *Biospectroscopy*, vol., 5, pp. 219-227.
- [39] Hoi-Ying N. H., C. M. Michael, A. B. Eleanor, B. Kathy, R. M. Wayne, 2000 "IR spectroscopic characteristics of cell cycle and cell death probed by synchrotron radiation based Fourier transform IR spectroscopy," *Biopoly. Biospectrosc.*, vol., 57, pp. 329-335,.
- [40] Casal H. L., H. H. Mantsch, Polymorphic phase behaviour of phospholipid membranes studied by infrared spectroscopy. *Biochem. Biophys. Acta* 779 (1984) 381-401.
- [41] Jamin N., L. Miller, J. M. Fridman, W. H. Dumas and J. L. Teillaud, 2003 "Chemical heterogeneity in cell death: combined synchrotron IR and fluorescence microscopy studies of single apoptotic and necrotic cells," *Biopoly. Biospectrosc.*, vol., 72, pp. 366-373,.
- [42] Mittler R, 1998 "In when cells die: A comprehensive evaluation of apoptosis and programmed cell death," Lockshin,R., Zakeri Z., Tilly J., Eds.; *Wiley-Liss*: New York, pp.147-174,.
- [43] Birge R., E. Fajardo, B. Hempstead, 1998 "In when cells die: A comprehensive evaluation of apoptosis and programmed cell death," Lockshin,R., Zakeri Z., Tilly J., Eds.; *Wiley-Liss*: New York, pp. 347-384,.
- [44] El-Shahawy A., N. M. Elsayi, W. S. Baker, F. A. Khorshid, N. S. Geweely, 2010 "Spectral analysis, molecular orbital calculations and antimicrobial activity of PMF- G fraction extracted from PM-701" *Int. J. Pharm. Bio. Sci.*, vol., 1, no. 2.
- [45] Matsuzaki K., "Magainins as paradigm for the mode of action of pore forming polypeptides" *Biochem. Biophys. Acta.*, vol., 1376, pp. 391-400, 1998b.
- [46] Shai Y., 1999 "Mechanisms of the binding, insertion and destabilization of phospholipids bilayer membrane by α -helical antimicrobial and cell nonselective membrane-lytic peptides" *Biochem. Biophys. Acta*, vol., 1462, pp. 55-70.
- [47] Zasloff M., 1987 "Magainins, a class of antimicrobial peptides from *Xenopus* skin: Isolation, characterization of two active forms, and partial c DNA sequence of a precursor" *Proc. Natl., Acad. Sci. USA*, vol., 84, pp. 5449-5453.
- [48] Matsuzaki K., O. Murase, N. Fujii, K. Miyajima, 1995 "Translocation of a channel-forming antimicrobial peptide, magainin 2, across lipid bilayers by forming a pore" *Biochemistry*, vol., 34, pp. 6521-6526,.
- [49] Raouf G. A. , F. A. Khorshid, S. M. El-Hamidy, G. S. Al-amri, N. A. Alotaibi, T. Dakhkhni, "PMF nano-shells and Quantum dots for cancer therapy," unpublished paper.
- [50] Brian M., R. Melissa, D. Max, and R. W. Bayden, 2005 "Mie-Type Scattering and non-Beer-Lambert Absorption Behavior of Human Cells in infrared Microspectroscopy, " *Biophysical J.*, vol., 88, pp. 3635-3640.
- [51] Brewer K.A., 1979 "Mechanism of carcinogenesis: Comments on therapy" *J. Int. Acad. Prev. Med.* , vol., 5, pp. 29-53,.
- [52] Sartori H. E., 1984 "Cesium therapy in cancer patients," *Pharm. Biochem. & Behavior*, vol., 21, pp. 11-13.

Analysis of intraoperative complication of ruptured cerebral aneurysm with detachable coils embolizationXu Hao-wen¹; Tan Song²; Song Bo², Sun Shi-lei², Xu Yu-ming²¹ Department of Interventional Radiology, the First Affiliated Hospital of Zhengzhou University, Zhengzhou, Henan 450052, China.² Department of Neurology, the First Affiliated Hospital of Zhengzhou University, Zhengzhou, Henan 450052, ChinaCorresponding author: Xu Yu-ming, xuyuming@zzu.edu.cn

Abstract: Objective: To report the incidence of intraoperative complications of coiling of ruptured cerebral aneurysms leading to permanent disability or death in a consecutive series of 341 patients and to identify risk factors for these events. Methods: Between January 2007 and May 2011, 341 consecutive patients with ruptured intracranial aneurysms were treated with detachable coils. Procedural complications of coils embolization leading to death or neurologic disability at the time of hospital discharge were recorded. For patients with procedural complications, odds ratios (OR) with corresponding 95% confidence intervals (CI) were calculated for the following patient and aneurysm characteristics: patient age and sex, use of a supporting balloon, aneurysm location, timing of treatment, clinical condition at the time of treatment, and aneurysm size. Results: Procedural complications occurred in 21 of 341 patients (6.16%; 95% CI, 4.2% to 8.1%), leading to death in 9 patients (procedural mortality, 2.6%; 95% CI, 1.6% to 4.2%) and to disability in 12 patients (procedural morbidity, 3.5%; 95% CI, 2.0% to 5.3%). There were 4 procedural ruptures and 17 thrombotic complications. The significant risk factors for the occurrence of procedural complications were use of supporting balloon (OR, 5.3; 95% CI, 2.3 to 16.1%) and stent (OR, 8.4; 95% CI, 4.1 to 20.5%). Conclusion: Procedural complication rate of coiling of ruptured aneurysms leading to disability or death is 6.16%. In this series, the use of a temporary supporting balloon and stent in the treatment of wide-necked aneurysms was the risk factors for the occurrence of complications. [**Analysis of intraoperative complication of ruptured cerebral aneurysm with detachable coils embolization.** Life Science Journal. 2011;8(3):543-546] (ISSN: 1097-8135). <http://www.lifesciencesite.com>.

Keywords: cerebral aneurysm; complication; coil; embolization**1. Introduction**

Endovascular coiling of ruptured cerebral aneurysms has become an accepted treatment with good clinical results and valuable protection against rebleeding^[1,2]. However, intraoperative complications during the endovascular treatment can result in poor patient outcome. Complications of endovascular coiling consist of procedural perforation by the microcatheter, microguidewire, or coil and thrombotic complications. In this study, we report the incidence of procedural complications of coiling of ruptured intracranial aneurysms leading to permanent disability or death in a consecutive series of 341 patients. In addition, we tried to find risk factors associated with the occurrence of procedural complications.

2. Methods**2.1 Subjects**

Between January 2007 and May 2011, 341 consecutive patients with ruptured intracranial aneurysms were treated with detachable coils. There were 107 men and 234 women with a mean age of 53.2 years (median, 52 years; range, 19–83 years).

Clinical grading according to the Hunt and Hess scale (HH) at the time of treatment was:HHI– II, 219 patients; HH III, 61 patients; and HH IV– V, 61 patients. Mean size of the 341 ruptured aneurysms was 8.0 mm (median, 7; range, 2– 40 mm). Timing of treatment after SAH was < 3 days in 158 patients, between 4 and 10 days in 117 patients, and > 11 days in 66 patients. Size and locations of the aneurysms are listed in Table 1.

2.2 Coiling Procedure

All patients were treated with coil embolization under general anesthesia and systemic heparinization. Heparin was continued intravenously during the procedure, Coiling was performed with detachable coils. The aim of coiling was to obtain an attenuated packing of the aneurysm, until not a single coil could be placed. 30 (8.8%) and 45 (13.2%) wide-necked aneurysms were coiled with the aid of a supporting balloon and stent, respectively. In the occurrence of aneurysm perforation during coiling, heparin was reversed instantaneously and coiling was continued until the bleeding stopped. In the occurrence of thromboembolic complications, usually

a selective bolus injection of 200,000 –750,000 U of urokinase was administered in the involved vessel.

Table 1: Location of 341 ruptured aneurysms treated with detachable coils

location	N
Posterior circulation (N= 21)	
Basilar tip	3
Basilar trunk	3
Vertebral artery	4
Posterior inferior cerebellar artery	8
Superior cerebellar artery	3
Anterior circulation (N =320)	
Anterior communicating artery	88
Posterior communicating artery	101
Carotid tip	4
Carotid ophthalmic artery	25
Anterior choroideal artery	9
Middle cerebral artery	93

2.3 Procedural Complications

Procedural complications (aneurysm rupture or thrombotic) of coiling leading to death or neurologic disability at the time of hospital discharge were prospectively recorded in our data base during a weekly joint meeting with neuroradiologists, neurosurgeons, and neurologists. For comatose patients, thrombotic complications were considered to have caused neurologic deficit if this was either clinically evident or if there were infarctions on subsequent CT scans in the territory of the involved vessel. Procedural rupture in comatose patients who subsequently died was considered procedural mortality. Outcome of surviving patients with procedural complications was assessed according to the Glasgow Outcome Scale (GOS) at the joint outpatient clinic at 6 weeks. All procedural aneurysm ruptures, independent of clinical consequences were recorded.

2.4 Statistical Analysis

For patients with procedural complications, odds ratios (OR) with corresponding 95% confidence intervals (CI) were calculated using univariate logistic regression analysis for the following patient and aneurysm characteristics. Separate univariate logistic regression analyses were performed for the same patient and aneurysm characteristics for thromboembolic complications and procedural ruptures.

3. Results

Procedural complications occurred in 21 of 341 patients (6.16%; 95% CI, 4.2% to 8.1%), leading to death in 9 patients (procedural mortality, 2.6%; 95% CI, 1.6% to 4.2%) and to disability in 12 patients (procedural morbidity, 3.5%; 95% CI, 2.0% to 5.3%). There were 4 procedural ruptures and 17 thrombotic complications. Two of 4 procedural ruptures and seven of 17 thrombotic complications led to mortality (Table 2). Of 12 patients with procedural morbidity, 5 had a nondisabling neurologic deficit and were independent (GOS 4) and 7 were dependent (GOS 3) at 6 weeks after coiling. There were no patients in vegetative state (GOS 2).

Table 2: Morbidity and mortality for 4 procedural ruptures and 21 thromboembolic events in 341 patients

	Procedural Rupture	Thrombotic event
Morbidity	5	5
Mortality	2	7
Total	9	12

Overall rupture during coiling occurred in 15 patients (4.4%) and was without clinical sequelae in 11 (73.3%). These 11 patients with procedural rupture without clinical consequences were not included in statistical analysis of procedural complications. were not included in statistical analysis of procedural complications.

In the 30 patients with wide-necked aneurysms treated with a supportive balloon, 5 complications leading to disability or death occurred (16.7%); thrombotic complications in 5 patients and no procedural rupture. In the 45 patients with wide-necked aneurysms treated with a assisted stent, 9 complications leading to disability or death occurred (20%); procedural ruptures in 1 and thromboembolic complications in 8 patients. The significant risk factors for the occurrence of procedural complications were use of supporting balloon (OR, 5.3; 95% CI, 2.3 to 16.1%) and stent (OR, 8.4; 95% CI, 4.1 to 20.5%). Results of univariate logistic regression for the different variables for occurrence of all complications are listed in Table 3.

4. Discussion

We found that procedural complications of coiling of ruptured intracranial aneurysms leading to permanent disability or death occurred in 6.16% of patients. Thromboembolic complications accounted for 80% and procedural rupture for 20% of

complications. The overall complication rate is in concordance with previous studies: Sluzewski et al^[3] reported, in a meta-analysis of 1256 patients, a 3.7% procedural complication rate leading to permanent deficits. In a meta-analysis limited to posterior circulation aneurysms, Lozier et al^[4] found 1.4% procedural mortality and 5.1% procedural morbidity. Henkes et al^[5] reported a procedural mortality of 1.5% and morbidity of 5.0% in 1034 coiled ruptured aneurysms.

Table 3: Odds ratios for different patient and aneurysm characteristics for the occurrence of all procedural complications leading to disability or death in 341 patients

Variable	OR	95% CI
Men	0.71	0.34–1.48
Timing after SAH		
3 d	0.75	0.39–1.44
4 ~ 10 d	0.81	0.40–1.62
10d	1.90	0.94–3.84
Aneurysm location		
Posterior circulation	0.67	0.30–1.48
Anterior cerebral artery	1.00	0.52–1.92
Middle cerebral artery	1.47	0.50–4.32
Carotid artery	1.23	0.61–2.47
balloon	5.3	2.31–16.32
stent	8.4	4.12–20.54
HH		
HH I–II	0.67	0.35–1.28
HH III	1.49	0.78–2.84
HH IV–V	0.79	0.32–1.93
Aneurysm size (mm)		
5	0.76	0.39–1.51
5-10	0.59	0.31–1.13
> 10	1.58	0.79–3.13

The risk factors for the occurrence of complications was the use of balloon and stent to assist in coiling of wide-necked aneurysms. This may be explained by the following 3 reasons: first, the technique requires the introduction of an additional balloon microcatheter, with inherent higher risk of thromboembolic events as was shown by Soeda et al^[6] in a study using diffusion-weighted MR imaging. Second, the (thrombotic) coil mesh in a wide necked aneurysm has a large surface area in contact with blood. Third, there is a higher tendency for

procedural rupture when the microcatheter is fixed by the balloon or stent and coils are deployed^[7].

Incidence of procedural rupture was similar to that reported by others: in a meta-analysis of 1248 ruptured aneurysms by Ross et al^[8], the procedural rupture rate was 4.1%, leading to mortality in 1.8% and morbidity in 0.2%. Henkes et al^[5] reported a procedural rupture rate of 5.0% in 1034 ruptured aneurysms. Most aneurysm perforations remain without clinical sequelae. Countermeasures such as reversal of anticoagulation and securing the perforation site with additional coils seem to be effective in preventing disability or death in most cases.

The thrombotic complication rate is comparable with that reported in other studies: Henkes et al^[5] found a thromboembolic complication rate of 4.7% in 1034 ruptured aneurysms. The rate of thromboembolic stroke was 6% in a series of 118 patients by Ross^[8]. In the occurrence of clot formation, local intra-arterial fibrinolysis with urokinase, abciximab, or recombinant tissue plasminogen activator may help to recanalize the occluded artery, but even complete recanalization may not prevent a major neurologic deficit^[9]. Aneurysmal rebleeding due to intraarterial fibrinolysis has been observed in this setting and has a poor prognosis. Thrombotic complications occurred significantly less often in posterior circulation aneurysms. We do not have a solid explanation for this finding. It is possible that the access to posterior circulation aneurysms is less difficult and time-consuming than for anterior circulation aneurysms.

In the present study, patient age, clinical condition, timing of treatment, and aneurysm size and location had no influence on the occurrence of procedural complications. The interval between endovascular treatment and SAH did not affect periprocedural morbidity rates in a study of 327 patients by Baltsavias et al^[10]. Lubicz et al reported that thrombotic events during embolization of a ruptured aneurysm were more frequent in elderly people than in younger patients (9.6% versus 1.4%), but this could not be confirmed by Lubicz et al, who found a permanent morbidity as a result of thromboembolic complications of 2.9% in 68 patients older than 65 years.

In conclusion, the procedural complication rate of coiling of ruptured aneurysms leading to disability or death is 6.16%. The use of a temporary supporting balloon in the treatment of wide-necked aneurysms is the only risk factor for the occurrence of complications

References

1. Molyneux A, Kerr R, Stratton I, et al. International Subarachnoid Aneurysm Trial (ISAT) Collaborative Group: International Subarachnoid Aneurysm Trial (ISAT) of neurosurgical clipping versus endovascular coiling in 2143 patients with ruptured intracranial aneurysms: a randomised trial. *Lancet*. 2002; 360:1267–1274.
2. Sluzewski M, van Rooij WJ, Beute GN, et al. late rebleeding of ruptured intracranial aneurysms treated with detachable coils. *AJNR Am J Neuroradiol*. 2005; 26:2542–2549.
3. Sluzewski M, van Rooij WJ. Early rebleeding after coiling of ruptured cerebral aneurysms: incidence, morbidity, and risk factors. *AJNR Am J Neuroradiol*. 2005; 26:1739–1743.
4. Lozier AP, Connolly ES Jr., Lavine SD, et al. Guglielmi detachable coil embolization of posterior circulation aneurysms: a systematic review of the literature. *Stroke*. 2002; 33: 2509–2518.
5. Henkes H, Fischer S, Weber W, et al. Endovascular coil occlusion of 1811 intracranial aneurysms: early angiographic and clinical results. *Neurosurgery*. 2004; 54:268–280.
6. Soeda A, Sakai N, Murao K, et al. Thromboembolic events associated with Guglielmi detachable coil embolization of asymptomatic cerebral aneurysms: evaluation of 66 consecutive cases with use of diffusion-weighted MR imaging. *AJNR Am J Neuroradiol*. 2003; 24:127–132.
7. Malek AM, Halbach VV, Phatouros CC, et al. Balloon-assist technique for endovascular coil embolization of geometrically difficult intracranial aneurysms. *Neurosurgery*. 2010; 56:1397–1406.
8. Ross IB, Dhillon GS. Complications of endovascular treatment of cerebral aneurysms. *Surg Neurol*. 2005; 64:12–18.
9. Sedat J, Dib M, Lonjon M, et al. Endovascular treatment of ruptured intracranial aneurysms in patients aged 65 years and older: follow-up of 52 patients after one year. *Stroke*. 2008; 39:2620–2625.
10. Baltsavias GS, Byrne JV, Halsey J, et al. Effects of timing of coil embolization after aneurysmal subarachnoid hemorrhage on procedural morbidity and outcomes. *Neurosurgery*. 2005; 52:1320–1331.
11. Lubicz B, Leclerc X, Gauthier JY, et al. Endovascular treatment of ruptured intracranial aneurysms in elderly people. *AJNR Am J Neuroradiol*. 2004; 25: 592–595.

9/1/2011

Construction of HSV-1 HF based replication defective vector

Li Xiang, Xinjing Liu, Huitao Liu, Zhiqiang Han, Jiameng Lu and Yuming Xu *

Department of Neurology, the First Affiliated Hospital of Zhengzhou University, Zhengzhou, Henan province, 450052, P. R. China. yumingxu@zzu.edu.cn

Abstract: Due to the unique biological features of original virus, HSV-1 derived vectors are rendered a number of advantages, such as broad cell tropism, including infection non-dividing mammalian cells across a broad range of species, and large capacity for foreign gene delivery. To date, two types of recombinant HSV-1 vectors known as replication competent vector and replication defective vector, derived from different HSV-1 strains, such as strain KOS and strain 17 have been developed as gene delivery vehicles and applied in fundamental studies and clinical trials for gene therapy. However, so far, no HSV-1-HF strain derived recombinant vector has been reported yet. Since the features of HSV-1 vectors are largely associated their original virus strains, the HSV-1 vectors from different strains may vary in their infection ability, tropism and cytotoxicity. Here, we described the construction of a HSV-1-HF strain based replication defective vector by a homologous recombination approach in bacteria.

[Li Xiang, Xinjing Liu, Huitao Liu, Zhiqiang Han, Jiameng Lu and Yuming Xu. **Construction of HSV-1 HF based replication defective vector.** Life Science Journal. 2011; 8(3):547-553] (ISSN: 1097-8135).

<http://www.lifesciencesite.com>.

Key words: HSV-1, homologous recombination, replication defective vectors

Introduction

Herpes simplex virus type 1 (HSV-1) is an important human pathogen that causes a variety of diseases from mild skin diseases, such as herpes labialis to life-threatening diseases, such as devastating herpes encephalitis (1-2). Due to its unique features, such as broad cell tropism to infect a wide variety of cell types including the most proliferating and non-dividing mammalian cells across a broad range of species, the large transgene capacity after deleting non-essential genes, and the neurotropic property to infect the nervous system in both anterograde and retrograde directions, HSV-1 derived vectors have been widely used in gene transfer and gene therapy studies and hold promising potential for human disease gene therapy and vaccine application (3). Since it does not integrate into host chromosomes, HSV-1 derived vectors strongly reduce the risk of insertional mutagenesis. To date, two classes of recombinant HSV-1 vectors known as replication competent vector and replication defective vector, derived from different HSV-1 strains, such as strain KOS and strain 17 have been developed as gene delivery vehicles and applied in fundamental studies and clinical trials, including delivery and expression of human genes to cells of the nervous system, selective destruction of cancer cells and prophylaxis against infection with HSV or other infectious diseases (2-3). The replication defective HSV-1-based vectors are herpes viruses in which genes that are essential for viral replication have been either mutated or deleted so as to reduce their cytotoxicity and, together with other deletions involving nonessential genes, have also created space to introduce distinct and independently regulated

expression cassettes for different transgenes(3). A replication-defective HSV vector for the treatment of chronic pain, such as inflammatory pain, neuropathic pain and pain caused by cancer in bone, has recently entered in phase I clinical trial(3-4) and replication-competent (oncolytic) vectors have reached phase II/III clinical trials. (3). Since the features of HSV-1 vectors are largely associated with the biological character of their original virus strains, the HSV-1 vectors from different strain may vary in their infection ability, tropism and cytotoxicity. Although several replication-defective HSV-1 vectors have been constructed mainly from HSV-1 strain 17+(5), and strain KOS(6-8), however, so far, there is no HSV-1-HF strain derived recombinant vector was reported yet. HSV-1 strain HF is an especially weak pathogenic laboratory strain(9) and has its specific biological characters, such as reduced neurovirulent pathogenicity compared with HSV-1 strains 17 syn+ and KOS and high levels of thymidine kinase activity (10). We previously cloned the whole genome of HSV-1 Strain HF into a bacterial artificial chromosome of F plasmid, named BAC- HSV-1-HF (11), and we here described the construction of a HSV-1-HF based replication defective vector by using of a simple and highly efficient BAC recombineering approach in bacteria (12).

Materials and methods

Cells: African green monkey kidney (Vero) cells, CNE cells (human nasopharyngeal carcinoma epithelioid cell line), HFL-1 cells (human lung fibroblasts strain) and 293A cells (human embryonic kidney cell strain) were purchased from Shanghai

Institute of Biochemistry and Cell Biology, Chinese Academy of Sciences. The 2-2 cell line is kindly provided by Dr Jia laboratory in The Prostate Centre at Vancouver General Hospital, Vancouver, British Columbia, Canada. All cells were grown in Dulbecco's Modified Eagle Medium (DMEM), except HFL-1 cells in MEM, supplement with 10% fetal calf serum in humidified 37°C, 5% CO₂ incubator.

Plasmids and bacteria: The plasmid pYD-C255, a GalK-kan (galactokinase-kanamycin) dual-expression cassette and a recombinering E. coli strain SW105 were gifted by Dr Yu, Washington University in St. Louis; The plasmid BAC-HSV-1-HF was constructed by our laboratory as described previously(11), which is able to produce infectious HSV-1 HF virus when transfected it into HSV permissive cells;

Virus: The infectious HSV-1-HF virus were prepared by transfecting vero cells with BAC- HSV-1-HF

plasmid DNA

Constructed a replication defective BAC-HSV-1 HF vector:

As shown by a schematic diagram below, we constructed a replication defective BAC-HSV-1 HF vector by using of a simple Red recombination approach(12) in SW105 bacteria in two steps: the first step was to delete the essential IE gene ICP27 by a positive selection to construct a BAC-HSV-1-HF- Δ ICP27 replication defective vector, which harbored galK-kan selection genes; The next step was to introduce a hTERT-ICP27 cassette into the BAC-HSV-1-HF- Δ ICP27 replication defective vector by a negative selection and replaced galK-kan sequences simultaneously for engineering a tumor specific replication competent oncolytic virus vector, BAC-HSV-1-HF- hTERT- ICP27.

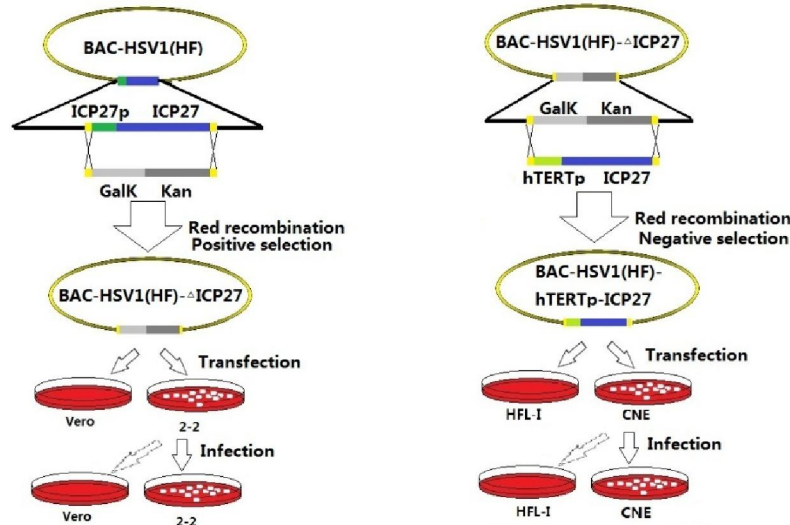


Fig.1. Schematic diagram showing the flowchart of the construction of recombinant BAC-HSV-1-HF- Δ ICP27 replication defective vector by a positive selection and a tumor specific replication competent oncolytic virus vector, BAC-HSV-1-HF-hTERT-ICP27 by a negative selection.

1. Construction of BAC-HSV-1-HF- Δ ICP27 replication defective vector by positive selection scheme

To delete the ICP27 gene (DQ889502:103991-106290) from BAC-HSV-1-HF, a Red recombination was applied through galK positive selection scheme in SW105 bacteria strain and the GalK-kan cassette, containing homology arms to the flanking region of UL54 was inserted, by homologous recombination, into the in BAC-HSV-1-HF. The brief procedure is as follows:

1) The GalK-kan primers design and GalK-kan cassette PCR amplification:

GalK-kan primers with 50 bp homology to the area flanking the UL54 site was designed and synthesized at the following sequences: the forward primer 5'-

TGGCGCTTCACTACGAGCAGGAGATCCAGAGG
 CGCCTGTTTGATGTATGACCTGTTGACAATTAA
 TCATCG-3'and the reverse primer
 5'-GTTATGTCCGGGGCCCGTAAGAACAGGTTGG
 TGAGGGGGGTCGCTGTTCATCTCAGCAAAAGTT
 CGATTTA-3'. PCR amplification 2278 bp fragment of the GalK-kan cassette using the primers designed above, a PrimeSTAR HS DNA Polymerase -mix and 2 ng pYD-C255 plasmid as template at the program of 94°C 15s, then 94°C/8s, 59°C/1m, 68°C 2.5m for 25 cycles and 68°C extension for 3 min. The PCR products were subjected to a digestion by adding 1 ul DpnI into the PCR reaction at 37°C for 3 hours and gel-purified the 2.3 kb PCR product into 50 ul ddH₂O for a transformation.

2) Transduction of the PCR products into BAC-HSV-1-HF recombinering bacteria

To induce a homology recombination, 23 μ l of electrocompetent SW105 bacteria harboring BAC-HSV-1-HF was electroporated with 2 μ l of PCR product at 1,750V, 6ms. After electroporation of the PCR product, the bacteria were recovered in 1 ml LB for 5 hr at 31°C in 10 ml culture tube in a 31°C shaking water bath and grow on kan⁺/cm⁺ plate over night at 31°C in a cabinet-type incubator. After incubation, a few amp^r, kan⁺, cm⁺ colonies were picked and streaked onto MacConkey + galactose + chloramphenicol indicator plates for another 24 hrs incubation at 31°C and pick a single, bright red (GalK⁺) colony to inoculate a 5 ml LB +chloramphenicol overnight culture at 31°C.

3) Identification of ICP27 deletion from BAC-HSV1-HF plasmid construct PCR analysis
Three pairs of PCR primers were designed and used to identify the ICP27 deletion from BAC-HSV-HF plasmid construct :

UL53-F:ACCTGGTGT~~TTTT~~GCTCC and GalK- R TCCTGGGTTTAGTTCCTC, UL53-F and GalK- R were designed to bind to UL53 and GalK sequences respectively and amplify a 329bp fragment .Kan-F GTTGGACGAGTCGGAATC and UL55-R CGCAAAGAAAAGCAGTG, Kan-F and UL55-R were designed to bind to Kanamycin and UL55 sequences respectively and amplify a 464bp fragment. ICP27 primers: UL54-138-F 5'-GGACGAGGACATGGAAGA-3 and UL54-500-R 5'-GGTTGCGATTGGTTCTGG-3', UL54-138-F and UL54-500-R were designed to bind to Kanamycin and UL55 sequences respectively and amplify a 380bp fragment. PCR was performed by using the Plasmid DNA extracted from positive recombinant clones as templates and the primers above at the program of 94°C for 5min for initial denaturation, 94°C for 30sec, 55°C for 30sec, and 72°C for 30sec in 30 cycles, and a final extension step at 72°C for 7min. PCR products were subjected to a 1% agarose gel separation.

4) Functional analysis to test infective BAC-HSV1-HF- Δ ICP27 vector virus generation in Vero cells and 2-2 cells

The BAC-HSV-HF- Δ ICP27 plasmid was extracted from PCR identified positive clone with the Qiagen Plasmid Mini Kit (25) (Cat.No.12123) followed the manufacturer's instruction. Vero cells and 2-2 cells (1.2×10^5 cells/well) grown on the 6-well plate were transfected with 2 μ g of BAC-HSV-HF- Δ ICP27 plasmid DNA using lipofectamine 2000 following the manufacturer's protocol. The virus was harvested 5 to 7 days after transfection, when CPE was observed, by three freeze/thaw cycles and sonication of collected cells. Recombinant viruses were used to infect the Vero cells again to test the virus production by observation GFP fluorescence.

2. Engineering the foreign gene(s) or cassette(s) of interest into the recombinant BAC-HSV-1-HF- Δ ICP27 replication defective vector

To engineer the foreign gene(s) or cassette(s) of interest into the recombinant BAC-HSV-1-HF- Δ ICP27 replication defective vector and test the function of the vector, we introduced a PCR product containing a hTERT promoter driven ICP27 cassette with the same flanking homology sequences to replace the GalK-kan cassette into the vector by a negative selection scheme as the following procedure.

1) hTERT promoter cloning: Clone of hTERT promoter

PCR to amplify hTERT promoter of genome was performed with the primers of forward: 5'-TTTGGATCCCGATTTCGACCTCTCTCCGCTGGGCG-3' and reverse: 5'-TTTCTCGAGCAGGGCTTCCACGTGCGCAGCAG-3' for a 410bp band by using of the 293A cell genomic DNA as a template with the condition of : 94°C for 5min for initial denaturation, 94°C for 30sec, 59°C for 30sec, and 72°C for 30sec in 30 cycles, and a final extension step at 72°C for 7min. The PCR products were cloned to pMD18-T vector via TA cloning method. Plasmid pMD-hTERTp extracted from positive colonies was sequence confirmed.

2) ICP27 gene cloning: Clone of ICP27 gene

PCR amplification of ICP27 gene from HSV-1 genome was performed with the primers: forward, 5'-CGACAGCTCTGAAATGGCGACTGACATTGATATGC-3' and reverse: 5'-GTTTTGCGCCGCTAAATCCGTCCCCGTTCC-3' for a 1.7K band by using of the HSV-1(HF) virus stock as a template with the condition of : 94°C for 5min for initial denaturation, 94°C for 30sec, 63.2°C for 30sec, and 72°C for 2min in 30 cycles, and a final elongation step at 72°C for 7min. PCR production was cloned to pGM-T vector via TA cloning method. The pGM-ICP27 DNA extracted from the correct clone was sequenced.

3) Construction of The plasmid pMD-hTERTp-ICP27

The plasmid pMD-hTERTp-ICP27 was subject to serially digestion and gel purification in the following order: pMD-hTERTp, digested by XhoI to get linear DNA, blunt by Klenow fragment and dephosphorylated by FastAP, then was ligated with the 1.7 kb ICP27 fragment acquired from pGM-ICP27, digested by EcoRI and blunted by Klenow fragment. The plasmid pMD18-hTERTp-ICP27 was restriction analyzed to identify the correct clone.

4) PCR amplification of hTERT promoter driven

ICP27 expression cassette
 PCR primers were designed with 5'ends same as the homology arms used in the ICP27 knock out step and 3'ends binding to the upstream sequence of hTERT promoter and downstream sequence of ICP27 expression cassette respectively:
 5'-TGGCGCTTCACTACGAGCAGGAGATCCAGAGGCGCCTGTTTGATGTATGACGATTCGACCTCTCTCCGCTGGGGC -3' and the reverse primer:
 5'-GTTATGTCCGGGGCCCGTAAGAACAGGTTGGTGAGGGGGGTCGCTGTCATTAATCCGTCCTCCGTTCC-3'. PCR amplification of 2.2 KB fragment was performed at the program of 94°C 15S, then 94°C/8s, 59°C/1m, 68°C 2.5m for 25 cycles and 68°C extension for 3 min by using pMD18-hTERTp-ICP27 plasmid as the template. The procedure of PCR products DpnI digestion, gel purification, electroporation in the bacteria of BAC-HSV-1HF- Δ ICP27-galk was same as described above.

5) Recombinant colonies selection
 the recovered bacteria from electroporation were washed twice with 1ml 1 \times M9 salts and the pellet at 13,200 rpm/15s, was re-suspend, Plated on cm⁺ galk negative selection plates and Incubated at 31°C for 2 days until small colonies grow out. The colonies grown on Kan plate (negative) & cm⁺ plate were picked and the BAC DNA was prepared for restriction digestion, PCR and functional analysis.

6) PCR analysis
 PCR was carried out to identify the recombinant BAC-HSV1-HF-hTERT-ICP27 clones by the same primers and conditions as used in positive selection step except templates by using the plasmid DNA from selected colonies from the negative selection.

7) Functional analysis by testing infective virus generation in HFL-I and CNE cells
 The BAC-HSV1-HF-hTERT-ICP27 plasmid was extracted from selected PCR identified correct clone with the Qiagen Plasmid Mini Kit (25)(Cat.No.12123) followed the manufacturer's instruction. HFL-I and CNE (1.2 \times 10⁵ cells/well) plated in 6-well plate were

transfected with 2 μ g of BAC-HSV1-HF-hTERT-ICP27 plasmid DNA using lipofectamine 2000 respectively following the manufacturer's protocol. The virus were harvested 5 to 7 days after transfection, when CPE was observed, by three freeze/thaw cycles and sonication of collected cells. Recombinant viruses were used to infect the HFL-I and CNE again to determine the virus generation by observation GFP fluorescence.

Results:

1. Construction of BAC-HSV-1-HF- Δ ICP27

replication defective vector by positive selection

Through galk positive selection of a Red recombination scheme in SW105 bacteria strain, we obtained recombinant bacteria colonies, which were grown on MacConkey + galactose + chloramphenicol indicator plates. In Figure 2, recombinant bacteria colonies were shown in bright red color.

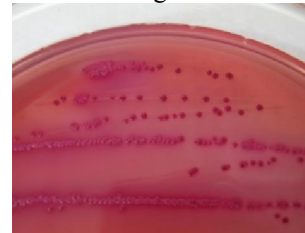


Fig. 2. Recombinant bacteria colonies showing in bright red color on MacConkey + galactose + chloramphenicol indicator plates

PCR analysis of galk-kan gene and ICP27 from the selected recombinant clones showed the ICP27 gene was deleted from BAC-HSV-1-HF genome. In Figure 3, agarose gel electrophoresis showed the correct PCR products of galk-kan gene with the primers of UL53F/GalR in A, KanF/UL55R in B and ICP27 F/R in C.

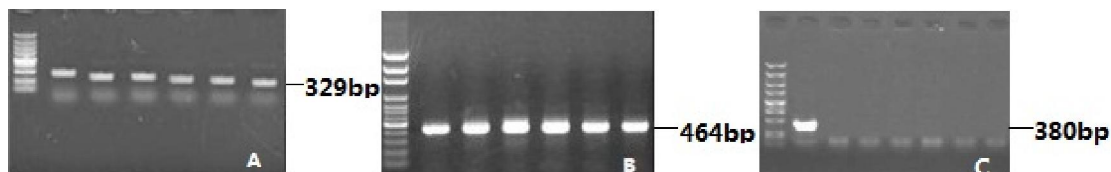


Fig. 3. Agarose gel electrophoresis showing a 329bp band of UL53F/GalR PCR product of galk gene in A, a 464bp band of KanF/UL55R PCR product of Kanamycin gene in B and 380bp of ICP27 F/R PCR product of ICP27 in C.

Identification of ICP27 deletion from BAC-HSV-HF plasmid constructs: Functional analysis to test infective BAC-HSV-HF- Δ ICP27 vector virus

generation in Vero cells and 2-2 cells. After transfection of the Vero cells and 2-2 cells with BAC-HSV1-HF- Δ ICP27 plasmid DNA from PCR

identified recombinant clone, CPE was observed in 2-2 cells, but not in Vero cells. As shown in Figure 4, When infected the Vero cells and 2-2 cells with the harvested supernatants from the transfected Vero cells and 2-2 cells, the CPE and GFP fluorescent was only observed in the cells infected by the harvested supernatants from

2-2 cells. Whereas a parallel positive control, transfection with BAC-HSV1-HF plasmid DNA was observed CPE and GFP fluorescent only in the transfection step and neither the CPE and GFP fluorescent in the infection step always. These results indicated that ICP27 gene was successfully deleted.

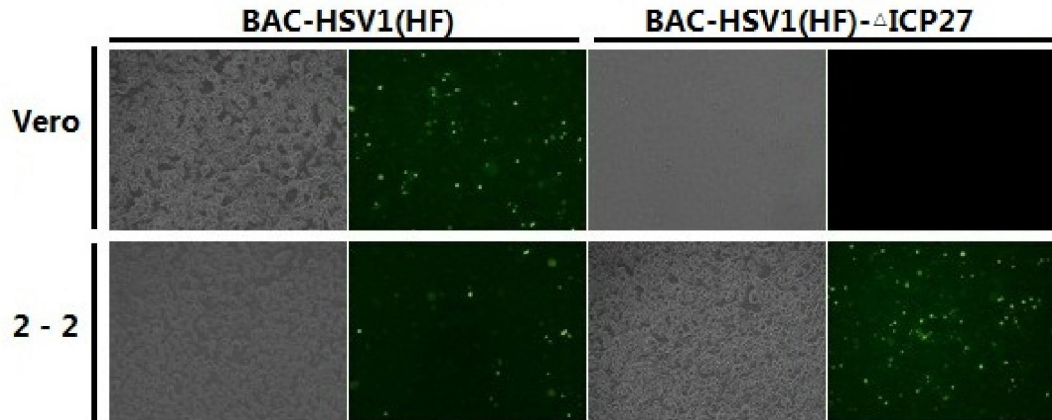


Fig.4. CPE and GFP fluorescence observation in Vero cells and 2-2 cells infected with BAC-HSV1-HF plasmid in the left panel and BAC-HSV1-HF- Δ ICP27 plasmid in the right panel.

The CPE in the transfection step with BAC-HSV1-HF- Δ ICP27 plasmid and GFP fluorescence in the infection step with harvested supernatant from the transfection step were only observed in 2-2 cells, but not in Vero cells, while in a positive control with BAC-HSV-HF plasmid, CPE and GFP fluorescence were observed in both Vero cells and 2-2 cells.

Based on the results obtained above, we concluded that a replication defective vector BAC-HSV-HF- Δ ICP27 was constructed.

2. Engineering the a hTERT promoter driven ICP27 cassette into the recombinant BAC-HSV-1-HF- Δ ICP27 replication defective vector

To test the function of recombinant BAC-HSV-1-HF- Δ ICP27 replication defective vector, we introduced a hTERT promoter driven ICP27 cassette into the vector by a negative selection to engineer a BAC-HSV-1-HF-hTERT-ICP27.

By PCR amplifications, we successfully obtained a 410 bp hTERT promoter element and a 1.7Kb ICP27 element and cloned them into a pMD-18T vector to result a hTERT promoter driven ICP27 cassette. The agarose gel electrophoresis showed the correct size of the PCR products sequence confirmed of hTERT promoter and ICP27 element gene structure (Data not show). The hTERT promoter driven ICP27 cassette with the same homology arm of ICP27 deletion, was amplified by PCR and electro transformed into the BAC-HSV1-HF- Δ ICP27 competent bacterial.

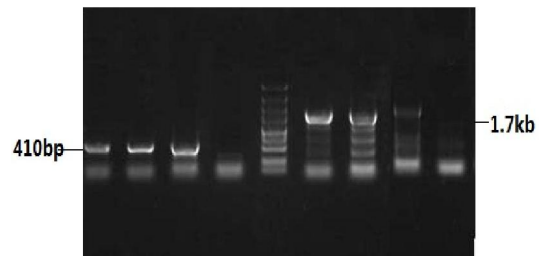


Fig. 5. Agarose gel electrophoresis analysis BAC-HSV1-HF-hTERT-ICP27, showing a 410bp band of hTERT promoter PCR fragment and a 1.7Kb band of ICP27 gene PCR fragment in respectively.

PCR analysis showed recombinant colonies carrying hTERT promoter and ICP27 sequences, indicating hTERT-ICP27 cassette was successfully engineered into BAC-HSV-HF- Δ ICP27 vector, As shown in fig.5. Through a negative selection, the recombinant colonies grown on Kan plate (negative) & cm (positive) plate were obtained. This identified the absent of the galK-Kan elements. The recombinant bacteria have lost the galK-kan cassette by a deletion, and the rest will be truly recombinant clones.

After transfection of HFL-I and CNE cells with the plasmid DNA BAC-HSV1-HF-hTERT-ICP27 extracted from recombinant clone, the CPEs and GFP fluorescence were observed only in CNE cells, but not in HFL-I cells, indicating the infective virus were restricted in the tumor cells. To determine if the infective virus were selectively generated in tumor cell specific manner, we thus collected the supernatant from

the transfected cells and infected the HFL-I and CNE cells respectively again and took the CPE and GFP fluorescence observation. After infection, as shown in Figure 6, the CPE and GFP fluorescence were restrictively observed CNE cells, but still not in HFL-I cells indicating the infective virus were specifically generated in tumor cells. As a parallel negative control,

BAC-HSV1-HF- Δ ICP27 failed to generate any CPE after transfection and nor infective GFP fluorescence after infection with harvested supernatant. These results suggested that recombinant BAC-HSV1-HF-hTERT-ICP27 is tumor selective replication competent oncolytic virus.

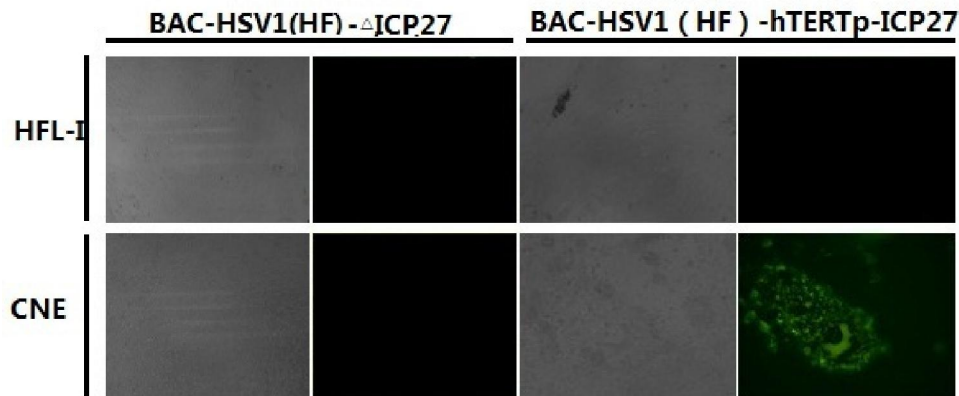


Fig.6. CPE and GFP fluorescence observation in HFL-I and CNE cells, which were treated with the supernatants from corresponding cells transfected with BAC-HSV1-HF- Δ ICP27 and BAC-HSV1-HF-hTERT-ICP27 vector.

Discussions

Utilizing a red homologous recombination technique in bacteria, we successfully constructed a BAC-HSV-1HF based recombinant replication defective vector by deleting ICP27 and leaving a GalK-Kan cassette in UL54 locus for foreign gene clone selection, which enabled us to develop a tumor-specific replication competent oncolytic virus for cancer therapy studies. Red homologous recombination technique is rapid and high efficient novel recombination technique, which makes it simple and easy to knock out, mutant or engineer almost any foreign gene(s) or cassette(s) into the BAC plasmid carried large DNA molecule, including the whole genome of HSV-1 virus compared with traditional homologous recombination techniques in mammalian cells. We used a two step scheme to delete the essential IE gene UL54, encoding ICP27 protein, by a galk-Kan cassette instead and to construct a replication defection vector, which allowed foreign gene cassette(s) to be engineered into the vector by a simply negative selection. Our recombinant HSV replication defective vector has potential for development of both tumor-specific replication competent Oncolytic HSV virus and gene delivery vectors for gene therapy of different diseases. Although different oncolytic virus have been developed and applied to preclinical and clinical studies, for example, the first-Generation HSV Vectors were designed to mutant a single gene so as to restrict their replication in dividing cells, the second Generation HSV Vectors was resulted in multigenic

mutations, and the third-Generation Vectors was designed to delete some essential genes plus US12 gene, encoding ICP47 protein to block MHC class I-mediated antigen presentation, for immune-modulation, however, the last Generation Vectors would be designed to develop the transgene-expressing vectors so as to further augment their antitumor efficacy by incorporation of expression cassettes for the delivery of various transgenes (3). By using this strategy, Dr. Jia et al 2010 developed a novel targeting replication HSV-1 viruses by dual-regulating viral essential gene expression of ICP27 in both transcriptional and translational levels to increase viral lytic activity and tumor specificity by systemic treatment advanced and metastatic prostate cancers(13). Therefore, the development of conditional replication competent HSV-1 viruses armed with multiple transgenes might present the future direction in oncolytic virotherapy. HSV-1 strain HF is a laboratory strain and has been demonstrated to have especially weak pathogenic via a intravaginal inoculation (9). Compared with HSV-1 strains 17 syn+ and KOS it exhibited reduced neurovirulent pathogenicity in mouse brains, although could also produce a lethal infection, but was completely avirulent after footpad inoculation (10). In addition, HSV-1 strain HF was also demonstrated to have high levels of thymidine kinase activity. As HSV-1 HF derivative clone 10 (HF10), a spontaneously occurring, highly attenuated virus of HSV-1-HF, was demonstrated to have strong anti-tumor activity both in animal model

studies and clinical trial (14-15), therefore, our

BAC-HSV-1-HF- Δ ICP27 replication defective vector

would have a promising potential to be modified by engineering method to acquire less neurovirulent and more efficient oncolytic effects than natural mutant HF10 to be used for cancer therapy. Furthermore, RNA interference is a recently developed novel gene silencing technique and has been demonstrated to be able to efficiently knock down targeting gene by both synthetic small interfering RNAs (siRNAs) and expressed small hairpin RNA (shRNA) in many cell types, including in neurons, however, in vivo delivery of RNAi remains a major challenge, thus limiting its applications. Recently, replication-defective herpes simplex viral (HSV-1) vectors have been demonstrated to be a highly efficient method for in vivo gene silencing in dorsal root ganglia (DRG) using HSV-mediated delivery of short-hairpin RNA (shRNA) targeting reporter genes (16). Therefore, our BAC-HSV-1HF based recombinant replication defective vector might be an ideal shRNA delivery vehicle for gene silencing in nerve system.

Conclusion

We have for the first time constructed a herpes simplex virus type 1 strain HF based recombinant replication-deficient vector, in which the UL54 gene locus was replaced by galk-Kan cassette, thus making it easy to introduce any gene(s) of interest into the vector by a simple negative selection. Our HSV-1 HF based replication defective vector might be ideal platform for gene delivery, oncolytic virotherapy and vaccine development as well.

Corresponding author: Dr. Yuming Xu,
yumingxu@zzu.edu.cn. Mailing address: 1 East Jianshe Road, Zhengzhou, Henan province, 450052, P. R. China

References

1. Watanabe D. Medical application of herpes simplex virus. *J Dermatol Sci*. 2010 Feb;57(2):75-82.
2. Fraefel C, Marconi P, Epstein AL. Herpes simplex virus type 1-derived recombinant and amplicon vectors. *Methods Mol Biol*. 2011;737:303-43.
3. Manservigi R, Argnani R, Marconi P. HSV Recombinant Vectors for Gene Therapy. *Open Virol J*. 2010 4:123-56.
4. Wolfe D, Mata M, Fink DJ. A human trial of HSV-mediated gene transfer for the treatment of chronic pain. *Gene Ther*. 2009 Apr;16(4):455-60.
5. Krisky DM, Marconi PC, Oligino TJ, Rouse RJ,

Fink DJ, Cohen JB, Watkins SC, Glorioso JC. Development of herpes simplex virus replication-defective multigene vectors for combination gene therapy applications. *Gene Ther*. 1998 Nov;5(11):1517-30.

6. Wu N, Watkins SC, Schaffer PA, DeLuca NA. Prolonged gene expression and cell survival after infection by a herpes simplex virus mutant defective in the immediate-early genes encoding ICP4, ICP27, and ICP22. *J Virol*. 1996 Sep;70(9):6358-69.
7. DeLuca NA, McCarthy AM, Schaffer PA. Isolation and characterization of deletion mutants of herpes simplex virus type 1 in the gene encoding immediate-early regulatory protein ICP4. *J Virol*. 1985 Nov;56(2):558-70.
8. McCarthy AM, McMahan L, Schaffer PA. Herpes simplex virus type 1 ICP27 deletion mutants exhibit altered patterns of transcription and are DNA deficient. *J Virol*. 1989 Jan;63(1):18-27.
9. Nishiura H, Hayakawa K, Matsui Y, Sawada M, Nii S. Experimental studies on genital herpetic infection in mice. *Biken J*. 1980 Dec;23(4):169-77.
10. Sedarati F, Stevens JG. Biological basis for virulence of three strains of herpes simplex virus type 1. *J Gen Virol*. 1987 Sep;68 (Pt 9):2389-95.
11. Liu X, Song B, Lu J, Wang Q, Han Z, Xu Y. The Construction of BAC-HSV-1 Strain HF with GFP Reporter Gene and the research of Its Infectious Progeny Virus. *Chinese journal of virology*, 2011; 27 (3) 238-243.
12. Warming S, Costantino N, Court DL, Jenkins NA, Copeland NG. Simple and highly efficient BAC recombineering using galK selection. *Nucleic Acids Res*. 2005 Feb 24;33(4)
13. Lee CY, Bu LX, DeBenedetti A, Williams BJ, Rennie PS, Jia WW. Transcriptional and translational dual-regulated oncolytic herpes simplex virus type 1 for targeting prostate tumors. *Mol Ther*. 2010 May;18(5):929-35.
14. Takakuwa H, Goshima F, Nozawa N, Yoshikawa T, Kimata H, Nakao A, Nawa A, Kurata T, Sata T, Nishiyama Y. Oncolytic viral therapy using a spontaneously generated herpes simplex virus type 1 variant for disseminated peritoneal tumor in immunocompetent mice. *Arch Virol*. 2003 Apr;148(4):813-25.
15. Mori I, Liu B, Goshima F, Ito H, Koide N, Yoshida T, Yokochi T, Kimura Y, Nishiyama Y. HF10, an attenuated herpes simplex virus (HSV) type 1 clone, lacks neuroinvasiveness and protects mice against lethal challenge with HSV types 1 and 2. *Microbes Infect*. 2005 Dec;7(15):1492-500.
16. Anesti AM, Peeters PJ, Royaux I, Coffin RS. Efficient delivery of RNA Interference to peripheral neurons in vivo using herpes simplex virus. *Nucleic Acids Res*. 2008 36(14)

9/20/2011

Structure, Electrical Conductivity and Dielectric properties of bulk, 2-amino-(4,5-diphenylfuran-3-carbonitrile)

A.A. Hendi

Physics Department, Sciences Faculty for girls, King Abdul Aziz University, Jeddah, Saudi Arabia
dr.asmahendi@hotmail.com

Abstract: X-ray diffraction patterns showed that the powder of 2-amino-(4, 5-diphenylfuran-3-carbonitrile) has polycrystalline nature with triclinic structure. Miller's indices, (hkl), values for each diffraction peak in XRD spectrum were calculated. The Electrical conductivity, dielectric constant ϵ' and dielectric loss ϵ'' have been calculated for bulk in the frequency range from 40 Hz to 5MHz and at the temperature (298-473) K. The obtained results have been discussed in terms of the correlated barrier hopping (CBH) model, which is well adapted to 2-amino-(4,5-diphenylfuran-3-carbonitrile) semiconductor material. The dc conductivity, σ_{dc} , is described by the variable range hopping (VRH). The values of dielectric constant, ϵ' , and dielectric loss, ϵ'' decreased with increasing the frequency due to the interface states capacitance and the decrease in conductance with increasing both the frequency and temperature.

[A.A. Hendi Structure, Electrical Conductivity and Dielectric properties of bulk, 2-amino-(4,5-diphenylfuran-3-carbonitrile)] Life Science Journal, 2011; 8(3): 554-559] (ISSN: 1097-8135). <http://www.lifesciencesite.com>.

Keyword: X-ray, Electrical conductivity, furan, Dielectric.

1. Introduction

Organic semiconductors are of steadily growing interest as active components in electronics and optoelectronics. Due to their flexibility, low cost and ease of production they represent a valid alternative to conventional inorganic semiconductor technology [1]. The increasing environmental consciousness throughout the world has triggered a search for new products and processes that are compatible with the environment. The furan[2,3-d] pyrimidopyrimidine ring system, because of a formal isoelectronic relationship with purine, is specifically of biological interest [2,3], it has numerous pharmacological and agrochemical applications viz. herbicides[4], antimalarials [5], antihypertensive [6] and potential radiation protection agents[7]. The understanding of charge transport mechanism in the composite materials is very important both from fundamental and technological point of view. Dielectric measurements are important means for studying the dynamic properties (capacitance, conductance, permittivity and loss factor) of dielectrics, this work deals with the electrical conductivity and dielectric properties of 2-amino-(4,5-diphenylfuran-3-carbonitrile). This is done for two reasons: firstly, to determine the possible conduction and dielectric relaxation mechanisms. Secondly, very little articles are found to deal with the dc and ac electrical conductivities of 2-amino-(4,5-diphenylfuran-3-carbonitrile).

2. Experimental procedures

2.1. Materials

The starting materials for the syntheses were purchased from Aldrich and used as received.

2.2. Synthesis

A mixture of the solution benzoin (0.01 mol) (1) and malonitrile $\text{CH}_2(\text{CN})_2$ (0.01 mol) (2) in ethanol (10 ml) we added basic alumina (20 g) and montmorillonite (15 g) with constant stirring.

The mixture was air dried at room temperature, placed in an alumina bath and subjected to MWI for

1.3 min/ 4 min respectively [8] as shown in scheme (1).

2.3. Measurements

The structural characteristics of 2-amino-(4,5-diphenylfuran-3-carbonitrile) was investigated

by X-ray diffraction patterns (XRD). Using a Philip X-ray diffractometer (model X-pert) with utilized monochromatic CuK_α radiation and operated at 50 kV and 40 mA. The diffraction patterns were recorded automatically with a scanning speed of 2deg/min.

2-amino-(4,5-diphenylfuran-3-carbonitrile) were firstly compressed under a pressure of $\sim 2 \times 10^8 \text{ N/m}^2$ in the form of a pellet and sandwiched between two evaporated gold, Au, electrodes which provide ohmic contacts to the sample.

A programmable automatic RLC bridge, model Hioki 3532 Hitester, was used to measure the frequency F , impedance Z , the capacitance C , and the loss tangent ($\tan\delta$) directly. The range of frequencies was 42 Hz-5MHz. The temperature of the sample was measured by a thermocouple over a temperature range 298-423 K. The total conductivity was calculated from the following equation: $\sigma_t(\omega) = d/ZA_0$, where d is the thickness of the sample and A_0 is the cross-section area. The dielectric constant, ϵ_1 , was calculated from the equation: $\epsilon_1 = dC/A_0 \epsilon_0$, where ϵ_0 is the permittivity of free space.

3. Results and discussion

X-ray powder diffraction (XRD) of 2-amino-(4,5-diphenylfuran-3-carbonitrile) was taken for the first time in a 2θ range from 5 to 40° , and its spectrum is presented in Fig. 2. As shown in this figure, the pattern has many diffraction peaks with different intensities indicating that the powder of 2-amino-(4,5-diphenylfuran-3-carbonitrile) has a polycrystalline nature. The unit cell parameters of 2-amino-(4,5-diphenylfuran-3-carbonitrile) were determined for the first time by using the CRYSFIRE computer program [9].

The data analysis of the structure is highly matched with a triclinic structure with lattice constant $a=11.63, b=18.933, c=22.226, \alpha=96.72, \beta=55.14, \gamma=132.66$ and space group $P1$. The value of Miller indices, (hkl) , and lattice spacing, d_{hkl} , corresponding to each diffraction line was indexed using CHECKCELL program [10]. Table 1 gives the values of Miller indices (hkl) for each diffraction peak, 2θ and the interplaner spacing (d_{hkl}) before and after refinement.

The variation of $\sigma_{ac}(\omega)$ as a function of frequency (42-5MHz) at different temperature range (298-423) K is shown in Fig. 3 for 2-amino-(4,5-diphenylfuran-3-carbonitrile) bulk sample. It is seen that $\sigma_{ac}(\omega)$ remains almost constant at low frequency and after a certain characteristic crossover frequency, ω_o , it increase with power law fashion. Similar behaviour has been observed in many organic materials in bulk and thin film forms [11–14].

The electrical conductivity, $\sigma_{ac}(\omega)$, of many materials including glasses, organic, polymer and crystal materials over wide range of frequency and temperature are given using the relation [15]

$$\sigma_{ac}(\omega) = \sigma_{tot}(\omega) - \sigma_{dc}(\omega) \quad (1)$$

where $\sigma_{tot}(\omega)$ is the total electrical conductivity at a particular angular frequency ω at a certain temperature. In this equation, the dc conductivity is taken to represent the ac conductivity in the limit $\omega \rightarrow 0$.

The values obtained from extrapolation of the experimental data of $\sigma_{tot}(\omega)$ at low frequencies up to zero frequency are assumed to be equivalent to the dc conductivity for 2-amino-(4,5-diphenylfuran-3-carbonitrile) at each temperature is shown in Fig. 4.

In general, in the case of semiconductors, the dc conductivity varies exponentially with temperature and is given by the Arrhenius equation:

$$\sigma_{dc} = \sigma_o \exp(\Delta E / k_B T) \quad (2)$$

where ΔE is the dc electrical activation energy, T is the absolute temperature, k_B is Boltzmann's constant and σ_o is the pre exponential factor including the charge carrier mobility and density of states. The value of ΔE was found to be 0.20 eV.

The experimental data could be analyzed using Mott's variable range hopping conduction process and the following expression for the dc conductivity was used [16]:

$$\sigma(T) \sqrt{T} = \sigma_{oo} \exp(-B T^{-1/4}) \quad (3)$$

where σ_{oo} and B are constants and B is given by

$$B^4 = T_o = \frac{18.1 \alpha^3}{k_B N(E_F)} \quad (4)$$

The hopping distance and hopping energy are given by [19]:

$$R = \left(\frac{9L_{loc}}{8\pi k T N(E_F)} \right)^{1/4}, \quad (5)$$

$$W = \left(\frac{3}{4\pi R^3 N(E_F)} \right), \quad (6)$$

where T_o is the characteristic temperature and $\alpha = 1/L_{loc} = 10^{-7}$ cm

The corresponding T_o has been evaluated from the linear slope of $\ln(\sigma_{dc} T^{1/2})$ versus $T^{-1/4}$ as depicted in Fig. 5.

The value of parameter T_o was found to be 3.725×10^8 K. In addition, the density of localized states at Fermi level, $N_{(EF)}$, has been calculated taking a constant value of α^{-1} (10^{-7} cm) and found to be 5.63×10^{17} eV⁻¹ cm⁻³. The values of R and W are calculated and found to be 5.2×10^{-6} cm and 299 meV respectively. The value of W and αR according to [16] should have a value greater than $k_B T$ and unity respectively.

The $\sigma_{ac}(\omega)$ is commonly characterized by an approximate power law over a wide range in frequency represented by Jonscher's law [17]:

$$\sigma_{ac}(\omega) = A \omega^s \quad (6)$$

where A is constant, ω is the angular frequency, $\omega = 2\pi f$, and s is the frequency exponent.

The frequency exponent, s , can be calculated from the slope of the straight lines in Fig.6 for high ranges of frequencies. The calculated values of s decrease from 0.98 at 303 K to 0.67 at 413 K.

This behavior was associated with a hopping mechanism in terms of correlated barrier hopping (CBH) model for ac loss, first developed by Pike [18] for single-electron hopping, and has been extended by Elliot [19] for simultaneous two electrons hopping. According to the correlated barrier hopping (CBH) model, values of s decrease with increasing temperatures. In this model, carrier motion occurs by means of hopping over the Coulomb barrier separating two defect centers. A Coulomb correlation between the charged defect centers results in the relaxation variable W of the Coulomb barrier and the intersite separation

The $\sigma_{ac}(\omega, T)$ conductivity in the CBH model to a first approximation is given as [20]:

$$\sigma_{ac}(\omega) = \frac{\pi(N_{(EF)})^2 \varepsilon}{24} \left(\frac{8e^2}{\varepsilon W_m} \right)^6 \frac{\omega^s}{\tau_o^{1-s}} \quad (7)$$

where ε is the dielectric constant, W_m is the maximum barrier height over which the electrons hop E_{opt} (optical band gap), e is the electronic charge and τ_o is the effective relaxation time. According to reference [20], τ_o is expected to have a value of the order of an inverse phonon frequency ($=10^{-13}$ s).

The frequency exponent s for this model is given by

$$s = 1 - \frac{6k_B T}{[W_m + k_B T \ln(\omega \tau_o)]} \quad (8)$$

A first approximation of this equation gives the simple expression for the frequency exponent s :

$$s - 1 = \frac{6k_B T}{W_m}, \quad (9)$$

The binding energy W_m is related to the maximum barrier height at infinite interstatic separation, which is called the polaron binding energy.

Fig. 7 show the ac conductivity $\ln \sigma_{ac}(\omega)$ as a function of the reciprocal temperature $1000/T$ in the investigated temperature range at different frequencies. From the figure, $\sigma_{ac}(\omega)$ increases linearly with increasing temperature. This may indicate that the ac conductivity is a thermally activated process it can be analyzed according to the well-known Arrhenius equation:

$$\sigma_{ac}(\omega) = \sigma^* \exp(-\Delta E_{ac}/kT) \quad (10)$$

where σ^* is constant and ΔE_{ac} is the activation energy for conduction.

The obtained values of the ac activation energy for different frequencies are decreased from 0.24eV to 0.15 eV.

Dielectric dispersion implies the variation of real and imaginary parts at fixed temperatures.

The complex dielectric function for the investigated organic dye is expressed as [21]:

$$\epsilon^*(\omega) = \epsilon_1(\omega) + i\epsilon_2(\omega) \quad (11)$$

where $\epsilon_1(\omega)$ and $\epsilon_2(\omega)$ are the dielectric constant and the dielectric loss respectively. The dielectric constant is associated with the polarization of the material under the influence of sub-switching ac field [22]. The dielectric constant $\epsilon'(\omega)$ and $\epsilon''(\omega)$ were calculated in the range of frequency 42Hz-5MHz and temperature range (298-423)K. Figs. (8 and 9) show the variation of $\epsilon_1(\omega)$ and $\epsilon_2(\omega)$ with frequency at different temperatures, respectively. As seen in Figs. (8 and 9) $\epsilon_1(\omega)$ and $\epsilon_2(\omega)$ decrease with increasing frequency. The decrease of $\epsilon_1(\omega)$ with frequency can be explained as follows; at low frequencies the dielectric constant $\epsilon_1(\omega)$ for polar materials is due to the contribution of multi-component of polarizability, deformational polarization (electronic and ionic polarization) and relaxation polarization (orientational and interfacial polarization) [23].

When the frequency is increased, the dipoles will no longer be able to rotate sufficiently rapidly, so that their oscillations begin to lag behind those of the field. As the frequency is further increased, the dipole will be completely unable to follow the field and the orientation polarization stopped, so $\epsilon'(\omega)$ decreases at higher frequencies approaching a constant value due to the interfacial or space charge polarization only [24, 25].

Conclusion

Structural investigation using X-ray confirmed that the powder of 2-amino-(4,5-diphenylfuran-3-carbonitrile) has a triclinic structure with lattice constant $a=11.63$, $b=18.933$, $c=22.226$, $\alpha=96.72$, $\beta=55.14$, $\gamma=132.66$ and space group $P1$. Electrical conductivity and dielectric properties of bulk, 2-amino-(4,5-diphenylfuran-3-carbonitrile) was measured as a function of frequency range 42Hz-5M kHz and temperature range 298-423K in a compressed pellet, with evaporated ohmic Au electrodes. The dc conductivity was explained according to the VRH mechanism. The ac conductivity $\sigma_{ac}(\omega)$ was found to vary as ω^s in the

frequency at high range of frequency the frequency exponent, s , was less than unity and decreases with the increase in temperature indicating a dominant correlated barrier hopping (CBH) mechanism.

The calculated ac activation energy was found to decrease with increasing frequency. This may be indicated that the ac conductivity is a thermally activated process. The dielectric constant, $\epsilon_1(\omega)$ was found to decrease by increasing frequency. The dielectric loss, $\epsilon_2(\omega)$, was also found to be decreased by increasing frequency.

Corresponding author

A.A. Hendi

Physics Department, Sciences Faculty for girls, King Abdul Aziz University, Jeddah, Saudi Arabia

dr.asmahendi@hotmail.com

References:

- [1] W. Brütting, Phys. Stat. Solidi A 201 (2004) 1035.
- [2] A. Gangjee, R. Devraj, L.R. Barreus, J. Med. Chem., 37(1994)1169.
- [3] H. Shimamura, R. Terajima, A. Kawase, Y. Ishizuka, I. Kimura, A. Kama, M. Kataoka, Jpn. Kokai tokkyo koho JP05,112,559; Chem. Abstr. 119(1993)160315.
- [4] R. G. Edie, R. E. Hackler, E. V. Krumkains, Eur Pat. Appl. Ep. 49; Chem. Abstr. 116(1992)128957.
- [5] M. P. Roer, Eu. Pat., 164268; Chem. Abstr., 105(1986)242726.
- [6] R. G. Melik, Ogandzhanyan, A. S. Gapoyan, V. E. Khachatryan, Sint. Geterosiki Soedin, 12(1981)24
- [7] S. Furukawa, M. Takada, H. N. Castle, J. Heterocycl. Chem., 18(1981)581
- [8] M. Kidwai, S. Rastogi, R. Venkataraman, Bull. Chem. Soc. Jpn, 76(2003)204.
- [9] R. Shirley, the CRYSFIRE System for Automatic Powder Indexing: User's Manual, the Lattice Press, Guildford, Surrey GU2 7NL, England, 2000.
- [10] J. Laugier, B. Bochu, LMGP-Suite suite of Programs for the interpretation of X-ray Experiments, ENSP/Laboratoire des Matériaux et du Génie Physique, BP46.38042, Saint Martin d'Heres, France, 2000.
- [11] R.D. Gould, A.K. Hassan, Thin Solid Films, 223 (1993) 334
- [12] A.O. Abu-Hilal, A.M. Saleh and R.D. Gould, Materials Chemistry and Physics, 94(2005)166.
- [13] M.M. El-Nahass, A.F. El-Deeb, F. Abd-El-Salam, Org. Electron., 7 (2006) 261
- [14] A.A. Atta, J. Alloys Compd., 480 (2009)564
- [15] S.R. Elliott, *Physics of Amorphous Materials* (John Wiley & Sons, Inc, New York, 1983)
- [16] N.F. Mott, E.A. Davis, *Electronic Processes in Noncrystalline Materials* (Clarendon Press, Oxford, 1979)20.
- [17] A.K. Jonscher, Nature, 267 (1977)673
- [18] G.E. Pike, Phys. Rev., B6(1972)1572.
- [19] Pike, G.E., Philos. B. Mag., 6(1972)1582.
- [20] S.R. Elliott, Philos. Mag., 36 (1977)1291
- [21] I. G. Austin, N.F. Mott., Adv. Phys., 18(1969) 41.
- [22] P. Venkaterwarlu, A. Laha, S.B. Krupanidhi, Thin solid Films, 474 (2005)1
- [23] B. Tareev, *Physics of Dielectric Materials* (Mir Publishers, Moscow, 1975)
- [24] S. Kurien, J. Mathew, Sebastian S, Potty SN, George KC. Mater Chem Phys., 98(2006)470.

[25] P.S. Anantha, K.Harihanan, Mater Sci Eng
B;121(2005)12.

Table.1 X-ray for powder of 2-amino-(4,5-diphenylfuran-3-carbonitrile) .

No	$2\theta_{\text{measured}}$	$2\theta_{\text{calculated}}$	d_{measured}	$d_{\text{calculated}}$	I/I_0	(hkl)
1	6.735	6.727	13.113	13.13	15.73	(001)
2	7.078	7.095	12.477	12.488	100	(010)
3	10.596	10.591	8.342	8.302	41.16	(0 $\bar{1}$ 1)
4	10.872	10.843	8.131	8.153	6.27	(002)
5	11.071	11.087	7.985	7.947	15.41	(101)
6	13.994	14.006	6.323	6.318	16.19	(100)
7	14.220	14.218	6.223	6.224	63.88	(020)
8	15.292	15.301	5.789	5.786	4.97	(1 $\bar{3}$ 1)
9	15.449	15.418	5.731	5.742	6.81	(0 $\bar{1}$ 2)
10	15.801	15.81	5.604	5.599	1.56	(113)
11	17.016	17.002	5.203	5.211	7.78	(111)
12	17.868	17.89	4.959	4.954	1.88	(114)
13	19.996	20.003	4.437	4.435	33.28	(2 $\bar{4}$ 0)
14	20.251	20.247	4.381	4.382	2.97	(1 $\bar{4}$ 0)
15	20.581	20.581	4.312	4.312	1.24	(2 $\bar{1}$ 5)
16	21.025	21.022	4.222	4.223	1.75	(1 $\bar{2}$ 4)
17	21.406	21.397	4.147	4.149	3.12	(030)
18	21.645	21.636	4.102	4.104	3.23	(1 $\bar{2}$ 3)
19	22.009	22.027	4.035	4.032	4.14	(124)
20	22.276	22.28	3.987	3.987	17.10	(202)
21	22.434	22.436	3.959	3.991	11.75	(205)
22	22.868	22.875	3.885	3.884	6.73	(1 $\bar{0}$ 2)
23	24.134	24.135	3.685	3.681	9.34	(3 $\bar{4}$ 4)
24	24.361	24.362	3.651	3.651	11.75	(3 $\bar{3}$ 2)
25	25.945	25.931	3.431	3.433	16.55	(2 $\bar{3}$ 2)
26	26.262	26.264	3.391	3.393	3.82	(213)
27	26.698	26.698	3.336	3.338	1.85	(3 $\bar{3}$ 1)
28	26.996	27.042	3.300	3.291	3.02	(3 $\bar{5}$ 4)
29	27.701	27.714	3.218	3.216	1.82	(216)
30	28.003	28.003	3.184	3.184	5.10	(212)
31	29.926	29.927	2.983	2.983	2.98	(117)
32	30.528	30.528	2.925	2.924	8.21	(2 $\bar{5}$ 3)
33	31.321	31.320	2.853	2.854	9.41	(1 $\bar{2}$ 6)
34	31.525	31.535	2.835	2.832	3.60	(0 $\bar{4}$ 1)
35	38.7525	38.751	2.321	2.322	1.67	(2 $\bar{5}$ 5)
36	39.1759	39.176	2.297	2.296	1.69	(301)
37	40.596	40.596	2.220	2.221	1.27	(048)

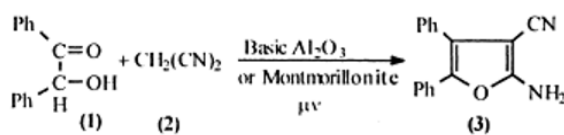
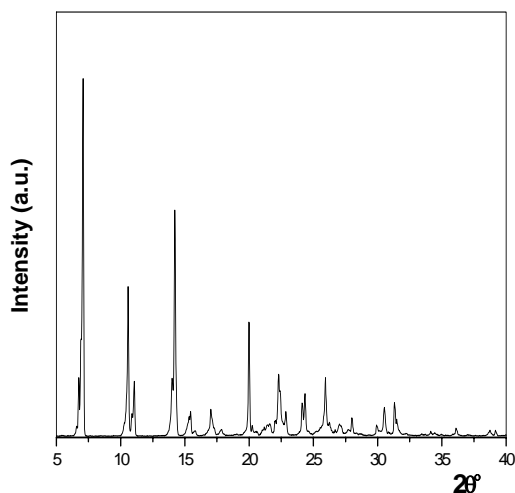
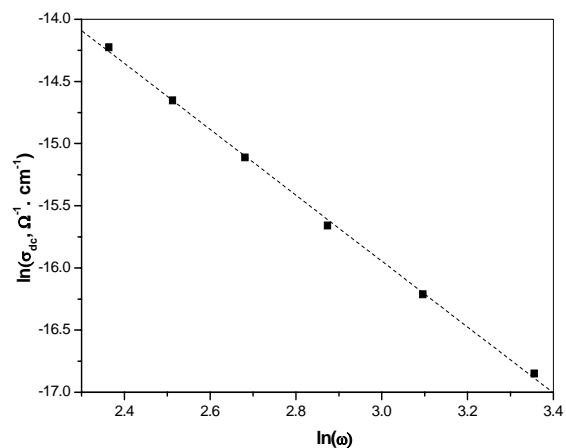
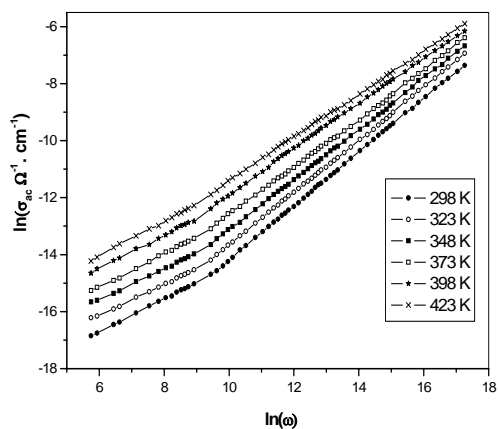
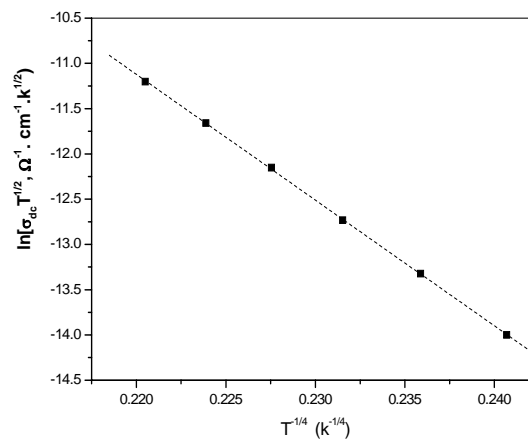
Fig. 1: Scheme 1. Synthesis of -amino-(4,5-diphenylfuran-3-carbonitrile).**Fig. 2:** XRD of 2-amino-(4,5-diphenylfuran-3-carbonitrile) in the powder form.**Fig. 4:** Temperature dependence of DC conductivity of 2-amino-(4,5-diphenylfuran-3-carbonitrile).**Fig. 3:** Frequency dependence of AC conductivity $\sigma_{ac}(\omega)$ of 2-amino-(4,5-diphenylfuran-3-carbonitrile) at various temperatures**Fig. 5:** Plots of $\ln(\sigma_{dc} T^{1/2})$ versus $T^{-1/4}$ for 2-amino-(4,5-diphenylfuran-3-carbonitrile).

Fig. 6: Temperature dependence of the frequency exponent s for 2-amino-(4,5-diphenylfuran-3-carbonitrile).

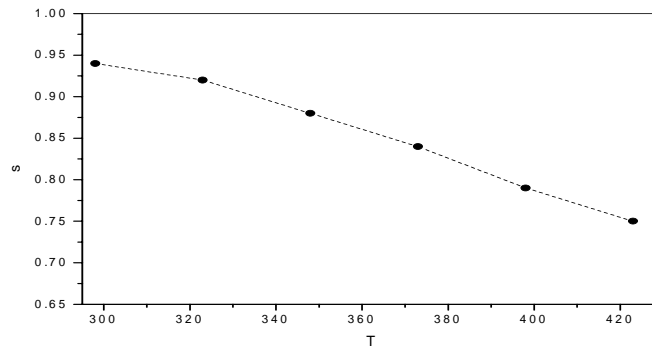


Fig. 7: Variation of AC conductivity, $\sigma_{ac}(\omega)$, with temperature at different frequencies for 2-amino-(4,5-diphenylfuran-3-carbonitrile). (4,5-diphenylfuran-3-carbonitrile).

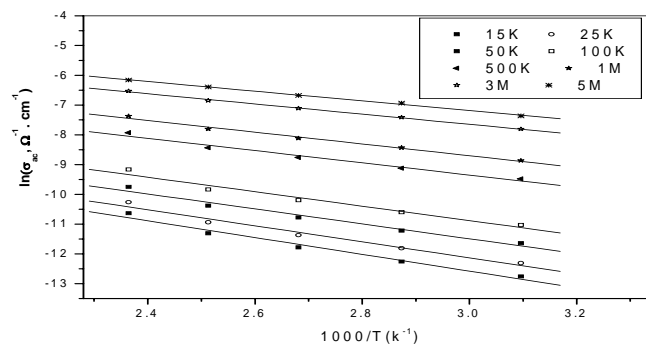


Fig. 8: Variation of the dielectric constant $\epsilon'(\omega)$ with frequencies at different temperature at for 2-amino-(4,5-diphenylfuran-3-carbonitrile).

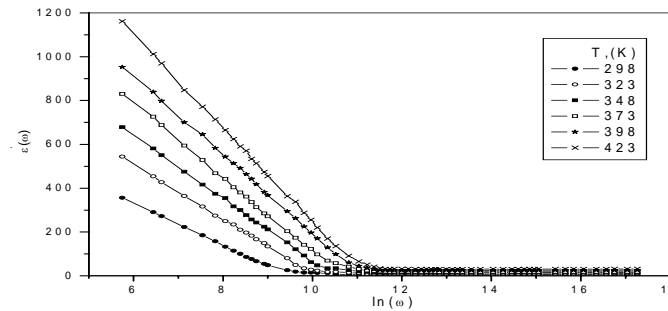
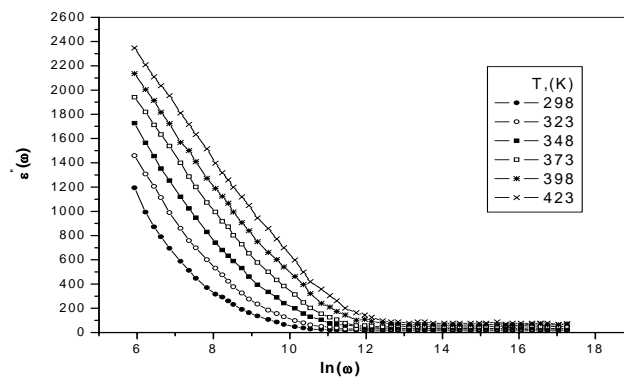


Fig. 9: Variation of the dielectric loss $\epsilon''(\omega)$ with frequencies at different temperature for 2-amino-(4,5-diphenylfuran-3-carbonitrile).



Study of Electrical Properties of TlInSe Layered Single Crystal

S. E. Al Garni

Physics Department, Sciences Faculty for Girls, King Abdulaziz University-KSA.
algarnisabah@gmail.com

Abstract: Single crystals layered compound TlInSeS were grown by modified Bridgman method. The crystals were identified by X-ray diffraction. In the present paper we describe and analyze conductivity and Hall effect measurements, performed on TlInSeS single crystals over the temperature range 148-558 K. The Hall Effect measurements revealed the extrinsic p-type conduction in the low temperature range of investigation. The dependence of the Hall coefficient conductivity, Hall mobility and charge carrier concentration on temperature were presented graphically. The analysis of the temperature dependent electrical conductivity and carrier concentration reveal that the acceptor level is located at 0.028 eV above the valence band of TlInSeS. From the obtained experimental data, the main characteristic parameters of the crystals have been estimated. Energy gap and acceptor concentration were 0.727 eV and $1.305 \times 10^{14} \text{ cm}^{-3}$ respectively. The anomalous behavior of $\ln \mu$ and $\ln T$ in the low temperature range was checked.

[S. E. Al Garni **Study of electrical properties of TlInSeS layered single crystal**. Life Science Journal. 2011;8(3):560-563] (ISSN:1097-8135). <http://www.lifesciencesite.com>.

Keywords: TlInSeS; Hall Effect; DC electrical conductivity; energy gap; acceptor level.

1. Introduction

Determination of the application potential for new semiconducting materials in solid state physics requires the growth and the examination of physical properties of the materials. Some binary and ternary layer-chain structured semiconductors such as the group III chalcogenides (InSe, GaSe, GaTe, TlInSe₂, TlInS₂, TlGaSe₂ etc.) have been explored thoroughly and proved already their applicability in solid state physics, for instance in optoelectronic devices [1]. One of the methods for modifying their physical properties is the production of solid solutions of these semiconductors. The experimental studies carried out on TlInS₂ and TlInSe₂ demonstrate that investigations for the physical properties of the TlInS₂-TlInSe₂ system should be rewarding in view of the production of a new candidate material for optical devices in the visible range. Quaternary thallium chalcogenide TlInSeS is formed from the TlInS₂-TlInSe₂ system and has a direct band gap of 2.328 at 10 K [2]. X-ray powder diffraction was used to characterize the TlInSeS crystals. The parameters of the monoclinic unit cell [3] were found to be $a=0.72850$, $b=0.45380$, $c=0.78357$ nm and $\beta=106.22^\circ$. The lattice of TlInSeS crystals consists of two dimensional layers arranged parallel to the (001) plane. Each layer is oriented perpendicular with respect to the previous one. There is interlayer bonding between Tl and Se (S) atoms whereas the bonding between In and Se (S) atoms is an interlayer type. Infrared reflection and Raman spectroscopy were studied [4,5]. In view of possible optoelectronic device application in the visible region, a great deal of attention has been devoted to the study of the

photoelectric, optical and electrical properties of thallium chalcogenides [6-10]. Information about the trapping centers and their distributions in undoped TlInSeS layered single crystals by thermally stimulated current measurements were published [11]. The photoluminescence (PL) spectra of TlInSeS crystals have been investigated [12].

In spite of its importance in technological application as a candidate material for optical devices, and also for the understanding of its basic physics, so far very little information on the physical properties of this compound. To our knowledge, there is no information about the DC electrical conductivity and Hall coefficient and its temperature dependence. Hence, we report the results of the electrical conductivity and Hall coefficient of TlInSeS layered single crystal in the temperature range 148–558 K. As a result of this study we were able to calculate most of the physical parameters of this compound. To the best of the authors knowledge, the data presented in this work have not been reported before.

2. Experimental procedures

2.1 Material and sample preparation

TlInSeS single crystals were grown from the melt by a modified Bridgman technique from a stoichiometric melt of starting materials sealed in evacuated ($\approx 10^{-6}$ Torr) and carbon coated silica tubes (15 mm in diameter and about 25 cm in length) with a tip at the bottom. All the starting materials used were of extra pure elements (99, 9999 %). To prevent the ampoule from exploding, it was heated in a temperature gradient furnace, so that the sulphur

condensed at the cold end and slowly reacted with the heated elements at the hot end. The ampoule was kept at temperature higher than the melting point for 10 hours to ensure homogenization. The growth was achieved by lowering the ampoule from the hot side of the furnace at 1053 K, to the cold side at 703 K at a speed of 1.6 mmh⁻¹. In the cold zone, the crystal cooled down slowly within a couple of days. The resulting ingots had no cracks and voids on the surface. The time required for this process was about 17 days. The crystals obtained have a layered structure (red in color) showed good optical quality and the freshly cleaved surfaces were mirror-like. The samples were identified by means of X-ray analysis. The X-ray diffraction analysis confirmed that TlInSeS compound have a monoclinic structure with the lattice parameters a=1.111, b=1.062 and c=1.592 nm. The samples for measurement were taken from the middle part of the ingots, by the razorblade. The freshly cleaved platelets (along the cleavage planes) were mirror-like. That is why no further polishing and cleaning treatments were required. Details for crystal growth are described elsewhere [13].

2.2. Electrical conductivity and Hall effect measurements.

Parallelepiped samples with mean dimensions 9.4×2.8×1.6 mm³ and mirror surfaces were prepared for electrical measurements. These were performed in a vacuum cryostat in the temperature interval 148 to 558 K using a specimen container evacuated to 10⁻³ Torr. Electrical conductivity and Hall coefficient were measured by a DC compensation method. Electrical measurements were made with the aid of silver paste contact. These contacts were Ohmic in the range of the applied voltage. The Ohmic nature of the contact was checked by recording the current-voltage characteristics. A study of the Hall effect was carried out in a static magnetic field employing a direct current. A magnetic field of 0.5 Tesla was employed for Hall coefficient measurement. The current direction was parallel and the field direction was perpendicular to the cleavage plane. In order to avoid thermogalvanomagnetic effects [14], several measurements were carried out for temperature values by reversing the direction of the current and the magnetic field. Welded copper and constantan wires (Ø 0.1 mm) served as junctions for measuring thermocouples. The temperature was varied above room temperature up to 558 K, with the help of electrically insulated heater. Temperatures below room temperature up to 148 K were achieved using liquid nitrogen. The measured Hall voltage was corrected for the finite ratio of the sample length to width according to calculated correction factors [15]. The apparatus and procedure of measurements are

mainly the same as those described in previous work [16].

3. Results and discussion

The result presented in the figures are that for TlInSeS single crystal with room temperature conductivity equal to 1.43×10⁻⁵ Ω⁻¹ cm⁻¹. Fig. 1 shows the temperature dependence of electrical conductivity. The complete temperature range can be subdivided into three regions: below transition, transition region and above transition. These curves are quite similar to semiconductor behaviour. These regions are clearly shown in fig. 1; with increasing temperature, the electrical conductivity increased slowly. Secondly, it reached the transition region at 190 K, then passed through a minimum and rose again. This pattern of change in the electrical conductivity is due to the appearance of impurity and intrinsic conductivity respectively and to the variation of hole mobility and concentration with temperature. The fall in the electrical conductivity was due to a decrease in mobility, since the carrier density in this temperature region remained practically constant (N_A-N_D = constant), until the intrinsic region was reached. At temperatures above the transition point, the conductivity rose rapidly. The temperature dependence exhibited a transition from a region of lower slope to one of higher slope. The transition region stretches from 190 to 460 K. The slopes of the curve increased with increasing temperature, and were higher at higher temperature due to carriers being excited from the extended state of the valence band into the conduction band. The width of the forbidden zone as calculated from the slope of the curve in the high temperature region was found to be 0.727 eV.

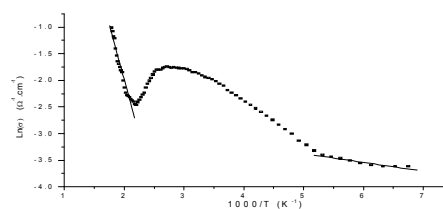


Fig.1. Electrical conductivity of TlInSeS as a function of temperature

The temperature dependence of the conductivity can be expressed in the form

$$\sigma = \sigma_0 \exp\left(\frac{-\Delta E_g}{2KT}\right)$$

Where σ_0 is the pre-exponential factor and ΔE_g is the width of energy gap. The calculated energy gap

width is smaller than that reported in the literature. This value contrasts with data of other authors [2,3]. Not only our results contradict to those obtained by other authors, but also the published values for ΔE_g disagreed with each other. We may attribute the discrepancy in the values of ΔE_g partially to the presence of a large number of intrinsic defects that affects strongly the motion of the scattering of current carriers and phonons. On the other hand it is thought that the technology used to grow this crystal may influence its physical properties. In this paper, we tried to elucidate this confusion, but more experimental data were necessary to explain this contradiction. In the extrinsic region the electrical conductivity increases slowly with temperature due to the fact that the carrier concentration, in this region is determined by the number of ionized acceptors liberated from the impurity level. From this region the ionization energy was calculated indicating the acceptor centre lay at 0.028 eV. The temperature dependence of the Hall coefficient for TlInSeS is positive in the entire range of investigation. This indicates that the compound TlInSeS is an excellent p-type semiconductor. The Hall coefficient at room temperature was evaluated as $R_H=4.786 \times 10^4 \text{ cm}^3/\text{C}$. We can see from the figure at the beginning of the curve the Hall coefficient shows a less rapid dependence on temperature. The sample exhibits a considerable fall of the Hall coefficient when temperature is increased up to the transition region in which the experimental $\text{Ln}R_H$ versus $10^3/T$ curve deviates from linearity. In the intrinsic conduction region the Hall coefficient fall rapidly. Determination of the energy gap and ionization energy from Hall data is possible by plotting the relation between $\text{Ln}R_H T^{3/2}$ and $10^3/T$ as shown in fig.3. In the temperature region in which the conductivity is predominately intrinsic, the forbidden band was estimated to be 0.727 eV. The depth of the acceptor centre was determined from the region in which conductivity is predominantly due to impurity atoms and was found to be 0.028 eV. These values are in good agreement with the values obtained from the temperature dependence of electrical conductivity. Combination of the Hall measurements and the electrical conductivity data were used to study the temperature dependence of the mobility of the charge carriers. The nature logarithm of $R_H \sigma$ against $\text{Ln}T$ is plotted in figure 4. This plot results in a straight line slope which allows the determination of the exponent. It was found that the exponent n in the relation $\mu \sim T^n$ below 190 K is 0.23, whereas in the high temperature range ($T > 460\text{K}$), the mobility decreases according to the low $\mu \sim T^{-2.94}$. This dependence indicates that phonon scattering is the mechanism responsible for

this mobility behaviour in the high temperature range. The highest measured value of the hole mobility at 148K is $9408.793 \text{ cm}^2/\text{V}\cdot\text{sec}$. The fall in the mobility below $7267.517 \text{ cm}^2/\text{V}\cdot\text{sec}$ as the temperature decreases, implies that other scattering mechanisms become more important but the small value of n are unusually compared with those obtained for impurity scattering in other semiconductors. However the variation of mobility with temperature in these defected semiconductors has not been previously reported, there is still insufficient experimental data to throw a clear light upon this behaviour. This may be associated with the presence of high density of stoichiometric vacancies and the creation of defects. The exact nature of defects in these semiconductors remains uncertain, but from structural considerations and also by analogy with III-V compounds, vacancies and anti-site defects are likely to play important role. Stoichiometric cation vacancies present are themselves not neutral, but their presence is responsible for easy restoration of radiation ejected atoms into lattice sites across low energy barriers. The room temperature value of the mobility was found to be $6864.25 \text{ cm}^2/\text{V}\cdot\text{sec}$.

Carrier density versus reciprocal temperature measurements indicates acceptor level at 0.02 eV as shown in figure 5. At low temperatures and indeed (148-190 K) in TlInSeS the carrier concentration is determined by the number of ionized acceptors and the variation of the carrier concentration is quite slow. Since, the TlInSeS sample exhibited an intrinsic behavior above 460 K, then the expected value for the intrinsic concentration will be given as

$$p_i = 2 \left(\frac{2 \pi K}{h} \right)^{3/2} (m_p^* m_n^*)^{3/4} T^{3/2} \exp \left(\frac{-\Delta E_g}{2 K T} \right)$$

Where symbols have their usual significance and the energy gap width as deduced from this relation is 0.727 eV. The carrier concentration at room temperature as calculated from the R_H curve is $1.305 \times 10^{14} \text{ cm}^{-3}$. The diffusion coefficient is related to the mobility of charge carriers, its value for holes can be deduced as $D_p=177.78 \text{ cm}^2/\text{sec}$. The relaxation time as well as the diffusion length for holes were evaluated to be $3.88 \times 10^{-7} \text{ sec}$ and $8.305 \times 10^{-3} \text{ cm}$ respectively.

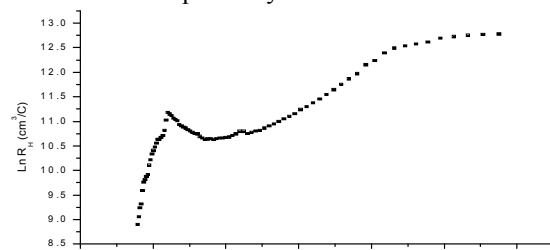


Fig.2. Variation of Hall coefficient with temperature for TlInSeS single crystal

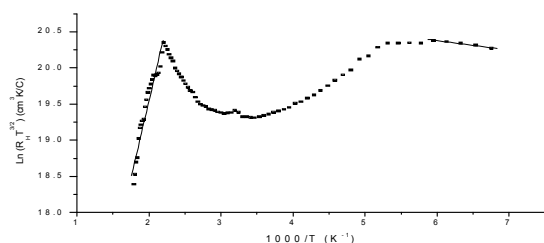


Fig.3. Relation between $R_H T^{3/2}$ and $10^3/T$ of TlInSeS single crystals

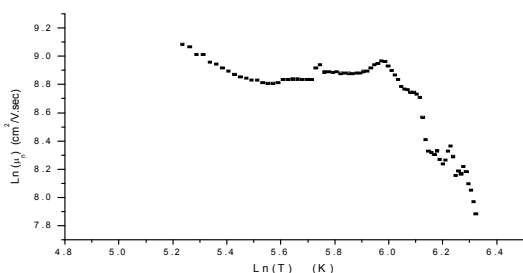


Fig.4. Temperature dependence of charge carrier mobility of TlInSeS

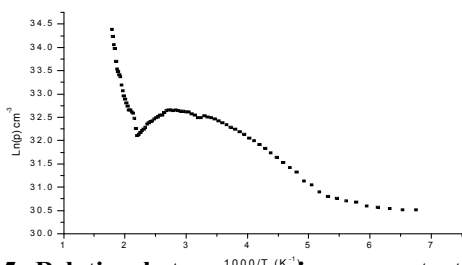


Fig.5. Relation between carrier concentration in TlInSeS and temperature

4. Concluding remarks

Thallium indium sulphur selenide single crystal was grown from the melt by a special modified Bridgman technique. Crystal perfection was checked by means of the x-ray diffraction technique. Measurements of electrical conductivity and Hall effect between 148 and 558 K were carried out on TlInSeS. The study was carried out with the current parallel to the c-axis and the magnetic field perpendicular to the c-axis. From the electrical conductivity and Hall effect measurements, the band gap of p-type TlInSeS and the depth of the impurity level was determined to be 0.727 eV and 0.028 eV respectively. The present investigations is the first one on electrical conductivity and Hall coefficient of

TlInSeS lead to the determination of the variation of carrier concentration and mobility with temperature. The variation of mobility with temperature shows small value of temperature exponents in the low temperature range. This anomalous behavior can not be understood by the usual theory of semiconductors. An attempt to explain this unusual character by assuming localized phonons due to stoichiometric vacancies are expected to play an important role in the behaviour TlInSeS while additional contribution may be presented due to creation of defects.

Corresponding author

S. E. Al Garni

Physics Department, Sciences Faculty for Girls, King Abdulaziz University-KSA.

algarnisabah@gmail.com

References

1. Abay B., H.S. Giider, H.Efeoglu, Y.K.. Yogurtcu(2001) J.Phys and Chem. Of Sol., 62: 747.
2. Akhmedov A.M., A.E.Bakhyshov, A.A. Lebedov, and M.A.Yakobon (1978) Sov. Phys. Semi Cord. 12: 299.
3. Gasanly N.M. and I.Guler(2008) Int.J.Mod. Phys., B22: 3931.
4. Nusov Sh., V.M. Burlakov, E.A. Vinogzodov, N.M. Gasanly and B.M. Dzhavadov(1986) Phys. Stat. Solidi., B 137: 121.
5. Vinogzadov E.A., N.M. Gasanly, A.F. Concharov, B. M. Dzhavadov and V. I. Tagirov(1980) Sov. Phys. Sol. Stat., 22: 526.
6. Harios M., K. Anagnostopoulos, K. Kambaa and J. Spyridelis(1989) Physica., B 160: 154.
7. Kalomiros J.A. and A.N. Anagnostopoulos(1994) Phys. Rev. B 50: 7488.
8. Ibrohimov T.d. (1994) I.I. Aslonov, Sol. Stat. Commun. 123: 339.
9. Samedov S.R., O. Baykan and A. Gulybayov(2004) International J. Infrared and Millimeter Waves, 25: 735.
10. Gasanly N.M(2010). Cyst. Res. Technol., 45: 528.
11. Galer I. and N.M. Crosanly(2009) J.Alloy and Compounds, 485: 41.
12. Gasanly N.M., A. Aydinli and N.S. Yuksek(2002) J.Phys. Condens. Matter., 14: 13685.
13. Hussein S.A. and A.T. Nagat(1989) Crystal. Res. Technol., 24: 283.
14. Runyan W.R. (1975). Semiconductor Measurements and Instrumentation Mc. Crows-Hill, ltd..
15. Kundov G.A.A. and T.G. Kerimova(1966) Phys. Stat. Sol., 16: 15.
16. Nagat A.T., S. A. Hussein, Y. H. Gameel and A. E. Belal(1990) Indian J. Of Pure and Applied Phys., 28: 586.

9/20/2011

Effect of Citrus Waste Substrate on the production of Bioactive Component, and Antioxidant and Antitumor Activity of *Grifola frondosa*

Jung Hyun Kim¹, Min Young Kim²

¹. Department of Tourism and Food Service Cuisine, Cheju Tourism College, Jeju 695-900, Republic of Korea

². Faculty of Biotechnology, College of Applied Life Sciences, Jeju National University, Jeju 690-756, Republic of Korea

jeffmkim@jejunu.ac.kr

Abstract: The contents of bioactive compounds, and antioxidant and anticancer activities of *Grifola frondosa* cultivated on citrus waste substrates such as citrus peel and premature Hallabong fruit drop were investigated in the present study. The total phenolics and naringin were 80- and 500-folds higher in the extracts from *Grifola frondosa* mycelia cultivated on citrus waste than those in the extracts of *Grifola frondosa* mycelia cultivated on the sawdust, which was reported in the previous findings. Moreover, IC₅₀ values of the extracts from *Grifola frondosa* mycelia cultivated on citrus waste in the DPPH radical scavenging assay were much lower than that of mushroom cultivated on the conventional substrate. The premature Hallabong mushroom extract showed the highest phenolic content (126.7 mg/g) and the best antioxidant activity. The IC₅₀ values of the premature Hallabong mushroom extract were 0.52, 0.38 and 0.46 mg/mL in the DPPH radical scavenging, superoxide radical scavenging and xanthine oxidase inhibition assays, respectively. Anticancer effects of *Grifola frondosa* cultivated on citrus waste in human colon and breast cancer cells were analyzed. Results demonstrated that *Grifola frondosa* cultivated on citrus waste exhibited antiproliferative effects in both HT-29 and MCF-7 cancer cells. Taken together, citrus waste can be utilized as a viable substrate to improve the antioxidant and anticancer activities as well as to increase total phenolic content of *Grifola frondosa*.

[Jung Hyun Kim, Min Young Kim. **Effect of Citrus Waste Substrate on the production of Bioactive Component, and Antioxidant and Antitumor Activity of *Grifola frondosa***. Life Science Journal. 2011;8(3):564-571] (ISSN:1097-8135). <http://www.lifesciencesite.com>.

Keywords: *Grifola frondosa*; citrus waste; Bioactive component; Antioxidant activity; Anticancer activity

1. Introduction

Globally citrus fruit production was estimated as 120 million tons per year (Terol et al., 2010). Almost half of these fruits is squeezed to juice, and the remainder including peel, segment membranes and other by-products is considered as citrus wastes. Traditional use for these residues is as cattle feed which currently does not have sufficient value to cover the production and transportation costs. Therefore, a large fraction of citrus waste is still deposited, leading to economical and environmental disadvantages, and health problem to human beings.

Grifola frondosa, a traditional and edible mushroom, has gained in popularity among consumers, not only because of its taste and flavor, but also because of its reported medicinal value (Borchers et al., 2004; Masuda et al., 2009). Extensive research has been carried out on the most efficient cultivation methods for mushrooms because its optimal growing conditions exist within a limited range of temperature, moisture, humidity and other environmental factors (Garibay-Orijel et al., 2007; Zhong and Tang, 2004; Sanchez, 2010; Chen et al., 2010). As one of the greatest challenges to

mushroom cultivation, investigators have recently exerted their efforts to optimize existing cultural techniques for edible and medicinal mushrooms using cheap and locally sourced substrate materials such as agricultural and food wastes (Gregori et al., 2009; Xiaoke and Shunxing, 2005; Chiu et al., 2000). Moreover, these studies done on mushrooms that have nutritional or pharmacological value focuses on the development of cultivation strategies that make it easy to obtain target compounds. Accordingly, our objective was to determine the potentiality of using citrus wastes such as peels and premature fruit drops as a basic raw material for growing *Grifola frondosa* mycelia. In addition, to investigate the health-promoting values of *Grifola frondosa* mycelia cultivated on citrus wastes, namely their bioactive compounds, antioxidant and anticarcinogenic properties were evaluated.

2. Material and Methods

2.1. Substrate

The peel waste of citrus fruit (*Citrus unshiu* Marc) after juice extraction was obtained from a local food processing company (Jeju Provincial

Development Co., Jeju, Korea). The fruit peels were dissected, weighed, lyophilized and then ground into a fine powder using a blender. Premature Hallabong (*[C. unshiu* Marcov \times *C. sinensis* Osbeck] \times *C. reticulata* Blanco) fruit drops, kindly supplied by commercial orchards (Seogwipo-si, Jeju, Korea), were washed, dried in an oven with air circulation at 40 °C, and ground with a mortar and pestle. The powdered substrates were stored at -20 °C prior to use.

2.2. Microorganism, inoculum and sample preparation

Grifola frondosa (KACC 50027), obtained from the RDA-Genbank Information Center, Suwon, Korea, was maintained on potato dextrose agar (PDA, Difco, Detroit, MI, USA) slant at 4 °C. Fungal inoculum was prepared from mycelia grown on PDA for 5 days at 24 °C in the dark and agar plugs taken from the periphery of the growing colony were used to inoculate media. An agar disk of the strain was inoculated (2%, v/v) in a 50 mL of a medium (pH 5) containing 50 mg of powdered substrate, 100 mg of CaCO₃ and 1 g of agar. After incubation for 10 days at 27 °C, the 50 mL culture was added to 1 L media which consisted of powdered substrate (1 kg) and CaCO₃ (50 g). The fermentations were implemented in a 5-liter jar fermenter for 15 days at a 25 °C. One gram of free-dried mycelia was ground into powder, extracted with 60 mL of 80% ethanol solution by ultrasonication at room temperature for 6 h, and then purified by using a Sep-Pak C₁₈ cartridge and a 0.45 μ m membrane filter (Waters, Milford, MA, US), were used directly for analysis of their bioactive components, antioxidant and antitumor activities.

2.3. Analysis of total phenolic content

The amount of total phenolics was determined by the modified method described previously (Zhang et al., 2010). Briefly, an aliquot of filtrate (20 μ L) was diluted with double-distilled water (30 μ L). Folin-Ciocalteu reagent (100 μ L) was dissolved in diluted solution, shaken, and then incubated for 5 min at room temperature. One hundred microliters of 20% Na₂CO₃ solution and double-distilled water until a total volume of 2 mL were added to the mixture. After incubation for 2 h at 23 °C, the absorbance *versus* a blank was determined at 760 nm. Three replicates were measured per sample class.

2.4. Analysis of naringin and hesperidin contents

The naringin and hesperidin contents of samples were determined using a modification of the procedure described previously (Abeysinghe et al., 2007; Kanaze et al., 2003). The mobile phase

consisted of 75 mM citric acid and 25 mM ammonium acetate in methanol/double-distilled water (40:60, v:v). The filtrate (20 μ L) of each sample was injected onto a C-18 symmetry (5 μ m, 3.9 mm \times 150 mm) column of the Waters HPLC system equipped with a 626 pump, a 486 UV detector fixed at 280 nm plus autosampler (Waters, Milford, MA) with the flow rate of 1 mL/min. The retention times and spectra were compared to those of authentic standards.

2.5. 1,1-diphenyl-2-picrylhydrazyl (DPPH) free radical scavenging assay

The radical scavenging assays were conducted by the modified method described previously (Cavin et al., 1998). Briefly, 100 μ L of each test compound with various concentrations was prepared in 96-well plates and equal volume of 0.4 mM DPPH in methanol was added to each well. The solution was kept in the dark for 10 min at room temperature and absorbance of the solution was measured at 517 nm using an ELISA reader (EL340, Bio-Tek). A methanolic solution of DPPH was used as control, whereas L-ascorbic acid, quercetin and curcumin were used as reference compounds. Percent inhibition was calculated according to the formula: Inhibition percentage = [(Control absorbance - Test absorbance) / Control absorbance] \times 100. A dose response curve was plotted to determine the IC₅₀ values. IC₅₀ is defined as the concentration sufficient to obtain 50 % of a maximum scavenging capacity. All tests were performed in triplicate.

2.6. Superoxide scavenging activity

The superoxide anion scavenging capacity of the test extracts was analyzed by estimation of the reduction product of nitroblue tetrazolium (NBT), as described previously (Chang et al., 1996; Furuno et al., 2002). The reaction mixture contained 50 mM Na₂CO₃ buffer, 3 mM xanthine, 3 mM ethylenediamine tetraacetic acid, 0.5 mM NBT and bovine serum albumin solution. Test extracts were added to the reaction mixture and incubated at 25 °C for 10 min. The reaction was started with the addition of xanthine oxidase (XO) (0.25 units/mL). After further incubation at 25 °C for 25 min, absorbance was recorded at 560 nm using an ELISA reader, against blank samples, which did not contain the enzyme. The superoxide production was confirmed by superoxide dismutase, which inhibited the reactions of NBT reduction in a concentration-dependent manner (data not shown). Each experiment was performed at least in triplicate.

2.7. XO inhibitory activity

XO activity was measured based on the procedure explained by Nguyen et al. (2004) with minor modifications. Assays were performed in 96-well plates with 115 μ L reaction mixtures containing 35 μ L of 200 mM phosphate buffer (pH 7.5), 30 μ L of XO (0.05 units/mL in 200 mM phosphate buffer), and 50 μ L of test plant extracts in deionized water. After preincubation at 25 °C for 15 min, the reaction was started by adding 60 μ L of 0.5 mM xanthine in 200 mM phosphate buffer (pH 7.5) to the mixture. The reaction mixture was incubated at 25 °C for 30 min and then the absorption increments at 290 nm, which indicated the formation of uric acid, were determined with an ELISA reader. The control group contained no test agent and allopurinol was used as a reference compound. Three replicates were made for each test sample to calculate IC₅₀ values.

2.8. Determination of the cell viability by using MTT assay

The human fibroblast cells (HS-68), colon cancer cells (HT-29) and breast cancer cells (MCF-7) were obtained from the Korean Cell Line Bank (Seoul, Korea). HS-68 and MCF-7 cells were cultured in Dulbecco's modified Eagle's Medium (DMEM) (GIBCO/BRL, NY, US) supplemented with 10% heat-inactivated fetal bovine serum, 100 units/mL penicillin, 100 μ g/mL streptomycin and 2 mM L-glutamine at 37 °C with 5% CO₂ in a humidified atmosphere. HT-29 cell lines were maintained in RPMI 1640 medium supplemented as above with L-glutamine, antibiotics and 10% heat-inactivated horse serum (Lonza, Walkersville, MD, US).

The inhibitory effect of samples on the proliferation of human normal and cancer cells was determined using 3-(4,5-dimethylthiazol-2-yl)-2,5-diphenyl tetrazolium bromide (MTT) assay. Briefly, HS-68, HT-29 and MCF-7 cells (2×10^3 /well) were loaded into 96-well culture plates and treated with fresh medium containing various concentrations (0-1,000 μ M) of each extract for 24 h. Cells were washed once with phosphate-buffered saline and reacted with the MTT solution (Boehringer Mannheim, Indianapolis, IN) at 37 °C for 4 h to produce the formazan salt. Finally, the formazan salt formed in each cultured cells was dissolved in DMSO, and the optical density (OD) value of each solution was measured at 540 nm using an ELISA reader (Bio-Tek, Winnoski, VT, US). The OD value detected for the control (cells without treatment with any samples) from the treated cells was plotted on the x-axis, designated as proliferation (% control), to demonstrate the effect of each sample on the viability of the related cells.

2.9. Statistical analysis

All analyses were replicated three times. Each data presented as means \pm standard deviation. The data were statistically analyzed one-way analyses of variance followed by Duncan's multiple range tests (SPSS 12.0). Difference with *p* value less than 0.05 was considered statistically significant. After multiple comparisons, the means in the following table and figures were followed with different small letter "a-d" based on their values and statistical differences. In the case that a mean was followed with "ab", this mean was not significantly different from a mean with "a", and was not significantly different from another mean with "b". However, means with different letters were significantly different at the level of 0.05.

3. Results and Discussion

Phenolic compounds, aromatic secondary plant metabolites, which mainly include flavonoids, phenolic acids, stilbenes, coumarins and tannins (Robbins, 2003). In addition to vitamin C and carotenoids, a variety of phenolic compounds are present in fruit and vegetables, and exhibit a wide range of physiological and flavoring properties (Robbins, 2003). Until now, only a few authors have reported the content and composition of phenolic compounds of *Grifola frondosa*: It has been shown to contain high amounts of phenolic compounds (Lee et al., 2008) and 18 phenolic compounds including flavonoids being reported (Lee et al., 2010a). We, therefore, examined the total phenolic content of *Grifola frondosa* mycelial extracts cultivated on citrus waste substrate (Table 1).

Table 1. Total phenolic, naringin and hesperidine composition of *Grifola frondosa* mycelial extract cultivated on citrus waste substrate

Content (mg/g dry matter)	Citrus peel substrate	Premature Hallabong substrate	Citrus peel mushroom	Premature Hallabong mushroom
Total Phenolics	57.0 \pm 0.62 ^a	97.7 \pm 1.22 ^b	74.5 \pm 1.60 ^c	126.7 \pm 1.07 ^d
Naringin	nd ^{**}	2.7 \pm 0.05 ^b	nd	3.3 \pm 0.53 ^b
Hesperidin	5.8 \pm 0.10 ^a	13.3 \pm 0.07 ^b	6.2 \pm 0.06 ^c	13.7 \pm 0.10 ^d

*Mean \pm S.D. for n=3; **Not detected; ^{a-d}Values with different superscripts in a row are significantly different (*p* < 0.05)

The content of total phenols was significantly higher for *Grifola frondosa* mycelial extract cultivated on premature Hallabong substrate (premature Hallabong mushroom, 126.7 mg/g) than that for *Grifola frondosa* mycelial extract cultivated

on citrus peel substrate (citrus peel mushroom, 74.5 mg/g) ($p < 0.05$). These contents were 47- to 80-fold higher than previous result reported by other authors, who evaluated content of total phenols was 1.59 mg/g in the extract from *Grifola frondosa* mycelia cultivated on the sawdust (Mau et al., 2004). In addition, mushroom extracts using citrus peel and premature Hallabong as substrate shows more total phenolic contents than those of their substrates (57.0 and 97.7 mg/g), respectively ($p < 0.05$) (Table 1). This indicates that citrus waste substrate may be responsible for the total phenolic content as well as the growth of mushroom.

The extracts of *Grifola frondosa* mycelia cultivated on citrus waste were analyzed by a modified reversed-phase HPLC system to determine the content of naringin and hesperidin, which are two major flavonoids present in citrus fruits (Kanaze et al., 2003; Choi et al., 2007). There was significant variation in the contents of naringin and hesperidin in all mushrooms and their substrates (Table 1). Naringin was detected only in premature Hallabong mushroom (3.3 mg/g) and its substrate (2.7 mg/g), whereas hesperidin was found in the extracts of all mushrooms and their substrates. As expected from the result of total phenolic content, naringin and hesperidin were significantly higher in the extracts of citrus peel and premature Hallabong mushrooms than that in their substrates ($p < 0.05$), with the highest hesperidin content found in premature Hallabong mushroom (13.7 mg/g) (Table 1). Recently, Lee *et al.* reported that the naringin content of the extract from *Grifola frondosa* fruit body cultivated on the sawdust was 0.0278 mg/g (Lee et al., 2010a), which is 500-fold lower than those of mushroom cultivated on premature Hallabong fruit drops. This implies that citrus waste substrate might contribute to the increase in the contents of naringin as well as of total phenolics of *Grifola frondosa* mycelia as compared with conventional substrate. Flavonoids have been associated with the health benefits derived from their antioxidant activity (Heim et al., 2002), and could be a natural source of antioxidants as well as a major determinant of antioxidant potentials of foods (Parr and Bolwell, 2000). Therefore, our results may provide important information on utilization of citrus wastes as primary substrate for *Grifola frondosa* cultivation as a medicinal mushroom. Since the key role of phenolic compounds to scavenge free radicals has been emphasized in several reports (Rauha et al., 2000; Archana and Dasgupta, 2005), antioxidant properties of *Grifola frondosa* mycelial extracts cultivated on citrus waste substrates were investigated in the following experiments.

Scavenging activity for free radicals of DPPH has been widely used to evaluate the

antioxidant activity of natural products from plant sources (Huang et al., 2005; Zhu et al., 2004). As shown in Figure 1, dose-response curves for the DPPH radical scavenging activity were observed in all mushrooms and substrates. The most potent scavenging DPPH radical activity was observed in premature Hallabong mushroom (0.5 mg/mL IC_{50}), which possess significantly higher DPPH free radical scavenging activity than that of citrus peel mushroom (0.9 mg/mL IC_{50}) ($p < 0.05$). These IC_{50} values were much lower than that of extracts of *Grifola frondosa* mycelia cultivated on the sawdust (4.95 mg/mL) (Mau et al., 2004; Mau et al., 2002), indicating that mushrooms cultivated on citrus waste substrate were more effective in scavenging effects than mushroom cultivated on conventional substrate. However, citrus peels (1 mg/mL IC_{50}) and premature Hallabong fruit drops (0.6 mg/mL IC_{50}) showed the similar activity with mushroom extracts using it as a substrate, respectively, even though they showed lower IC_{50} values (Figure 1).

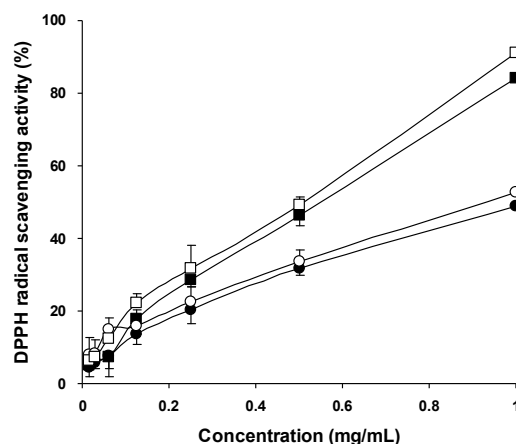


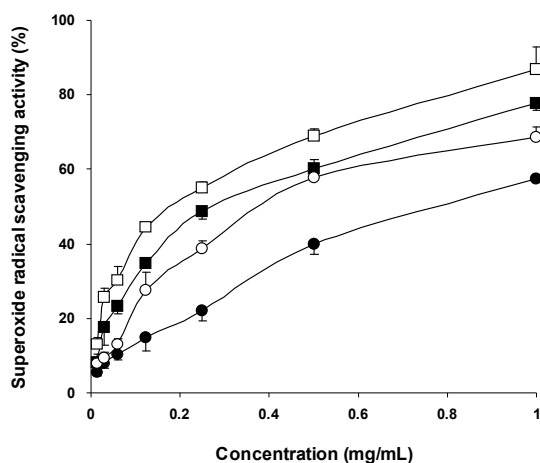
Fig. 1. DPPH radical scavenging activity of citrus

Sample	Citrus peel substrate	Premature Hallabong substrate	Citrus peel mushroom	Premature Hallabong mushroom
IC_{50} (mg/mL)	1.0±0.07 ^a	0.6±0.03 ^b	0.9±0.09 ^a	0.5±0.01 ^b

peel substrate (●), premature Hallabong substrate (■) and the extracts of *Grifola frondosa* mycelia cultivated on citrus peel substrate (○) and premature Hallabong substrate (□). Values are means ± S.D. of three separated experiments. ^{a-b}Values with different superscripts in a row are significantly different ($p < 0.05$).

Reactive oxygen species, including superoxide anions, hydrogen peroxide, hydroxyl radical, nitric oxide and peroxynitrite, play an

important role in oxidative stress related to the pathogenesis of various diseases such as inflammation, heart disease, diabetes, gout and cancer (Slater, 1984). In the present work, the activities were dose-dependent, and more effective antioxidant activity was found in premature Hallabong mushroom extracts (0.4 mg/mL IC_{50}) compared with that of citrus peel mushroom extracts (0.6 mg/mL IC_{50}), which exhibited superoxide scavenging activity using the NBT dye reduction assay (Figure 2).



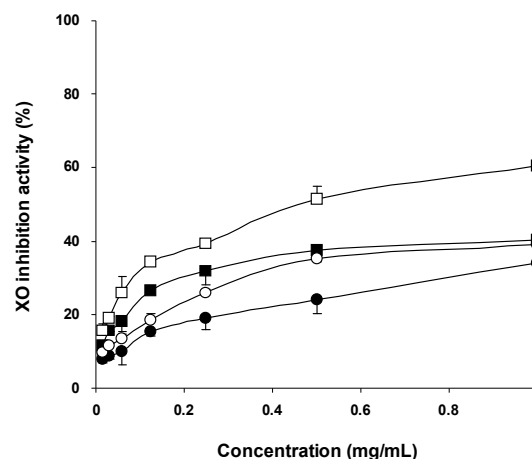
Sample	Citrus peel substrate	Premature Hallabong substrate	Citrus peel mushroom	Premature Hallabong mushroom
IC_{50} (mg/mL)	0.8±0.02 ^a	0.4±0.08 ^b	0.6±0.03 ^c	0.4±0.02 ^b

Fig. 2. Superoxide radical scavenging activity of citrus peel substrate (●), premature Hallabong substrate (■) and the extracts of *Grifola frondosa* mycelia cultivated on citrus peel substrate (○) and premature Hallabong substrate (□). Values are means ± S.D. of three separated experiments. ^{a-c}Values with different superscripts in a row are significantly different ($p < 0.05$).

When this method is used, the effect of the extract on the XO activity must be checked, because an inhibitory effect on the enzyme itself would also lead to a decrease of NBT reduction (Halliwell et al., 1995). In this regard, we evaluated the effect of *Grifola frondosa* mycelial extracts cultivated on citrus waste substrates on the XO activity by the metabolic conversion of xanthine to uric acid (Figure 3).

Addition of the extracts from all mushrooms and substrates to the reaction mixture (from 0.125 to 2.0 mg/mL) resulted in a dose-

dependent inhibition. The premature Hallabong mushroom extracts (0.6 mg/mL IC_{50}) showed a statistically higher XO inhibition activity than that of citrus peel mushroom extracts (1.2 mg/mL IC_{50}) ($p < 0.05$) (Figure 3). All the extracts from mushroom using citrus peel and premature Hallabong as substrate showed significantly higher ($p < 0.05$) activities in XO inhibition than those of their substrates (Figure 3). Mau et al. (2001) found that the metabolic extracts from mycelia of *Grifola frondosa* cultivated on the sawdust exhibited an IC_{50} values of 3.63, 3.67 and 3.49 mg/mL for antioxidant activity, reducing powder and chelating effect on ferrous ions, respectively, whereas no scavenging effect on hydroxyl radicals. All IC_{50} values in our study were below 1 mg/mL, indicating that utilization of citrus wastes as substrate enhanced antioxidant activity achieved by the scavenging of DPPH radical, superoxide radical, and XO inhibition, possibly because of the correlation between antioxidant activity and the content of total phenolics as mentioned above (Table 1).



Sample	Citrus peel substrate	Premature Hallabong substrate	Citrus peel mushroom	Premature Hallabong mushroom
IC_{50} (mg/mL)	1.5±0.14 ^a	1.1±0.11 ^a	1.2±0.06 ^b	0.6±0.04 ^c

Fig. 3. XOD inhibition activity of citrus peel substrate (●), premature Hallabong substrate (■) and the extracts of *Grifola frondosa* mycelia cultivated on citrus peel substrate (○) and premature Hallabong substrate (□). Values are means ± S.D. of three separated experiments. ^{a-c}Values with different superscripts in a row are significantly different ($p < 0.05$).

Previous studies demonstrated that the polysaccharide extracted from *Grifola frondosa* strongly enhances anticancer effect, suggesting that some component of *Grifola frondosa* extract may represent potential cancer chemopreventive substances (Adachi et al., 1987; Hishida et al., 1988; Nanba, 1995; Fullerton et al., 2000; Shi et al., 2007; Shomori et al., 2009). Fullerton et al. (2000) reported that a bioactive β -glucan from *Grifola frondosa* has a cytotoxic effect, through oxidative stress, on prostatic cancer PC-3 cells, leading to apoptosis. Furthermore, both water-insoluble polysaccharide and water-soluble extract from *Grifola frondosa* inhibited the proliferation of human gastric cancer cell lines (SGC-7901, TMK-1, MKN28, MKN45 and MKN74) (Shi et al., 2007; Shomori et al., 2009). However, there are few reports on the effects of *Grifola frondosa* extract on human cancer cell lines. Thus, it is necessary to perform the cell viability assay with *Grifola frondosa* extracts to investigate their antiproliferative effects in other types of cancer cells.

In the present study, colon cancer cells (HT-29) were treated with various concentrations (0-1 mg/mL) of extracts of mushrooms cultivated on citrus waste and their substrates separately for 24 h, and then analyzed by MTT cell viability assay for the cell viability, proliferation (% control), as shown in Figure 4A.

The formazan product of MTT assay was analyzed for quantification of the viability of cells. The extracts of all mushrooms and their substrates were found to exhibit significantly growth inhibitory effect in HT-29 cells, and premature Hallabong mushroom exhibited the most significant antiproliferative effect in HT-29 cells: it led to a maximum decrease of 41% at 1 mg/mL (Figure 4A). The antiproliferative effects of the mushrooms cultivated on citrus waste and their substrates in breast cancer MCF-7 cells were also investigated (Figure 4B). The number of viable cells slightly decreased after treatment with extracts of all mushrooms and their substrates. Premature Hallabong mushroom showed the most antiproliferative effect in MCF-7 cells, and their cell viability decreased by 27% at 1 mg/mL (Figure 4B). Based on the results obtained, the extracts of mushroom cultivated on citrus waste were effective in inhibiting colon (HT-29) and breast (MCF-7) cancer cell proliferations.

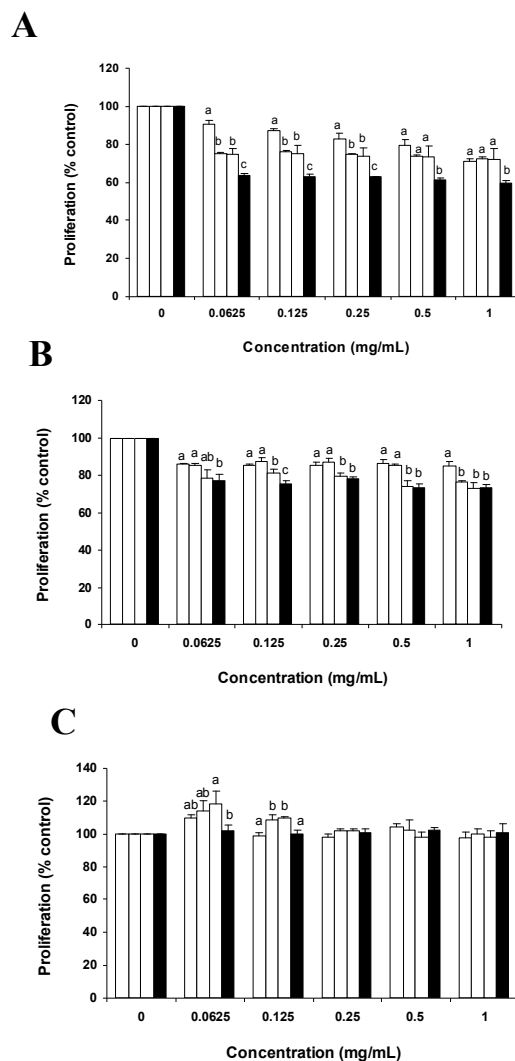


Fig. 4. Cell viability of human colon HT-29 cancer cells (A), breast MCF-7 cancer cells (B) and fibroblast HS-68 cells (C). Symbols: □, citrus peel; ▨, premature Hallabong; ▩, *Grifola frondosa* mycelial extract cultivated on citrus peel; ■, *Grifola frondosa* mycelial extract cultivated on premature Hallabong. Values are expressed as percentages compared to the baseline (0 mg/mL) value in the control (cells without treatment with any samples, considered to be 100%). Values are means \pm S.D. of three separated experiments. ^{a-c}Mean values not sharing the same letter above the bars are significantly different at $p < 0.05$ by one-way analyses of variance followed by Duncan's multiple range tests.

For the development of anticancer agents from natural products, it is important not only to screen the selectivity (or specificity) of the natural products among several cancer cells but also to assay if natural products exhibited any cytotoxicity in non-

cancer cells. Thus, the effect of extracts of mushrooms cultivated on citrus waste and their substrates on non-cancer cells (human fibroblast HS-68 cells) was tested. The HS-68 cells did not exhibit cytotoxic effect with any extract, indicating the potential specificity of the mushroom extracts against target cancer cells (Figure 4C).

In conclusion, citrus waste can be utilized as a practical substrate to improve the antioxidant and anticancer activities as well as to increase total phenolic content of *Grifola frondosa* and it, therefore, may be developed as natural antioxidant for food industry and other fields.

Corresponding Author:

Dr. Min Young Kim
Faculty of Biotechnology
College of Applied Life Sciences
Jeju National University
Jeju 690-756, Republic of Korea
E-mail: jeffmkim@jejunu.ac.kr

References

1. Abeyasingha DC, Lia X, Suna CD, Zhanga WS, Zhoua CH, Chen KS. Bioactive compounds and antioxidant capacities in different edible tissues of citrus fruit of four species. *Food Chemistry* 2007; 104: 1338-44.
2. Adachi K, Nanba H, Kuroda H. Potentiation of host-mediated antitumor activity in mice by beta-glucan obtained from *Grifola frondosa* (maitake). *Chemical and Pharmaceutical Bulletin* 1987; 35: 262-70.
3. Archana B, Dasgupta N. In vitro study of antioxidant activity of *Syzygium cumini* fruit. *Food Chemistry* 2005; 90: 727-33.
4. Borchers AT, Keen CL, Gershwin ME. Mushrooms, tumors, and immunity: an update. *Experimental Biology and Medicine* 2004; 229: 393-406.
5. Cavin A, Hostettmann K, Dyatmyko W, Potterat O. Antioxidant and lipophilic constituents of *Tinospora crispa*. *Planta Medica* 1998; 64: 393-96.
6. Chang WS, Lin CC, Chuang SC, Chiang HC. Superoxide anion scavenging effect of coumarins. *The American Journal of Chinese Medicine* 1996; 24: 11-7.
7. Chen HB, Huang HC, Chen CI, I YP, Liu YC. The use of additives as the stimulator on mycelial biomass and exopolysaccharide productions in submerged culture of *Grifola umbellata*. *Bioprocess Biosystem Engineering* 2010; 33: 401-6.
8. Chiu SW, Law SC, Ching ML, Cheung KW, Chen MJ. Themes for mushroom exploitation in the 21st century: Sustainability, waste management, and conservation. *The Journal of General and Applied Microbiology* 2000; 46: 269-82.
9. Choi SY, Ko HC, Ko SY, Hwang JH, Park JG, Kang SH, Han SH, Yun SH, Kim SJ. Correlation between flavonoid content and the NO production inhibitory activity of peel extracts from various citrus fruits. *Biological and Pharmaceutical Bulletin* 2007; 30: 772-8.
10. Fullerton SA, Samadi AA, Tortorelis DG, Choudhury MS, Mallouh C, Tazaki H, Konno S. Induction of apoptosis in human prostatic cancer cells with beta-glucan (Maitake mushroom polysaccharide). *Molecular Urology* 2000; 4: 7-13.
11. Furuno K, Akasako T, Sugihara N. The contribution of the pyrogallol moiety to the superoxide radical scavenging activity of flavonoids. *Biological and Pharmaceutical Bulletin* 2002; 25: 19-23.
12. Garibay-Orijel R, Caballero J, Estrada-Torres A, Cifuentes J. Understanding cultural significance, the edible mushrooms case. *Journal of Ethnobiology and Ethnomedicine* 2007; 3: 4.
13. Gregori A, Svagelj M, Berovic M, Liu Y, Zhang J, Pohleven F, Klinar D. Cultivation and bioactivity assessment of *Grifola frondosa* fruiting bodies on olive oil press cakes substrates. *New Biotechnology* 2009; 26: 260-62.
14. Halliwell B, Aeschbach R, Loliger J, Aruoma OI. The characterization of antioxidants. *Food Chemical Toxicology* 1995; 33: 601-17.
15. Heim KE, Tagliaferro AR, Bobilya DJ. Flavonoid antioxidants: chemistry, metabolism and structure-activity relationships. *The Journal of Nutritional Biochemistry* 2002; 13: 572-84.
16. Hishida I, Nanba H, Kuroda H. Antitumor activity exhibited by orally administered extract from fruit body of *Grifola frondosa* (maitake). *Chemical and Pharmaceutical Bulletin* 1988; 36: 1819-27.
17. Huang D, Ou B, Prior RL. The chemistry behind antioxidant capacity assays. *Journal of Agricultural and Food Chemistry* 2005; 53: 1841-56.
18. Kanaze FI, Gabrieli C, Kokkalou E, Georgarakis M, Niopas I. Simultaneous reversed-phase high-performance liquid chromatographic method for the

- determination of diosmin, hesperidin and naringin in different citrus fruit juices and pharmaceutical formulations. *Journal of Pharmaceutical and Biomedical Analysis* 2003; 33: 243-9.
19. Lee JS, Park BC, Ko YJ, Choi MK, Choi HG, Yong CS, Lee JS, Kim JA. *Grifola frondosa* (maitake mushroom) water extract inhibits vascular endothelial growth factor-induced angiogenesis through inhibition of reactive oxygen species and extracellular signal-regulated kinase phosphorylation. *Journal of Medicinal Food* 2008; 11: 643-51.
 20. Lee JS, Park SY, Thapa D, Choi MK, Chung IM, Park YJ, Yong CS, Choi HG, Kim JA. *Grifola frondosa* water extract alleviates intestinal inflammation by suppressing TNF- α production and its signaling. *Experimental and Molecular Medicine* 2010a; 42: 143-54.
 21. Masuda Y, Inoue M, Miyata A, Mizuno S, Nanba H. Maitake beta-glucan enhances therapeutic effect and reduces myelosuppression and nephrotoxicity of cisplatin in mice. *International Immunopharmacology* 2009; 9: 620-6.
 22. Mau JL, Chang CN, Huang SJ, Chen CC. Antioxidant properties of methanolic extracts from *Grifola frondosa*, *Morchella esculena* and *Ternitomyces albuminosus* mycelia. *Food Chemistry* 2004; 87: 111-8.
 23. Mau JL, Lin HC, Song SF. Antioxidant properties of several specialty mushrooms. *Food Research International* 2002; 35: 519-26.
 24. Nanba H. Activity of maitake D-fraction to inhibit carcinogenesis and metastasis. *Annals of the New York Academy of Sciences* 1995; 768: 243-245.
 25. Nguyen MT, Awale S, Tezuka Y, Tran QL, Watanabe H, Kadota S. Xanthine oxidase inhibitory activity of Vietnamese medicinal plants. *Biological and Pharmaceutical Bulletin* 2004; 27: 1414-21.
 26. Parr AJ, Bolwell GP. Phenols in the plant and in man. The potential for possible nutritional enhancement of the diet by modifying the phenols content or profile. *Journal of the Science of Food and Agriculture* 2000; 80: 985-1012.
 27. Rauha JP, Remes S, Heinonen M, Hopia A, Kahkonen M, Kujala T, Pihlaja K, Vuorela H, Vuorela P. Antimicrobial effects of Finnish plant extracts containing flavonoids and other phenolic compounds. *International Journal of Food Microbiology* 2000; 56: 3-12.
 28. Robbins RJ. Phenolic acids in foods: an overview of analytical methodology. *Journal of Agricultural and Food Chemistry* 2003; 51: 2866-87.
 29. Sanchez C. Cultivation of *Pleurotus ostreatus* and other edible mushrooms. *Applied Microbiology and Biotechnology* 2010; 85: 1321-37.
 30. Shi BJ, Nie XH, Chen LZ, Liu YL, Tao WY. Anticancer activities of a chemically sulfated polysaccharide obtained from *Grifola frondosa* and its combination with 5-Fluorouracil against human gastric carcinoma cells. *Carbohydrate Polymers* 2007; 68: 687-92.
 31. Shomori K, Yamamoto M, Arifuku I, Teramachi K, Ito H. Antitumor effects of a water-soluble extract from Maitake (*Grifola frondosa*) on human gastric cancer cell lines. *Oncology Reports* 2009; 22: 615-20.
 32. Slater TF. Free-radical mechanisms in tissue injury. *The Biochemical Journal* 1984; 222: 1-15.
 33. Terol J, Soler G, Talon M, Cercos M. The aconitate hydratase family from *Citrus*. *BMC Plant Biology* 2010; 10: 222.
 34. Xiaoke X, Shunxing G. Morphological characteristics of sclerotia formed from hyphae of *Grifola umbellata* under artificial conditions. *Mycopathologia* 2005; 159: 583-90.
 35. Zhang SJ, Lin YM, Zhou HC, Wei SD, Lin GH, Ye GF. Antioxidant tannins from stem bark and fine root of *Casuarina equisetifolia*. *Molecules* 2010; 15: 5658-70.
 36. Zhong JJ, Tang YJ. Submerged cultivation of medicinal mushrooms for production of valuable bioactive metabolites. *Advances in Biochemical Engineering/Biotechnology* 2004; 87: 25-59.
 37. Zhu YZ, Huang SH, Tan BK, Sun J, Whiteman M, Zhu YC. Antioxidants in Chinese herbal medicines: a biochemical perspective. *Natural Product Reports* 2004; 21: 478-89.

9/2/2011

The Impact of Explicit Teacher Feedback on Micro and Macro Level Features of the Performance of the EFL Students in Descriptive Writing

Afshin Soori¹, Arshad Abd. Samad², Kamariah Abu Bakar³

¹. Department of Foreign languages, Shiraz Branch, Islamic Azad University, Shiraz, Iran

². Associate Professor, Department of Language and Humanities Education, Faculty of Educational Studies, Universiti Putra Malaysia, UPM Serdang, Selangor D.E. Malaysia

³. Professor, Department of Language and Humanities Education, Faculty of Educational Studies, Universiti Putra Malaysia, UPM Serdang, Selangor D.E. Malaysia

Arshad@educ.upm.edu.my

Abstract: Teacher feedback is an essential aspect of any English language writing course. This is especially true now with the predominance of the process approach to writing that requires some kind of second party feedback, usually the instructor, on student drafts. Kroll describes feedback as one of the two components most central to any writing course with the other being assignments the students is given. Although teacher feedback seems an ideal one and most preferred by many students in second language instruction, its fruitfulness in developing students' writing is not so crystal clear. Moreover, many unanswered questions remain regarding micro and macro level features which have not been adequately attended by researchers. It seems the answers to these questions are not convincing, and there is a gap in this area. So, to fill the gap an investigation should be conducted to inform of whether this leads to improving the students' overall writing quality.

[Afshin Soori, Arshad Abd. Samad, Kamariah Abu Bakar. The Impact of Explicit Teacher Feedback on Micro and Macro Level Features of the Performance of the EFL Students in Descriptive Writing. Life Science Journal. 2011;8(3):572-576] (ISSN:1097-8135). <http://www.lifesciencesite.com>.

Keywords: Explicit teacher feedback; Micro level features; Macro level features

1. Introduction

Writing is a basic communication skill and a unique asset in the process of learning and teaching a second or a foreign language. Producing a successful written text is a task which requires simultaneous control over a number of language systems. Many scholars believe that teaching writing should be in a way that stimulates student output and only then should generate teacher response and conferencing (Raimes 1991, 1998; Reid, 1993).

Writing is the art of creating ideas and thoughts. So, writers are creators of words that convey meaning and through these words they communicate with the readers. Composing involves a series of decisions and choices that writers organize during the act of writing. Teaching ESL/EFL students to become successful writers is an especially complex task. But it can be a tremendously rewarding one as well.

During the last few decades researchers have delved deeper into the process of writing. This process includes several stages of composition development. While in the planning or prewriting stage, writers generate ideas and organization, they put these ideas into some rough order in writing stage. Then, during the revision stage, they hone organization and expression. Finally, during the editing stage, they correct surface errors like spelling, punctuation, and usage.

2. Developments in ESL composition instruction

Prior to considering the research compiled on the effects of feedback on students' compositions, it is essential to explore the development of approaches to teaching writing in ESL composition theories. The evolution of ESL composition theories and approaches has been discussed by Silva (1990). He mentions four major approaches as, Controlled Composition Approach, Current-traditional Rhetorical Approach, Process Approach, and Task-based Approach.

While the Controlled Composition Model primarily focused on formal accuracy and correctness and emphasized rigidly controlled programs of systematic habit formation to avoid errors, Current-traditional Rhetoric emphasized on the compared product rather than the composing process. The dissatisfaction with the "linearity and prescriptivism" of the first two approaches has brought the conception of the process approach. This approach, as the name suggests, focuses on the processes involved in composition writing, such as pre-writing, drafting, revising, and editing, to provide students with an efficient and effective composing process. The process-centred approach to writing assumes that students learn to write best using multiple drafts rather than just one final product (Bellah, 1995). Many composition faculties advocate multiple draft

assignments that build upon one another in order to promote student learning. Process approach was also criticized by advocates of English for Academic Purposes (EAP). Horwitz (in Dyer, 1996) suggests a task-based approach that merges process and product in the concept of communicative task.

3. Nature of Writing

The process/product debate continues in the field of writing instruction: should teachers focus on the writing process in the classroom or emphasize the importance of a correct final product in student writing? The process approach looks at writing from a new angle; it is completely different from previous approaches in writing. To Kroll (1990), this approach provides a positive, encouraging, and collaborative environment within which students, with sufficient time and less interference, can work through their composing processes. In process-based approach, writing is considered as a “non-linear, exploratory, and generative process whereby writers discover and reformulate their ideas as they attempt to approximate reason. Unlike the product-based approach, this approach focused on the writer’s need for guidance and intervention throughout the writing process, rather than on controlling lexical, syntactical, and organizational patterns. The process-based approach to writing instruction attempts to avoid the perhaps premature imposition of these patterns and instead adopts the notion that content, ideas, and the need to communicate would determine form (Silva,1990). According to expressivists, like Elbow, Murray, Macrorie, William Coles, and Emig, providing writer-students with linguistic feedback and correction is regarded as an interfering deleterious factor in the delicate process of their creative thinking and free-writing. They advocated classroom techniques that encourage students to take power in their own prose. (Kroll 1990). On the other hand, although cognitivists, like Zamel, Spack, Raimes, Kraples, and Fried Lander make any possible attempt to minimize interference of the writing teacher in the productive cognitive process of their students’ writing, they hold that besides teachers’ feedback on the macro level features of their students’ pieces, feedback on their micro level features also seems to be necessary.

4. The Importance of Feedback

Generally speaking, the philosophy of teaching is fostering students’ learning with helpful writing instruction and giving effective feedback is a central concern for any teacher of writing and an important area for both L1 and L2 writing research. However, one major issue that has obsessed the scholars’ minds is how to provide the students with

fruitful feedback that best contributes to students’ improvement in writing capabilities. So, teachers are required to provide the students with feedback that facilitates student mastery of writing. The purpose of giving feedback is to teach skills that assist students to improve their writing skills to the extent that the students are “cognizant of what is expected of them as writers and are able to produce it with minimal errors and maximum clarity.”(Williams, 2003, p.1) It remains no easy answer to the question of what kind of feedback the teacher should give the students. However, teachers should focus on implementing types of feedback that make students maximize utilizing the previous prior feedback on subsequent writing occasions.

5. Explicit teacher Feedback

Among the various types of teacher feedback, explicit teacher feedback is the main concern of this study. Direct or explicit feedback occurs when the teacher identifies an error and provides the correct form that seems more preferred by teachers and students (Ferris & Roberts, 2001; Ferris, Cheyney, Komura, Roberts, & McKee, 2000; Hadley, 2001; Komura, 1999; Rennie, 2000; Roberts, 1999). In direct feedback errors can not be tolerated and should be removed directly (Hadley, 2001).

Celce Murcia (2001) points out to the Lyster (1997) that provided the Canadian students with numerous feedback in immersion classrooms frequently in the middle of content-based exchanges. Their findings revealed that explicit correction and negotiated feedback had a positive value that “uptake” of correct grammatical forms occurred following such feedbacks.

6. Micro Level and Macro Level Features

In the present study the researcher concerns two aspects of writing as micro and macro level features. While at the micro level the emphasis is on the specific written forms at the level of word or sentence such as, grammatical conventions, spelling and punctuation, macro level features emphasize content inclusion, coherence like sequencing of ideas and linking, and organization (Ur, 1996). Unlike the previous research, this study focuses on micro and macro level features simultaneously. But the researcher tries to investigate the degree of impact of explicit teacher feedback on these two features. In fact, it will be carried out by considering the empirical data that will reveal the degree of improvement in writing skill over a course semester.

To sum up, methods of explicit teacher feedback as overt correction of errors, or marking errors, at both micro and macro levels will all be identified in this study to recognize whether explicit

teacher feedback has positive effects more on micro or macro level features by considering the number of errors in a number of writing tasks, the scores the students gain on the final product, and both quality and quantity of their writing including correctness at the end of the semester. In other words, the results of this study will reveal to what extent the students apply explicit teacher feedback more to the micro or macro level features of their writing.

7. Modes of writing in terms of purpose

In the past it was common to categorize writing with regards to its product. For instance, it was possible to find writing classes entitled “Letter Writing” or “Essay Writing” since the final outcome and the product was the main focus; however, today there is more emphasis on the process of writing and as a result students are motivated to concentrate on the purpose for which they write. To recognize the purposes in writing, it is necessary to review the modes of writing. Richards & Schmidt (2002) point out to different forms of writing and classified them into four types as: descriptive, narrative, expository, and argumentative writing. But among these modes of writing, description is the basic form of writing. At first look, it seems simple for academic discourse. But it is the opinion of those who did not write. Description is not simple, but it is “fundamental and the best way to lay the foundation of the writer’s craft.” (Murray; 1999, p.245). All types of writing encompass some elements of descriptive writing that cause a reader see, think, feel, and react. (Murray, 1999). Therefore, each mode of writing activates different types of processes in the mind of the writer and follows different procedures.

8. Discussions

8.1. Feedback on Writing: Micro Level versus Macro Level Features

There is an argument over teacher feedback on micro and macro level features. In contrast to Truscott (1996), who claimed grammar correction has no place in writing courses and should be abandoned, most researchers agree that attention must be paid to both micro and macro level features (Loewen, 2002; Skehan, 1988). What there is no agreement on is the degree of effect each has on improving students’ writing. Among numerous scholars, some recommend that teachers should emphasize macro level features and believe that micro level features should be focused on after ideas have been fully developed. (Elbow and Belanoff, 2000; Raimes, 1993; Sheppard, 1992; Truscott, 1999). But recent studies claim that except content, grammatical accuracy should be considered, because the lack of grammatical accuracy may prevent

students’ progress in university. (Ferris, 1995; Santos, 1988; Vann, Lorenz, & Meyer, 1991; Vann, Meyer, & Lorenz, 1984). But Ferris (2004) contends that it is far from complete to draw such conclusions. There remain many unanswered questions regarding micro and macro level features. The majority of the previous studies have investigated the impact of teacher feedback on grammar and content of ESL students’ writing, but they have revealed very little evidence of improvement in overall quality of the performance of EFL student writing. In other words, it is the time to look at the final product of the research on the effect of explicit teacher feedback on micro and macro level features and its impact on the improving the students’ writing abilities.

8.2. Benefits

Among the different skills, writing is an inseparable part of any language learning process. (Chastain, 1988; Rivers, 1981) Writing ability is the art of producing thought and ideas and inability in writing causes many problems for learners to do many different writing tasks in a second or a foreign language. Academic, educational, business, research tasks are just a few major ones. Poor writing ability is a main concern among the students. Here, teachers are responsible for assisting students to cope with problems. This investigation can shed light on how to provide effective feedback on students’ composition. In this case we may get some steps closer to finding a remedy for poor writing ability to contribute our students and meet their needs and to improve in writing ability. The outcomes of this investigation will have pedagogical implications and course developers will use them for material preparation for writing classrooms. Test designers will use the results as well. They recognize which aspect of writing they should consider more to focus in testing writing skills. The findings of this investigation will also indicate that whether the explicit teacher feedback is effective in improving the students’ writing abilities, and to what extent the teachers should provide the students’ writing with explicit teacher feedback. Finally, it will cater a new experience for language teachers to contribute their students to learn the writing skills in a faster and easier way.

Acknowledgements:

The authors would like to acknowledge Dr. Zahedi (the chancellor of Islamic Azad University, Larestan branch), and Dr. Mehrdad Jalalian (Universiti Putra Malaysia) for their support and contribution to this study.

Corresponding Author:

Prof. Dr. Arshad Samad

Department of Language and Humanities Education,
Faculty of Educational Studies, Universiti Putra
Malaysia, UPM Serdang, Selangor D.E. Malaysia
E-mail: Arshad@educ.upm.edu.my

References

- Bellah, M. (1995). *New Frontiers: Teacher comments, intervention, and the new rhetoric. Rhetorical invention and post-modern writing instruction.* Retrieved from <http://english.ttu.edu/courses/536/book/bellah.htm>.
- Celce-Murcia, M. (2001). *Teaching English as a Second or Foreign Language.* Heinle & Heinle, a division of Thomson Learning, Inc.
- Chastain, K. (1988). *Developing Second Language Skills: Theory and Practice.* 3rd ed. Orlando, Florida: Harcourt Brace Jovanovich.
- Dyer, B. (1996). L1 and L2 composition theories: Hillocks 'environmental mode' and task-based language teaching. *ELT Journal*, 50/4:312-317.
- Elbow, P. & Belanoff, P. (2000). *A Community of Writers: A workshop course in Writing.* McGraw-Hill Higher Education.
- Ferris, D.R. (1995). Students reactions to teacher response in multiple-draft composition classrooms. *TESOL Quarterly*, 29, 33,-53.
- Ferris, D.R., (2004). The "Grammar Correction" Debate in L2 Writing: Where are we, and where do we go from here. *Journal of Second Language Writing*, 13, 1, 49-62.
- Ferris, D.R. Chaney, S.J., Komura, K. Roberts, B.J., & McKee, S. (2000). Perspectives, problems, and practices in treating written error. In Colloquium presented at International TESOL Convention, B.C., March 14-18, 2000.
- Ferris, D. and Roberts, B., (2001). Error feedback in L2 writing classes: How explicit does it need to be? *Journal of Second Language Writing* 10, pp. 161-184.
- Hyland, F. (1998). The impact of teacher written feedback on individual writers. *Journal of Second Language Writing*, 7(3), 255-286.
- Hadley, A.O., (2001). *Teaching Language in Context.* Heinle & Heinle, a division of Thomson Learning, Inc.
- Komura, K. (1999). Student response to error correction in ESL classrooms. Unpublished Master's thesis California State University, Sacramento.
- Kroll, B. (1990). *Second Language Writing: Cambridge, England and New York: Cambridge University Press.*
- Kroll, B. (2001). Considerations for teaching an ESL/EFL writing course. In M. Celce Murcia (Ed.), *Teaching English as a Second or Foreign Language* (3rd ed.) (pp.219-232). Boston, MA: Heinle and Heinle.
- Loewen, S. (2002). The occurrence and effectiveness of incidental focus on form. Unpublished doctoral thesis, University of Auckland.
- Lyster, R. (1997). Recasts, repetition, and ambiguity in L2 classroom discourse. *Studies in Second Language Acquisition* 20, 51-81.
- Murray, D.M. (1999). *Write to Learn.* Harcourt Brace College Publishers.
- Raimes, A. (1991). Out of the Woods: Emerging Traditions in the Teaching of Writing. *TESOL Quarterly*, 25, 407-30.
- Reid, J. (1993). *Teaching ESL Writing.* Englewood Cliffs, NJ: Regents Prentice Hall.
- Rennie, C. (2000). Error Feedback in ESL Writing Classes: What do students really want? Master's thesis, California State University, Sacramento.
- Richards, J.C. & Schmidt, R. (2002). *Longman Dictionary of Language Teaching & Applied Linguistics.* Pearson Education Limited.
- Rivers, W.M. (1981). *Teaching Foreign Language Skills.* Chicago: The University of Chicago Press.
- Roberts, B. J. (1999). Can error logs and grammar feedback on ESL students' final drafts. Master thesis, California State University, Sacramento.
- Santos, T. (1988). Professors' reactions to the academic of writing of non-native-speaking students. *TESOL Quarterly* 22(1), 69-90.
- Sheppard, K. (1992). Two feedback types: do they make a difference? *RELC Journal* Vol. 23 (1) 103-109.
- Silva, T. (1990). Second language composition instruction: Developments, issues and directions in ESL. In B. Kroll (Ed.), *Second Writing: Research insights for the classroom* (pp. 11-23). New York: Cambridge University Press.
- Skehan, P. (1988). A Cognitive Approach to Language Learning. *System* 17: 223-234.
- Truscott, J. (1996). The case against grammar correction in L2 writing classes. *Language Learning*, 46, 327-369.
- Truscott, J., (1999). "The case for grammar correction in L2 writing classes": A response to Ferris. *Journal of Second Language Writing* 8, 111-122.
- Ur, P. (1996). *A Course in Language Teaching: Practice and theory.* Cambridge University Press.
- Vann, R. J., Lorenz, F. O., & Meyer, D. M. (1991). Error gravity: Faculty response to errors in the written discourse of nonnative speakers of

- English. In L. Hamp-Lyons (Ed.), *Assessing Second Language in Academic Contexts* (pp. 181-195).
32. Vann, R. J., Meyer, D.E., & Lorenz, F. O. (1984). Error gravity: A study of faculty opinions of ESL errors. *TESOL Quarterly*, 18, 427-440.
33. Williams, J. C. (2003). Providing Feedback on ESL Students' Written Assignments. *The Internet TESL Journal*, IX, 10. [http:// iteslj.org](http://iteslj.org)..

5/5/2011

Interleukin-4 Polymorphism in Egyptian Patients with Type-2 Diabetic Nephropathy

Mohamed M. El-Shabrawi¹, Nervana M. K. Bayoumy² and Hamdi H. Hassan³

¹Clinical and Chemical Pathology Department, Faculty of Medicine, Suez Canal University, Egypt

²Physiology Department, College of Medicine, King Saud University Saudi Arabian

³Internal Medicine Department, Faculty of Medicine, Suez Canal University, Egypt
zeinash2003@yahoo.com

Abstract: The effects of environmental and genetic factors on the development of diabetic complications are well-documented. The roles of inflammatory processes on the development of these complications including diabetic nephropathy were established. Cytokines have great roles in the development of diabetic nephropathy. Polymorphism in the 590-region of interleukin-4 gene is associated with the regulation of expression of this gene. During these investigations, peripheral blood was collected from 100 patients with type-2 diabetes mellitus with nephropathy and 100 diabetics without nephropathy (control). DNA was extracted and a polymerase chain reaction restricted fragment length polymorphism (PCR-RFLP) technique was performed to examine polymorphisms in the -590 region of the IL-4 gene. Obtained results revealed that the frequency of allele T was higher among patients with diabetic nephropathy than among the control. In addition, most of patients with allele T had overt albuminuria, higher blood pressure, renal dysfunction and dyslipidemia than patients with allele C. In conclusion, these findings suggest that patients with allele T are more liable to develop diabetic nephropathy with most of the micro- and macro-vascular complications.

[Mohamed M. El-Shabrawi, Nervana M. K. Bayoumy and Hamdi H. Hassan **Interleukin-4 Polymorphism in Egyptian Patients with Type-2 Diabetic Nephropathy**] Life Science Journal, 2011; 8(3):577-582] (ISSN: 1097-8135). <http://www.lifesciencesite.com>.

Keywords: Interleukin-4, Diabetic nephropathy, Polymorphism.

Introduction

Diabetes mellitus is one of the complex diseases that are increasing globally. Type-2 DM is the most common type (Ahluwalia *et al*, 2009). Several environmental and genetic factors had been incriminated in its pathogenesis and its complication (Kang *et al*, 2008). It has been suggested that DM is an immune-mediated disease, in which the expression of several cytokines are changed (Cruz *et al*, 2008; Yih-Hsin *et al*, 2009).

Cytokines and cytokine receptor axis (Kang *et al*, 2008) are the subject of several recent studies for their roles in the pathogenesis of DM as well as their role in the pathogenesis of its complications (Ahima, 2009; Hyum *et al*, 2009). Increase in the serum level of several cytokines such as interleukin (IL) 18, IL-6, IL-12, IL-17 and tumor necrosis factor α were documented in patients with type-2 DM and its nephropathic complications (Ahluwalia *et al*, 2009).

Interleukin 4 is secreted by T helper 2 (Th2) cells. Important roles have been identified for IL-4 in the context of the immune response (Feve *et al*, 2009). It stimulates the development of Th2 lymphocytes by acting upon the undifferentiated T cells after exposure to antigens, it induces the shift from IgM and IgG towards IgE production by plasmocytes, and it determines the secretion of the whole Th2 cytokine spectrum. In addition, it has an inhibitory effect upon interferon (IFN) secretion and the differentiation of Th2 lymphocytes (Dinarello *et al*, 2010; Enriquez *et al*, 2010).

The association of IL-4 with immunological disorders such as multiple sclerosis, systemic lupus erythematosus (SLE), nephrotic syndrome, graft rejection, asthma, and type-1 and 2 DM is well established (Colin, 2003). The key roles of IL-4 as an inhibitory cytokine of autoimmunity and inflammations raise questions concerning the impacts of this cytokine on the pathogenesis of some diseases including nephropathic type 2 DM (Elbe-Burger, 2002; Arabadadi *et al*, 2010).

In hypercholesterolemia, the accumulated low density lipoproteins (LDL) in the arterial wall would be oxidized to release oxidation products that lead to activation of inflammatory responses (Cornicelli *et al*, 2000). In mice model, severe hypercholesterolemia is associated with a switch to Th2 immune response, with increased IL-4 expression in the atherosclerotic lesions (Feve *et al*, 2009; Yuxia *et al*, 2011). IL-4 mRNA can also be detected in atherosclerotic lesions in human body. The micro-environmental IL-4 in the atherosclerotic lesions has multiple effects on atherogenesis, such as augmentation of LDL cholesterol esterification by a concentration- and time- dependent manner. In addition, IL-4 can regulate the expression of 15-lipoxygenase (15-LO), a key enzyme in LDL oxidation (Jingfang *et al*, 2010).

It had been demonstrated that the adipocyte layer in the dermis is reduced in IL-4 transgenic mice. Accordingly, local micro-environmental expression of IL-4 is suggested to be involved in the atherogenic process (Hyun *et al*, 2009).

IL-4R α is a crucial component for binding and signal transduction of IL-4. It is reasonable that polymorphisms located in IL-4R α , which alter the binding affinity to IL-4 or downstream signaling pathways and thus contribute to the fine tune of IL-4 responsive phenotypes, would also be linked to disease development (Dinarello *et al*, 2010; Hyun *et al*, 2009). Several studies have reported that genetic polymorphisms of IL-4 and IL-4R α are associated with genetic predisposition to diseases, possibly through their influences on the activity of these genes or their products (Dinarello, 2011).

Although the initiation and etiology of T2DM still await identification, accumulating evidences have proved the hypothesis that DM type 2 is a state of chronic inflammation, with increased acute phase proteins and various cytokines (Ming-Yuh *et al*, 2009). Genetic studies exploring susceptible or resistant genes for T2DM could provide clues for understanding the mystery of diabetic pathogenesis and for future design of diabetic treatment (Brown, 2010).

It seems likely that the risk for diabetes-associated kidney disease is magnified by inheriting risk alleles at several susceptibility loci (Hyun *et al*, 2009). Genome-wide linkage studies have recently identified several chromosomal regions that likely contain diabetic nephropathy susceptibility genes. Previous studies had documented two polymorphisms affected gene for IL-4. One of these polymorphisms is a single nucleotide polymorphism (SNP) at region -590 in the promoter region (Mohammad, 2010).

Secretion of IL-4 can be affected by its polymorphisms in -590 region (Mohammad, 2010). This study was done aiming at studying the polymorphism of this gene at 590-region in patients with type-2 diabetic nephropathy.

2. Materials and Methods

Patients' selection:

Type 2 diabetic patients with albuminuria attending Suez Canal University hospital. 100 patients were selected up-on the following criteria as well as 100 patients as control (diabetics without nephropathy). All patients had established Diabetic Nephropathy—defined as persistent albuminuria (>300 mg/24 h or >200 μ g/min or >200 mg/L) in two of three consecutive measurements on sterile urine samples—with or without renal failure.

Patients were excluded from the study if having Reno-vascular and/or uncontrolled Hypertension, congestive heart failure, chronic kidney disease, urinary tract infection, haematuria and acute febrile illness. Also, patients with other diabetic complications other than nephropathy such as retinopathy were also excluded.

All patients underwent detailed clinical and biochemical evaluation: duration of Diabetes, overt albuminurea, renal insufficiency and hypertension.

Blood urea, serum creatinine, blood sugar fasting and post prandial, fasting lipid profile, 24-hr urinary albumin excretion (enzyme immunoassay) were measured in all patients. Serum creatinine concentration was assessed by a kinetic Jaffe method. Lipid profile was measured by a conventional laboratory technique. These laboratory investigations were done using fully-automated spectrophotometer Hitachi-912 (Roche Diagnostics, Boehringer Mannheim, Germany).

DNA extraction:

DNA was extracted using commercially available Spin-column technique kit for DNA extraction from human whole blood (QIAamp®DNA Blood Mini Kit, QIAGEN, 28159 Avenue Stanford, Valencia, CA 91355, USA). The extracted DNA samples were stored at -20°C for further use.

Determination of IL-4 genotypes:

Determination of IL-4 genotyping was done using polymerase chain reaction (PCR) using primers having the following sequences:

The sense primer:

5'-TAAACTTGGGAGAACATGGT-3'

The anti-sense:

5'-TGGGGAAAGATAGAGTAATA-3'

The PCR was carried out using a ready to use PCR buffer (Gen-Taq Master Mix, BIORON, Germany). The buffer is composed of Taq DNA Polymerase (recombinant) in reaction buffer (0.1 unit/ μ l), antibodies to Taq DNA polymerase, concentration adjusted for the effective inhibition of DNA polymerase activity at 37°C, 32 mM (NH₄)₂SO₄, 130 mM TrisHCl, pH 8.8 at 25 °C, 0.02% Tween-20, 5.5 mM MgCl₂ and dNTPs (dATP, dCTP, dGTP, dTTP): 0.4 mM of each. The PCR mixture reaction was prepared as follow: 30 μ l of a ready for use master mix, 2 μ l of forward primer (0.5 μ mol), 2 μ l of reverse primer (0.5 μ mol), 3 μ l of template DNA (100 – 500 ng) and 3 μ l of sterile deionized water to reach a final mixture volume of 40 μ l.

The PCR condition was an initial denaturation at 95°C for 5 minutes, followed by 35 cycles of melting at 95°C for 50 seconds, annealing at 53°C for 50 seconds, and extension at 72°C for 45 seconds, with a final extension step of 5 minutes at 72°C, using thermal cycler (ThermoHybaid PX2, UK). The PCR product of IL-4 (-590 C/T) was a 195-bp fragment and was digested with *Ava*II (Fermentas, Germany) into 175-bp and 20-bp fragments. The digested products were run on a 2.5% agarose gel and studied after staining with ethidium bromide (Mohammad, 2010).

Statistical analysis:

Collected data was analyzed using SPSS version 13 program. For dichotomous variables,

ANOVA and regression analysis tests were used, and chi-square was used for categorical variables. A p value (two sided) of <0.05 was considered to be significant.

3. Results

The mean±standard deviation age of this study group was 45.21±2.34 years and 46.32±2.37 years old for control group. There were statistically significant difference between both groups regarding serum triglycerides, serum total cholesterol, serum HDL-cholesterol, serum LDL-cholesterol, albuminuria level and estimated glomerular filtration rate (GFR) with a p-value of less than 0.05 (table 1).

In study patients, mean FBG, total cholesterol, triglyceride and LDL level were 230 ± 40 mg/dl, 290 ± 10 mg/dl, 350 ± 12 mg/dl and 180 ± 11 mg/dl respectively. On the other hand, in control group, mean FBG, total cholesterol, triglyceride and LDL level were 171 ± 15 mg/dl, 150 ± 6 mg/dl, 100 ± 4 mg/dl and 100 ± 9 mg/dl respectively. Mean blood

urea and serum creatinine was 94.0 ± 12.8 mg/dl and 2.6 ± 0.3 mg/dl respectively among study group. Among control group, they were 71 ± 10.2 and 1.9 ± 0.2 respectively.

Regarding the distribution of the different genotypes among the study group, it was CC (n= 26), TC (n= 61) and TT (n= 13), while in the control group it was CC (n= 30), TC (n= 67) and TT (n= 3) (table 3).

In patients having genotype CC (n = 26), majority (75%) of patients developed overt albumiuria, having lesser degree of hypertension, renal dysfunction, and dyslipidemia than TC and TT genotypes (p<0.005). On the other hand, Urinary albumin excretion (UAE), SBP, DBP, TG, S.Cr. and LDL-C were significantly higher (p-value <0.05) in patients of TT type than CC and TC groups (table 2).

Odds ratio (OR) for the high risk allele (T) is 1.34 with 95% confidence interval (CI) from 0.90 to 2.00. Thus the high risk allele of IL-4 is 1.3 times in patients than in controls (p-value 0.001).

Table 1: Characteristics of Type 2 Diabetic Patient with Nephropathy and Controls:

Variable	Study	Control
Age, year	45.21±2.34	46.32±2.37
Drug therapy	Oral	Oral
Duration of DM (years)	7 ± 0.9	6 ± 0.3
Serum Triglycerides, mg/dL	350 ± 12	100 ± 4*
Serum total cholesterol, mg/dL	290 ± 10	150 ± 6*
Serum HDL- cholesterol, mg/dL	24 ± 2	40 ± 3*
Serum LDL- cholesterol, mg/dL	180 ± 11	100 ± 9*
Fasting blood sugar, mg/dL	230 ± 40	171 ± 15
Albuminuria, mg/dL	899 ± 50	25 ± 1*
Estimated GFR, mL/min	72 ± 3	120 ± 5*

HDL indicates high-density lipoprotein; LDL, low-density lipoprotein; and GFR, glomerular filtration rate.

* p-value<0.05

Table 2: Patient Characteristics and Distribution of IL-4 genotypes:

Characteristics	Genotypes		
	TT (n= 13)	TC (n= 61)	CC (n= 26)
Age, Years	43.8±1.3	47.6±2.5	45.2±2.6
SBP, mmHg	178±8	162±8	146±4*
DBP, mmHg	92±6	82±4	76±6*
Urine Alb., mg/ day	1364±72	1193±38	576±30*
S. creat. mg/ dl	3.65±0.98	2.81±.45	1.97±0.31*
T. Chol, mg/ dl	233±45	229±29	185±25*
TG, mg/ dl	281±51	233±30	191±32*
LDL, mg/ dl	165±27	150±25	105±22*
Estimated GFR, ml/ min	60 ± 4	70 ± 5	78 ± 3*

*p-value <0.05

Table 3: Polymorphisms of Interleukin-4 Gene in Nephropathic Type 2 Diabetic Patients and Controls

Genetic Parameter	Study	Controls
Genotype		
CC	26 (26%)	30 (30%)
TC	61 (61%)	67 (67%)
TT	13 (13%)	3 (3%)*
Allele		
C	113 (56.5%)	127 (63.5%)
T	87 (43.5%)	73 (36.5%)*

*p-value < 0.05



Figure 1: Electrophoretic patterns of different IL-4 genotypes

4. Discussion

The main etiological cause of type 2 DM and its inflammatory complications such as nephropathy has yet to be clarified (Arababadi *et al*, 2009). It seems that immune-related factors play important roles in the etiology and pathogenesis of type 2 DM and its associated renal complications (Ikeuchi *et al*, 2009).

The crucial role of the cytokines network in orientation of immune responses is documented (Hyun *et al*, 2009). Several factors such as infectious agents, hormonal conditions, and cytokine gene polymorphisms regulate expression and secretion of cytokines (Lee *et al*, 2005). Study findings indicated a significant difference between type 2 diabetic patients with nephropathy and non-nephropathic diabetic controls regarding genotypes and alleles of the -590 region of IL-4 gene. A similar study was done by Mohammad K. on Iranian population and revealed the similar results (Mohammad, 2010).

In the present study, 74% of the patients belonged to both TC and TT genotypes. Clinical correlation revealed that most patients in this group have macro and micro vascular complications: represented by greater degree of albuminuria and

severe renal insufficiency ($p < 0.05$). These findings indicate that the presence of the allele T of IL-4 gene is associated with greater risk of diabetic nephropathy compared with C allele.

Many studies were done to evaluate the relation of IL-4 polymorphism to the onset of DM type 2, while few only were done to show its relation to the development of its complications (Arababadi *et al*, 2009; Mohammad, 2010). Previous data revealed that there was no relation between several promotor polymorphisms including T-590C and type 2 diabetic patients without nephropathy (Ming-Yuh *et al*, 2009); therefore, based on the current and previous studies, it seems likely that the polymorphisms are associated with nephropathic complications rather than type 2 DM (Hyun *et al*, 2009).

Some studies have investigated these polymorphisms in type 1 and 2 DM without nephropathy and in non-diabetic nephropathies (Arababadi *et al*, 2009; Hyun *et al*, 2009). For example, Ikeuchi and colleagues Parry and coworkers showed that the polymorphisms in the IL-4 gene are not associated with minimal change nephrotic syndrome. Mittal and Manchanda reported that these polymorphisms are related with

susceptibility to end-stage renal disease (Mittal and Manchanda, 2007).

Another study in a Japanese population showed that IL-4 polymorphisms could influence disease susceptibility and progression in immunoglobulin A nephropathy (Masutani *et al.*, 2003).

A significant relation between IL-4 polymorphisms and type 2 DM was reported by Bid and colleagues, in the north Indian population (Bid *et al.*, 2008). Another study demonstrated that there were no significant differences in the IL-4 polymorphisms between patients with type 1 DM and healthy controls (Mohammad, 2010).

A probable reason for the discrepancy between results could be that populations are different in race and genetics from area to another as well as, the small number of patients studied and the probable small effect of the mutation.

Conclusion

The study explored the potential scope of one of the genetic approaches to risk assessment in development of diabetic nephropathy, with its interaction with other conventional factors. The study notified that the presence of allele T in both genotypes TC and TT is strongly associated with increased risk for developing diabetic nephropathy. These observations emphasize the need to monitor these patients to reduce the susceptibility to nephropathy and then ESRD especially in the developing countries where the transplantation is so difficult. Further, the complex interplay between genetic and environmental factors should be considered in order to evaluate the etiological role of IL-4 polymorphism in nephropathic DM.

Corresponding author

Mohamed M. El-Shabrawi
Clinical and Chemical Pathology Department,
Faculty of Medicine, Suez Canal University, Egypt
zeinash2003@yahoo.com

References

- Ahima R. (2009): Connecting obesity, aging and diabetes. *Nat Med*; 15:996-7.
- Ahluwalia T., Khullar M. and Ahuja M. (2009): Common variants of inflammatory cytokine genes are associated with risk of nephropathy in type 2 diabetes among Asian Indians. *PLoS ONE*; 4: e5168
- Arababadi M., Pourfathollah A. and Daneshmandi S. (2009): Evaluation of relation between IL-4 and IFN-g polymorphisms and type 2 diabetes. *Iran J Basic Med Sci*; 12:100-4.
- Arababadi M., Pourfathollah A., Jafarzadeh A. and Hassanshahi G. (2010): Serum levels of Interleukin (IL)-10 and IL-17A in occult HBV infected south-east Iranian patients. *Hepat Month*; 10:31-5.
- Bid H., Konwar R., Agrawal C. and Banerjee M. (2008): Association of IL-4 and IL-1RN (receptor antagonist) gene variants and the risk of type 2 diabetes mellitus: a study in the north Indian population. *Indian J Med Sci*; 62: 259-66.
- Brown S. (2010): Estimation of glomerular filtration rate with creatinine-based versus cystatin C-based equations in kidney transplant recipients. *Iran J Kidney Dis*; 4:169-70.
- Colin G. (2003): Type 2 diabetes as an inflammatory disorder. *British Journal of Diabetes & Vascular Disease*; 3(1):36-41.
- Cornicelli J., Butteiger D. and Rateri D. (2000): Interleukin-4 augments acetylated LDL-induced cholesterol esterification in macrophages. *J Lipid Res*; 41: 376-83.
- Cruz M. and Maldonado-Bernal C. (2008): Glycine treatment decreases proinflammatory cytokines and increases interferon-gamma in patients with type 2 diabetes. *J Endocrinol Invest*; 31:694-9.
- Dinarello C. (2011): Interleukin-1 in the pathogenesis and treatment of inflammatory diseases. *Blood*; 117(14): 3720 - 32.
- Dinarello C., Donath M. and Mandrup-Poulsen T. (2010): Role of IL-1beta in type 2 diabetes. *Curr Opin Endocrinol Diabetes Obes*; 17(4):314-21.
- Elbe-Bürger A., Egyed A. and Olt S. (2002): Overexpression of IL-4 alters the homeostasis in the skin. *J Invest Dermatol*; 118: 767-78.
- Enriquez R., Sirvent A., Andrada E. (2010): Cryoglobulinemic glomerulonephritis in chronic hepatitis B infection. *Ren Fail* 2010; 32:518-22.
- Fève B. and Bastard J. (2009): The role of interleukins in insulin resistance and type 2 diabetes mellitus. *Nat Rev Endocrinol*; 5(6):305-11.
- Hyun Y., Park J., Song Y., Shin K., Chae J., Kim B., Ordovas J. and Lee J. (2009): Interleukin-6 (IL-6) -572C->G promoter polymorphism is associated with type 2 diabetes risk in Koreans. *Clin Endocrinol (Oxf)*, 70: 238-244.
- Ikeuchi Y., Kobayashi Y., Arakawa H., Suzuki M., Tamra K. and Morikawa A. (2009): Polymorphisms in interleukin-4-related genes in patients with minimal change nephrotic syndrome. *Pediatr Nephrol*; 24:489-95.
- Jingfang L., Bingyin S., Shuixiang H., Xiaoli Y., Mark D. Willco and Zhenjun Z. (2010): Changes to tear cytokines of type 2 diabetic patients with or without retinopathy. *Molecular Vision*; 16:2931-2938.
- Kang K., Reilly S. and Karabacak V. (2008): Adipocyte-derived Th2 cytokines and myeloid PPARdelta regulate macrophage polarization and insulin sensitivity. *Cell Metab*; 7: 485-95.
- Lee S., Lee T., Ihm C., Kim M., Woo J. and Chung J. (2005): Genetics of diabetic nephropathy in type 2 DM: candidate gene analysis for the pathogenic role of inflammation. *Nephrology (Carlton)*; Suppl: S32-6.

- Masutani K., Miyake K. and Nakashim H. (2003): Impact of interferon-gamma and interleukin-4 gene polymorphisms on development and progression of IgA nephropathy in Japanese patients. *Am J Kidney Dis*; 41:371-9.
- Ming-Yuh S., Chien-Ning H., Kuo-Ting H. and Yih-Hsin C. (2009): Association of IL-4 promoter polymorphisms in Taiwanese patients with type 2 diabetes mellitus. *Endocrine Abstracts*, 20 P337.
- Mittal R. and Manchanda P. (2007): Association of interleukin (IL)-4 intron-3 and IL-6 -174 G/C gene polymorphism with susceptibility to end-stage renal disease. *Immunogenetics*; 59:159-65.
- Mohammad K. (2010): Interleukin-4 Gene Polymorphisms in Type 2 Diabetic Patients with Nephropathy. *IJKD*; 4:302-6.
- Parry R., Gillespie K., Parnham A., Clark A. and Mathieson P. (1999): Interleukin-4 and interleukin-4 receptor polymorphisms in minimal change nephropathy. *Clin Sci (Lond)*; 96:665-8.
- Yih-Hsin C., Chien-Ning H. and Ming-Yuh S. (2009): Cytokines, Metabolism, and Type 2 Diabetes Mellitus. *J Biomed Lab Sci*; Vol 21 No 4
- Yuxia W., Lingfang K., Xueying W., Yanli C. and Yuping S. (2011): The association between C-572G polymorphism of the Interleukin 6 gene promoter and type 2 diabetes mellitus in a Chinese Han population. *International Journal of the Physical Sciences*, Vol. 6, (13), pp. 3255-3262, 4.

9/2/2011

Evaluation of changes the qualitative & quantitative yield of horse bean (*Vicia Faba*L) plants in the levels of humic acid fertilizer

*Simin Haghighi¹, Tayeb Saki Nejad², Shahram Lack³

1- Department of Agriculture. Science and Research Branch, Islamic Azad University, Khuzestan, Iran.

2- Assistant Professor Department of Physiology, Ahvaz branch, Islamic Azad University, Ahvaz, IRAN (*Thesis Supervisor*)

3- Department of Agriculture. Science and Research Branch, Islamic Azad University, Khuzestan, Iran.

*Corresponding Author: haghighi.simin@gmail.com

Abstract :Much of the farmland in IRAN was consisting of soils arid and semi-dry, which of organic matter are also poor. Organic compounds used in these areas can improve the physical properties, chemical, and soil fertility, In this regard, this test was performed in 2010 year; design was used split plot randomized complete block with 3 replications. Main plots, cultivars with 3 levels: BAREKAT (V₁), JAZAYERI (V₂) and the SHAMI (V₃) and sub-plots, treated with acid Humic 4 levels including: controls (F₀), acid humic (F₁), humic acid +macro- elements (F₂) and humic acid + micro-elements (F₃) were considered. Acid composition of micro and macro elements humic in the prolonged stages of bean growth was caused increase the number of seeds per pod, seed yield, harvest index, grain protein percentage. Among the traits related to yield, most yield-related biological treatment (V₃F₂) with a numeric value and the highest grain yield 6233 kg ha treatment (V₃F₂) 2,942 kg per hectare with the average number of seeds won.

[Simin Haghighi, Tayeb Saki Nejad, Shahram Lack. **Evaluation of changes the qualitative & quantitative yield of horse bean (*Vicia Faba*L) plants in the levels of humic acid fertilizer.** Life Science Journal. 2011; 8(3):583-588] (ISSN: 1097-8135). <http://www.lifesciencesite.com>. 91

Keywords: horse bean, humic acid, qualitative and quantitative yield

Introduction

Clate Humic producing acid from various nutrients such as sodium, potassium, magnesium, zinc, calcium, iron, copper, and Humic acid solution used in the food category growth, and nitrogen content in the aerial roots (and not your Nvpamvr, 1979) and the disappearance of chlorosis in corn leaves (Fernandez, 1968) and was Lupine (Santiago et al, 2008). In a three-year study of three amounts of phosphorus acid with and without Humic it looked on the growth of potatoes. The results showed that the phosphorus content of leaflets on treatments with acid Humic 03 . 0% increase. Treated with acid to humic tuber yield more than 10 times increase in 2 to 3 years of study. The results showed that treatment with acid humic tumor had no significant effect on density.

The researchers used the acid levels in the soil Humic the spraying and application of quantitative and qualitative yield of the pepper. The results showed that acid humic significant effect on chlorophyll content of leaves, especially on a chlorophyll b. The experimental spray Humic acid 200 mg per liter, an increase of 38 percent, 74 percent of the plant to absorb nitrogen and phosphorus uptake of barley was 72% (Yvsv et al, 1996) and Khazaei Sabzevari (2009) Effect of spraying acid levels Humic (0, 100, 200 and 300 milligrams per liter) at four different times (tillering, stem elongation, flag leaf emergence and pollination) on growth and yield characteristics were investigated. The results

showed that acid humic dry weight, leaf area, stem height was a significant effect. Turkmen et al (2004) showed that tomato plants grown in quantities of 1000 mg .kg humic acid soil increased tomato yield was increased.

Avayd and Chen (1990) showed that acid Fvlvyk Humic acid in concentrations of 25 to 300 milligrams per liter in the nutrient solution is able to stimulate the growth of stem plants. In the pilot stage of development in wheat spikes Humic spray materials in high winds and hot dry conditions, yield 7 to 8 percent increase compared to the control treatment (Zvdan, 1986). 8 to 20 percent yield increase in the use of acid Humic, 14 percent rice and 44% in the radishes (and Meyer, 1998). In terms of greenhouse effect, acid Humic on oat growth were investigated. The results showed that application of Humic acid 100 mg per pot had a significant effect on dry matter yield.

Karakart and colleagues (2008) 5 Humic acid concentration on yield and fruit quality in pepper leaf and soil treatments were studied. Treatments were applied at the beginning of the fourth week after planting. Humic significant effect on acid stability, length and diameter did fruit. The use of acid fruits with low sugar levels through both increased Humic. Humic acid also have significantly effective in leaf chlorophyll content and its effect on the content of chlorophyll in the leaves. Humic acid in 20 mL quantities of water, a spray of dirt and leaves the

chlorophyll content was highest. Humic acid also significantly increased compared to the total weight of fruit.

Soil health is one of the key factors in determining the yield of crops. 20 kg ha Humic acid with 100% NPK, plus a 12% increase in the uptake of onions in the highest yield and lowest yield of NPK with control (0 Humic acid and 0 NPK) was. To NPK, respectively, to 105 3 . 199, 9 . 7 to 63.12 and 132 to 139 mg per kg of soil during the experiment by adding acid and fertilizer increased Humic.

The researchers tested three types of acid Humic (uptake, k-Humate, Eko-Fer) on the yield and characteristics such as weight, amount of permeability, PHP, color, and ascorbic acid in tomato fruit and stem thickness were investigated. The results showed that most of the fruit, the flowers and fruit weight (3 . 67 g) using 600 cc . da Eko-Fer Humic acid were obtained. Most of the gum and the highest ascorbic acid was about 5 . 25 mg per 100 g fruit acid used cc.100 300 Humic Uptake and maximum stem thickness (685.10 mm) using the 500 cc.100 Acid Uptake Humic income (safeguards and Akal, 1999.)

Martin (1967) found that the use of derivatives Humic acid in tomatoes grown in pots, especially in the final stages of the yield increased significantly. Humic treated with acid to increase in number of fruit to fruit size, especially in the first harvest was five. I went to see the high quality fruit. Humic acid application also increased 200 percent in the first harvest was in tomatoes.

Branl and colleagues (1987) in a field trial of the combination of oxidized Humic extracted from tomatoes, cotton and grape were investigated. As a soil treatment at the beginning of another growing season and were applied as a spray in mid-growth period.

Duvall (1998) during the testing of various amounts of up to 400 pounds on two species of rapeseed (*Brassica rapa* L.) and (*Brassica hirta* L.) with three different cultures on one-year period studied. The study found no difference in plant growth parameters. The fourth week of rain on the second planting eliminates the increased survival of plants.

The test of spraying acid and nitrogen Humic on durum wheat was investigated. Results showed a significant increase in acid Humic shoot and root dry weight in wheat. Humic acid also increased photosynthetic activity of plant enzyme activity was increased (Difayn et al, 2005). Johns et al (2004) the acid test Humic on spring wheat yield were investigated. The results showed that humic acid phosphorus and other nutrients to increase and the increase in yield was significant.

Salmon and colleagues (2005) in a field trial of the three hybrids of watermelon contains acid Humic Sugar belle, Aswan, Gizal looked. Humic acid to drip

irrigation in the values of zero (control), 2.4 and 6 liters of the Fdan and fruit yield and quality were investigated. The results showed that the hybrid had the lowest yield Sugar belle largest and Aswan. Humic acid concentrations on 6 liters significantly increased the yield of 3 hybrids.

Seeds were evaluated. The results showed that seed number, plant height and spike traits that were most responsive to acid Humic. The late planting dates (stress), Hybrid 18F average yield was lower than optimal conditions (Yvlykan, 2008). Humic acid and positive direct effects on crop growth (Linnaeus Vagan and Han, 2004), peas (Vagan, 1974) and chicory (Valdryty et al, 1996) found. Treated was with acid in plant growth response curve showed that increasing the concentration of acid Humic Humic increased plant growth. The reduction in growth was seen in very high concentrations (Chen and Avayd, 1990), 1986. Infrequently reported and Associates, 1988. Avayd and Chen, 1990. Moscow et al, 1999 and Noble, 2002.)

1. Material and Method

Land preparation and planting procedures

In order to run tests on the grounds of the 7.25.88 irrigation, plowing to a depth of 20 cm, 15 cm and depth of the disk was trowel. Urea nitrogen of 30 kg of pure nitrogen per hectare as basal fertilizer was applied at planting. After preparation, the size plot of land was design on the map, the dimensions of a test plot were 6 × 4 m and 6 m in length planted in each plot was 7 lines. Between two rows of 60 cm and 15 cm between rows of seeds were on. The manual method was performed on 08.03.89.

The final performance of the final harvest

The number of plants per unit area and yield components of four components, namely the number of nodes contained in the plant, pod, pods, seed number per pod and average seed weight is the significance of the number of pods per plant and average seed weight in order to function as important components.

At the end of the growing season of lines 3 and 4 as the final area of one square meter were the yield and its parameters (number of pods per plant, average seed number per pod, seed weight) were measured. This test was used in the following formula:

$$U = \frac{K \cdot L \cdot Z \cdot A}{10^5}$$

K: number of plants per square meter

L: average number of pods per plant

Z: The average number of seeds per pod

A: thousand seed weight (g)

Statistical computing

Analysis of variance, split plot design with the computer software EXCELL, MSTATC bonds was to compare the attributes of the LSD test was used.

2. Result

2.1.1. Qualitative and quantitative components of the production

2.1.1.1. Yield

A result of the variance shows that the number of humic acid and their interactions in the 1% level has significant effect on yield. The number of treatments on grain yield at 5% level is significant.

Comparisons with the average highest and lowest yield of the macro humic acid treatment and the lowest value in 2765 to control with the numeric value are 2,122 kg per hectare. High yield in positive physiological effects of the macro humic acid treatment effects on plant cell metabolism that plants can increase yield (and infrequently reported, 2002). Alqmry and colleagues (2009) the effect of acid on plant Humic Bean said Humic acid increases the yield and yield components. In a study of spray Humic cluster development stage of wheat, yield 7 to 8 percent increase compared to the control treatment (Zvdan, 1986). Humic acid used in wheat, rice, radish, respectively, 20 and 14 and a 44% increase in yield (and Meyer, 1998).

Based on the comparisons yield the highest average number of islands with the lowest value in 2514 and 2412 the average amount allocated to it is a blessing. Higher performance in a number of islands can be most affected by the number of pods per plant and number of fertilizers, he said.

In examining the interaction of different varieties of acid Humic and comparisons with the highest average performance compared to the macro Humic SHAMI and acid value of 2942 kg per hectare and the lowest figure of the blessing and acid Humic macro with value 1733 kg hectares respectively.

2.1.2. Yield components

2.1.2.1. The number of pods per plant

Due to the variance and number of treatments and their interactions on acid Humic pods on the plant is significant at 5% level. Comparison tests for the effects of acid on the number of pods per plant showed Humic highest number of pods plant to acid treatment Humic macro with the number of pods per plant and the minimum value 20.11 in value with the control pod number 19.14 plant is achieved.. Macro Humic acid prevents loss due to the elements essential to plant flowers that will have enhanced performance. The loss in grain yield of flowers is one of the limiting factors.

Mean table comparisons, the highest and lowest number of pods per plant in treated compared to

the number of islands with a numeric value associated with 17.19 and 12.16 the number of pods per plant varieties have been blessed with a numeric value.

The study compared the results for the interaction of acid Humic and more pods per plant varieties and cultivars to acid Humic macro SHAMI with 63.21 and the lowest value of the macro and the amount of acid Humic blessed with the value 2.13 the number of pods in the plant.

Among yield components, number of pods per plant, one of the most important yield components and grain yield than is. Ability of the flowers and pods of beans in the actual production potential is high, but this depends on the genetic makeup and environmental conditions are perfect, and because changes in the yield is very high.

2.1.2.2. The number of seeds per pod

Results of the variance at 1% level indicating that the effects of acid treatments and their interactions humic figure on the number of seeds per pod were significant. The comparisons in Table (2-4) treated with acid Humic highest average acid value of 5.02 seeds per pod and the lowest value in the two quarters is the number of seeds per pod. However, seeds per pod and the number of acid and acid Humic Micro Humic no significant difference.

Comparisons in the average number of treatments to the highest and lowest average value in order to figure blessed with 5.09, and SHAMI with the figure number 93. 4 is the number of seeds per pod. Examining the interaction between the largest number of seeds per pod and number of acid

Humic SHAMI were with the value 5.53 the number of seeds and the lowest number of islands and micro humic acid value of 4.07. Unlike the number of pods per plant, one of the variable component is the number of seeds per pod, grain yield, grain yield is the most constant, because the number of oocytes in the ovaries is almost equal.. The number of seeds per pod and its changes, the effect of fluctuations is not the same as the number of pods. During elongation of seed per pod and seed filling also effective

Harvest index

Harvest index of grain yield to biological function can be divided. Harvest index is the distribution coefficient assimilates and that part of what made assimilate the tank has been transferred. Results showed that 1% of the variance in the number humic acid and their interactions were significant. Comparison tests showed that the treatment of various acids Humic highest and lowest average harvest index, respectively related to the treatment and control of macro Humic acid value was 77.46 and 08.42.

The test compares the average invoice amount for the highest and the lowest harvest index to the figures islands blessed with a numerical average of 63.45 and 09.45 shows.

In reviewing the test results compared to the number of factors and interactions of acid and acid Humic SHAMI Humic highest harvest index compared to the minimum number of macro and micro Humic islands and is acid.

Although the number of islands has a lot of grain, but many of its biological function, provided that the division of these two numbers are low harvest index. But the figure has blessing to yield fewer but much less allocated to dry matter accumulation. this result with two more harvest index is provided. This phenomenon should be studied in a number of islands, which accounts for the biological function of dry matter yield, harvest index is low, and that figure is shrinking.

The percentage of grain protein

Analysis of variance showed that the 1% level humic acid on seed protein content is significant. Comparisons with the average highest and lowest percentage of protein in the seeds treated with acid Humic macro Humic the acid value was 1.30 and the rate was 41.25.. Protein function is a function of plant nitrogen. Humic acids by increasing nitrogen increased leaf area and plant protein does. Increasing membrane permeability of root cells in Humic acid absorption and transport are more elements (Akynsy et al, 2009). In a study Noble et al (2002) showed that the use of Humic acid in corn increased 23% and 39% dry weight of shoot and root dry weight increased significantly in soil nitrogen and nitrogen concentrations than the control plants were stored.

Due to the variance effect on grain protein percentage figure is significant at the 5% level. Average highest and lowest average number of treatments in accordance with comparisons of seed proteins, respectively, compared to the islands of 24.26 and 92.25 the number of blessings. I figure between the average grain protein percentage a blessing and SHAMI, there was no significant difference.

The study compared the effects of two treatments Humic acid and the highest number of acid treatments and the number of macro Humic blessed with 53.30 and the lowest value of the acid treatment and the number of macro Humic SHAMI rate was 73.21.

The synthetic amino acid protein is an integral part of the protein nitrogen. The amount of nitrogen to protein can be increased.

A stepwise regression to yield

According to Table 4-6 of the components in the stepwise regression yield the greatest impact on grain yield, biological yield and harvest index have. So

we need to achieve higher yield on harvest index and biological function to work. Since the harvest index of economic performance Tqsm biological function is achieved, thus increasing the economic performance can be increased harvest index.

Table 1. The stepwise regression for yield and other traits as the dependent variable as independent variables

1	2	3	Variable added to model
-29.719	-10.2227	-36.2031	Constant
59.0**	45.0**	48.0**	Total dry weight
	03.50**	32.45**	Harvest index
		-10.0 ^{ns}	Shoot dry weight
93.99	94.99	95.99	R ²

Ns and **: Stepwise regression coefficients in the last stage is Significant at the 1% level

Reference

1. Aso, S., and sakai, J. studies on the physiological effects of humic acid. I uptake of humic acid by crop plants and ies physiological effects. Soil science, plant Nutrition, 9: 85-91.
2. Aydin, A., Turan, M., and sezem, y. 1999. Effect of fulvic humic application on yield nutrient uptake in sunflower (*Heliantus annuus*) and corn (*zea mys*) soil sciences, 6:249-252.
3. Ayuso, M., Hernandez, T., and Gercia, C. 1996. Effect of humic fractions from arban wastes and other more evolved orgamic materials on seed germination. Journal of science of food end ayricultur, 72(4): 461-468.
4. Azam, F., and Mauk, k.A. 1983. Effect of humic acid soaking on seeding growth of wheat (*Triticum aestivuml.*) under different conitions, Pakistan Journal of Botany, 15: 31-38.
5. Bar-tal, A., Bar-yosef, B., and chen, y. 1988. Effects of fulvic acid and PH on zinc sorption on montmorillonite. Soil science, 146:367-373.
6. Brownell, J.R., Nordstrom, D., Marihart, I., and Jorgensen, G. 1987. Crop responses form two new Leonardite ex tracts. Science and Environment. 62:492-499.
7. Chen, Y., and Aviad, T. 1990. Effects of humic substans on plant Growth InP. Macarthy et al. Eds. Humic substance in soil and crop science: selected Reading. American society of A gronomy Madison. WI: 161-186.

8. Cooper, J., and Liu, Ch. 1998. Influence of humic acid substances on rooting and nutrient content of creeping Bentgrass. *Crop Science*, 38:1639-1644.
9. Cordovilla, M.D. Ligeró, F. and C. Liuch. 1999. Effects of NaCl on growth and nitrogen fixation and assimilation of inoculated and KNO₃ fertilized faba and *Pisum sativum* L. plants. *Plant. Sci.* 140,127-136.
10. Crawford, J.H., Senn, T.L., and Stembridge, G.E. 1968. The influence of humic acid fractions on sprout production and yield of the Carogold sweet potato. *S. Carolina Ag. Exp. Sta. Tech. Bull.* 1028.
11. Delfino, S., Tognetti, R., Desiderio, E., and Alvino, A. 2005. Effect of foliar application of N and humic acid on growth and yield of durum wheat. *AgronomySustain. Dev.* 25: 183-191.
12. Dixit, V.K., and Kishore, N. 1967. Effects of humic acid and fulvic acid fraction of soil organic matter on seed germination. *Indian Journal of science.* 1: 202-206
13. Dormaar, J.F., 1970. Effects of humic substance from Chernozem Ah horizon on nutrient uptake by phaseolus vulgaris and Festuca scabrella. *Can. Journal soil science.* 55:111-1118.
14. Dursun, A., Gurenc, I., and Turan, M. 2002. Effects of different levels of humic acid on seedling growth and macro- and micronutrient contents of tomato and eggplant. *ACTA. Agrobotanical.* 56: 81-88.
15. Duval, J.R. 1998. Evaluating Leonardite as crop growth enhancer for turnip and mustard greens, *Plant Culture Technology*, 8(4): 564-567.
16. Ervin, E. H., Zhay, X., and J. Roberts, C. 2007. Improving root development with foliar humic acid applications during Kentucky Bluegrass sod establishment on sand. *ISHS Acta Horticulture*, 783.
17. Fernandez. Escobar, R., Benlloch, M., Barrmed, D., Duenas, A., and Gutierrez Ganán, J.A., 1996. Response of olive trees to foliar application of humic acid extracted from Leonardite. *Scientia Horticulture* 4:3-4:191-200.
18. Fuhr, F., and Sauerbeck, D. 1967. B. The uptake of straw decomposition products by plant roots: 317-327. In Report FAO/IAEA Meeting, Vienna, Pergamon Press, Oxford.
19. Fuhr, F., and Sauerbeck, D. 1967. The uptake of colloidal organic substances by plant roots as shown by experiment with C-labelled humus compounds: 73-82. In Report FAO/IAEA Meeting, Vienna, Pergamon Press, Oxford.
20. Iswaran, V., and Chonkar, P.K., 1971. Action of sodium humate and dry matter accumulation of soy beans in saline alkali soil. In B. Novak et al. *Humic ET planta*: 613-615.
21. Jones, C.A., Jacobson, J.S., and Mugaas, A. 2004. Effect of humic acid phosphorus availability and spring wheat yield. *Fact. Fertilizer*, 32.
22. Karakurt, Y., Huvnlü, H., Unlu, H. and Adem, P. 2008. The influence of foliar and soil fertilization of humic acid on yield and quality of pepper. *Plant soil science.*
23. Kauser, A., and Azam, F. 1985. Effect of humic acid on wheat seedling growth. *Environmental and Experimental Botany.* 25:245-252.
24. Kelting, M., Harris, J.R., Fanelli, J., and Appleton, 1998. Bio stimulants and soil amendment effect two-year posttransplant growth of red maple and washing ton hawthorn. *Hort science*, 33: 819-822.
25. Koo, E.S., 2006. Humic acid or fulvic acid: which organic acid accelerates the germination of the green mung beans? *California State Science.* 1617.
26. Lee, Y.S., and Bartlett, R.J. 1976. Stimulation of plant growth by humic substances. *Soil science. Sec. American Journal.* 40: 876-879.
27. Lee, Y.S., and Bartlett, R.J. 1976. Stimulation of plant growth by humic substances. *Soil science. sec American Journal.* 40: 876-879.
28. Linehan, D.J., and Shepherd, H. 1979. A comparative study of the effects of natural and synthetic ligands on ion uptake by plant. *Plant soil*, 52: 281-289.
29. Liu, C., and Cooper, R.J. 2000. Humic substances influence creeping bentgrass growth. *Golf. Course Management*, 33: 1023-1025.
30. Liu, C., Cooper, R.J., and Bownan, D.C. 1998. Humic acid application effects- photosynthesis, root development, and nutrient content of creeping bentgrass. *Horticulture science.*
31. Lobartini, J.C., Tan, K. H., and Pape, C. 1998. Dissolution of aluminum and iron phosphate by humic acids, 29(516) *Commun. Soil science plant and*: 535-544.
32. Lojo, A.M., 2000. Bio-Organic Fertilizer production and Application, Industrial Research and Development office Sugar Regulatory Administration, Quezon City, Philippines, PP, 11, 19, 20, 26.)
33. Mallikarjuna, M., Govindasamy, R., and Chandrasekaram, S. 1987. Effect of humic acid on sorghum vulgare var. CSH-9. *Current Science*, 56:1273.
34. Martin, J.A., Malcolm, R.E., and MacCarthy, T.L. 1967. The influence of various rates of nitrogen and humic acid derivatives on the growth and yield of greenhouse tomato. *S. Carolina Ag.*
35. Mishra, B., and Srivastava, L.L. 1988. Physiological properties of an isolated form of humic acid from soil association of Bihar. *Soil Science.* 36:1-89.
36. Mylonas, V.A., and McCants, C.B., 1980. Effects of humic and fulvic acid on growth of tobacco. *Tabacco growth and ion uptake. Journal of plant Nutrition*, 2:377-393.
37. Nardi, S., Pizzeghello, D., Gessa, C., Ferrarese, L., Trainotti, L., and Cusadoro, G. 2000. A low molecular weight humic fraction on nitrate uptake

- and protein synthesis in maize seeding, soil biology. *And biochem*, 32(2000) 415-419.
38. Padem, H., and Ocal, A. 1999. Effects of humic acid application on yield and some characteristics of processing tomato. *ISHS Acta Hortical turae*. 159-163.
 39. Piccolo, A., Celano, G., and Pietramelara, G. 1993. Effects of fractions of coal-derived humic substances on seed germination and growth of seed lings (*Lactuca sativa* and *Lycopersicon esulentum*) *Biology and ferti of soi*. 16: 11-15.
 40. Piccolo, A., Nardi, S., and Concheri, G. 1992. structural characteristics of humic substances as related to nitrate up take and growth regulation in plan systems. *Soil biology and biochem*, 24(4): 373-380.
 41. Pinton, R., Cesco, S., Iacoletting, G., Astolfi, S., and varanini, z. 1999. Modulation of No₃-uptake by watter-extractable humic substances: involvement of root plasma membrane lttATP ase . *plant and soil* , 215: 155-161.
 42. Rauthan, B.S., and Schnitzer, M. 1981. Effects. Of soil fulvic acid on the growth and nutrient content of cucumber (*cucumis sativus*) plants. *Plant soil*. 63: 491-495.
 43. Salman, S.R., Abou- Hussein, S.D., Abdolmawgoud A.M.R., and El-nemr, M.A. 2005. Fruit yield and Quality of watermelon as Affected by hybrids and humic acid Application.J
 44. Sanchez-Conde, M.P., and Ortega, C.B. 1968. Effect of humic acid on the developement and the mineral nutrition of the pepper plant: 745-755. In *Contool dela Fertiliza cion delas plants as cultiradas, 2"* Cologuia Evr. Medit. Cent. E dafal. Biol. Aplic. Cuartos Sevilla, Spain.
 45. Sangeetha, M., Sing aram, P., and Vma Devi, 2006. Effect of lignite humic acid and fertilizer on yield of onion and nutrient availability. *International Union of soil sciences*, 21:163.
 46. Santi, S., Locci, G., Pinton, R., Cesco, s., and varanini, Z. 1995. Plasma membrane H⁺- ATPase in maize roots induced for No₃-uptak
 47. Schmidt, K.E., and zhang, X. 1998. How humic substances help turf grass grow. *Golf Course Management*: 65-68.
 48. Sheriff, M. 2002. Effect of Lignite coal derived HA on growth and yield of wheat and maize in alkaline soil. PhD. The sis, NW FD Agricultural Universioy, Pe shawar, Pakistam.
 49. Sladky, Z. 1965. Anatomic and physiological and ternations in sugar beet receiring foliar applications of humic substances, *biology plant*, 7:251-26.
 50. Sladky, Z., and Tichy . 1959. Applications of humic substances to overground organs of plantes. 1: 9-15.
 51. Stephan, w.k., and Charles, W.J. 1994. Experimentation with Arkansas lignite to identify organic soil supplemenes sui table to regional agricultural needs. Proposal. Arkanssas Tech University.
 52. Turkmen, O., Dursun, A., Turan, M., and Erdinc, C. 2004. Cal cium and humic acid effect seedgermination, growth and nutrient content of tomato(*lycopersicon esculentumL*) seed lings under saline soil conditionspp. *Acta Agriculture scandinavica*, 7:168-174.
 53. Ulukan, H. 2008. Effect of soil applied humic acid at different sowirg times on some yield colponenes in wheat hybrids. *Interna tional Journaly of Botany*. 4(164): 175.
 54. Ulukan, H., 2007. Humic acid application into field crops cultivation science Eng 11(2).
 55. Valdrighi, M.M., Pear, A., Agnolucci, M., Frassinetti, S., Lunardi, D., and vallini, G. 1996. Effects of compost- derived humic acids on Vegetable biomass production and microbial growth within a plant soil system. *Comparative study. Agric Ecosyst. Environ*, 58: 133- 144.

2/12/2011

The Renoprotective Effect of Honey on Paracetamol - Induced Nephrotoxicity in Adult Male Albino Rats

Basma K. Ramadan^{1*} and Mona F. Schaalán²

¹Physiology Department, Faculty of Medicine for Girls, Al-Azhar University

²Biochemistry Department, Faculty of Pharmacy, Misr International University

basma_phy@hotmail.com

Abstract: Objectives: Oxidative stress plays a crucial role in the development of drug-induced nephrotoxicity. Honey has been known to be effective against oxidative stress-induced diseases. The study aims to investigate the antioxidant and ameliorative protective impact of clover flowers honey against paracetamol- induced nephrotoxicity in rats.

Material and methods: Forty adult male albino rats (120-180 gram b.wt.) were divided into four groups (n= 10 in each group). The animals in the control group (group I) did not receive any treatment, while those in group II received clover flowers honey (2 g/kg/day, p.o) for 4 weeks. The animals in group III received paracetamol (640 mg/kg, p.o), while in group IV, rats were pretreated with clover flowers honey (2 g/kg/day, p.o) for 4 weeks before paracetamol administration. At the end of the experiment, 24hrs urine was collected for glucose and protein determination, while blood was sampled for serum GSH, urea and creatinine determination. The kidneys were removed for assessment of tissue SOD, CAT and tumor necrosis factor (TNF-alpha).

Results: Exposure of rats with a nephrotoxic dose of paracetamol disturbed the kidney function tests; blood urea nitrogen (BUN) and serum creatinine (SC) levels, decreased the antioxidant capacity of GSH and SOD and elevated renal TNF-alpha. The protective use of clover flowers honey before paracetamol-induced nephrotoxicity resulted in a significant improvement in all evaluated parameters, rendering most of the disturbed parameters to their normal levels.

Conclusion: Results of the present study suggest that the protective activity of clover flowers honey may be related to its anti-inflammatory and antioxidant properties.

[Basma K. Ramadan and Mona F. Schaalán. **The Renoprotective Effect of Clover Flowers Honey on Paracetamol - Induced Nephrotoxicity in Adult Male Albino Rats**[Life Science Journal 2011;8(3):589-596]. (ISSN:1097-8135).

<http://www.lifesciencesite.com>.92

Key Words: Paracetamol-induced nephrotoxicity, SOD, CAT, GSH and TNF- α

1. Introduction

Prevention is better than cure, a prophylactic concept that should be applied in cases of drug induced nephrotoxicity which is a serious and common danger. The use of nephrotoxic drugs has been implicated as a causative factor in up to 25% of all cases of severe acute renal failure in critically ill patients (*Pannu and Nadim, 2008*). This is probably because the kidney is supplied with a large volume of blood accounting for 20% of total cardiac output. Therefore, the kidney is likely to be affected by secondary effects of drugs and their metabolites that are accumulated through the urine concentrating mechanism (*Marieb, 2006*).

Paracetamol, PCM, or Acetaminophen, is a drug of para-aminophenol group which is considered one of the commonly used and safe over-the-counter antipyretic and analgesic drugs, when administered at recommended doses (*Ozkaya et al., 2010*). The main problem with this medication remains its misuse through intentional or unintentional ingestion of supra-therapeutic dosages which usually lead to hepatic necrosis. When administered at normal doses, PCM is primarily metabolized by conjugation with sulfate and glucuronic acid. A minor pathway through CYP450 has also been reported to yield a highly reactive metabolite, *N*-acetyl-*p*-benzoquinonimine (NAPQI).

This metabolite is generally stabilized through conjugation with glutathione (GSH) and eliminated *via* the kidney. However, when an overdose of PCM is administered, the production of NAPQI exceeds the capacity of GSH to detoxify it. The excess NAPQI then causes liver damage associated with oxidative stress (*Roberts and Bukley, 2007*). PCM overdose is also known to be associated with inflammation, marked by an increase in the inflammatory cytokines; tumor necrosis- α (TNF- α), interleukins, as well as the upregulation of nitrogen oxide (NO) from serum, macrophages and hepatocytes (*Jaeschke et al., 2003*). Even in sensitive individuals, such as persons with renal insufficiency, therapeutic doses of paracetamol have also been implicated in kidney damage (*Stern et al., 2005*).

Oxidative stress is reported to constitute a major mechanism in the pathogenesis of PCM-induced liver and renal damage in experimental animals. Because toxic overdoses of APAP were reported to have life-threatening impacts on the kidney, e.g. hepatic necrosis and renal failure in both human and experimental animals, early protection from APAP-induced nephrotoxicity has life-saving importance (*Ghosh and Sil, 2007, Demirbag et al., 2010*). Therefore, supplementation with antioxidants is very crucial to

delay, prevent or remove oxidative damage. There are numerous reports indicating that PCM-mediated oxidative stress or hepato-renal toxicity is attenuated by use of naturally occurring antioxidants and/or free radical scavengers such as vitamins, medicinal plants and flavonoids. Recently, the flavonoids have aroused considerable interest because of their potential beneficial effects on human health. The antioxidant capacity of these molecules seems to be responsible for many of their beneficial effects and confers a therapeutic potential in diseases such as cardiovascular diseases, gastric or duodenal ulcers, cancer and hepatic pathologies.

Honey is a natural popular sweetener and is being used to treat a variety of illnesses due to its pleiotropic medicinal properties such as its antibacterial, hepatoprotective, hypoglycemic, reproductive, antihypertensive and antioxidant effects. The therapeutic role of honey in the treatment of various ailments has been receiving considerable attention recently, and its therapeutic value has been partly attributed to its antioxidant properties because it contains both aqueous and lipophilic antioxidants. These properties enable honey to act at different cellular levels as an ideal natural antioxidant (*Aljadi and Kamaruddin, 2004*). Honey with higher water content and with darker color proved to have a higher antioxidant activity. The antioxidant compounds present in honey include vitamin C, monophenolics, flavonoids, and polyphenolics (*Schramm et al., 2003*).

The aim of the present study is to shed further light on the possible nephroprotective ameliorative effects of clover flowers honey on PCM-induced acute nephrotoxicity in albino rats.

2. Material and Methods

Animals:

The experimental protocol and animal handling were approved and performed according to the guidelines of animal use of the Ethical Committee, El-Azhar University. In this study, 40 healthy adult local strain male albino rats, weighing 120-180 g were utilized. They were housed in room temperature and regular light: dark cycle and fed rodent chow and water *ad libitum*. They were fasted 17 hours (4: 00 p.m- 9: 00 a.m) before the experiments, but were allowed free access to water.

Experimental design

Rats were kept in plastic cages during the experimental period. One week acclimatization period was allowed before initiation of the experiment. On the start of the 2nd week, rats were divided into four equal groups:

Group I: Control group (C) was supplied with access water and ordinary rat chow.

Group II: Control group receiving 2 gm/kg/day clover flowers honey (*Omotayo et al., 2010*) by oral route using a gastric gavage tube for 4 weeks (C/H).

Group III: Acute nephrotoxic group (N) were induced by single oral dose (640mg/kg b.wt.) of paracetamol using gastric gavage tube (*Deviet et al., 2005*). The animals were treated between 9:00 and 10.00 A.M to minimize the possible diurnal effects in tissue glutathione concentration influencing the experimental results.

Group IV: Rats administered clover flowers honey (2 gm/kg b.wt./day) for 4 weeks by gastric gavage tube and at the end of the fourth week single oral dose of paracetamol (640 mg/kg b.w) was administered by the same route (H/N).

Blood and tissue samples were collected 72 hours after paracetamol administration in groups treated by paracetamol; group III (acute paracetamol-induced nephrotoxic group, N) and group IV; (H/N).

Blood sampling:

Animals were anesthetized and blood samples were withdrawn from retro – orbital sinus by heparinized capillary tubes under light ether anesthesia after 12-14 hours fasting period. The withdrawn blood was collected in centrifuge tubes for serum separation, by allowing the blood to clot for an hour at room temperature and centrifugation at 3000 rpm for 15 minutes. Sera were separated and stored at – 20 C° until used for estimation of serum urea (BUN), serum creatinine (SC) and glutathione content (GSH). Assessment of serum glutathione (GSH) content was performed using Cayman's GSH assay kit, serum urea was according to modified *Berthelot – Searcy* method (*Henry, 1991*), while serum creatinine activity was determined using the application of Jaffe reaction (*Wilson and Walkes, 2000*).

Determination of cytosolic catalase (CAT) activity was according to the method of *Claiborne (1985)*, while the cytosolic superoxide dismutase (SOD) activity was according to *Marklund (1985)*.

Kidney tissue sampling and preparation of its homogenate

Under light ether anesthesia, the animals were subjected to a dorsal midline incision by dissection of the muscle to reach renal bed and expose the kidneys. Careful dissection was done to the renal pedicle which was rapidly cut. The kidneys were removed and dissected free from the fat and connective tissue. The left kidney was longitudinally sectioned, and renal cortex was homogenized in cold potassium phosphate buffer (0.05 M, pH 7.4). The renal cortical homogenates were centrifuged at 5000 rpm for 10 min at 4 °C. The resulting supernatant was used for the

determination of the activities of SOD and catalase (CAT) using colorimetric assay.

The protein content in each supernatant sample was estimated according to **Lowry *et al.*, 1951**.

The right kidney was homogenized in 175 μ l of lysis buffer for 10 minutes and the tissue was centrifuged for 20 minutes at 15,000 rpm. 350 μ l of SV RNA dilution buffer was added to 175 of tissue homogenate, the mixture was placed in a water bath at 70°C for 3 minutes. The mixture was centrifuged at 12,000-14,000rpm for 10 minutes at 20-25°C.

For detection of TNF- α gene expression, RNA was extracted, reversely transcribed into cDNA and amplified by PCR and then detected using agarose gel electrophoresis (**Williams, 1989**). RNA was extracted from the kidney tissue using SV total RNA isolation system (Promega, Madison, WI, USA).

Statistical Analysis:

Data input and analysis were done using SPSS computer program. All results were expressed as the mean \pm standard error. Mean values of the different groups were compared using a one way analysis of variance (ANOVA). Least significant difference (LSD) post hoc analysis was used to identify significantly different mean values. *P* value < 0.05, 0.0005 was accepted to denote a significant difference.

Table 1: The serum profile of kidney functions and GSH level in the experimental groups

	Group I (C)	Group II (C/H)	Group III (N)	Group IV (H/N)
BUN (mg/dl)	25.75 \pm 1.1	26.92 \pm 3.7	59.75 \pm 3.2 *	28.25 \pm 0.5 **
SC(mg/dl)	0.31 \pm 0.01	0.30 \pm 0.3	0.84 \pm 0.05 *	0.32 \pm 0.02#
Urinary albumin (mg/dl)	0	0	43.6 \pm 0.1*	0.5 \pm 0.1**
Urinary glucose (mg/dl)	0	0	125 \pm 5*	3 \pm 0.05**
Serum GSH (mg%)	37.69 \pm 0.55	37.01 \pm 0.1	24.94 \pm 0.73*	36.91 \pm 0.68 #

Values shown are mean \pm SE(n=10 rats per each group). The experimental groups include control group; C, control group+ honey; C/H, paracetamol-induced nephrotoxic group; N, honey pretreatment to nephrotoxic group; H/N. As compared with control group (*), N group (#) (one-way ANOVA) followed by LSD test), *P* < 0.05, *P* < 0.0005.

Effect of paracetamol-induced nephrotoxicity and their pretreatment with clover flowershoney on the assessed oxidative stress indicators

72 hours after induction of acute kidney failure by paracetamol in group III(N), the serum level of GSH was significantly reduced (*P* < 0.05) to reach nearly 33% of its normal level in the control animals (Table 1). This highlights the hampered antioxidant system, which was further extended to the renal tissues.

Renal activities of SOD and CAT were significantly depressed (-72%, -52.5%, respectively at *P* < 0.0005) in group III, compared to the control group.

Results

Effect of paracetamol-induced nephrotoxicity and their pretreatment with clover flowers honey on the renal functions

Table 1 depicts the paracetamol-induced nephrotoxicity as reflected by the disturbed kidney functions. The applied model of paracetamol-induced nephrotoxicity in group II(N) caused a significant elevation of serum levels BUN (2.8 times, *P* < 0.0005) and SC (2.2 times, *P* < 0.0005), compared to the normal control group. The disturbance of the kidney functions was further reflected on its defective reabsorptive capacity of albumin and protein, which led to their appearance in high quantities in the urine.

Pretreatment with clover flowers honey (2 gm/kg b.wt./day) for 4 weeks prior to paracetamol administration (Group IV, H/N) showed significant depression of the levels of BUN(-52.7%), SC (-62%); both reaching their normal levels, when compared to nephrotoxic group II (N), at *P* < 0.0005. The significant depletion of urinary albumin (-98.8%, *P* < 0.0005) and urinary glucose (-97.6%, *P* < 0.0005), which were rendered non-traceable in the urine, indicated a successful renoprotective impact of clover flowers honey.

Pretreatment with clover flowers honey for 4 weeks succeeded to restore the total antioxidant capacity at the blood as well as the renal tissues. It prevented the GSH depletion by causing a significant increase in its level (62%, *P* < 0.0005), when compared to the nephrotoxic group III (N).

The amelioration of the renal SOD and CAT activities in group III, due to the prophylactic use of clover flowers honey, was reflected on a 2.7 fold increase in renal SOD activity and a 1.9 fold increase in renal CAT activity in group IV (H/N), at *P* < 0.0005 (Figure 1).

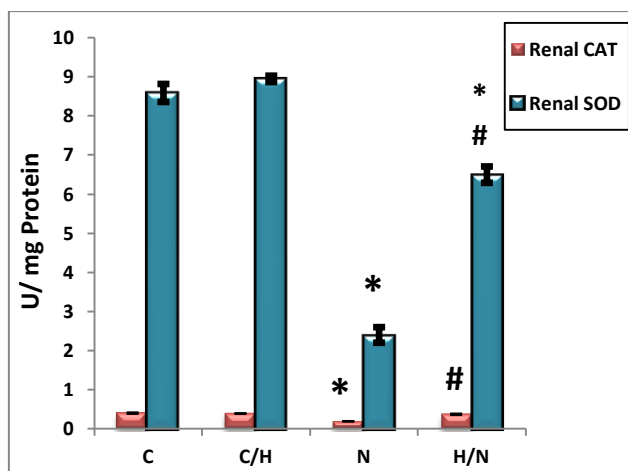


Fig. 1: Mean activities of renal SOD and CAT \pm SE. The experimental groups include control group; C, control group + honey; C/H, paracetamol-induced nephrotoxic group; N, honey pretreatment to nephrotoxic group; H/N. As compared with control group (*), N group (#) (one-way ANOVA) followed by LSD test), $P < 0.05$, $P < 0.0005$.

Effect of paracetamol-induced nephrotoxicity and their pretreatment with clover flowershoney on renal TNF- α gene expression:

Figure 2 illustrates the impact of the nephrotoxic model on the renal tissue gene expression of the apoptotic indicator, TNF- α . The induced nephrotoxicity significantly elevated the renal tissue TNF- α gene expression (5.6 times, $P < 0.003$) when compared to normal. The anti-apoptotic effect of clover flowershoney was reflected by the significant amelioration of the renal tissue TNF- α gene expression (-31%, $P < 0.0005$), an effect that could be correlated to its antioxidant activity.

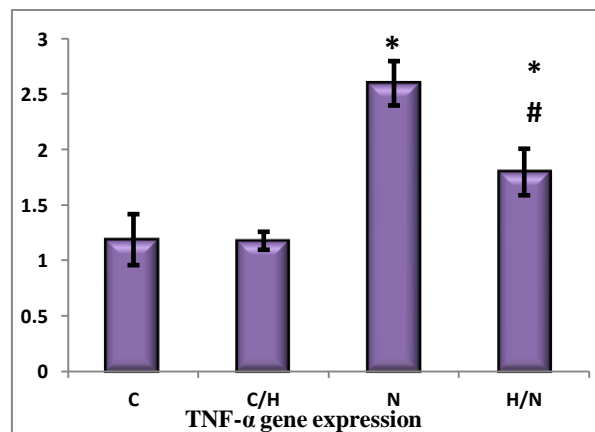


Fig. 2: Mean TNF- α gene expression \pm SE. The experimental groups include control group; C, control group + honey; C/H, paracetamol-induced nephrotoxic group; N, honey pretreatment to nephrotoxic group; H/N. As compared with control group (*), N group (#) (one-way ANOVA) followed by LSD test), $P < 0.05$, $P < 0.0005$.

4. Discussion

Paracetamol toxic overdose is often linked to many metabolic disorders including serum electrolyte, urea and creatinine derangements. Serum urea and creatinine are considered nephrotoxicity markers, but serum urea concentration is often considered a more reliable renal function predictor than serum creatinine (Palani *et al.*, 2009).

In the present study, administration of nephrotoxic dose of paracetamol to rats resulted in a significant elevation of serum levels of urea and creatinine in paracetamol administered group when compared to the normal control group. These results are in agreement with that observed by Isik *et al.* (2006) who noticed an elevation in serum urea and creatinine in rats after 1 g/kg b.w. of paracetamol administration. Moreover Satirapoj *et al.* (2009) reported an elevation in serum urea and creatinine in a woman following therapeutic dose of paracetamol three days before hospital admission.

Karadeniz *et al.* (2008) and Ajami *et al.* (2010) explained this elevation in the levels of urea and creatinine by the presence of strong correlation between nephrotoxicity and oxidative stress. The elevated H_2O_2 and O_2^- production alters the filtration surface area and modifies the filtration coefficient; both factors could decrease the glomerular filtration leading to accumulation of urea and creatinine in the blood.

Acute paracetamol intoxication induced significant appearance of glucose and protein in urine. These results are in agreement with that observed by Melo *et al.* (2006) who noticed an increase in the urinary excretion of albumin and glucose after paracetamol injection associated with augmented serum urea and creatinine, both indicating glomerular damage. Abdel-Raheem *et al.* (2009) reported that detection of small quantities of urinary albumin is one of the early biomarkers of altered glomerular permeability. The appearance of glucose and protein may be attributed to the dysfunction of the proximal convoluted tubule because glucose and proteins are completely absorbed from the proximal convoluted tubules under normal conditions. These results are supported by the findings of Abdel-Zaher *et al.* (2008), who stated that the nephrotoxicity induced by paracetamol overdose was characterized by damage and necrosis in the proximal tubule.

Abbate *et al.* (2006) reported that progressive renal damage by proteinuria may be a mechanism that exerts destructive effect on the kidney. Proteinuria may accelerate kidney disease progression to end stage renal failure and whenever proteinuria is decreased by treatment, progression to end stage renal dysfunction is reduced.

Several studies have clearly demonstrated that acute paracetamol overdose induces renal oxidative

stress as manifested by a decrease in antioxidant enzymes and an increase in lipid peroxidation product (malondialdehyde) (*Abdel – Zaher et al., 2007 and Ghosh & Sil, 2007*).

The current study showed that the administration of paracetamol (APAP) in acute single toxic dose resulted in a significant decrease in renal SOD and CAT activities when compared to control group. The present results are in agreement with that observed by *Palani et al. (2009)* and *Demirbag et al. (2010)* who observe a significant decrease in levels of SOD and CAT after acute paracetamol overdose administration to rats when compared with normal control rats and explain these results on the base that paracetamol overdose enhances lipid peroxidation or inactivates the antioxidative enzymes. In addition, *Linares et al. (2006)* reported that, during kidney injury, superoxide radicals are generated at the site of damage and modulate SOD and CAT, resulting in the loss of activity and accumulation of superoxide radical, which damages kidney. SOD and CAT are the most important enzymes involved in ameliorating the effects of oxygen metabolism.

Current evidence suggests that intracellular GSH plays an essential role in detoxification of APAP and prevention of APAP-induced toxicity in the liver and kidney (*Newton et al., 1996 and Richie et al., 1996*). The generation of the reactive oxygen species appears as an early event which precedes intracellular GSH depletion and cell damage in paracetamol toxicity (*Manov et al., 2003*).

In the present study, paracetamol overdose administration caused a significant decrease in serum GSH content. This decrease in GSH level could be considered another mechanism for the observed paracetamol nephrotoxicity and suggests that the administration of high dose of paracetamol saturates the metabolic pathway, decreases the liver clearance of APAP and allows higher amounts of the un-metabolized drug to come in contact with the kidney (*Gu et al., 2005*). Because the same enzyme system as the liver is also present in the kidney, it is most probable that N-acetyl-P-benzoquinone imine (NAPQI) will also be formed in the kidneys, giving rise to toxicity but much later than in the liver (*Roberts and Bukley, 2007*). The major pathway of metabolism during toxicity is via CYP-450 due to saturation of glucuronidation and sulfation pathways forming the intermediate NAPQI in high amounts which in turn will be conjugated with GSH to detoxify this product with consequent exhaustion of cellular GSH reserve (*Sener et al., 2005*). At sufficiently high doses, GSH becomes depleted leaving NAPQI free (*Dai et al., 2006*). The free NAPQI is strongly electrophilic and binds covalently and irreversibly to critical cellular, protein causing cellular necrosis (*James et al., 2003*).

Tumor necrosis factor- α is one of the most important proinflammatory cytokines that can cause cell death through binding to its specific receptor tumor necrosis factor receptor on the cell surface. Accordingly, it was described to be increased in many diseases in which apoptosis is included in its mechanism such as glomerular injury, acute renal failure and chronic renal affection (*Locksley et al., 2001*).

The present study showed a significant increase in the renal TNF- α gene expression after acute paracetamol overdose administration. These results are supported by the study of *Das et al. (2010)* who reported that paracetamol administration at a single dose of 2g/kg body weight orally to male adult albino mice increased plasma level of blood urea, creatinine and TNF-alpha. This increase is explained in terms of the induction of renal damage through oxidative stress.

The increased TNF- α gene expression could be attributed to activation of apoptosis pathways. Apoptosis can result from the activation of death receptors in response to ligand binding (*Servais et al., 2008*). *Abeet et al. (2004)* reported another mechanism that increases TNF- α which is proteinurea that can result in complement activation, production of reactive oxygen species and cytokines synthesis e.g. TNF- α . *Morais et al. (2005)* reported that the exposure of proximal tubular cells to albumin produced strong upregulation in the expression of Fas and Fas ligand and apoptotic response. This finding correlates with the present results that showed proteinurea associated with an increase in some apoptotic markers as TNF- α .

Ghosh et al. (2010) stated that, exposure of rats with a nephro-toxic dose of APAP altered a number of biomarkers (like blood urea nitrogen and serum creatinine levels) and decreased the renal oxidative stress markers with elevation of renal tumor necrosis factor-alpha, these changes were occurred as a result to inactivation of the mitochondrial pathway during APAP-induced cell death.

The therapeutic role of honey in the treatment of various ailments has been receiving considerable attention recently, and its therapeutic value has been partly attributed to its anti-inflammatory, anti-apoptotic and antioxidant properties.

Interestingly, the present study revealed that prophylactic administration of clover flowers honey for 4 weeks before acute paracetamol overdose administration resulted in improvement of the kidney functions in the form of nearly complete absence of glucose and protein from urine, which could be attributed to the glomerular repair. These results are in accordance with *Jaganathan and Mandal (2009)* who reported an improvement in kidney functions after honey administration in rats with induced nephrotoxicity.

The current study showed that a significant elevation of the oxidative stress enzymes SOD, CAT and GSH enzyme activities results from honey administration. This increase coincides with *Omotayo et al. (2010)* who reported that honey supplementation ameliorates oxidative stress in kidneys of diabetic rats, which was proved by significant reduction of the activities of catalase (CAT) and glutathione. Also *Cavuşoğlu et al. (2009)* reported that the protective role of the honey in cases of cadmium induced genotoxicity in mice may be attributed to its anti-oxidant effect.

The present results are also consistent with those of *Jaganathan and Mandal (2009)* who reported that improvement of kidney functions and the correction of decreased level of oxidative stress enzymes in the form of SOD, CAT and Serum GSH by the use of honey are related to some minor constituents of honey, which is believed to have antioxidant properties. Among these constituents are flavonoids and phenolic acids, certain enzymes (glucose oxidase, catalase), ascorbic acid, carotenoid-like substances, organic acids, amino acids, and proteins.

Clover flowers honey supplementation for 4 weeks before paracetamol administration protected against paracetamol induced renal damage as indicated by reducing the elevated serum urea and creatinine. These results are inconsistent with *Al-Waili et al. (2006)* who noticed a significant decrease in serum urea and creatinine after honey treatment as it corrects the influence of hemorrhage and food restriction on renal functions.

The obtained results showed reduction in TNF- α gene expression in paracetamol induced nephrotoxicity after honey treatment which could be attributed to the anti-inflammatory, antiapoptotic and healing effect of honey.

These results are consistent with *Majtan et al. (2010)* who reported that, honey decreases the elevated TNF alpha and plays an important role in healing through degradation of type IV collagen in the basement membrane of tissues. So, honey may accelerate wound healing process.

The anti-inflammatory properties of honey were also proved by the histopathological evaluation of the inflamed eyes of rabbits treated by honey in the study of *Öztürk et al. (2002)*. They found that the degree of inflammatory cell infiltration was significantly lower in the group treated with topical honey. This suppression of the inflammatory cells could be the cause of the decreased gene expression of TNF- α after honey treatment in APAP induced nephrotoxicity.

Similar findings were also recorded by *Han et al. (2007)* who reported that honey has immunomodulatory properties which could be useful in inhibiting the production of inflammatory cytokine and NO production in neurodegenerative diseases.

In conclusion, our study showed that honey has the ability to contribute to glomerular and tubular repair and recovery of the kidney from nephrotoxicity, which is proved by the improvements of the kidney function parameters and the decrease of the antioxidant and anti-inflammatory markers. Thus, honey is suggested to have a beneficial effect on renal tissue through potent paracrine anti-apoptotic and anti-inflammatory mechanisms.

Corresponding author

Basma K. Ramadan

Physiology Department, Faculty of Medicine for Girls,
Al-Azhar University

basma_phy@hotmail.com

References

- Abbate, M.; Zoja, C. and Remuzzi, G. (2006):** How does proteinuria cause progressive renal damage? *J Am SocNephrol.*, 17: 2974-2984.
- Abdel – Zaher, A.; Abdel – Hady, R.; Mahmoud, M. and Farrag, M. (2008):** The potential protective role of alpha-lipoic acid against acetaminophen-induced hepatic and renal damage. *Toxicol.*, 243 (3): 261 – 70.
- Abdel-Raheem, I.T.; Abdel-Ghany, A.A. and Mohamed, G.A. (2009):** Protective effect of quercetin against gentamicin-induced nephrotoxicity in rats. *Biol. Pharm. Bull.* 32(1): 61-67.
- Abdel-Zaher, A.; Abdel-Rahman, M.; Hafez, M. and Omran, F. (2007):** Role of nitric oxide and reduced glutathione in the protective effects of aminoguanidine, gadolinium chloride and oleanolic acid against acetaminophen-induced hepatic and renal damage. *Toxicol.*, 234 (1-2): 124-34.
- Abe, K.; Li, K.; Sacks, S.H. and Sheerin, N.S. (2004):** The membrane attack complex, C5b-9, up regulates collagen gene expression in renal tubular epithelial cells. *Clin. Exp. Immunol.*, 136: 60-66.
- Ajami, M.; Eghtesadi, S.; Pazoki-Toroudi, H.; Habibey, R. and Ebrahimi, S.A. (2010):** Effect of *Crocus sativus* on gentamicin induced nephrotoxicity. *Biol Res.*, 43: 83-90.
- Aljadi, A.M. and Kamaruddin, M.Y. (2004):** Evaluation of the phenolic contents and antioxidant capacities of two Malaysian floral honeys. *Food Chemistry.* 85: 513-518.
- Al-Waili, N.S.; Saloom, K.Y.; Akmal, M.; Al-Waili, F., Al-Waili, T.N.; Al-Waili, A.N. and Ali, A. (2006):** Honey ameliorates influence of hemorrhage and food restriction on renal and hepatic functions,

- and hematological and biochemical variables. *Int J Food Sci Nutr.*, 57(5-6): 353-62.
- Cavuşoğlu, K.; Yapar, K. and Yalçın, E. (2009):** Royal jelly (honey bee) is a potential antioxidant against cadmium-induced genotoxicity and oxidative stress in albino mice. *J Med Food*, 12 (6): 1286-92.
- Claiborne, A. (1985):** Catalase activity: In: handbook of method for oxygen radical research. Green Wald, R.A. (ed), Boca Raton, Florida: CRC. Press, PP: 283-4.
- Dai, G.; He, L.; Chou, N. and Wan, Y. (2006):** Acetaminophen metabolism does not contribute to gender difference in its hepatotoxicity in mouse. *Toxicol. Sci.*, 92(1): 33-41.
- Das, J.; Ghosh, J.; Manna, P. and Sil, P.C. (2010):** Taurine protects acetaminophen-induced oxidative damage in mice kidney though APAP urinary excretion and CYP2E1 inactivation. *Toxicology*. 269(1): 24-34.
- Demirbag, S.; Uysal, B.; Guven, A.; Cayci, T.; Ozler, M. and Ozcan, A. (2010):** Effects of medical ozone therapy on acetaminophen-induced nephrotoxicity in rats. *Renal failure*, 32:493-499.
- Devi, K.P; Sreepriya, M; Balakrishna, K. and Devaki, T. (2005):** Protective effect of Premnatomentosa extract (*L.verbanacae*) on acetaminophen-induced mitochondrial dysfunction in rats. *Mol. CollBiochem.*, 272(1-2): 171-177.
- Ggosh, A. and Sil, P.C. (2007):** Anti-oxidative effect of a protein from *Cajanusindicus L* against acetaminophen-induced hepato-nephrotoxicity. *J. Biochem. Mol. Biol.*, 40(6): 1039-49.
- Ghosh, J.; Das, J.; Manna, P. and Sil, P.C. (2010):** Acetaminophen induced renal injury via oxidative stress and TNF-alpha production: therapeutic potential of arjunolic acid. *Toxicology*. 268 (1-2): 8-18.
- Gu, J.; Cui, H.; Zhang, L.; Zhang, Q.; Yang, W.; Hinson, J. and Ding, X. (2005):** In vivo mechanisms of tissue-selective drug toxicity: effects of liver-specific knockout of the NADPH-cytochrome P450 reductase gene on acetaminophen toxicity in kidney, lung, and nasal mucosa. *Mol. Pharmacol.*, 67(3): 623-30.
- Han, S.; Lee, K.; Yeo, J.; Kweon, H.; Woo, S.; Lee, M.; Baek, H.; Kim, S. and Park, K. (2007):** Effect of honey bee venom on microglial ceels nitric oxide and tumor necrosis factor-alpha production stimulated by LPS. *J Ethnopharmacol*, 111(1): 176-81.
- Henry, J. (1991):** Clinical diagnosis and management. 18th ed. Pbl. Philadelphia, W.B. Saunders Company. PP.156-9.
- Isik, B.; Bayrak, R.; Akcay, A. and Sogut, S. (2006):** Erdosteine against acetaminophen-induced renal toxicity. *Mol.Cell. Biochem.*, 287 (1-2): 185-91.
- Jaganathan, S.K. and Mandal, M. (2009):** Honey constituents and its apoptotic effect in colon cancer cells. *Journal of Apiprodukt and Apimedical Science*, 1:29-36.
- James, L.; McCullough, S.; Lamps, L. and Hinson, J. (2003):** Effect of N-acetylcysteine on acetaminophen toxicity in mice: relationship to reactive nitrogen and cytokine formation. *Toxicol. Sci.*, 75(2): 458-67.
- Jaeschke H, Knight TR, Bajt ML (2003):** The role of oxidant stress and reactive nitrogen species in acetaminophen hepatotoxicity. *ToxicolLett*; 144:279-88.
- Karadeniz, A; Yildirim, A.; Simsek, N.; Kalkan, Y. and Celebi, F. (2008):** Spirulinaplatis protects against gentamicin-induced nephrotoxicity in rats. *Phytother.Res.* 22, 1506-1510.
- Linares, M.V.; Belles, M.; Albina, M.L.; Sirvent, J.J. and Sanchez, D.J. (2006):** Assessment of the pro-oxidant activity of uranium in kidney and testis of rats. *ToxicolLett.*, 167: 152-61.
- Locksley, R.M.; Killeen, K.N. and Lenardo, M.J. (2001):** The TNF and TNF receptor superfamilies: integrating Mammalian Biology. *Cell*, 104: 487-501.
- Lowry, O.H.; Rosebrough, N. J., Farr, A. L., and Randall, R. J. (1951):** Protein Measurement with the Folin Phenol Reagent. *J. Biol. Chem.*, 193: 265-275.
- Majtan, J.; Kumar, P.; Majtan, T.; Walls, A.F. and Klaudiny, J. (2010):** Effect of honey and its major royal jelly protein 1 on cytokine and MMP-9 mRNA transcripts in human keratinocytes. *ExpDermatol.*, 19(8): e73-9.
- Manov, I.; Hirsh, M. and Iancu, T.C. (2003):** Acetaminophen hepatotoxicity and mechanisms of its protection by N-acetylcysteine: a study of Hep 3B cells. *Exp. Toxicol. Pathol.*, 53:489-500.
- Marieb, E. (2006):** Urinary system. In: Essentials of human anatomy and physiology. 8th ed., pbl. Pearson Benjamin Cummings, San Fransisco, Boston, New York, London and Madrid ip: PP. 501-26.

- Marklund, S.L. (1985):** Pyrogallol Antioxidation. In: Handbook of method for oxygen radical research. Greenwald, R.A. (Ed), pbl. Boca Raton, Florida: CRC. Press, USA, PP. 243-247.
- Melo, D.; Sociura, V.; Poloni, j.; Oliveira, C.; Filho, J.; padilha, R.; Reichel, C.; Neto, E.; Oliveira, R.; Davila, L.; Kessler, A. and Oliveira, J. (2006):** Evaluation of renal enzymuria and cellular excretion as a marker of acute nephrotoxicity by APAP overdose in Wistar rats. *Clinica. Chemica.Acta*, 373: 88-91.
- Morais, C.; Westhuyzen, J.; Metharom, P. and Healy, H. (2005):** High molecular weight plasma proteins induce apoptosis and Fas/FasL expression in human proximal tubular cells. *Nephrol. Dial. Transplant.*, 20: 50-58.
- Newton, J.; Hoefle, D.; Gemborys, M.; Mugege, G. and Hook, J. (1996):** Metabolism and excretion of glutathione conjugate of acetaminophen in the isolated rat kidney. *J. Pharmacol. Exp. Ther.*, 237: 519-524.
- Omotayo, E.O.; Gurtu, S.; Sulaiman, S.A., AbWahab, M.S.; Sirajudeen, K.N. and Salleh, M.S. (2010):** Hypoglycemic and antioxidant effect of honey supplementation in streptozotocin-induced diabetic rats. *Int. J. Vitam Nutr Res.*, 80 (1): 74-82.
- Ozkaya, O.; Genc, G.; Bek, K. and Sullu, Y. (2010):** A case of acetaminophen (paracetamol) causing renal failure without liver damage in a child. *Renal Failure*, 32: 1125-1127.
- Öztürk, F.; Kurt, E.; Cerçi, M.; Emiroglu, L.; Inan, U.; Türker, M. and Ilker, S. (2000):** The effect of propolis extract in experimental chemical corneal injury. *Ophthalmic Res.*, 32(1): 13-18.
- Palani, S.; Raja, S.; Praveen Kumar, R.; Soumya Jayakumar, B. and Senthil, K. (2009):** Therapeutic efficacy of *Pimpinella tirupatiensis* (Apiaceae) on acetaminophen induced nephrotoxicity and oxidative stress in male albino rats. *International Journal of Pharm Tech Research*, 1(3): 925 – 934.
- Pannu, N. and Nadim, M. (2008):** An overview of drug induced acute kidney injury. *Crit. Care Med.*, 36 (4 supp): S216-23.
- Richie, J.R.; Long, C.A. and Chen, T.S. (1996):** Acetaminophen-induced depletion of glutathione and cysteine in aging mouse kidney. *Biochem. Pharmacol.*, 44: 129-135.
- Roberts, D. and Buckley, N. (2007):** Pharmacokinetic considerations in clinical toxicology: Clinical Applications. *Clin. Pharmacokinet.*, 46(11): 897-939.
- Satirapoj, B.; Lohacit, P. and Ruamvang, T. (2009):** Therapeutic dose of acetaminophen with fatal hepatic necrosis and acute renal failure. *J. Med. Assoc. Thai.*, 90 (6): 1244-47.
- Schramm, D.D.; Karim, M.; Schrader, H.R.; Holt, R.R.; Cardetti, M. and Keen, C.L. (2003):** honey with high levels of antioxidants can provide protection to healthy human subjects. *J Agric Food Chem.*, 51(6): 1732-1735.
- Sener, G.; Sehirli, O.; Cetinel, S.; Yegen, B. Gedik, N. and Ayanoglu-Dugler, G. (2005):** Protective effects of MESNA (2-mercaptoethane sulphonate) against APAP hepatorenal oxidative damage in mice. *J. Appl. Toxicol.*, 25: 20-9.
- Servais, H.; Ortiz, A.; Devuyt, O.; Denamur, S.; Tulkens, P.M. and Mingeot-Leclercq, M.P. (2008):** Renal cell apoptosis induced by nephrotoxic drugs: cellular and molecular mechanisms and potential approaches to modulation. *Apoptosis*, 13: 11-32.
- Stern, S.; Bruno, M.; Hennig, G.; Horton, R.; Roberts, J. and Cohen, S (2005):** Contribution of acetaminophen- cysteine to acetaminophen nephrotoxicity in CD-1 mice. 1. Enhancement of acetaminophen nephrotoxicity by acetaminophen – cysteine. *Toxicol. Appl. Pharmacol*, 202 (2): 151-9.
- Williams, J.F. (1989):** Optimization strategies for the polymerase chain reaction. *Biotechniques*, 7: 762-769.
- Wilson, K. and Walker, J. (2000):** Practical Biochemistry: Principles and Techniques. 5th ed. Pbl. Cambridge, Cambridge University Press. PP: 630-89.

Non-Ulcer Dyspepsia: Abnormal Myoelectrical Activity and Gastric Emptying, Fact Or Fiction?.

Amal S. Bakir, Adel A. Mahmoud, Tarek M. Yousef and Mohamed A. Mostafa

Internal Medicine Department, Gastroenterology and Hepatology unit. Ain-Shams University, Cairo, Egypt

Amalshawky_mb@hotmail.com

Abstract: Background/Aim: Functional or non-ulcer dyspepsia is the presence of bothersome postprandial fullness, early satiation, epigastric pain and or epigastric burning sensation with no evidence of organic disease, systemic disease and/ or metabolic disease which explain the symptoms. The pathophysiology of non-ulcer dyspepsia is complex and includes many theories. This work was conducted to study the gastric myoelectrical activity and gastric emptying in Egyptian patients with non-ulcer dyspepsia. **Study design and methods:** This study was carried out on 150 subjects classified into three groups: **Group I:** included 50 patients with non-ulcer dyspepsia and *H.pylori* infection. **Group II:** included 50 patients with non-ulcer dyspepsia and without *H.pylori* infection. **Group III:** included 50 age and sex matched "healthy" asymptomatic volunteers; 25 positive and (IIIa) and 25 negative (IIIb) for *H.pylori*. All participants were subjected to abdominal ultrasonography for assessment of gastric emptying, Elecrogastrography for Gastric electrical activity recording and *H.pylori* infection was detected by histopathology of antral gastric biopsies for patient groups and by detection of antigen in stool for the control subjects. **Results:** Dominant frequency, percent of normal rhythm both fasting and after test meal, power of dominant frequency both fasting and after the test meal, and power ratio showed statistically non-significant difference between patients with non-ulcer dyspepsia and *H-pylori* infection and healthy subjects with *H-pylori* infection [2.8±0.56 vs. 2.79±0.39, 67.8±27.6 vs. 76.1±19.1, 75.57±23.18 vs. 71.9±18.53, 3280±2223.1 vs. 2309.8±1543.0, 5068.3±3037.8 vs. 5498.4±2751.3, and 2.44±3.68 vs. 2.94±1.92, respectively, with $p > 0.05$ in all comparisons]. Dominant frequency, percent of normal rhythm both fasting and postprandial, power of dominant frequency both fasting and postprandial, and power ratio was statistically non-significantly different on comparing patients with non-ulcer dyspepsia and without *H-pylori* infection and healthy subjects without *H-pylori* infection [3.01±0.26 vs. 2.95±0.35, 65.57±26.58 vs. 69.5± 31.36, 73.04±28.2 vs. 68.8±34.8, 2952.1±1765.19 vs. 2142.8±763.5, 3185.1±1859.9 vs. 4441.5±2124.3, and 1.48± 1.52 vs. 2.1±0.7 and $p > 0.05$ for all comparisons]. On comparing patients with non-ulcer dyspepsia and *H-pylori* infection to healthy subjects with *H-pylori* infection; Full emptying time was significantly shorter in patients with non-ulcer dyspepsia [12.85±3.17 vs. 15.4± 3.34, $p < 0.05$], while ½ emptying time, antral dimension both postprandial and fasting were statistically non-significantly different [5.06±2.02 vs. 6.39±2.43, 7.3±1.69 vs. 8.44± 3.8, and 4.14±1.37 vs. 4.3± 1.58, respectively, with $p > 0.05$ for all comparisons]. On comparing patients with non-ulcer dyspepsia without *H-pylori* infection and healthy subjects without *H-pylori* infection ; there was no significant statistical difference regarding the full emptying time, ½ emptying time, full antrum dimension, and fasting antrum dimension [15.45±2.79 vs. 15.7±2.75, 7.05±3.52 vs. 6.7±1.39, 7.71±1.39 vs. 8.85± 2.44, and 3.68±1.13 vs. 3.68±0.73 with $p > 0.05$ for all comparisons]. There was no significant statistical difference between the patients with *H-pylori* infection and non-ulcer dyspepsia before and after *H-pylori* eradication therapy regarding the dominant frequency, percent of normal rhythm both fasting and postprandial, power of the dominant frequency both fasting and postprandial, and power ratio [2.8±0.56 vs. 2.93±0.44, 67.8±27.6 vs. 80.67±23.0, 75.57±23.18 vs. 79.9±23.09, 3280±2223.1 vs. 3073.25±1465.96, 5068.3±3037.78 vs. 6167.15±2339.94, and 2.44±3.68 vs. 2.22±0.85, and $p > 0.05$ for all comparisons]. On comparing patients with non-ulcer dyspepsia and *H-pylori* infection before and after eradication therapy there was a non-significant statistical difference in full emptying time [12.85±3.17 vs. 14.45±1.85 and $p > 0.05$], but ½ emptying time was statistically significantly longer after eradication than that before [5.06±2.02 vs. 6.05±1.09 and $p < 0.05$], but, full antrum dimension and fasting antrum dimension was statistically non-significantly different before and after eradication therapy [7.3±1.69 vs. 7.37± 1.8 and 4.14± 1.37 vs. 4.12±1.19 with $p > 0.05$ for both comparisons. **Conclusion:** gastric myoelectrical activity is the same in patients with non-ulcer dyspepsia patients and healthy subjects regardless of the *H-pylori* status. *H-pylori* infection in non-ulcer dyspepsia patients may accelerate gastric emptying and *H-pylori* eradication therapy improves that abnormal gastric emptying. Non-ulcer dyspepsia patients without *H-pylori* infection may have different pathophysiological mechanisms than those with *H-pylori* infection.

[Amal S. Bakir, Adel A. Mahmoud, Tarek M. Yousef and Mohamed A. Mostafa. **Non-Ulcer Dyspepsia: Abnormal Myoelectrical Activity and Gastric Emptying, Fact Or Fiction?** *Life Sci J* 2011;8(3):597-603] (ISSN:1097-8135). <http://www.lifesciencesite.com>. 93

Key words: non-ulcer dyspepsia, abnormal myoelectrical activity and gastric emptying.

1. Introduction

Functional or non-ulcer dyspepsia [NUD] is the presence of bothersome postprandial fullness, early satiation, epigastric pain and or epigastric burning sensation with no evidence of organic disease [including at upper endoscopy], systemic disease and/or metabolic disease which explain the symptoms. These symptoms should be present in the last 3 months and symptoms onset at least 6 months prior to the diagnosis. There are two subcategories, the postprandial distress syndrome and the epigastric pain syndrome [1].

The pathophysiology of NUD includes many theories; dysmotility has been the prim focus of interest in functional dyspepsia including delayed gastric emptying, accelerated gastric emptying, impaired fundic accommodation, unsuppressed postprandial fundic contractility, antral distension, and duodenal dysmotility [2]. Visceral hypersensitivity is present in 30-40% of patients with functional dyspepsia based on the barostat technique and water load test [3]. Aberrant cerebral processing of visceral stimuli in the form of lack of activation of the medial pain system and activation of the lateral pain system components at lower distending pressures occurs in NUD patients with visceral hypersensitivity [4]. Gastric tone and motility are influenced by duodeno-gastric reflexes, whose dysfunction has been proposed to play a role in the pathogenesis of symptoms in NUD. Receptors involved in this reflex include those for CCKA, dopamine, 5-HT1A, and gastrin releasing peptide [5]. Gastric myoelectrical abnormality such as tachygastric, bradygastric and flat line pattern has been reported in patients with NUD [6].

Gastric colonization by *H.pylori* has been found in 33-79% of patients with non-ulcer dyspepsia [7]. The possible effect of *H.pylori* infection on gastric motor function may be mediated by alternation of gastrin levels, gastric acid hypersecretion and release of cytokines (IL-1B, IL-6, IL-8, and TNF) [8]. Interaction between polymorphisms of genes responsible for components of the immune response and *H.pylori* infection among some patients with functional dyspepsia is suggested by a Japanese study [9].

Aim of the work:

This work was conducted to study the gastric myoelectrical activity and gastric emptying in Egyptian patients with non-ulcer dyspepsia.

2. Study design and methods:

This study was carried out on 150 subjects classified into three groups: Group I: included 50 patients with non-ulcer dyspepsia and *H.pylori* infection, 20 females and 30 males with mean age 44 ± 15.64 years. Group II: included 50 patients with non-ulcer dyspepsia and without *H.pylori* infection, 20

females and 30 males with mean age 42 ± 14.42 years. Group III: included 50 age and sex matched "healthy" asymptomatic volunteers; 25 positive (IIIa) and 25 negative (IIIb) for *H.pylori*. The following were excluded from the study; patients with diabetes mellitus, patients with end-organ failure [e.g. renal and liver cell failure], patients with calculic and non-calculic cholecystitis, pregnant females, females taking contraceptive pills, patients taking drugs affecting gastric motility [e.g. prokinetics, anticholinergics, antibiotics like macrolides, dopaminergic agonists, adrenergic agents], patients with previous abdominal surgery and patients with systemic illness. All participants were subjected to the following: 1. Full history taking; Subjects were asked about dyspeptic symptoms (e.g. nausea, vomiting, belching, fullness, bloating, epigastric pain). 2. Thorough clinical examination. 3. Laboratory investigations; Complete blood count, ESR, fasting and 2-hour postprandial blood sugar, liver function tests [serum albumin, total proteins, total and direct bilirubin, transaminases, Prothrombin time], kidney function tests [BUN, creatinine, Serum electrolytes], Urinalysis, stool analysis. 4. Chest X-ray, abdominal ultrasonography [U/S]. 5. Upper gastrointestinal endoscopy for patients with NUD and antral biopsies were taken. 6. Histopathological examination of antral biopsied tissue for *H.pylori* infection determination. 7. Abdominal ultrasonography for assessment of gastric emptying: All subjects were fasting for at least 6 hours before examination, abdominal U/S was performed with 3.5 array transducer. With the subject sitting in a chair and slightly inclined backwards, the sonographic probe was positioned at the epigastrium to measure the pre-spinal antral area at the level of antrum-body junction in a single section. The superior mesenteric vein and the aorta were used as a reference points to standardize the scan position. Both patient's sitting position and small volume of liquid meal (<300ml water) are safe factors against floating of gastric contents in the corpus and fundus. The following markers of gastric motility were measured: A. Basal antral area: was the mean of two measurements taken 5 and 0 min. before the meal. B. Maximal postprandial antral area: was measured after maximal widening of the antrum had occurred, usually within 2 min. postprandial. C. Minimal postprandial antral area: was the smallest area measured at any time postprandial. D. Half emptying time: was the time in minutes to observe a 50% decrease in maximal antral area [t ½ time], Calculated by linear regression analysis from the linear part of antral emptying curve. Antral emptying curves were obtained by plotting antral area vs. time [10]. 8. Electrogastrigraphy: Gastric electrical activity was recorded from five disposal pre-gelled silver chloride surface electrodes placed on the upper abdomen. This was done after the skin has been carefully abraded to

decrease resistance to obtain a good signal to noise ratio. The patient was kept in a reclining position to minimize motion artifacts. Four EGG signals were recorded bipolar from these five electrodes as the potential differences between each of the four electrodes, and one central electrode. A reference electrode was placed at the left clavicle. The electrical signals are recorded with appropriate amplification and filtering. One hour recording while the patient is fasting was done, then given a standardized test meal [pastes and 250ml milk] and postprandial recording for one hour was done. After the recording session the EGG signals were subjected to spectral analysis [Fast Fourier Transform]. The dominant frequency [The frequency with the highest power], the percent of normal rhythm both fasting and postprandial, the power of the dominant frequency [The dominant power] both fasting and postprandial, and the power ratio [the ratio of the power of the mean spectrum of the postprandial state to the power of the mean spectrum of the fasting state, indicative of the postprandial increase in gastric motor activity] were determined for each subject. Dysrhythmia was defined as follows: A tachygastric was considered to be present when the power spectrum contained a sharp-peaked component with a frequency >3.7 cpm and <10.8 cpm, which was not of respiratory origin. For a definite diagnosis of tachygastric it was required that at the same time the normal gastric signal (2.6-3.7 cpm) was absent in all four EGG signals and that the abnormal rhythm was present for at least 2min. A so-called bradygastric was defined as presence of a sharp peak at a frequency less than 2.6 cpm, in the absence of a normal 3 cpm component in all four EGG leads. 9. *Helicobacter pylori* eradication therapy: An eradication triple regimen for *H.pylori* [omeprazole 20mg bid, amoxicillin 1g bid and clarithromycin 500mg bid] was given for 10 days for every *H.pylori* positive patient, followed by 20 days of omeprazole. 10. Endoscopy, electrogastrigraphy, and measurement of gastric emptying time using ultrasonography, were repeated one month after completion of therapy. 10. Detection of *H.pylori* status in the control group: *H.pylori* status in the control group V was assessed by detection of *H.pylori* antigen in stool. 11. Statistical analysis of results: student *t* test was used for comparison between different groups and a *p* value < 0.05 was considered statistically significant.

Informed consent was obtained from all participants before enrollment in the study. The study was approved by the local ethical committee.

Statistical analysis:

Data were analyzed using Statistical Program for Social Science (SPSS) version 17.0. Quantitative data were expressed as mean \pm standard deviation (SD). Comparison between two independent mean groups for

parametric data using student T test, the probability of error at or less than 0.05 was considered significant.

3. Results:

Dominant frequency, percent of normal rhythm both fasting and after test meal, power of dominant frequency both fasting and after the test meal, and power ratio showed statistically non-significant difference between patients with non-ulcer dyspepsia and *H.pylori* infection and healthy subjects with *H.pylori* infection [2.8 \pm 0.56 vs. 2.79 \pm 0.39, 67.8 \pm 27.6 vs. 76.1 \pm 19.1, 75.57 \pm 23.18 vs. 71.9 \pm 18.53, 3280 \pm 2223.1 vs. 2309.8 \pm 1543.0, 5068.3 \pm 3037.8 vs. 5498.4 \pm 2751.3, and 2.44 \pm 3.68 vs. 2.94 \pm 1.92, respectively, with *p* > 0.05 in all comparisons [Table 1].

Dominant frequency, percent of normal rhythm both fasting and postprandial, power of dominant frequency both fasting and postprandial, and power ratio was statistically non-significantly different on comparing patients with non-ulcer dyspepsia and without *H.pylori* infection and healthy subjects without *H.pylori* infection [3.01 \pm 0.26 vs. 2.95 \pm 0.35, 65.57 \pm 26.58 vs. 69.5 \pm 31.36, 73.04 \pm 28.2 vs. 68.8 \pm 34.8, 2952.1 \pm 1765.19 vs. 2142.8 \pm 763.5, 3185.1 \pm 1859.9 vs. 4441.5 \pm 2124.3, and 1.48 \pm 1.52 vs. 2.1 \pm 0.7, respectively, and *p* > 0.05 for all comparisons.] [Table 2].

On comparing patients with non-ulcer dyspepsia and *H.pylori* infection to healthy subjects with *H.pylori* infection; Full emptying time was significantly shorter in patients with non-ulcer dyspepsia [12.85 \pm 3.17 vs. 15.4 \pm 3.34, *p* < 0.05], while $\frac{1}{2}$ emptying time, antral dimension both postprandial and fasting were statistically non-significantly different [5.06 \pm 2.02 vs. 6.39 \pm 2.43, 7.3 \pm 1.69 vs. 8.44 \pm 3.8, and 4.14 \pm 1.37 vs. 4.3 \pm 1.58, respectively, with *p* > 0.05 for all comparisons] [Table 3].

On comparing patients with non-ulcer dyspepsia without *H.pylori* infection and healthy subjects without *H.pylori* infection; there was no significant statistical difference regarding the full emptying time, $\frac{1}{2}$ emptying time, full antrum dimension, and fasting antrum dimension [15.45 \pm 2.79 vs. 15.7 \pm 2.75, 7.05 \pm 3.52 vs. 6.7 \pm 1.39, 7.71 \pm 1.39 vs. 8.85 \pm 2.44, and 3.68 \pm 1.13 vs. 3.68 \pm 0.73, respectively, with *p* > 0.05 for all comparisons] [Table 4].

There was no significant statistical difference between the patients with *H.pylori* infection and non-ulcer dyspepsia before and after *H.pylori* eradication therapy regarding the dominant frequency, percent of normal rhythm both fasting and postprandial, power of the dominant frequency both fasting and postprandial, and power ratio [2.8 \pm 0.56 vs. 2.93 \pm 0.44, 67.8 \pm 27.6 vs. 80.67 \pm 23.0, 75.57 \pm 23.18 vs. 79.9 \pm 23.09, 3280 \pm 2223.1 vs. 3073.25 \pm 1465.96, 5068.3 \pm 3037.8 vs. 6167.15 \pm 2339.94, and 2.44 \pm 3.68 vs. 2.22 \pm 0.85,

respectively, with $p > 0.05$ for all comparisons][Table 5].

On comparing patients with non-ulcer dyspepsia and *H-pylori* infection before and after eradication therapy there was a non-significant statistical difference in full emptying time[12.85±3.17 vs. 14.45±1.85 and $p > 0.05$], but ½ emptying time was

statistically significantly longer after eradication than that before[5.06±2.02 vs. 6.05±1.09 and $p < 0.05$], but, full antrum dimension and fasting antrum dimension was statistically non-significantly different before and after eradication therapy[7.3±1.69 vs. 7.37± 1.8 and 4.14± 1.37 vs. 4.12±1.19, respectively, with $p > 0.05$ for both comparisons][Table 6].

Table 1: Comparison between Group I and control [group III a] regarding EGG parameters expressed as mean ± SD:

Group EGG	Group I n=50	Group IIIa n=25	t value	P
DF (cpm)	2.8 ±0.56	2.79 ±0.39	0.07	>0.05
% normal rhythm [fasting]	67.8±27.6	76.1±19.1	0.84	>0.05
% normal rhythm [post prandial]	75.57±23.18	71.9 ±18.53	0.43	>0.05
Power- DF[fasting]	3280±2223.1	2309.8±1543.0	1.23	>0.05
Power- DF[post prandial]	5068.3±3037.8	5498.4 ±2751.3	0.38	>0.05
Power ratio	2.44 ±3.68	2.94 ±1.92	0.4	>0.05

DF; dominant frequency. Cpm; cycle per minute.

Table 2: Comparison between Group II and control [Group IIIb] regarding EGG parameters expressed in mean ± SD:

Group EGG	Group II n=50	Group IIIb n=25	t- value	P
DF (cpm)	3.01 ±0.26	2.95±0.35	0.49	>0.05
% normal rhythm [fasting]	65.57±26.58	69.5±31.36	0.36	>0.05
% normal rhythm [postprandial]	73.04 ±28.2	68.8 ±34.8	0.35	>0.05
Power -DF [fasting]	2952.1±1765.19	2142.8±763.5	1.37	>0.05
Power-DF [postprandial]	3185.1 ±1859.9	4441.5±2124.3	1.66	>0.05
Power ratio	1.48 ±1.52	2.1±0.7	1.2	>0.05

Table 3: Comparison between Group I and control [group IIIa] regarding gastric emptying parameters expressed in mean ± SD:

Group Emptying	Group I n=50	Group IIIa n=25	t -value	P
Full emptying time(min.)	12.85 ±3.17	15.4±3.34	2.04	<0.05
1/2 emptying time(min.)	5.06±2.02	6.39±2.43	1.59	>0.05
Full antrum (cm2)	7.3±1.69	8.44±3.8	1.13	>0.05
Fasting antrum(cm2)	4.14±1.37	4.3±1.58	0.3	>0.05

Table 4: Comparison between Group II and control [group IIIb] regarding gastric emptying parameters expressed in mean ± SD:

Group Emptying	Group II N=50	Group IIIb n=25	t- value	P
Full emptying time (min.)	15.45±2.79	15.7±2.75	0.23	>0.05
1/2 emptying time(min.)	7.05±3.52	6.7±1.39	0.26	>0.05
Full antrum(cm2)	7.71±1.39	8.85±2.44	1.64	>0.05
Fasting antrum(cm2)	3.68±1.13	3.87±0.73	0.48	>0.05

Table 5: Comparison among Group I patients before and after eradication therapy as regards EGG parameters expressed in mean \pm SD:

Group EGG	Before Eradication therapy	After Eradication therapy	t- value	P
DF (cpm)	2.8 \pm 0.56	2.93 \pm 0.44	1.05	>0.05
% normal rhythm [fasting]	67.8 \pm 27.6	80.67 \pm 23.0	1.38	>0.05
% normal rhythm Postprandial]	75.57 \pm 23.18	79.9 \pm 23.09	0.6	>0.05
Power-DF [fasting]	3280.0 \pm 2223.1	3073.25 \pm 1465.96	0.31	>0.05
Power-DF [postprandial]	5068.3 \pm 3037.78	6167.15 \pm 2339.94	1.27	>0.05
Power ratio	2.44 \pm 3.68	2.22 \pm 0.85	0.27	>0.05

Table 6: Comparison between group I patients regarding gastric emptying parameters before and after eradication therapy expressed in mean \pm SD:

Group Emptying	Before eradication therapy	After eradication therapy	t- value	P
Full emptying time (min.)	12.85 \pm 3.17	14.45 \pm 1.85	2.22	>0.05
1/2 emptying time (min.)	5.06 \pm 2.02	6.05 \pm 1.9	1.74	<0.05
Full antrum (cm ²)	7.3 \pm 1.69	7.37 \pm 1.8	0.13	>0.05
Fasting antrum(cm ²)	4.14 \pm 1.37	4.12 \pm 1.19	0.06	>0.05

4. Discussion:

The absence of statistically significant difference in EGG parameters between patients with non-ulcer dyspepsia with *H-pylori* infection and healthy subjects with *H-pylori* colonization. Also, the absence of significant difference in EGG parameters before and after *H-pylori* eradication in non-ulcer dyspepsia patients. Furthermore, the absence of significant difference in EGG parameters between non-ulcer dyspepsia patients without *H-pylori* infection and healthy subjects without *H-pylori* infection suggest the EGG as a non-useful test in the assessment of non-ulcer dyspepsia patients and question the contribution of abnormal gastric myoelectrical activity to non-ulcer dyspepsia with or without *H. pylori* infection. That results are in accordance with the results reported by **Holmvall and Lindberge** who concluded that severe functional dyspepsia is not associated with abnormal EGG parameters. Also, that conclusion agree with the conclusion reported by **Oba-Kuniyoshi and his colleagues**, who suggested that postprandial symptoms in dysmotility-like functional dyspepsia are not related to disturbance of gastric myoelectrical activity [11,12]

Furthermore, **Abid and Lindberg** reported poor correlation between EGG parameters and antro-duodenal manometry and suggested doubtful clinical usefulness in adults [13].

In addition, some studies reported that *H-pylori* infection in very common among non-ulcer dyspepsia

patients and its role in pathogenesis is debatable [14-16].

But, this is not in agreement with some studies confirming abnormal EGG parameters in non-ulcer dyspepsia patients, although they are not necessary to show the similar abnormalities in various patient groups [17- 19].

Also, our results do not agree with the results obtained by some studies demonstrating that *Helicobacter pylori* infection causes both inflammation and the co-existing motor disorders in functional dyspepsia patients with improvement of both symptoms and correction of the abnormal rhythm and power after eradication therapy of *H-pylori* [20, 21].

The great differences between different studies may be explained by the fact that EGG is still an investigational, yet, non-standardized tool in medicine with building of its standards which needs accumulation of tremendous number of studies with consequent systematic review and meta-analysis of that studies for conclusion of its rules to apply on human diseases.

The significantly shorter gastric full emptying time in patients with non-ulcer dyspepsia and *H. pylori* infection than healthy subjects with *H. pylori* colonization and the significant prolongation of the gastric half emptying time after *H. pylori* eradication in that group of patients suggests that accelerated gastric emptying rather than delayed gastric emptying is an associated finding in non-ulcer dyspepsia patients with

H. pylori infection and eradication therapy of *H. pylori* may improve that enhanced gastric emptying. The absence of that change in non-ulcer dyspepsia patients without *H. pylori* infection suggests the disease a different pathophysiological entity than *H. pylori* associated non-ulcer dyspepsia.

That results are in agreement with results reported by **Miyaji and his colleagues**, who found that *H. pylori* infected non-ulcer dyspepsia patients may have delayed gastric emptying, normal gastric emptying or accelerated gastric emptying and *H. pylori* eradication corrects the disturbed gastric emptying [22]. Also, accelerated rather than delayed gastric emptying associated with *H. pylori* infection was reported by Caldwell and his colleagues and **Minocha and his colleagues** [23,24]. However, our results are in contradiction to results obtained by some studies reporting lack of association of *H. pylori* infection or eradication therapy with gastric emptying abnormality in functional dyspepsia patients [25- 27].

Also, our results contradicts with the results of a study reporting delayed gastric emptying in *H. pylori* infected non-ulcer dyspepsia patients [28].

The accelerated gastric emptying in *H. pylori* infected functional dyspepsia patients may be explained by enhanced postprandial gastric sensation due to abnormal afferent function and irritable stomach syndrome [29].

The normal gastric emptying in *H. pylori* negative functional dyspepsia patients in our study is not in agreement with the results obtained by some studies reporting delayed gastric emptying in 24-78% of patients with functional dyspepsia [30, 31].

Conclusion:

Gastric myoelectrical activity is the same in patients with non-ulcer dyspepsia patients and healthy subjects regardless of the *H.pylori* status. *H.pylori* infection in non-ulcer dyspepsia patients may accelerate gastric emptying and *H.pylori* eradication therapy improves that abnormal gastric emptying. Non-ulcer dyspepsia patients without *H. pylori* infection may have different pathophysiological mechanisms than those with *H. pylori* infection.

Corresponding author

Amal S. Bakir

Internal Medicine Department, Gastroenterology and Hepatology unit. Ain-Shams University, Cairo, Egypt
Amalshawky_mb@hotmail.com

References:

1. Drossman DA, Corazziari E, Delvaux M, Spiller R, Talley NJ, Thompson WG, Whitehead WE (2006). Rome III: The Functional Gastrointestinal Disorders. 3rd Edition Degnon Associates, McLean, VA,.

2. Tack J, Bisschops R, Sarnelli G. (2004). Pathophysiology and treatment of functional dyspepsia. *Gastroenterology*; 127:1239-55.
3. Van den Elzen BD, Bennink RJ, Holman R. (2007). Impaired drinking capacity in patients with functional dyspepsia: intragastric distribution and distal stomach volume. *Neurogastroenterol Motil*; 19:968-76.
4. Vandenberghe J, Dupont P, Van Oudenhove L. (2007). Regional cerebral blood flow during gastric balloon distension in functional dyspepsia. *Gastroenterology*; 132: 1684- 93.
5. Eamonn MM and Quigley M (1999): Advances in basic science hold promise for new therapies in gastrointestinal dysmotility. *Eurp. Gastroenterol. Week*.
6. Chen JD and McCallum RW: (1993). Clinical applications of electrogastronomy. *Am J Gastroentrol*; 88:1324.
7. Lin Z, Chen JDZ, Parolisi S: (2001). Prevalence of gastric myoelectrical abnormalities in patients with non-ulcer dyspepsia and *H. pylori* infection: resolution after eradication. *Dig Dis Sci.*; 46(4): 739-745.
8. Koskenpato J, Tommola TK, Kairemok M: (2000) Long -term follow up study of gastric emptying and *H.pylori* eradication among patients with functional dyspepsia. *Dig Dis Sci*; 45(9):1763-1768.
9. Arisawa T, Tahara T, Shibata T. (2007) Genetic polymorphism of molecules associated with inflammation and immune response in Japanese subjects with functional dyspepsia. *Int J Mol Med*;25:1343-50.
10. Portincasa P, Diciaula A, Palmieri V (1997): Impaired gall bladder and gastric motility and pathological gastroesophageal reflux in gall stone patients. *Europ. J. Clin. Invest.*;27: 653.
11. Holmval P, Lindberg G(2002). Electrogastronomy before and after a high-caloric, liquid test meal in healthy volunteers and patients with severe functional dyspepsia. *scand J Gastroenterol*;37:1144-48.
12. Oba-kuniyoshi AS, Olveira Jr JA, Moraes ER, Troncon IE.(2004) Postprandial symptoms in dysmotility-like functional dyspepsia are not related to disturbances of gastric myoelectrical activity. *Braz J Med Biol Res*; 37:47-53.
13. Abid S, Lindberg G. (2007) Electrogastronomy: poor correlation with antro-duodenal manometry and doubtful clinical usefulness in adults. *World J Gastroenterol*;13[38]:5101-07.
14. Hamilton JW, Bellahsene BE, Reichelderfer M, Webster JG, Bass P. Human electrogastronomy, comparison of surface and mucosal recordings. *Dig. Dis. Sci.*;31:33-9.

15. Talley NJ, Janssens J, Lauritsen K, Racz I, Bolling-Sternevald E(1999). Eradication of *Helicobacter pylori* in functional dyspepsia: randomized double blind placebo controlled trial with 12 months follow up. *BMJ*;318:833-7.
16. Talley NJ, Vakil N, Ballard EDIL, Fennerty MB(1999). Absence of benefit of eradicating *Helicobacter pylori* in patients with nonulcer dyspepsia. *N. Engl. J. Med.*;341 : 1106-11.
17. Lu CL, Chen CY, Chang FY(2001). Impaired postprandial gastric myoelectrical activity in Chinese patients with non-ulcer dyspepsia. *Dig. Dis. Sci.*; 46:242-9.
18. Lin X, Chen JZ.(2001) Abnormal gastric slow waves in patients with functional dyspepsia assessed by multichannel electrogastrography. *Am. J. Physiol.*; 280:G1370-5.
19. Koch KL, Hong SP, Xu L. (2000). Reproducibility of gastric myoelectrical activity and the water load test in patients with dysmotility-like dyspepsia symptoms and in control subjects. *J. Clin. Gastroenterol.* ; 31:125-9.
20. Lin Z, Chen JDZ, Parolisi S, Shifflett J, Peura DA, MacCallum RW. (2001). Prevalence of gastric myoelectrical abnormalities in patients with non-ulcer dyspepsia and *H.pylori* infection, resolution after *H.pylori* eradication. *Dis. Dis. Sci*; 46:739-45.
21. Thor P, Lorens K, Tabor S, Herman R, Konturek JW, Konturek SJ, (.1996). Dysfunction in gastric myoelectric and motor activity in *Helicobacter pylori* positive gastritis patients with non-ulcer dyspepsia. *J. Physiol. Pharmacol.*; 47:469-76.
22. Miyaji H, Azuma T, Ito S, Abe Y, Ono H, Suto H, Ito Y(1999). The effect of *Helicobacter pylori* eradication on gastric antral myoelectrical activity and gastric emptying in patients with non-ulcer dyspepsia. *Aliment Pharmacol Ther.*; 13[11]:1473-80.
23. Caldwell SH, Valenzeula G, Marshall BJ, Dye KR, Hoffman SR, Plankey MW, MacCallum RW. (1992). *Helicobacter pylori* infection and gastric emptying of solids in humans. *Neurogastroenterology & motility*;4:113-117
24. Minocha A, Mokshangundam S, Gallo SH, Rahal PS. (1994). Alterations in upper gastrointestinal motility in *H. pylori* non-ulcer dyspepsia. *Am J Gastroenterol*; 89:1797-800
25. Leontiadis GI, Minopoulos GI, Maltezos S, Kotsios S, Manolas KI, Hatseras D(2004). Effects of *Helicobacter pylori* infection on gastric emptying rate in patients with non-ulcer dyspepsia. *World J Gastroenterol.*;10[12]:1750-4
26. Goh KL, Paramsothy M, Azian M(1997) Does *Helicobacter pylori* infection affect gastric emptying in patients with functional dyspepsia?. *J Gastroenterol Hepatol* 12 [12]: 790-4.
27. Poong-Lyul R, Young-Ho K, Hee J S, Jae J K, Kwang C K, Seung W P, Jong C R(1999). Lack of association of *Helicobacter pylori* infection with gastric hypersensitivity or delayed gastric emptying in functional dyspepsia. *Am J Gastroenterol*; 11:3165-69.
28. Mearin F, deRibot X, Balboa A. (1995) Does *H. pylori* infection increase gastric sensitivity in functional dyspepsia? *Gut*; 37:47-51.
29. Thumshirm M, Camilleri M, Saslow SB, Williams DE, Burton DD, Hanson RB(1999). Gastric accommodation in non-ulcer dyspepsia and the roles of *Helicobacter pylori* infection and vagal function. *Gut*;44:55-64
30. Talley N, Verlinden M, Jones M (2001). Can symptoms discriminate among those with delayed or normal gastric emptying in dysmotility like dyspepsia? *Am J Gastroenterol*; 96: 1422-8.
31. Timmons S, Liston R, Moriarty KJ. (2004) Functional dyspepsia: motor abnormalities, sensory dysfunction, and therapeutic options. *Am J Gastroenterol Apr*;99(4):739-49.

6/18/2011